

# **UNDERSTANDING AGE AND DIABETES RELATED CHANGES IN ERYTHROCYTE MEMBRANE**

**Yanisleidys Pantoja**

**Doctor of Philosophy**

**Aston University**

**September 2024**

© Yanisleidys Pantoja, 2024, asserts their moral right to be identified as the author of this thesis.

This copy of the thesis has been supplied on condition that anyone who consults it is understood to recognise that its copyright belongs to its author and that no quotation from the thesis and no information derived from it may be published without appropriate permission or acknowledgement.

## **Impact of COVID-19**

The global COVID-19 pandemic significantly impacted the progression of my research on erythrocytes. Due to restrictions implemented during the first year of the pandemic, including social distancing measures, limited access to laboratory facilities, and challenges in obtaining blood samples, I was unable to work directly with erythrocytes. To adapt to these circumstances, I shifted my focus to utilizing cell models, specifically U937 cells, to practice techniques that I would later apply to erythrocyte research. This transition allowed me to obtain relevant research experience despite the constraints posed by the pandemic, but in practice substantially delayed the main work on the project, which was carried out in only two years.

**This project has received funding from EU's Horizon 2020 research and innovation programme under MSC grant agreement N°847419.**

# Abstract

Type 2 Diabetes mellitus (T2DM) is an age-related disease with an inflammatory and oxidative aetiology. Hyperglycaemia significantly contributes to oxidative stress, leading to lipid peroxidation and the formation of advanced glycation or lipoxidation end products (AGEs/ALEs). Evidence indicates that T2DM and ageing affect erythrocyte membrane fluidity, though the mechanisms remain unclear. This project investigated the correlation between membrane fluidity, tension, and phospholipid composition to understand the interactions between membrane properties, oxidative stress, and lipid composition in erythrocytes. Erythrocytes from healthy volunteers were treated in vitro with high glucose levels, with and without glyoxal or methylglyoxal. Membrane fluidity increased with long-term glucose treatment at 100 mM and in the presence of glyoxal at 5 mM and 100 mM glucose, while ageing in 5 mM glucose showed no changes. Membrane tension increased for all participants at 22 mM glucose, but glyoxal and methylglyoxal results were inconsistent. Analysis of intracellular reactive oxygen species (ROS) was inconsistent, but aged cells showed increased phosphatidylserine exposure after 4-hour glucose treatment, which is indicative of changes in the membrane. Liquid chromatography-tandem mass spectrometry revealed erythrocytes aged in physiological glucose levels had increased PC 28:0|PC 14:0\_14:0, while higher glucose levels increased unsaturated fatty acyl chains, including PC 34:3, and PE 41:7|PE 19:2\_22:5 at 22 mM glucose. The 100 mM glucose treatment showed elevated levels of PE 41:7|PE 19:2\_22:5, PE 34:1|PE 16:0\_18:1, and PE 34:1|PE 16:0\_18:1. PC 28:0|PC 14:0\_14:0 and PC 28:0 remained high at 5 mM compared to 22 mM and 100 mM glucose. This increase in the number of double bonds in phospholipids at higher glucose levels likely contributed to the increased membrane fluidity observed at 100 mM glucose. These findings suggest that exposure of erythrocytes to high glucose induces changes in lipid composition, which can significantly affect membrane dynamics. This highlights the complex relationship between glucose levels, ageing, and erythrocyte membrane properties. The small sample size of the study and interindividual variability in oxidative stress markers emphasise the need for further research to elucidate these mechanisms and identify potential therapeutic targets for managing T2DM-related complications.

## **Acknowledgments**

### **Personal acknowledgements**

I would like to dedicate this work to my family.

In loving memory of my nan Maria, whose love continues to inspire me every day. Her strength and spirit remain a source of motivation, reminding me of the values she instilled in me. In loving memory of my grandad, Jose Delso, although not with us, his wit and sense of humour live on and continue to guide me every day.

To my mum Lilian, dad Stephen, and sister Amy, thank you for your unwavering support and encouragement throughout my studies. I would not be where I am today without your help, support and belief in me. Your love and guidance have been my foundation, and I am forever grateful. I could not have reached this milestone without your constant presence and reassurance.

To my other half Kirk, thank you for always being there for me throughout the entire PhD journey. Your understanding and support have been invaluable, helping to motivate me and push through moments of doubts and exhaustion.

### **Professional acknowledgements**

I would like to thank my supervisor, Prof. Corinne Spickett, and my co-supervisors, Dr Alan Goddard and Dr James Brown. Corinne, thank you for welcoming me into the group and for your guidance and advice over the last four years. I will be forever grateful for this opportunity. Alan and James, I deeply appreciate your help and support, which have greatly contributed to my research. Thank you all for sharing your knowledge and providing continuous encouragement throughout my PhD journey.

A special thanks goes to Ophelie, MB363 would have not been the same without you. I would also like to thank everyone in the oxidative stress group during my time at Aston University. I would also like to acknowledge the MemTrainees.

I acknowledge my industrial partner, Sciex, a special thanks to Cagakan Ozbaldi for his invaluable help with lipidomics. I would also like to extend my gratitude to Melissa, whose efforts in setting up the placement made this collaboration possible.

# Table of Contents

***Understanding age and diabetes related changes in erythrocyte membrane .... 4***

***Abstract..... 4***

***Chapter 1..... 16***

**General Introduction ..... 16**

1.1 Diabetes ..... 17

1.2 Erythrocytes..... 19

1.3 Erythrocyte glucose metabolism..... 20

1.4 Oxidative stress in erythrocyte under hyperglycaemic conditions ..... 21

1.6 Membrane Tension..... 31

1.7 Ageing ..... 36

1.8 Erythrocytes in diabetes and ageing..... 37

1.10 Knowledge Gap ..... 39

1.11 Overall aim of the project..... 39

***Chapter 2..... 41***

**Materials and Methods..... 41**

2.1 Ethics approval and participants..... 42

2.2 Materials ..... 42

2.2.1 Chemicals and Reagents ..... 42

2.2.2 Laboratory Consumables ..... 43

2.3 Methods..... 43

2.3.1 Erythrocyte preparation ..... 43

2.2.2 Preparation of treatments ..... 44

2.2.2.1 Mannitol treatment preparation ..... 44

2.2.2.2 Glyoxal and methylglyoxal preparation ..... 44

2.2.3 Erythrocyte membrane fluidity studies using the fluorescent probe laurdan ..... 44

2.2.3.1 Preparation of laurdan ..... 44

2.2.3.2 Preparation of Methyl- $\beta$ -cyclodextrin..... 44

2.2.3.3 Short term glucose treatment..... 45

2.2.3.4 Long term glucose treatment ..... 46

2.2.3.5 Laurdan fluorescence measurements and generalised polarisation (GP) calculations ... 47

2.2.4 Erythrocyte membrane tension studies ..... 47

2.2.4.1 Flipper-TR assay..... 47

2.2.4.2 Image acquisition ..... 48

2.2.4.3 Image analysis ..... 48

6

2.2.5 Erythrocyte ROS production and PS detection using the fluorescent probe carboxy-H2DCFDA and annexin V, respectively.....	48
2.2.5.1 Carboxy H <sub>2</sub> DCFDA and glucose treatment.....	48
2.2.5.2 Annexin V staining.....	49
2.2.5.3 Flow cytometry.....	49
2.2.6 Mass spectrometry analysis of erythrocyte lipids.....	50
2.2.6.1 Erythrocyte lipid extraction.....	50
2.2.6.2 Lipid preparation prior to LC-MS analysis.....	51
2.2.6.3 Liquid chromatography (LC) conditions.....	51
2.2.6.4 Mass Spectrometry.....	52
2.2.6.5 Data analysis.....	53
2.2.7 Statistical analysis.....	53
<b>Chapter 3.....</b>	<b>54</b>
<b>Effect of glucose and ageing, in the presence or absence of glyoxal and methylglyoxal, on erythrocyte membrane fluidity.....</b>	<b>54</b>
3.1 Introduction.....	55
3.2 Materials and Methods.....	61
3.3 Results.....	62
3.3.1 Short-term glucose treatment and its effect on erythrocyte membrane fluidity as the cells aged.....	62
3.3.2 Effect of increasing glucose concentrations on erythrocyte membrane fluidity as the cells aged <i>in vitro</i> .....	66
3.3.3 Effect of glucose in the presence or absence of methylglyoxal and glyoxal on erythrocyte membrane fluidity.....	70
3.4 Discussion.....	71
<b>Chapter 4.....</b>	<b>78</b>
<b><i>In vitro</i> studies of the effect of glucose and ageing on erythrocyte membrane tension.....</b>	<b>78</b>
4.1 Introduction.....	79
Aim and objectives:.....	84
4.2 Materials and methods.....	85
4.3 Results.....	85
4.3.1 Assaying membrane tension of untreated erythrocytes, in the presence or absence of hypertonic and hypotonic treatments using Flipper-TR.....	85
4.3.2 Effect of increasing glucose concentrations on erythrocyte membrane tension as the cells were aged <i>in vitro</i> for five days.....	89

5.3.3 Effect of increasing glucose concentrations in the presence of glyoxal and methylglyoxal on erythrocyte membrane tension as the cells were aged <i>in vitro</i> for five days.....	93
Discussion .....	99
<b>Chapter 5.....</b>	<b>106</b>
<b><i>In vitro</i> studies of the effect of glucose and ageing on erythrocyte reactive oxygen species (ROS) production and phosphatidylserine (PS) exposure on outer membrane leaflet.....</b>	<b>106</b>
5.1 Introduction.....	107
Aim and objectives.....	112
5.2 Materials and Methods.....	112
5.3 Results.....	112
5.3.1 Effect of glucose on the production of reactive oxygen species (ROS) as erythrocytes aged .....	112
5.3.2 Effect of glucose on phosphatidylserine (PS) exposure as erythrocytes aged .....	120
5.4 Discussion .....	124
<b>Chapter 6.....</b>	<b>129</b>
<b>Lipidomic analysis of erythrocyte phospholipids.....</b>	<b>129</b>
6.1 Introduction.....	130
6.1.1 Lipid composition of erythrocyte membranes .....	130
Aim and objectives.....	137
6.2 Materials and methods.....	138
6.3 Results.....	138
6.3.1 Effect of ageing on erythrocyte phospholipids .....	138
6.3.2 Effect of glucose treatments on erythrocyte phospholipids .....	152
6.3.3 Differences in lipid profiles between participants.....	166
6.4 Discussion .....	177
<b>Chapter 7.....</b>	<b>186</b>
<b>General Discussion .....</b>	<b>186</b>
<b>Chapter 8.....</b>	<b>194</b>
<b>References.....</b>	<b>194</b>
<b>Supplementary Data.....</b>	<b>221</b>

## ***List of abbreviations***

**ADP** - Adenosine diphosphate  
**AFM** - Atomic Force microscopy  
**ATP** - Adenosine triphosphate  
**BODIPY** - Fluorescent boron dipyrromethene  
**DCFH-DA** - Dichlorodihydrofluorescein diacetate  
**DDA** - Data dependent analysis  
**DHE** – Dihydroethidium  
**DMSO** - Dimethyl sulfoxide  
**DOPC** - 1,2-Dioleoyl-sn-glycero-3-phosphocholine  
**DPPC** – Dipalmitoylphosphatidylcholine  
**DTT** – Dithienothiophene  
**EDTA** - Ethylenediaminetetraacetic acid  
**ER** - Endoplasmic reticulum  
**FADs** – Fatty acid desaturases  
**FLIM** - Fluorescence lifetime imaging microscopy  
**FSC** - Forward scatter  
**GDM** - Gestational diabetes mellitus  
**GO** – Glyoxal  
**GP** - Generalised polarisation  
**GUV** - Giant unilamellar vesicles  
**IDA** – Information dependent acquisition  
**LC** - Liquid chromatography  
**LPC** – Lyso-phosphatidylcholine  
**LPE** – Lyso-phosphatidylethanolamine  
**MBCD** - Methyl- $\beta$ -cyclodextrin  
**MGO** – Methylglyoxal  
**MS** - Mass spectrometry  
**MTBE** – Methyl tert-butyl ether  
**NAD** - Nicotinamide adenine dinucleotide  
**NADH** - Nicotinamide adenine dinucleotide (NAD) +  
**NADPH** - Nicotinamide adenine dinucleotide phosphate  
**OT** – Optical tweezers  
**PBS** - Phosphate buffer saline

**PC** – Phosphatidylcholine  
**PE** – Phosphatidylethanolamine  
**PKC** – Protein kinase C  
**PS** – Phosphatidylserine  
**RBC** - Red blood cells  
**ROS** – Reactive oxygen species  
**SM** – Sphingomyelin  
**sn** - Stereospecific numbering  
**SSC** - Side scatter  
**St** – Sterol  
 $\tau$  - Fluorescence lifetime  
**TCSPC** - Time-correlated single photon counting  
**TOF** – Time of flight

## List of Figures

Figure 1.1 Signalling pathway involved in insulin secretion in $\beta$ -cells under normal physiology (A) and mechanisms leading to b-cell dysfunction (B).	19
Figure 1.2 Diagram showing the Fenton (a) and Haber-Weiss (b) reactions.	21
Figure 1.3 Lipid peroxidation.	23
Figure 1. 4. Non-enzymatic reaction leading to advance glycation end products (AGEs) formation.	24
Figure 1. 5. Polyol pathway.	26
Figure 1. 6 Glucose metabolism disorder in erythrocytes under hyperglycaemic conditions.	27
Figure 2. 1. Diagram explaining long-term glucose treatment.	33
Figure 2. 3. Diagram explaining long-term glucose treatment.	33
Figure 3. 1. Laurdan in the ground (a) and excited states (b).	56
Figure 3. 2. Illustration of the polarization-like state of laurdan due to a weak interaction of the dimethylamino group of laurdan with the ester groups of DOPC.	57
Figure 3. 3. Structure of cholesterol (A) and MBCD (B).	59
Figure 3. 4. Molecular structure of D-glucose (A) and D-mannitol (B).	61
Figure 3. 5. GP of laurdan in erythrocytes treated for one hour with glucose (A) and mannitol (B) on days 0 and 4.	63
Figure 3. 6. Effect of short-term glucose treatment on erythrocyte membrane fluidity.	65
Figure 3. 7. Effect of long-term physiological levels of glucose exposure on erythrocyte membrane fluidity, measured by laurdan.	67
Figure 3. 8. Long term erythrocyte treatment under physiological and pathological levels of glucose.	68
Figure 3. 9. Laurdan GP of erythrocytes, after the cells were kept for five days in different glucose concentrations (5 mM, 22 mM and 100 mM) in the presence or absence of glyoxal (1 $\mu$ M) or methylglyoxal (5 $\mu$ M).	70
Figure 4. 1. Different illustrations of methods used to measure membrane tension. small micropipette creating a tether.	80
Figure 4. 2. Molecular structure of Flipper-TR.	81

Figure 4. 3. Flipper TR and membrane tension..	81
Figure 4. 4. Explanation of fluorescent lifetime imaging.....	83
Figure 4. 5. Images acquired by FLIM of untreated erythrocytes and those under hypotonic and hypertonic conditions belonging to participant G..	86
Figure 4. 6. Erythrocyte membrane tension assayed by Flipper-TR on untreated (day 0) and control cells per participant.....	87
Figure 4. 7. Erythrocyte membrane tension assayed by Flipper-TR on untreated (day 0) cells ( $n=4$ ).....	88
Figure 4. 8. Images of erythrocytes, aged in different glucose concentration (day 4), belonging to participant G.....	90
Figure 4. 9. Erythrocyte membrane tension assayed by Flipper-TR on erythrocytes aged in media containing different glucose concentrations..	91
Figure 4. 10. Combined data of erythrocyte membrane tension measured by Flipper-TR fluorescent lifetime.....	93
Figure 4. 11. Images of RBCs corresponding to participant G.....	95
Figure 4. 12. Membrane tension assayed by Flipper-TR on erythrocytes aged in media containing 5 mM glucose in the presence or absence of glyoxal and methylglyoxal.....	96
Figure 4. 13. Membrane tension assessed by Flipper-TR on erythrocytes aged in media containing 22 mM and 100 mM glucose and treated with 1 $\mu$ M glyoxal and 5 $\mu$ M methylglyoxal. Fluorescent lifetime measurements were taken by FLIM.....	97
Figure 4. 14. Combined erythrocyte membrane tension data from three different participants ( $n=3$ ).....	98
Figure 5. 1. A flow cytometer has three main systems: optics, fluidics, and electronics..	109
Figure 5. 2. Light scattering properties of a cell.....	109
Figure 5. 3. The complex redox chemistry of carboxy- $H_2DCFDA$ .....	111
Figure 5. 4. ROS production of erythrocytes treated with 5 mM, 22 mM, and 100 mM glucose for 30 minutes (A) ( $n=3$ ), 1 hour (B) ( $n=4$ ), and 4 hours (C) ( $n=4$ ) on days 0 and 4..	114
Figure 5.5. Figure 4.5. ROS production of erythrocytes for each participant treated with glucose (A and C) and mannitol (B and D). .....	117
Figure 5. 6. Shows data belonging to participant D on day 0 at 1 hour treatment between 5 mM and 22 mM glucose.....	119
Figure 5. 7. Annexin V used to detect PS exposure on erythrocyte as a marker of apoptosis..	121
.....	12

Figure 5. 8. Annexin V used to detect PS exposure on erythrocytes as a marker of apoptosis for each participant on days 0 (A) and 4 (B) after 4-hour glucose treatment.....	123
Figure 6. 1. Chemical structure of phospholipids.....	131
Figure 6. 2. Structure of sphingomyelin.....	132
Figure 6. 3. Quadrupole mass analyser.....	133
Figure 6. 4. Diagram of Zeno TOF 7600 mass spectrometer.....	134
Figure 6. 5. Volcano plots were used to compare untreated and treated cells under 5 mM glucose..	140
Figure 6. 6. Information on PC 36:4  PC 18:2_18:2 obtained using positive ion mode.....	145
Figure 6. 7. Information on PC 34:2;O2 PC 16:0_18:2; O2 obtained using negative ion mode..	151
Figure 6. 9. Information on PS 25:0;O PS 18:0_7:0;O obtained using negative ion mode ..	157
Figure 6. 10. Volcano plots used to compare lipids extracted from erythrocytes under 5 mM and 100 mM glucose.....	159
Figure 6. 11. Information on PC 28:0 PC 14:0_14:0 obtained using positive ion mode. ....	163
Figure 6. 12. Information on PE 34:1 PE 16:0_18:1 obtained using negative ion mode.....	165
Figure 6. 13. Principal component analysis (PCA) plots, labelled (A) for positive ion mode and (B) for negative ion mode.....	167
Figure 6. 14. One-way ANOVA was performed on the data obtained from different participants in positive (A) and negative (B) ion modes..	168
Figure 7. 1. Summary of results investigating the effect of ageing on erythrocytes.....	187
Figure 7. 2. Summary of results investigating the effect of glucose on erythrocytes. ....	187
Figure S 1. Quality controls (QCs) obtained using negative ion mode. fragments. a. ....	222
Figure S 2. Quality controls (QCs) obtained using negative ion mode.....	223
Figure S 3. Quality controls (QCs) obtained using negative ion mode.Figure S 4. Quality controls (QCs) obtained using negative ion mode.....	223
Figure S 5. Quality controls (QCs) obtained using negative ion mode.Figure S 2. Quality controls (QCs) obtained using negative ion mode.....	223

Figure S 3. Quality controls (QCs) obtained using negative ion mode.	223
Figure S 4. Quality controls (QCs) obtained using negative ion mode.	223
Figure S 5. Quality controls (QCs) obtained using negative ion mode.	223
Figure S 6. Quality controls (QCs) obtained using positive ion mode.	224
Figure S 7. Quality controls (QCs) obtained using positive ion mode.	224
Figure S 8. Membrane fluidity studies. Results obtained for participant A, long term glucose treatment.	225
Figure S 9. Membrane fluidity studies. Results obtained for participant B, long term glucose treatment.	225
Figure S 10. Membrane fluidity studies. Results obtained for participant C, long term glucose treatment.	226
Figure S 11. Erythrocyte membrane tension assayed by Flipper-TR on untreated erythrocytes and those aged in media containing 5 mM for participant E.	227
Figure S 12. Membrane tension of fresh (day 0) and aged (day 4, 5 mM glucose) erythrocytes when exposed to hypotonic (A) and hypertonic solutions (B), which was assayed by Flipper-TR.	227
Figure S 13. Erythrocyte membrane tension assayed by Flipper-TR on untreated erythrocytes and those aged in media containing 5 mM for participant F.	228
Figure S 14. Membrane tension of fresh (day 0) and aged (day 4, 5 mM glucose) erythrocytes when exposed to hypotonic (A) and hypertonic solutions (B), which was assayed by Flipper-TR.	228
Figure S 15. RBC membrane tension assayed by Flipper-TR on untreated erythrocytes and those aged in media containing 5 mM for participant G.	229
Figure S 16. Membrane tension of fresh (day 0) and aged (day 4, 5 mM glucose) erythrocytes when exposed to hypotonic (A) and hypertonic solutions (B).	229
Figure S 17. Erythrocyte membrane tension assayed by Flipper-TR on untreated erythrocytes and those aged in media containing 5 mM.	230
Figure S 18. RBC membrane tension assayed by Flipper-TR on cells treated with hypotonic (A) and hypertonic (B) solutions on days 0 and 4.	230

## List of Tables

Table 2. 1. The components of Dulbecco's PBS purchased from Merck. ....	44
Table 2. 2. LC method involving a flow rate of 0.6 mL/min with a total duration of 15 minutes. The gradient used involved at 0 minutes 15% (B); 0-2 minutes 30% (B); 2-2.5 minutes 48% (B); 2.5-11 minutes 82% (B); 11-11.5 minutes 99% (B); 11.5-12 minutes 99% (B); 12-12.1 minutes 15% (B) and 12.1-15 minutes 15% (B).....	52
Table 6. 1. Diagnostic ions of major phospholipids found in erythrocytes ( <i>Leidl et al., 2008, Spickett et al., 2011</i> ).....	135
Table 6. 2. Significantly different lipids found between untreated (day 0) and treated cells under physiological glucose levels (day 4, 5 mM). ....	142
Table 6. 3. Significantly different oxidised phospholipids found between untreated (day 0) and treated cells under physiological glucose levels (day 4, 5 mM). ....	147
Table 6. 4. Significantly different lipids found between cells kept in media containing 5 mM and 22 mM glucose.....	155
Table 6. 5. Significantly different phospholipids found between cells kept in media containing 5 mM and 100 mM glucose.....	161
Table 6. 6. Significantly different diacyl phospholipids identified among untreated erythrocytes from different participants.....	170
Table 6. 7. Significantly different oxidised diacyl phospholipids identified among untreated erythrocytes from different participants.....	176

# Chapter 1

## General Introduction

## 1.1 Diabetes

Diabetes mellitus (DM) is a complex metabolic disorder, which is characterised by elevated blood glucose levels (hyperglycaemia), insulin deficiency or insulin insensitivity, or both (*Ighodaro, 2018*). Diabetes is diagnosed on the basis of hyperglycaemia, and it can be divided into two main types, type 1 and type 2 (*Pearson, 2019, Rains and Jain, 2011*). Type 1 diabetes has been linked to genetics and the production of autoantibodies that destroy pancreatic  $\beta$ -cells, which leads to no production, or producing small amounts, of insulin (*Rains and Jain, 2011*). On the other hand, type 2 diabetes mellitus is part of metabolic syndrome; a group of interconnected factors that include insulin resistance, visceral adiposity, atherogenic dyslipidaemia and genetic susceptibility (*Huang, 2009*). Its pathophysiology includes a combination of defective insulin secretion by pancreatic  $\beta$ -cells, and the inability of insulin-sensitive tissues to respond appropriately to insulin (*Galicia-Garcia et al., 2020*). Type 2 diabetes accounts for more than 90% of patients diagnosed with diabetes and it has been linked to factors such as obesity and age (*Rains and Jain, 2011*). While traditionally considered an age-related ailment, type 2 diabetes mellitus is now increasingly diagnosed in the young (*Vaiserman and Lushchak, 2019, Lascar et al., 2018*).

Oxidative stress, an imbalance between the production of oxidants (increase) and antioxidants (decrease), has become increasingly recognised and has gained great medical significance; it is considered a component of almost every inflammatory disease process including diabetes (*Dalle-Donne et al., 2003, Pizzino et al., 2017*). Free radicals are products of normal cellular metabolism and can be defined as an atom or molecule having one or more unpaired electrons in the outer shell (*Phaniendra et al., 2015*). This makes the free radical unstable, short lived and highly reactive (*Phaniendra et al., 2015*). Examples of free radicals include superoxide ( $O_2^{\bullet-}$ ), hydroxyl ( $OH^{\bullet}$ ) and peroxy radical ( $ROO^{\bullet}$ ) (*Di Meo and Venditti, 2020*). These examples are part of the broader category of reactive oxygen species (ROS), which are molecules containing oxygen that are highly reactive, whether or not they possess unpaired electrons. For instance, hydrogen peroxide is a ROS that is not a free radical. While ROS serve essential roles in cell signalling and host defence, excessive or uncontrolled production can lead to oxidative stress (*Milkovic et al., 2019*). In healthy organisms, the production of free radicals is low, and the antioxidant defence mechanisms rapidly removes them before they can cause damage to the cells (*Di Meo and Venditti, 2020*). The balance is not faultless, and some ROS-mediated damage occurs continuously. Hyperglycaemia is a major contributing

factor of oxidative stress, and it has been hypothesised to contribute to oxidative stress by either direct generation of ROS or by altering the redox balance.

Oxidative stress is involved in the pathogenesis of type 2 diabetes mellitus (*Rains and Jain, 2011*) and has been shown to compromise the two major mechanisms failing during diabetes; insulin secretion and insulin action (*Rains and Jain, 2011, Ighodaro, 2018*). Chronic hyperglycaemia leads to  $\beta$ -cell deterioration in the islets of Langerhans (*Robertson et al., 2004*). The mechanisms involved in  $\beta$ -cell deterioration (Figure 1.1) involves increased ROS production, which lead to the inhibition of calcium mobilisation and insulin release as well as the activation proapoptotic signals. Furthermore, hyperlipidaemia and hyperglycaemia, common in diabetes, induce endoplasmic reticulum (ER) stress (*Mustapha et al., 2021*). The cells respond to ER stress by initiating the activation of proapoptotic unfolded protein response (UPR), potentially leading to pro-apoptotic signalling pathways (*Mustapha et al., 2021*).

Moreover, sustained high glucose levels increase the biosynthesis of islet amyloid polypeptide (IAPP), which, through its aggregation into amyloid fibrils, contributes to  $\beta$ -cell dysfunction, reduced insulin secretion, and increased ROS generation (*Galicía-García et al., 2020, Alrouji et al., 2023*). The islets are considered among the most vulnerable of tissues during times of oxidative stress, exhibiting the lowest intrinsic antioxidant capacity compared to other metabolic tissues (*Robertson et al., 2004*). Beyond its implication in diabetes pathogenesis, oxidative stress as a result of hyperglycaemia can affect various cellular components of red blood cells, including the plasma membrane, haemoglobin and membrane protein skeleton.

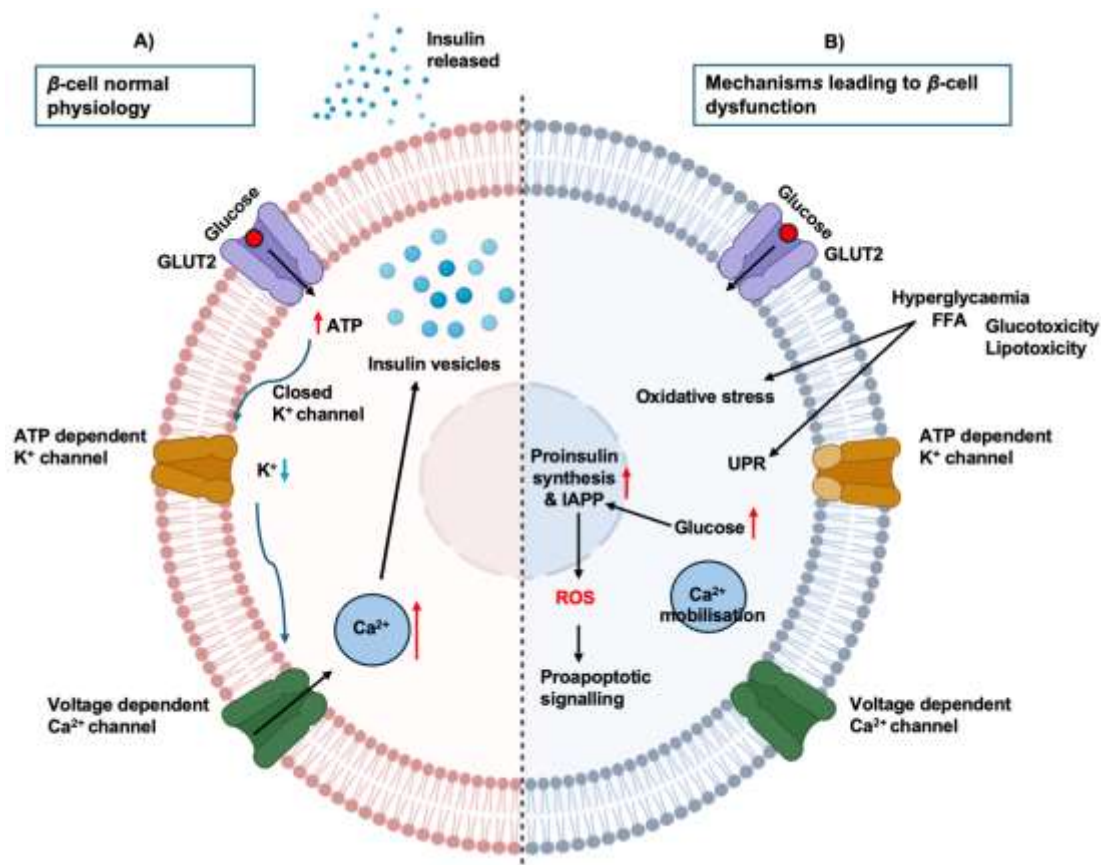


Figure 1.1 Signalling pathway involved in insulin secretion in  $\beta$ -cells under normal physiology (A) and mechanisms leading to  $\beta$ -cell dysfunction (B). Under normal conditions, insulin release is triggered in response to high glucose concentration, where glucose is internalised by GLUT2. Glucose metabolism increases the production of ATP, the ATP dependent potassium channels are closed and the change in membrane depolarisation, leads to calcium influx, which enables insulin exocytosis. B) Hyperglycaemia promotes oxidative stress leading to ROS production inhibiting calcium mobilisation and activating proapoptotic signals. Excess fatty acids and hyperglycaemia lead to activation of proapoptotic unfolded protein response (UPR) and generating endoplasmic reticulum stress. Continuous high glucose levels increase pro-insulin and islet amyloid polypeptide (IAPP) biosynthesis which generates ROS. Adapted from: (Galicia-Garcia et al., 2020) using Biorender.

## 1.2 Erythrocytes

Red blood cells (RBCs) are the most abundant cell type in the blood (*Byrnes and Wolberg, 2017*) and are continuously exposed to glucose in the plasma. For many years, the RBC membrane has been widely studied; much is known about its composition (*Burton and Bruce, 2011*). Erythrocytes have provided an easy and accessible source for early studies of basic membrane structure (*Marchesi, 1974*). Also, they cannot carry out protein or lipid synthesis de novo and are therefore unable to replace irreversibly oxidised proteins with newly

synthesised ones (*D'Alessandro et al., 2019a*). A healthy erythrocyte is anucleate, 7-8  $\mu\text{m}$  in diameter (*Han et al., 2018*) and is composed of a fluid-like lipid bilayer (contributing to the bending resistance), and an attached cytoskeleton (maintaining cell shape) (*Chang et al., 2017*). Due to the fluid nature of the lipid bilayer, and the elastic nature of the cytoskeleton, the RBC can undergo dramatic deformations in the narrow blood capillaries, as small as 3  $\mu\text{m}$  in diameter without damage (*Chang et al., 2017*). Haemoglobin, the most abundant protein found in the cytoplasm of erythrocytes, is widely known as the iron-containing protein in blood and is responsible for binding oxygen and carbon dioxide during gas exchange (*Maqsooda S., 2012, Gell, 2018*).

The renewal of phospholipids in the erythrocyte plasma membrane depends on mechanisms such as lipid exchange and acylation of fatty acids within plasma lipoproteins (*de Oliveira and Saldanha, 2010*). Lipids are very important in the maintenance of erythrocytes shape; small changes in the surface area (inner/outer) can lead to various abnormalities (morphological / functional) (*de Oliveira and Saldanha, 2010*). The phospholipids in the RBC membrane play a pivotal role in the maintenance of cell shape, cell permeability as well as movement of various compounds across the membrane. Changes in RBC membrane phospholipid composition, as a result of lipid peroxidation and glycation, may induce changes physio-chemical properties of the erythrocyte membrane as well as in fluidity/rigidity (*Rudrappa, 2011*).

### **1.3 Erythrocyte glucose metabolism**

Glucose metabolism plays an important role in erythrocyte function. Erythrocytes predominantly rely on two key metabolic pathways namely glycolysis and the pentose phosphate pathway to fulfil their energy and redox homeostasis requirements (*Chatzinikolaou et al., 2024*). Erythrocytes rely heavily on glycolysis to generate adenosine triphosphate (ATP) because they lack mitochondria and thus cannot produce ATP through oxidative phosphorylation (*Chatzinikolaou et al., 2024*). Glycolysis allows these cells to produce ATP anaerobically, which is crucial for maintaining their functionality, including membrane transport and preserving cell shape. Additionally, the pentose phosphate pathway (PPP) is particularly important for erythrocytes as it generates nicotinamide adenine dinucleotide phosphate (NADPH). NADPH is essential for maintaining the reduced state of glutathione, a critical antioxidant that protects erythrocytes from oxidative damage (*Sun et al., 2017*). This defence against oxidative stress is vital for the longevity and function of erythrocytes.

## 1.4 Oxidative stress in erythrocyte under hyperglycaemic conditions

Oxidative damage as a result of hyperglycaemia has been shown to decrease the life span of erythrocytes, by altering their shape and deformability (Morabito *et al.*, 2020). The erythrocytes contain numerous sources of oxidants, including high levels of molecular O<sub>2</sub> bound to haemoglobin. Autoxidation of haemoglobin (forming methaemoglobin), where the haem-iron is oxidised from the ferrous (Fe<sup>2+</sup>) to the ferric (Fe<sup>3+</sup>) state, which is unable to bind haemoglobin, leads to the production of O<sub>2</sub><sup>•-</sup> radical (Tam *et al.*, 2013, Mohanty *et al.*, 2014). Dismutation of O<sub>2</sub><sup>•-</sup> radical produces hydrogen peroxide (Gwozdziński *et al.*, 2021), which can react with free soluble iron (Fe<sup>2+</sup>) and produce ROS (hydroxide and hydroxyl radical) by the Fenton reaction (Figure 1.2A). Additionally, O<sub>2</sub><sup>•-</sup> radical can also interact with hydrogen peroxide in the presence of ferrous iron to produce hydroxide and hydroxyl radical through the Haber-Weiss reaction (Figure 1.2B). So, haemoglobin is a major factor initiating oxidative stress within the RBCs (Gwozdziński *et al.*, 2021).

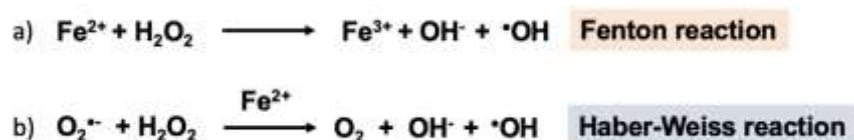


Figure 1. 1. Diagram showing the Fenton (a) and Haber-Weiss (b) reactions.

One of the consequences of uncontrolled oxidative stress is damage to lipids. Hydroxyl radical (HO<sup>•</sup>) is one of the most prevalent ROS that can affect lipids. It is a small, highly mobile, water soluble and chemically the most reactive ROS (Ayala *et al.*, 2014). Lipid peroxidation proceeds in three steps, which are initiation, propagation and termination (Figure 1.3). In the initiation step, a free radical attacks a polyunsaturated fatty acid (PUFA), causing the loss of a hydrogen and leads to the formation of a carbon-centred lipid radical. In the propagation step, oxygen reacts with the lipid radical generated in the initiation step to form a lipid peroxy radical (Augustine *et al.*, 2020). The lipid peroxy radical can then abstract hydrogens from adjacent unsaturated fatty acids which also generates another lipid radical, as in the initiation step. The cycle occurs until termination takes place, where antioxidants such as vitamin E donate a hydrogen to the lipid peroxy radical species and form a corresponding vitamin E radical that reacts with another lipid peroxy radical forming non-radical products (Ayala *et al.*, 2014). In erythrocytes the degree of lipid peroxidation has been found to be proportional to the glucose concentration *in vitro* (Jain, 1989).

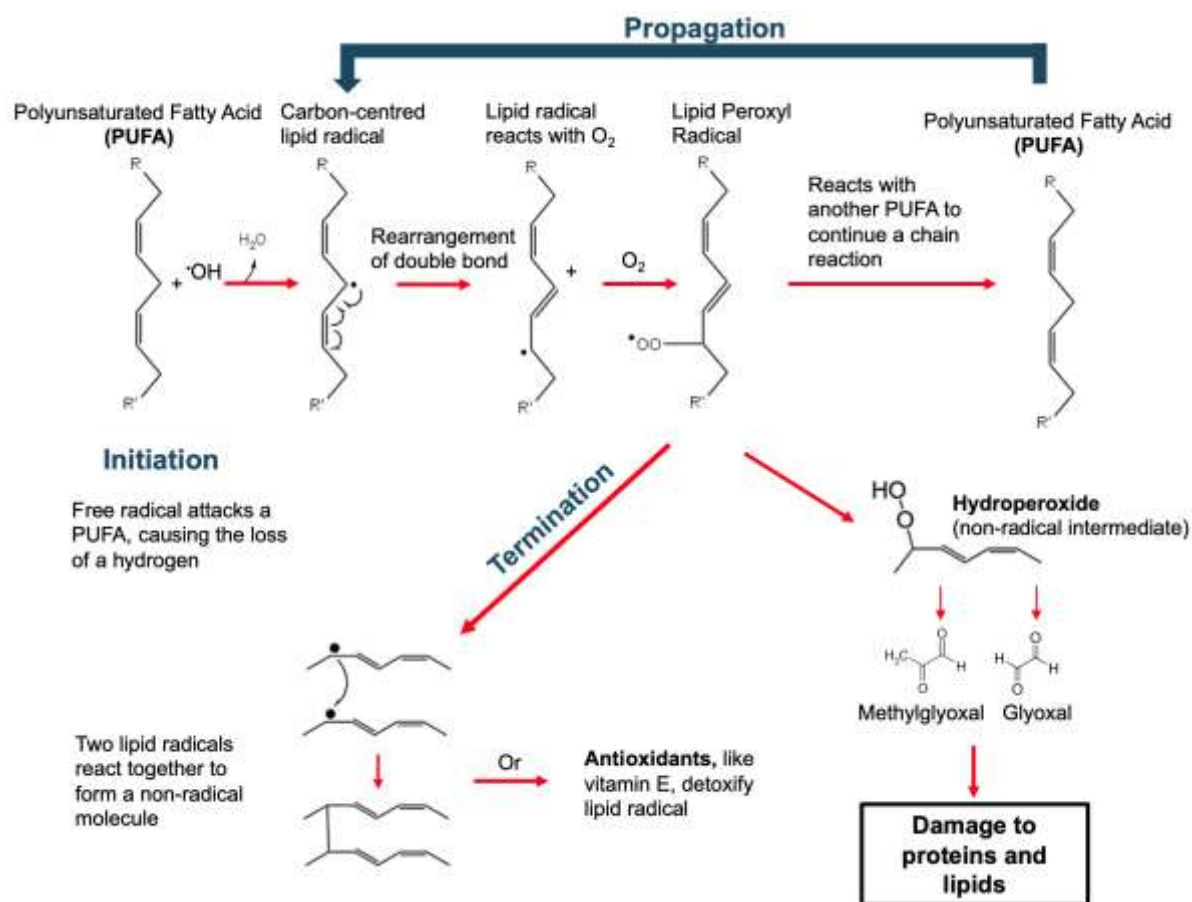


Figure 1. 3. Lipid peroxidation. In the initiation step of lipid peroxidation, a free radical such as hydroxyl radical initiates the process by attacking a polyunsaturated fatty acid (PUFA), leading to the loss of a hydrogen atom and the formation of a carbon centred lipid radical. Subsequently, in the propagation step, oxygen reacts with the lipid radical generated in the initiation step to produce a lipid peroxyl radical. During the propagation phase, the lipid peroxyl radical can abstract hydrogen atoms from adjacent unsaturated fatty acids, creating another lipid radical, thus perpetuating the cycle in the initiation step. This chain reaction continues until termination occurs. Termination is facilitated by antioxidants such as vitamin E, which donate atoms to the lipid peroxyl radical species. This donation forms a corresponding vitamin E radical that can react with another lipid peroxyl radical, resulting in the formation of non-radical products. Adapted from: (Wang *et al.*, 2017).

Unsaturated phospholipids and cholesterol are known for being targets of damaging peroxidative modifications (Ayala *et al.*, 2014). One of the major products of cholesterol peroxidation in diabetic RBC membrane is 7-keto-cholestadiene, and it correlates with HbA1c levels (Inouye, 1999). An increase in lipid peroxidation leads to the formation of lipid hydroperoxides (Reis and Spickett, 2012). In the cell membrane, lipid peroxides are more hydrophilic than native fatty acid side chains. These lipid peroxides tend to migrate to the membrane surface to interact with water, leading to disruption of the membrane structure by altering fluidity and making the membrane leaky (Pamplona, 2011). Also, lipid peroxides can

degrade and form lipid aldehydes (reactive carbonyl species), such as glyoxal and methylglyoxal (*Augustine et al., 2020, Pamplona, 2011*). These reactive aldehydes can react with nucleophilic groups of proteins and amino-phospholipids resulting in irreversible modifications and the formation of advanced lipoxidation end products (ALEs) (*Pamplona, 2011*). Reactive aldehydes can be produced excessively under oxidative stress conditions, have cytotoxic effects and play important roles in the pathophysiology of diabetes mellitus through the involvement in the progression of the disease (*Moldogazieva et al., 2019*). Lipid aldehydes tend to be more stable than ROS and can propagate oxidative injury by diffusing to sites distant from their origin (*Augustine et al., 2020*).

Besides damage to lipids, other factors such as glycated protein formation induced by hyperglycaemia, together with increased ROS generation, contribute to oxidative stress (*Morabito et al., 2020*). The Maillard reaction begins when a carbonyl group of a reducing sugar reacts with an amino group of a protein forming a Schiff base (*Wautier and Schmidt, 2004*). The Schiff base can undergo re-arrangements to yield a more stable Amadori product. These Amadori products can undergo further re-arrangements to form irreversible advanced glycated end products (AGEs) (Figure 1.4) (*Wautier and Schmidt, 2004*). The significance of the Maillard-like reactions in vivo was first recognised in 1968, with the study of haemoglobin A1c (HbA1c), which is known to be elevated in diabetic patients (*Rahbar, 1968*). HbA1c represents a post-translational adduct of glucose with the N-terminal valine amino group of haemoglobin  $\beta$  chain. Consequently, HbA1c is used as a diagnostic tool in assessing diabetes (*Wautier and Schmidt, 2004*). However, it is essential to note that HbA1c is not a perfect diagnostic tool, as it can be artificially high/low in relation to plasma glycation. The levels of HbA1c and fructosamine (glycation in plasma proteins, mainly albumin) are highly correlated (*Cohen et al., 2003*). Discrepancies between the levels of glycated haemoglobin and fructosamine can lead to what is known as glycation gap (*Rodriguez-Segade et al., 2012*). Patients who exhibit extremes of the glycation gap, whether positive or negative, tend to have a higher mortality rate (*Dunmore et al., 2018*).

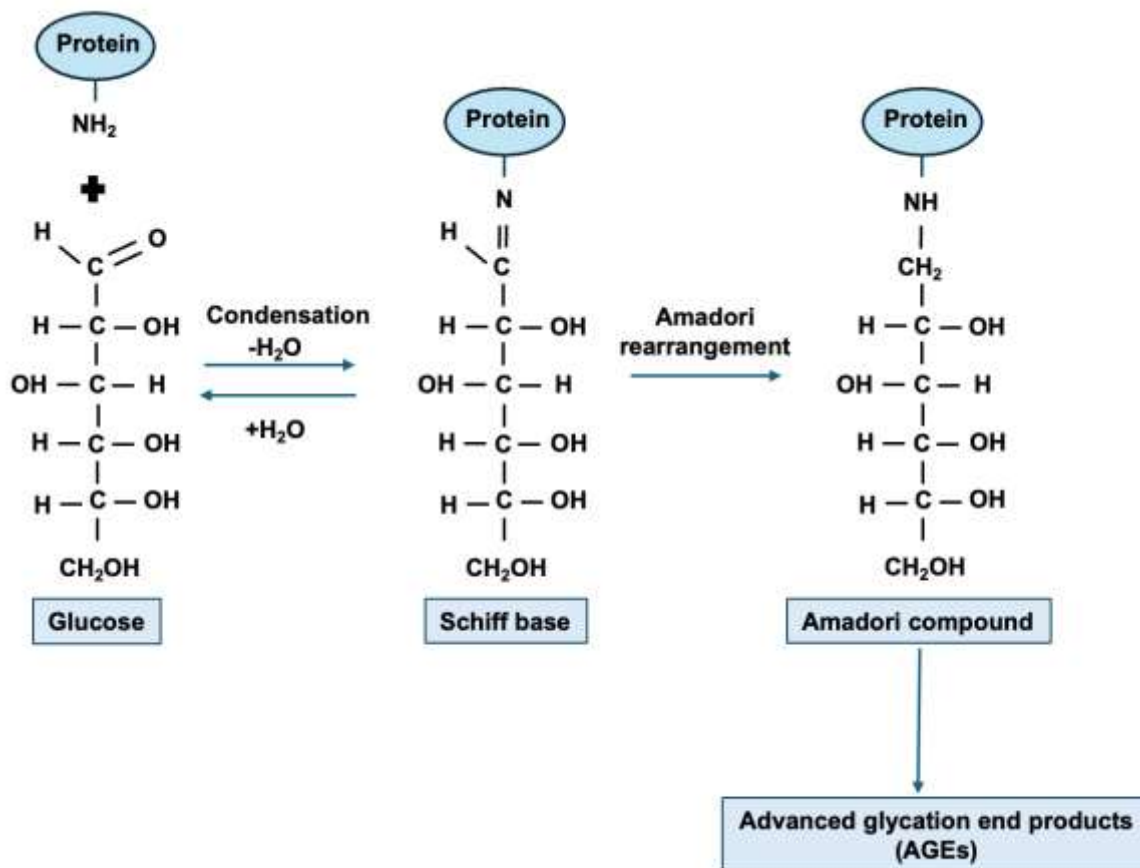


Figure 1. 2. Non-enzymatic reaction leading to advanced glycation end products (AGEs) formation. This process begins with the carbonyl group of reducing sugar, like glucose, reacting with an amino group found in proteins or amino-containing lipids such as lysine or arginine. The reaction forms a reversible Schiff base. Over time, the Schiff base undergoes intermolecular rearrangement, leading to the formation of a more stable compound known as Amadori product. The Amadori product can undergo further irreversible chemical reactions, including oxidation and fragmentation. These reactions give rise to a complex mixture of compound collectively known as advanced glycation end-products (AGEs). AGEs are characterised by the formation of new crosslinks between proteins or other molecules, contributing to various pathological processes associated with ageing and diabetes mellitus (Neelofar and Ahmad, 2015). Diagram adapted from: (Stirban et al., 2014).

Some AGEs and advanced lipoxidation end products (ALEs) share the same structure since they arise from common precursors. ALEs are formed through the oxidation of lipids. For instance, carboxymethyl lysine (CML) is generated by glyoxal, which is formed through both lipid and sugar oxidative degradation pathways (Vistoli et al., 2013). CML has shown to be elevated in blood serum of type 1 and type 2 diabetics; and has a strong association with retinopathy and nephropathy complications as a result of diabetes (K et al., 2007, Monnier et al., 2005, Kilhovd et al., 1999). Both ALEs and AGEs can interact with the receptor for AGEs (RAGE) (Arivazhagan et al., 2022). AGEs on the surface of erythrocytes can bind to RAGE

receptors on monocytes, macrophages and endothelial cells (Goldin *et al.*, 2006). Activation of the AGE/RAGE signalling pathway initiates a complex cascade of intracellular events, involving the activation of NADPH oxidase and nuclear factor (NF)- $\kappa$ B (Younessi and Younessi, 2011). These pathways converge to induce cellular stress and dysfunction through various mechanisms (Ramasamy *et al.*, 2011). NADPH oxidase activation leads to an increased production of superoxide radicals, contributing to oxidative stress within the cells. Additionally, activation of NF- $\kappa$ B leads to upregulation of pro-inflammatory genes, including tumour necrosis factor-alpha (TNF- $\alpha$ ), which in turn stimulates the production of interleukin-6 (IL-6), thereby promoting an inflammatory state (Younessi and Younessi, 2011). Furthermore, intracellular proteins are also a target of modifications and AGE formation, leading to functional impairment (Nowotny *et al.*, 2015). In erythrocytes, glycation of haemoglobin induced by hyperglycaemia leads to a reduced oxygen carrying capacity; glycation of cytoskeletal proteins leads to reduced deformability, and eryptosis and glycation of channel proteins leads to electrolyte disturbances (Wang *et al.*, 2021). Eryptosis refers to the process of programmed cell death in erythrocytes. It is characterised by cell shrinkage, membrane blebbing, and exposure of phosphatidylserine (PS) on the cells' surface, which signals macrophages to remove the dying cells from circulation (Repsold and Joubert, 2018). Eryptosis is analogous to apoptosis in nucleated cells and serves to remove damaged or aged erythrocytes, thereby maintaining cellular homeostasis and preventing haemolysis (Repsold and Joubert, 2018). Furthermore, AGEs are formed in high amounts in diabetes and also during aging; and have been implicated in various diabetes- and age-related diseases (Gkogkolou and Bohm, 2012).

Moreover, oxidative stress in erythrocytes as a result of hyperglycaemia has been thought to take place via the polyol pathway (Figure 1.5). Excess glucose can enter the polyol pathway where glucose is converted to sorbitol by aldose reductase, using NADPH, and then oxidised to fructose by sorbitol dehydrogenase (Wang *et al.*, 2021). This can cause excessive consumption of NADPH due to increased aldose reductase activity, and thus a decrease in the levels of glutathione and suppression of the antioxidant system leading to oxidative stress in the cells (Ighodaro, 2018). The accumulation of sorbitol and fructose inside the cells can lead to glycation of proteins and lipids (Rolfsson *et al.*, 2017), as well as cellular hyperosmotic stress that also generates oxidative stress (Vincent *et al.*, 2004).

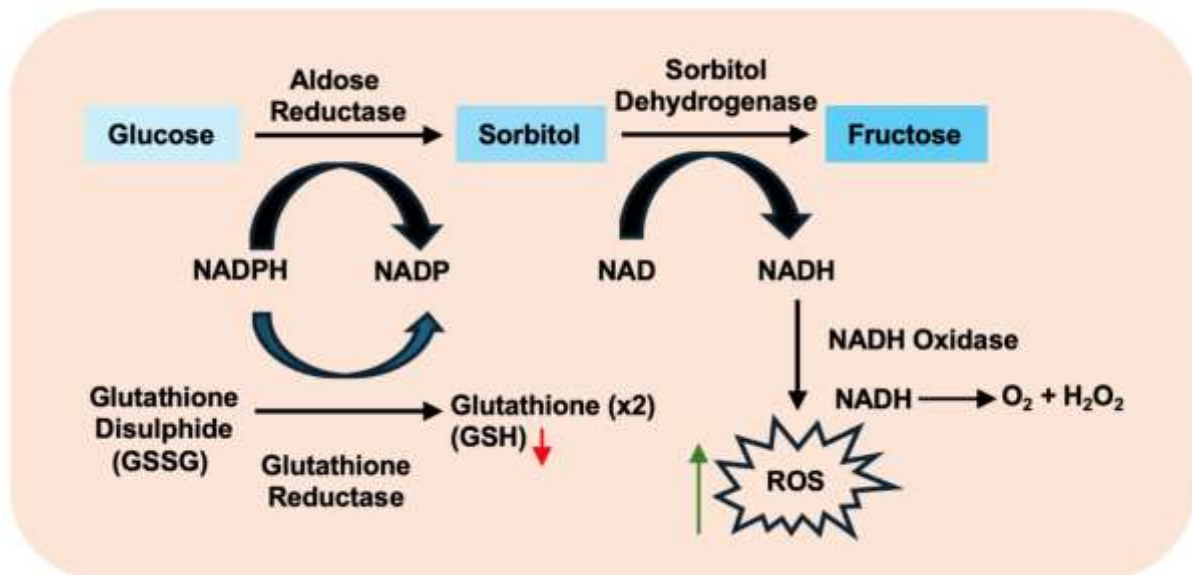


Figure 1. 3. Polyol pathway. Glucose is converted to sorbitol by aldose reductase, NADPH is used in the process. Glutathione reductase also competes for NADPH to convert glutathione disulphide to two molecules of glutathione. When glucose concentration is high, this can lead to a decrease in glutathione production and hence increased ROS. Sorbitol is then converted to fructose by sorbitol dehydrogenase, where NAD is used and converted to NADH. RBCs are known to have NADH oxidases and these convert NADH to oxygen and hydrogen peroxide leading to an increase in ROS (Mohanty et al., 2014). (Figure taken from (Tang et al., 2012), some modifications were carried out, and it is licenced under non-commercial 3.0 (CC BY-NC 3.0).

The dysregulation of glucose metabolism in diabetes (Figure 1.6) triggers a cascade of cellular damage pathways in erythrocytes, contributing to multiple pathways of cellular damage contributing to oxidative stress, glycation and the formation of AGEs. Hyperglycaemia can also induce dyslipidaemia, disrupting adipose tissue fat storage and resulting in the release of free fatty acids (FFA) from adipocyte stores (Galicia-Garcia et al., 2020). The increased extracellular FFA consequently alter membrane lipid composition, impacting membrane fluidity (Wang et al., 2021).

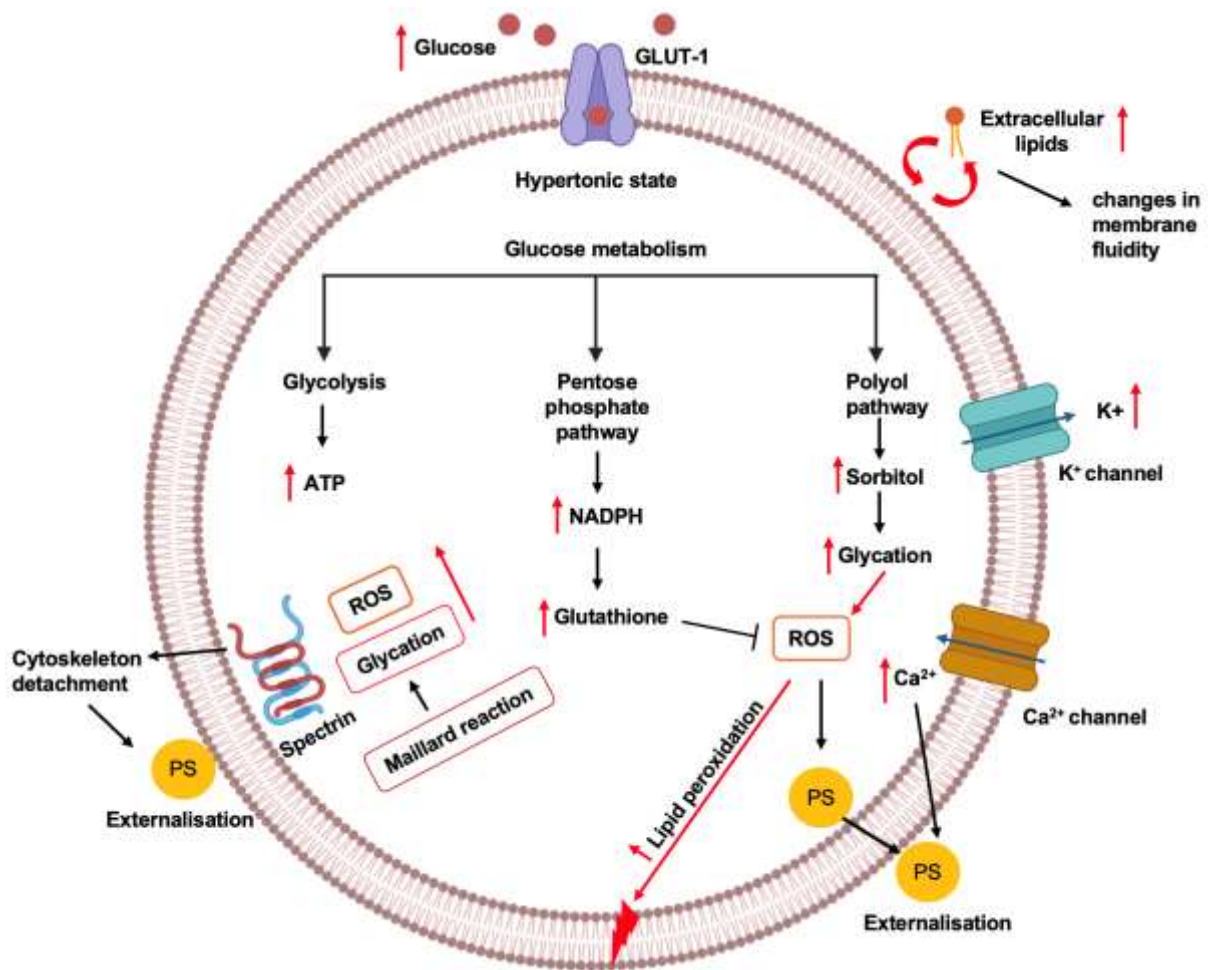


Figure 1. 4 Glucose metabolism disorder in erythrocytes under hyperglycaemic conditions. Glucose transporter 1 (GLUT1) mediates insulin independent glucose transport based on a concentration gradient in erythrocytes. As glucose levels increases in the blood, more glucose enters erythrocytes and accelerates glucose metabolism. Glycolysis is the main source of energy (ATP). The pentose phosphate pathway also gets activated and helps generate NADPH to reduce oxidative stress. Excess glucose, however, enters the polyol pathway and is converted to sorbitol, which leads to increased glycation, the formation of AGEs and the production of ROS. Glycation can also occur the Maillard reaction, and glycation of cytoskeletal proteins, such as spectrin can lead to cytoskeleton detachment, impacting membrane tension and causing phosphatidylserine externalisation. Increasing levels of ROS can lead to increased lipid peroxidation causing changes in membrane fluidity. Hyperglycaemia-induced dyslipidaemia prompts the release of free fatty acid (FFA) from adipocyte store. Increased extracellular FFA can modify membrane lipid composition, further influencing membrane fluidity. Adapted from: (*Wang et al., 2021*) using Biorender.

## 1.5 Membrane fluidity

The plasma membrane consists of a semipermeable lipid bilayer that separates the cytoplasm from the external environment; the maintenance of this fluidity is essential for cell function and viability (*Hollan, 1996*). The movement of the membrane components, phospholipids and proteins, within the membrane is referred to as membrane fluidity and it is a biophysical property of the membrane. The shear viscosity of the membrane, which measures its resistance to deformation under an applied force, is intrinsically linked to fluidity (*Espinosa et al., 2011*). A more fluid membrane exhibits lower shear viscosity, allowing for easier movement of membrane components (*Espinosa et al., 2011*). Conversely, a more rigid membrane, with higher shear viscosity, resists such movements. The balance between these properties is fundamental to the functioning of membranes in different environmental and physiological conditions.

Membrane fluidity can be affected by several factors, which include the class of phospholipids, the degree of saturation of fatty acids, length of the acyl chains, type and number of sterols (or similar molecules e.g., free cholesterol decreases membrane fluidity) (*de Oliveira and Saldanha, 2010*) and temperature (Figure 1.7). It is important to note that membrane fluidity at a given temperature will depend on the lipid class, acyl chain composition and the sterol content (*de Kroon et al., 2013*). Lower cholesterol content and higher unsaturation of phospholipid fatty acyl chains are associated with more fluid membranes (*Fajardo et al., 2011*).

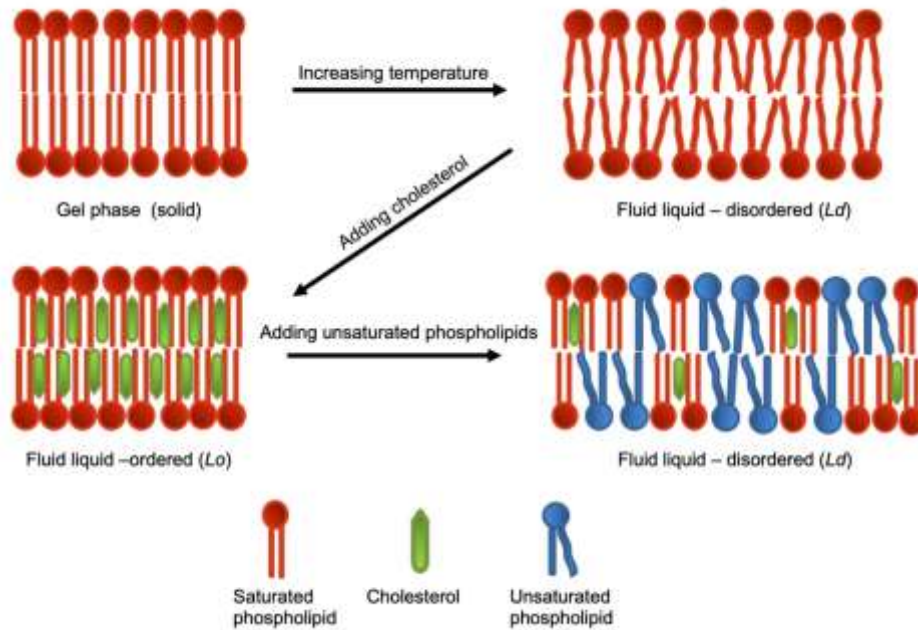


Figure 1. 7. Diagram showing different phases of the lipid bilayer depending on the phospholipid composition and temperature. By increasing the temperature, the bilayer goes from a solid, gel phase to a more liquid phase (when the lipids go through their transition temperature). By incorporating cholesterol, the effect of temperature is stabilised. Cholesterol positions between the phospholipid tails create a denser packing and decreasing membrane fluidity. The addition of polyunsaturated phospholipids, especially those containing *cis* double bonds, creates ‘kinks’ and impairs the packing, leading to increased fluidity. Diagram underwent minor modifications and was adapted from: (Zalba and Ten Hagen, 2017) under CC BY-NC-ND 4.0 (<https://creativecommons.org/licenses/by-nc-nd/4.0/>).

Cholesterol accounts for 30% of total lipidic membrane content of eukaryotic membranes (Mouritsen and Zuckermann, 2004), including erythrocytes (de Oliveira and Saldanha, 2010). It is found evenly distributed between phospholipids of the inner and outer bilayer leaflets (Goodman and Shiffer, 1983) and plays an important role in membrane fluidity. However, it has been shown that free cholesterol from plasma can exchange with that in RBCs (Quarfordt and Hilderman, 1970), and that diet can affect cholesterol content in RBC membranes (Lankinen et al., 2018) (Song and Jensen, 2021). On the other hand, it has also been shown that fish oil supplements lead to an increase in polyunsaturated fatty acids in the RBC plasma membrane (Kamada et al., 1986, Lund et al., 1999). More recently it has been suggested that RBCs have an active role in reverse cholesterol transport (Lai et al., 2019).

The position of cholesterol in the membrane plays a role in membrane fluidity i.e., cholesterol near the surface restricts the passage of molecules by increasing the packing of phospholipids (decreasing membrane fluidity) (Subczynski et al., 2017). The small hydroxyl group is the only

polar group in the molecule and the remainder is highly apolar (Yang *et al.*, 2016). Cholesterol intercalates into the membrane with a polar hydroxyl group positioned between the phospholipid polar headgroups, and its rigid ring structure reaches approximately the depth of the C9-C10 carbon atoms of the phospholipid acyl chains (Subczynski *et al.*, 2017). Furthermore, it has been shown that in polyunsaturated bilayers cholesterol positions with the hydroxyl group located in the centre of the membrane (Marquardt *et al.*, 2016, Ermilova and Lyubartsev, 2018). At high temperatures, cholesterol stabilises the membrane and raises its melting point by positioning between the phospholipid tails and restricting their movement. At low temperatures it prevents the hydrocarbon chains of phospholipid from clustering together and thus increases fluidity.

Cholesterol normally oxidises at a lower rate than polyunsaturated fatty acids (Van der Paal *et al.*, 2016). One of the major products of cholesterol peroxidation in the diabetic RBC membrane is 7-keto-cholestadiene, which correlates with HbA1c levels (Inouye, 1999). When a cholesterol fatty acid is oxidised, it behaves similarly to unoxidized cholesterol in terms of membrane fluidity (Kulig *et al.*, 2015). On the other hand, ring-oxidised cholesterols, which is the case of 7-keto-cholestadiene, can acquire tilted orientations in the membrane leading to a stronger disruption of the membrane structure than unoxidized and tail-oxidised cholesterols (Kulig *et al.*, 2015). This can result in increased mobility of fatty acid chains (decreased order) and increased membrane fluidity (Kulig *et al.*, 2015).

Membrane fluidity is also determined by the acyl chain composition of the lipids. The transition temperature of the lipids increases as the acyl chain length increases (leading to decreased fluidity); and decreases with the presence of cis-double bonds in the acyl chains (leading to increased fluidity) (Renne and de Kroon, 2018). Furthermore, phospholipid species can exert an effect on membrane fluidity, independent of cholesterol content and unsaturation of their fatty acyl chains. The size of the phosphate head group and the hydration status of the head group through their interaction with water have been shown to alter membrane fluidity. This combination results in phospholipid species that can either increase (phosphatidylcholine) or decrease (phosphatidylethanolamine) fluidity (Fajardo *et al.*, 2011). Phosphatidylethanolamine has a smaller head group than phosphatidylcholine and can form hydrogen bonds between the positively charged amino head group and the negatively charged phosphate residue of adjacent lipids (Boggs, 1987). These properties cause tighter packing of phosphatidylethanolamine and its acyl chains, which results in a higher transition temperature

of phosphatidylethanolamine molecular species compared to the phosphatidylcholine species (Renne and de Kroon, 2018).

Sphingomyelin is a significant component of the RBC membrane (Slotte, 2013) and is commonly found in the outer leaflet (Op den Kamp, 1979). Sphingomyelins usually contain long saturated acyl chains and, due to the preferential interaction between sphingolipids and sterols, form liquid ordered domains (Mouritsen, 2010). Membrane rafts (also called lipid rafts) are ordered membrane domains enriched in cholesterol and sphingolipids, which possess lower fluidity (Korade and Kenworthy, 2008, Ripa et al., 2021). They are involved in membrane fluidity, trafficking of membrane proteins and regulation of different cellular processes (Korade and Kenworthy, 2008).

Some studies have reported that the plasma membrane of RBCs from diabetics present higher levels of lipids that promote a decrease in membrane fluidity such as: excess cholesterol excess sphingomyelin and excess saturated fatty acids (Bryszewska et al., 1986, Watala and Jozwiak, 1990, Clifton and Nestel, 1998). It has also been indicated or hypothesised that a high lipophilic index in RBCs resulting in lower membrane fluidity may be associated with higher risks of T2DM (Kroger et al., 2015). On the other hand, increased in membrane fluidity has also been reported in cases of diabetes mellitus (Mazzanti et al., 1992). Incubation of erythrocytes in different glucose concentrations have also led to variable results from no significant changes and a decrease in membrane fluidity (Zavodnik et al., 1997, Bryszewska and Szosland, 1988). The inconsistency in these findings highlights a significant knowledge gap. These alterations in lipid composition not only impact membrane fluidity but also have implications for membrane tension, the mechanical property determines the resistance of the membrane to stretching.

## 1.6 Membrane Tension

Membrane tension is defined by two main components; the in-plane tension in the lipid bilayer, primarily caused by changes in osmotic conditions, which lead to cell swelling and subsequent membrane stretching, and membrane-cytoskeleton adhesion, mediated by phospholipid binding proteins (Figure 1.8) (Gauthier et al., 2012). It represents the force resulting from lateral stretching or compression of the membrane (Kozlov and Chernomordik, 2015). This is distinct from other forms of membrane deformation, such as changes in membrane thickness, bending, or shear deformation (Lamparter and Galic, 2020). The lipidic component of

membranes is considered the major determinant of the lateral pressure across the bilayer (Grage *et al.*, 2022). The lipid bilayer can experience various pulling forces that cause changes in membrane tension (Figure 1.8A). For instance, plasma membrane tension caused by pulling forces from cytoskeletal attachments can generate contractile forces that pull on the membrane, thereby increasing membrane tension (Diz-Munoz *et al.*, 2013). Lipid rafts can alter the distribution of forces across the membrane contributing to an overall increase in membrane tension (Kuzmin *et al.*, 2005).

Increased lateral membrane tension causes conformational changes in integral membrane proteins, and affects membrane permeability, lipid lateral diffusion and organisation of lipid rafts (Muddana *et al.*, 2011). Studies have shown that lipid lateral diffusion increases with rising membrane tension (Reddy *et al.*, 2012, Muddana *et al.*, 2011). Additionally, higher membrane tension can reduce the thickness of the lipid bilayer, which may result in lipid phase separation or a mismatch between the hydrophobic regions of lipid acyl chains and the transmembrane domains of proteins leading to distortion of the lipid bilayer and concomitant protein conformational changes (Muddana *et al.*, 2011). Such distortions can alter membrane protein functionality, affecting processes such as signal transduction, transport and enzymatic activity as well as influencing interaction of membrane proteins with the cytoskeleton.

The erythrocyte cytoskeleton, composed of various proteins such as actin filaments and spectrin, forms a filament-like structure beneath the lipid bilayer (Li and Lykotrafitis, 2014). This cytoskeletal network plays a pivotal role in maintaining the cell shape, flexibility, and overall integrity (Lux, 2016). The actin filaments in erythrocytes are smaller than in other mammalian cells, although they provide the necessary structural support, flexibility and mechanical stability required in maintaining the integrity of the cell under mechanical stress (Nowak *et al.*, 2022). This intricate meshwork of proteins, strengthens the lipid bilayer and organises membrane lipids, facilitating the resilience of erythrocytes in the circulation (Lux, 2016). The erythrocyte cytoskeleton protects the cell against mechanical disruption, provide

structural support and acts as a crucial determinant of membrane tension, ensuring the ability of the cells to withstand mechanical stressors (Lux, 2016).

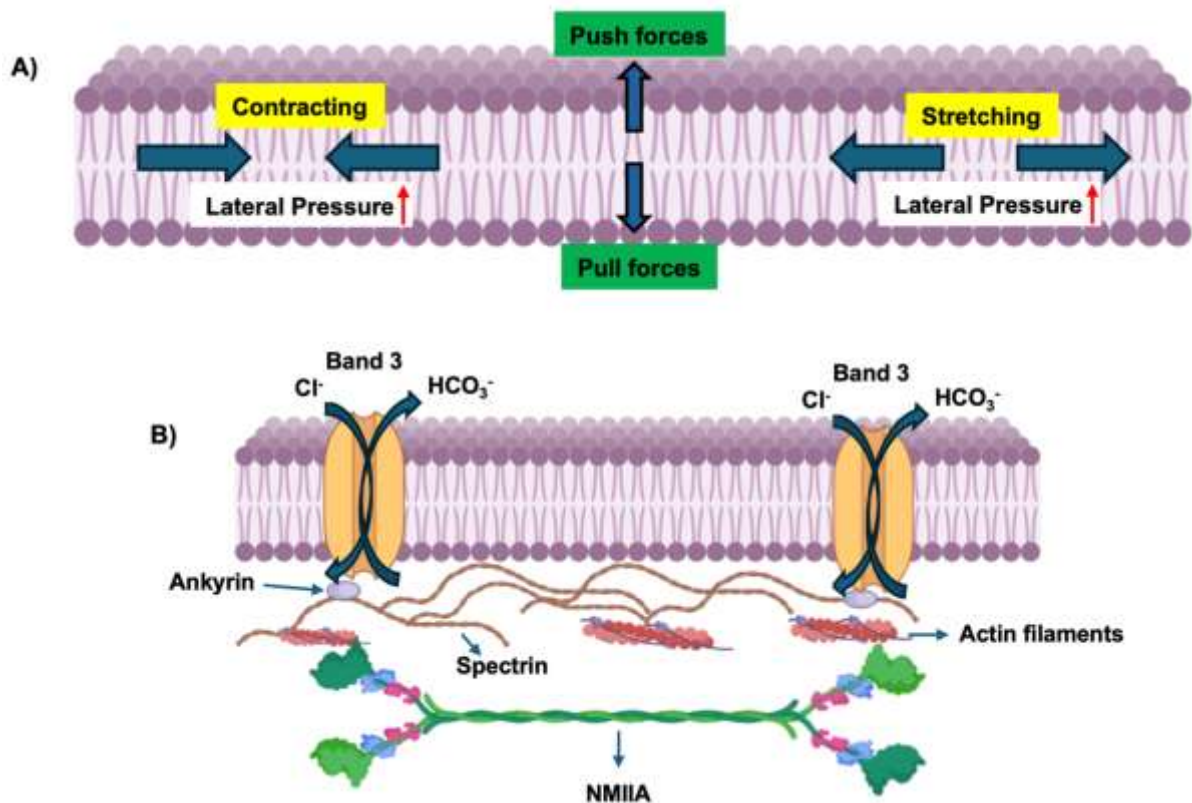


Figure 1. 8. Mechanical forces affecting membrane tension. A) Push and pull forces, which may lead to the membrane contracting or stretching and therefore affecting lateral pressure. B) Spectrin cross-links short actin filaments, attaching to the plasma membrane via associations with transmembrane proteins such as Band 3, which is the most abundant transmembrane protein found in erythrocytes. Band 3 functions to transport chloride into the cells and bicarbonate out of the cells. Non-muscle myosin IIA (NMIIA) contractile forces could promote membrane tension in the spectrin–actin filament network, maintaining normal biconcave shapes and controlling deformability. Section B was modified from (Smith *et al.*, 2018) using Biorender. Not drawn to scale.

Actin filaments in erythrocyte membranes interact with non-muscle myosin IIA (NMIIA) (Figure 1.8B), which plays a key role in maintaining the biconcave shape and deformability of red blood cells by regulating membrane tension (Smith *et al.*, 2018). The drug blebbistatin, which relaxes NMIIA, has been shown to reduce membrane tension and increase deformability, highlighting NMIIA's importance in controlling membrane dynamics and flickering (Smith *et al.*, 2018). Membrane flickering, refers to the rapid fluctuations of the plasma membrane due to thermal energy (Tomaiuolo, 2014). These fluctuations are a manifestation of the membrane mechanical properties, such as bending rigidity, shear elasticity and tension. Healthy cells

typically exhibit flickering, as it reflects a balance of these mechanical properties. In contrast, reduced flickering, such as in very stiff cells, can indicate an abnormal or compromised membrane state (Yoon *et al.*, 2009).

Membrane tension can also arise from the tendency of the cell to preserve its area (Diz-Munoz *et al.*, 2013, Sens and Plastino, 2015). This restorative tension is due to the inherent elasticity of the lipid bilayer and the associated proteins that prefer a specific membrane curvature and organization (Brown, 2012). When the membrane is stretched or compressed laterally, whether by external forces, interactions with the cytoskeleton, or changes in lipid composition, it tends to generate tension as it attempts to return to its equilibrium state. Membrane tension is not uniform and can vary significantly across different regions of the cell membrane, although there have been reports of membrane tension being able to propagate rapidly in cells and have a widespread effect (Cohen and Shi, 2020, Shi *et al.*, 2018). This heterogeneity is crucial for various cellular processes, allowing cells to adapt their shape and mechanical properties to their functional needs.

While there may not be many studies specifically focusing on membrane tension in diabetic conditions, there are several studies that have investigated alteration in erythrocyte membrane properties, which indirectly relate to membrane tension. Diabetes can affect erythrocyte membrane composition, including changes in lipids, protein structure and cytoskeletal organisation, which may influence membrane tension (S. AlSalhi *et al.*, 2018, Wang *et al.*, 2021, Gabreanu and Angelescu, 2016). Membrane tension is integral to understanding the deformability of erythrocytes, which is attributed to four primary factors. These factors include the surface area to volume ratio of the biconcave disc, the viscosity of the intracellular fluid (i.e., the cytoplasm) dominated by the presence of haemoglobin, the viscoelastic properties of the plasma membrane and the membrane skeleton (Tomaiuolo, 2014).

Increasing shear stress can increase membrane tension through a combination of direct mechanical forces, cytoskeletal interactions, activation of mechanosensitive channels and changes in membrane fluidity (Reddy *et al.*, 2012). The relationship between membrane tension and fluidity is complex. Experimental studies have suggested that membrane fluidity increases with increasing membrane tension as shown in endothelial and HeLa cells (Butler *et al.*, 2001, Haidekker *et al.*, 2000, Li *et al.*, 2018). A study on model bilayer membranes demonstrated that increasing osmotic pressure, which enhances membrane curvature, leads to increased membrane tension and fluidity (Nomoto *et al.*, 2018). Conversely, increasing the

cholesterol concentration in the membrane raised membrane tension while reducing fluidity (Nomoto *et al.*, 2018). This is likely due to the strengthened interactions between cholesterol and phospholipids, which limit the mobility of the molecules within the membrane. Thus, the impact of membrane tension on fluidity is not straightforward and varies with the molecular context of the membrane.

Studies have shown that increasing membrane tension can decrease both membrane thickness and hydration depth and increases membrane polarity (Reddy *et al.*, 2012, Zhang *et al.*, 2006). Increasing membrane tension is expected to change lipid packing by stretching the lipids away causing changes to membrane fluidity (Colom *et al.*, 2018). Polarity of the bilayer can increase due to the penetration of water into the hydrophobic interior. Hydration of the hydrophilic head groups plays an important role in the structure and function of the lipid bilayer (Reddy *et al.*, 2012). Membrane proteins, which are sensitive to changes in the lipid environment, may undergo structural changes in response to alterations in bilayer thickness or hydration depth. These changes in membrane polarity induced by membrane tension could potentially act as triggers for altering the structure of membrane proteins, thereby influencing their function (Reddy *et al.*, 2012).

Oxidative stress exerts its influence on cell membrane tension through various mechanisms. Firstly, it can modify lipid molecules by increasing lipid peroxidation, thereby altering the physical properties of the membrane, such as lipid packing and fluidity (Colom *et al.*, 2018, Pizzino *et al.*, 2017). Oxidised phospholipids often have altered shapes and packing properties, which subsequently can impact membrane tension (Schumann-Gillett and O'Mara, 2019). Moreover, increased oxidative stress can trigger calcium influx from the extracellular environment, which is known to activate protein kinase C (PKC) in erythrocytes (Betz *et al.*, 2009, Ermak and Davies, 2002). This activation can result in PS exposure (de Jong *et al.*, 2002). Overactivation of PKC has been shown to decrease membrane tension by 50% (Betz *et al.*, 2009). It is thought that activation of PKC weakens the spectrin-membrane interaction, as PKC phosphorylates the 4.1R protein, thereby dissolving the binding complex (Betz *et al.*, 2009). Furthermore, age related modifications can also exacerbate membrane susceptibility to oxidative damage and impair membrane integrity.

## 1.7 Ageing

Ageing is a complex, multifarious process characterised by the irreversibly progressive decline of physiological function, which eventually leads to age-related disorders such as T2DM, hypertension, Alzheimer's disease and cancer (*Das, 2021, Li et al., 2021*). In the late 1980's, Monnier and Cerami proposed the Maillard theory of ageing, hypothesising that a continuous accumulation of AGEs was a factor in ageing (*Monnier et al., 1988, Monnier, 1989*). In the first decade of glycation research, the focus was on extracellular glycation of collagen, which is correlated with ageing and shown to be important in the pathogenesis of diabetic complications (*Chaudhuri et al., 2018*). Accumulation of AGEs is an inevitable component of the ageing process in all eukaryotic organisms, including humans (*Chaudhuri et al., 2018*)

Erythrocytes experience a range of continuous metabolic and physical changes as they age, such as membrane vesiculation, haemoglobin modifications and progressive failure, cellular homeostasis and antioxidant defences. A major feature of the oxidatively distorted erythrocytes is the binding of oxidised haemoglobin to high affinity sites on Band 3, as well as haemoglobin crosslinking with spectrin, which is tightly correlated with increased membrane rigidity and decreased deformability (*Antonelou et al., 2010*). Glycated haemoglobin is used as a RBC age marker (*Bosch et al., 1992*). Distortion in calcium homeostasis is another age-related pathway, where increasing intracellular calcium levels leads to PS exposure in the outer membrane and also vesiculation (Hoerl and Scott, 1978).

The cell membrane is crucial for cellular functions, and its lipid content is essential for maintaining appropriate cell function. It has been proposed that there could be a correlation between cell membrane integrity and changes in its composition and ageing. The proposal suggests that lipid composition of the membrane plays an important role in the ageing process (*Das, 2021*).

Ageing is associated with alterations in membrane lipid composition and membrane physical properties (*Noble et al., 1999*). These changes in lipid composition can lead to changes in membrane fluidity and tension (*Horn and Jaiswal, 2019, Nomoto et al., 2018*). A study carried out in centenarians reported that extreme longevity appeared to be associated with a substantial integrity of erythrocytes. This study showed an evident increase in polyunsaturated fatty acids, which is likely to improve membrane fluidity in erythrocytes (*Caprari et al., 1999*). On the other hand, membrane fluidity has been shown to decrease in erythrocytes from elderly

subjects and significant differences have been reported between old healthy controls compared with T2DM with a decrease in membrane fluidity observed in diabetic individuals (Goi *et al.*, 2005, Emam, 2008). A more recent study, carried out in blood plasma, reported a decrease in omega 3 fatty acids (in particular levels of docosahexaenoic acid (C22:6) and eicosapentaenoic acid (C20:5)) and PEs with ageing (Hornburg *et al.*, 2023). Unsaturated fatty acids play a crucial role in maintaining membrane fluidity and their presence in the lipid bilayer helps to prevent the membrane from becoming too rigid, thereby ensuring proper cellular function and resilience against mechanical stress.

Ageing is also associated with a loss of cytoskeletal stability (Kim *et al.*, 2022). The cytoskeleton plays a crucial role in providing structural support and stabilisation of the membrane. AGEs, which are known to accumulate with age, can form crosslinks between proteins, including cytoskeletal proteins such as spectrin and cytoplasmic proteins such as haemoglobin, further affecting cellular function. These crosslinks compromise the integrity of the cytoskeleton and membrane, leading to decreased cellular stability and increased vulnerability to stress (Huang *et al.*, 2011, Antonelou *et al.*, 2010). These changes in the membrane can impair the morphological and physiological functions of erythrocytes.

### **1.8 Erythrocytes in diabetes and ageing**

The natural ageing process is further accelerated in individuals with diabetes, leading to alterations in the shape and composition of erythrocytes (Morley, 2008). Under hyperglycaemic conditions characteristic of diabetes, the typical biconcave shape of erythrocytes can change accompanied by reports of altered membrane phospholipid asymmetry such as a decrease in the cholesterol/phospholipid ratio (Rudrappa, 2011). These changes have functional implications, particularly in the exposure of PS. Interestingly, aged erythrocytes from diabetic patients exhibit higher levels of exposed PS compared to those from non-diabetics, potentially enhancing the internalisation of erythrocytes by endothelial cells and macrophages and contributing to vascular complications associated with diabetes (Yang *et al.*, 2024, Zhou *et al.*, 2018, Catan *et al.*, 2019). Also, aged cells have shown increased PS in the outer membrane as well as increased ROS production (Catan *et al.*, 2019). Analysis of stored erythrocytes has revealed a 40% decrease in glutathione levels, indicating a diminished defence mechanism against oxidative stress in aging cells (Pertinhez *et al.*, 2014).

Diabetes and aging share several common pathways affecting erythrocytes, including oxidative stress, altered membrane lipid composition and fluidity, membrane glycation, and the formation of AGEs, although AGEs are more pronounced in diabetes. Both conditions are associated with increased PS exposure, reduced erythrocyte deformability, and a shorter erythrocyte lifespan (*Catan et al., 2019, Racine and Dinunno, 2019*). A unique aspect of diabetes is chronic hyperglycaemia, which can lead to complications such as microangiopathy, further impairing erythrocyte function. HbA1c, a diagnostic marker of diabetes, also increases as erythrocytes age, and the cells become denser (*Cohen et al., 2008, Franco et al., 2013*).

Mass spectrometry studies carried out by Koehrer and colleagues have investigated changes in lipids in erythrocytes due to hyperglycaemia, revealing that long chain polyunsaturated fatty acids, such as arachidonic acid and docosahexaenoic acid, may play an important role in diabetes (*Koehrer et al., 2014*). The study found a decrease in levels of these fatty acids in the erythrocytes of diabetic patients, along with alterations in omega-3 and omega-6 polyunsaturated fatty acids and increased levels of saturated and monounsaturated fatty acids. Specifically, there was a reduction in phosphatidylethanolamine esterified with arachidonic acid and an increase in phosphatidylethanolamine esterified with saturated fatty acids (*Koehrer et al., 2014*). Similar results were observed when the effect of ageing was investigated in the blood plasma, showing decreased levels of omega 3 fatty acids and PEs (*Hornburg et al., 2023*). Furthermore, lipidomic studies in women with gestational diabetes and animal models of diabetes have shown significant lipid profile differences compared to controls (*Bukowiecka-Matusiak et al., 2018, Burzynska-Pedziwiatr et al., 2022, Lydic et al., 2009, Zhong et al., 2023*).

Apoptotic cells, senescent and long-stored RBCs display higher levels of ceramides, which may be produced from cell membrane sphingomyelins by sphingomyelinase (*Bicalho et al., 2013, Dinkla et al., 2012*). It has also been reported that blood plasma from diabetic subjects have higher levels of ceramides (*Wilkerson et al., 2019*). Furthermore, a mass spectrometry analysis by Zhang and colleagues revealed a higher abundance of glycated peptides in erythrocytes compared to blood plasma in diabetic patients (*Zhang et al., 2011*). Glycation is also elevated in aged cells compared to younger cells (*Mangalmurti et al., 2010*).

These findings collectively highlight the impact of hyperglycaemia and ageing on erythrocyte lipid profiles, emphasising the importance of understanding changes in erythrocytes during ageing and hyperglycaemia.

### **1.10 Knowledge Gap**

Studies on membrane fluidity in diabetes have produced inconsistent results, with some reporting increased or decreased fluidity, and some showing no changes at all. This inconsistency highlights a significant knowledge gap in our understanding of erythrocyte membrane dynamics under diabetic conditions. There has been limited research on erythrocyte membrane tension in diabetes, suggesting a need for further exploration in this area. Additionally, the mechanisms responsible for hyperglycaemia-induced membrane lipid peroxidation in diabetic erythrocytes required further clarification. Advanced techniques, such as mass spectrometry, could play a crucial role in this research by providing detailed insights into the lipid composition of erythrocyte membranes under diabetic conditions. Lipidomic analysis could reveal important information about changes in phospholipid classes, chain length, and saturation levels, potentially clinically significant. More comprehensive studies using mass spectrometry and lipidomic approaches are essential to address these gaps in our knowledge.

### **1.11 Overall aim of the project**

The aim of this project was to understand the molecular processes in diabetes and ageing that lead to erythrocyte dysfunction and how these may contribute to disease pathology. Specifically, the correlation between membrane fluidity, membrane tension, ROS production, and lipid composition in erythrocytes was the focus of the investigation. To achieve this, the following approach was planned over the course of a three-year PhD programme. Native human erythrocytes from healthy volunteers were treated *in vitro* with high levels of glucose, with and without the presence of oxidative stress, to simulate the hyperglycaemic conditions characteristic of diabetes. The effect of these treatments on membrane fluidity and tension as the RBCs aged was investigated using fluorescent probes laurdan and Flipper-TR, respectively, with laurdan assessing changes in membrane fluidity and Flipper-TR measuring membrane tension. Intracellular production of ROS was monitored using carboxy-H<sub>2</sub>DCFDA and flow cytometry to quantify oxidative stress within the erythrocytes under different treatment conditions. Additionally, lipidomic analysis was conducted on lipids extracted from the treated

erythrocytes using mass spectrometry, with the aim of identifying specific changes in lipid composition, including alterations in phospholipid classes, chain length, and saturation levels.

Erythrocytes were incubated for five days to investigate the effects of high glucose and oxidative stress on membrane properties. While this approach aimed to mimic some of the changes associated with ageing, it is important to note that the physiological half-life of erythrocytes is approximately 90 days. Therefore, describing the five-day incubation as 'ageing' is an oversimplification, and the findings should be interpreted with this limitation in mind.

By integrating these methodologies, the project sought to elucidate the complex interactions between membrane properties, oxidative stress, and lipid composition in erythrocytes, contributing to a better understanding of the pathophysiology of diabetes and ageing.

# Chapter 2

## Materials and Methods

## 2.1 Ethics approval and participants

This study received approval from the Aston University Research Ethics Committee (UREC) with REC reference number #954. The research protocol strictly adhered to ethical guidelines to ensure the rights and welfare of all participants involved. The participants consisted of postgraduate students and staff members from Aston University who were in good health. Prior to their involvement, all participants received comprehensive information regarding the study objectives, procedures, potential risks, and benefits. Informed consent was obtained from each participant. Furthermore, all data collected were analysed anonymously to protect participant confidentiality.

## 2.2 Materials

### 2.2.1 Chemicals and Reagents

Acetonitrile Optima LC/MS grade (cat. # A955-212), ammonium formate (cat. # 15635830), methanol Optima LC/MS grade (cat. # A456-212) and 2-propanol Optima LC/MS grade (cat. # A461-212) were purchased from Fisher Scientific (Waltham, Massachusetts, USA).

Carboxy-H<sub>2</sub>DCFDA (cat. # C400), methyl- $\beta$ -cyclodextrin (cat. # J66847.06), laurdan (6-Dodecanoyl-2-Dimethylaminona naphthalene) (cat. # D250), penicillin-streptomycin (cat. #15140122), RPMI media with no glucose (cat. # 11879020) and SILAC RPMI 1640 Flex Media (no glucose, no phenol red) (cat. # A2494201) were purchased from Thermo Fisher Scientific (Waltham, Massachusetts, USA).

Ammonium acetate (cat. # 73594), D (+)-glucose (cat. # G702), D-mannitol (cat. # M1902), dimethyl sulfoxide (DMSO) (cat. # D8418-100ml), Dulbecco's phosphate buffered saline (PBS) (cat # D8662), EDTA (Ethylenediaminetetraacetic acid) (cat. # E9884), foetal bovine serum (FBS) (cat. # TMS-013- B), formic acid (cat. # 399388), glyoxal (cat. # 50649), hydrogen peroxide solution (cat. # H1009), methylglyoxal (cat. # 67028) and sodium phosphate (Na<sub>3</sub>PO<sub>4</sub>) (cat. # 342483) were purchased from Merck (Kenilworth, New Jersey, USA).

Flipper TR (cat. # SC020) was purchased from Spirochrome (Stein Am Rhein, Thurgau, Switzerland). CytoFLEX Sheath Fluid (cat. # B51503) and FlowClean cleaning agent (cat. # A64669), were purchased from Beckman Coulter (Brea, California, USA). MTBE (tert-Butyl methyl ether) (cat. # 650560) was purchased from Honeywell/Riedel-de-Haën (Muskegon,

Michigan, USA). ESI positive and negative calibration solution X500 (Sciex, Connecticut, Massachusetts, USA).

## 2.2.2 Laboratory Consumables

EDTA anticoagulant tubes (cat # 455036) and 1.5 ml graduated flip top tubes (cat # 616201) were purchased from Greiner Bio One (Kremsmünster, AUSTRIA). The 96-well plates (black and flat bottom cat. # 611F96BK) were purchased from Thermo Fisher Scientific (Waltham, Massachusetts, USA). The slides (Thistle Scientific - Ividi) (cat. # IB-80426) were purchased from Thistle Scientific (Uddingston, Scotland). Acquity UPLC CSH C18 column (2.1x100mm; 1.7 $\mu$ m) and Acquity UPLC CSH C18 VanGuard pre-column (2.1x5mm; 1.7 $\mu$ m) were purchased from Waters (Milford, Massachusetts, USA).

## 2.3 Methods

### 2.3.1 Erythrocyte preparation

Human venous blood from twelve healthy young volunteers (self-reported as healthy), who gave informed consent to participate in the study, was obtained in 9 mL EDTA anticoagulant tubes. To ensure anonymity, no biometric or identifiable data were collected, and no formal clinical evaluation was conducted. Blood was centrifuged at 500g for 10 minutes at room temperature and the plasma and buffy coat were removed by aspiration. Subsequently, erythrocytes were washed twice in 20 mL sterile phosphate-buffered saline (PBS) solution (Table 2.1). The supernatant was discarded, the erythrocytes were resuspended in glucose free RPMI media containing 10% foetal bovine serum (FBS), 100 U/mL penicillin and 100  $\mu$ g/mL streptomycin and a final concentration 5 mM glucose (sterilised by filtration in 0.22  $\mu$ m syringe filters) was added. Then the erythrocytes were counted using a Neubauer haemocytometer chamber, resuspended to obtain  $1 \times 10^8$  cells/mL using glucose free RPMI media. A 1 M glucose stock was prepared in sterile PBS, and then filtered using a 0.2  $\mu$ m syringe filter. Glucose stocks of 50 mM, 110 mM, 220 mM, 50 mM and 1000 mM were prepared using sterile PBS and were 10 times the final concentrations required. Glucose was freshly prepared every day. Depending on the study carried out, either glucose was added to obtain a final concentration of 5 mM to keep the cells under physiological levels of glucose, or the cells were kept in media containing pathological levels of glucose (11, 22, 50 and 100 mM) to simulate diabetic conditions *in vitro*. The cells were kept for five days, incubated at 37°C and 5% CO<sub>2</sub>, and the media was changed every day.

Table 2. 1. The components of Dulbecco's PBS purchased from Merck.

Phosphate saline buffer (PBS) ingredients	g/L
Calcium chloride dihydrate ( $\text{CaCl}_2 \cdot 2\text{H}_2\text{O}$ )	0.133
Magnesium chloride hexahydrate ( $\text{MgCl}_2 \cdot 6\text{H}_2\text{O}$ )	0.1
Potassium chloride (KCl)	0.2
Potassium dihydrogen phosphate ( $\text{KH}_2\text{PO}_4$ )	0.2
Sodium chloride (NaCl)	8
Sodium phosphate dibasic anhydrous ( $\text{Na}_2\text{HPO}_4$ (anhydrous))	1.15

## 2.2.2 Preparation of treatments

### 2.2.2.1 Mannitol treatment preparation

A 1 M mannitol (Merck, Kenilworth, New Jersey, USA) stock was prepared in sterile PBS, and then filtered using a 0.2  $\mu\text{m}$  syringe filter. Mannitol stocks of 10 times the final concentrations required (50, 11, 22, 50 and 100 mM) were prepared.

### 2.2.2.2 Glyoxal and methylglyoxal preparation

Solutions of 1 M glyoxal and methylglyoxal (Merck, Kenilworth, New Jersey, USA) were prepared using sterile PBS. The solutions were filtered using a 0.2  $\mu\text{m}$  syringe filter. Then stocks 100 times (X100) the final concentrations, 100  $\mu\text{M}$  and 500  $\mu\text{M}$  for glyoxal and methylglyoxal respectively, were prepared using sterile PBS.

## 2.2.3 Erythrocyte membrane fluidity studies using the fluorescent probe laurdan

### 2.2.3.1 Preparation of laurdan

A 28 mM laurdan stock was prepared in dimethyl sulfoxide (DMSO). After vortexing and sonicating the mixture at room temperature, aliquots of 50 mL were stored at  $-20^\circ\text{C}$ . A 1 mM stock was prepared using DMSO, from which stocks 100 times (X100) the final concentration of laurdan (100  $\mu\text{M}$ ) were also made in DMSO.

### 2.2.3.2 Preparation of Methyl- $\beta$ -cyclodextrin

A solution of 37.8 mM methyl- $\beta$ -cyclodextrin (MBCD) was prepared in sterile PBS. The mixture was vortexed and was then filtered using 0.2 mm syringe filter.

### 2.2.3.3 Short term glucose treatment

Erythrocytes, initially kept in media with 5 mM glucose, were counted, centrifuged at 500 G for 5 minutes, the medium discarded, and the cells resuspended to obtain  $1 \times 10^6$  cell/mL using glucose free RPMI medium. The cells,  $1 \times 10^6$ , were added to each well of 24-well plate and treated with final glucose concentrations of 5 mM, 11 mM, 22 mM, 50 mM and 100 mM, respectively (this was performed in triplicate). Glucose treatments were carried out for 1, 4 and 24 hours on days 0, 2 and 4. Explanation of short-term glucose treatment is shown in Figure 2.1. Mannitol was used as an osmotic control, at the same concentrations as the glucose. Once the treatments were completed, the media was removed and discarded; 250  $\mu$ L of SILAC medium (containing no glucose, FBS, penicillin or streptomycin) was added to cells followed by a final concentration of 1  $\mu$ M laurdan (using x100 stock). DMSO was used as a vehicle control for laurdan. MBCD was used as a positive control to increase erythrocyte membrane fluidity; a final concentration of 5 mM was added to the cells immediately after laurdan was added. The cells were incubated for one hour at 37°C and 5% CO<sub>2</sub>. A low concentration of laurdan was used, as laurdan can form micelles that can emit fluorescence and interfere with the signal emitted from cells (Kozyra, 2003). Once laurdan treatment was completed, the contents of the wells were mixed gently, and 100  $\mu$ L of cells were placed in a black non-binding 96-well plate and laurdan fluorescence was measured using a BMG FLUOstar omega microplate reader.

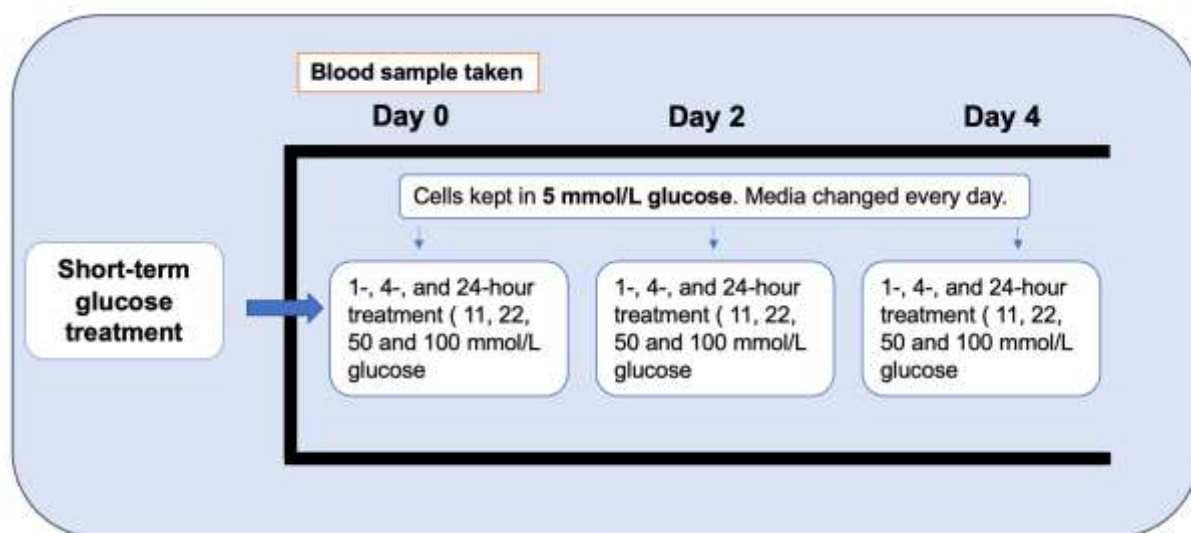


Figure 2. 4. Diagram illustrating short-term glucose treatment. Blood was collected on day 0, erythrocytes were isolated from whole blood and kept in RPMI media containing 5 mM glucose. The cells were treated with 11, 22, 50 and 100 mM glucose for 1, 4 and 24 hours on days 0, 2 and 4. The physiological control included treating the cells with 5 mM glucose.

#### 2.2.3.4 Long term glucose treatment

Erythrocytes were counted and resuspended to obtain  $1 \times 10^8$  cells/mL in glucose free RPMI medium. Then glucose at final concentrations of 5 mM, 11 mM, 22 mM, 50 mM and 100 mM were added to the cells. Explanation of long-term glucose treatment is shown in Figure 2.2. Some erythrocytes were treated with glucose (final concentrations of 5 mM, 11 mM, 22 mM, 50 mM or 100 mM) in combination with 1  $\mu$ M glyoxal or 5  $\mu$ M methylglyoxal. The erythrocytes were incubated at 37°C, 5% CO<sub>2</sub> for five days with fresh media every day. Glyoxal and methylglyoxal treatments were added every day after the media was changed. The medium contained 10% FBS, 100 U/mL penicillin and 100  $\mu$ g/mL streptomycin. To test for membrane fluidity changes, the cells were counted, centrifuged at 500 G for 5 minutes and resuspended in SILAC medium (containing no glucose, FBS, penicillin or streptomycin) to obtain a total cell number of  $1 \times 10^6$  cells in 250  $\mu$ L (or  $4 \times 10^6$  per mL). A 24-well plate was used and 250  $\mu$ L containing  $1 \times 10^6$  cells were added to the wells. A final concentration of 1  $\mu$ M laurdan (from x100) was added to the cells, followed by incubation for one hour at 37°C and 5% CO<sub>2</sub>. MBCD, at a concentration of 5 mM, was used as a membrane fluidising control and added to the cells immediately after laurdan. After laurdan treatment 100  $\mu$ L of cells were placed in a black non-binding 96-well plate and laurdan fluorescence was measured. Erythrocyte membrane fluidity, using laurdan, was tested on untreated (day 0) and treated cells (days 2 and 4). On day 0, membrane fluidity was checked before placing the cells in media containing different glucose concentrations.

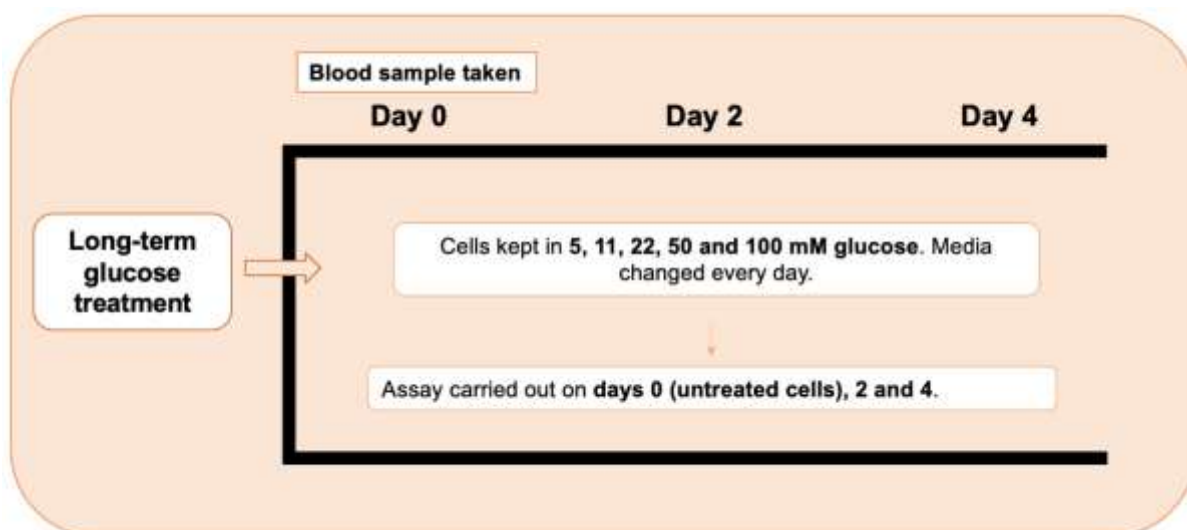


Figure 2. 5. Diagram explaining long-term glucose treatment. Blood was collected on day 0, Erythrocytes were isolated from whole blood and kept in RPMI media containing different glucose concentrations (5, 11, 22, 50 and 100 mM). Laurdan assay was carried out on days 0 (untreated cells), 2 and 4.

### 2.2.3.5 Laurdan fluorescence measurements and generalised polarisation (GP) calculations

Fluorescence was determined by using a fluorometer (BMG FLUOstar) with excitation at 355 nm and emission at 440 nm and 490 nm, and the temperature set at 37°C. The generalised polarisation (GP) was calculated by using the formula:

$$GP = (I_{440} - I_{490}) / (I_{440} + I_{490}) \text{ (Scheinpflug et al., 2017)}$$

$I_{440}$  and  $I_{490}$  denote the fluorescence intensities measured at 440 nm and 490 nm, respectively. Furthermore,  $(I_{440} - I_{490})$  represents the difference in fluorescence intensity between 440 nm and 490 nm, while  $(I_{440} + I_{490})$  represents their sum. The formula gives a possible range of values from -1 to +1, where negative values indicate higher polarity of laurdan environment (increased membrane fluidity), and positive values indicate lower polarity (decreased membrane fluidity).

### 2.2.4 Erythrocyte membrane tension studies

#### 2.2.4.1 Flipper-TR assay

For membrane tension studies, erythrocytes ( $1 \times 10^8$ /mL) were aged in media containing 5 mM, 22 mM and 100 mM glucose. The media was refreshed every day. The content of the vial of Flipper-TR was dissolved in 50  $\mu$ L DMSO to make a 1 mM stock solution and was stored at -20°C without aliquoting according to the manufacturer's recommendation. One mL of erythrocyte suspension containing  $1 \times 10^8$  cells was centrifuged for 5 minutes at 500 G and resuspended in 1 mL of PBS. A 5  $\mu$ L aliquot containing  $1 \times 10^6$  cells was placed in a well of a 4-well slide, followed by the addition of 495  $\mu$ L of PBS containing 1  $\mu$ M Flipper-TR and 5 mM, 22 mM, or 100 mM glucose. No more than two treatments were carried out at any one time and an empty well was left in between to avoid photobleaching of adjacent samples. The RBCs were incubated in the dark for 15 minutes at 37°C and 5% CO<sub>2</sub>. Following the 15-minute incubation period where the RBCs had already sedimented on to the bottom of the slide, the PBS was discarded to remove the Flipper-TR molecules that had not entered the membrane and reduce the background noise when the cells were imaged. Fresh PBS (500  $\mu$ L) containing either 5 mM, 22 mM, or 100 mM glucose were added to the cells in the respective wells. For the hypotonic control, the cells were placed in a solution containing 40% PBS containing 5 mM glucose and 60% sterile water. The hypertonic control was PBS containing 100 mM

mannitol. Some of the cells were treated with 1  $\mu$ M glyoxal or 5  $\mu$ M methylglyoxal in combination with glucose after the Flipper-TR incubation.

#### **2.2.4.2 Image acquisition**

FLIM was performed using a Leica TCS SP8 inverted microscope (DMi8) (Leica Microsystems CMS GmbH, Mannheim, Germany). Leica Application Suite X (LAS X) software was used to acquire and analyse the images. A 63x water apochromatic objective and hyD SMD1 (high sensitivity) detectors were used. From the dye assistant option Alexa 488 was selected. The laser configuration used a pulsed white light laser, which emits from 470 nm to 670 nm. The white light laser intensity was set to 2%, to get less than 1 photon per laser pulse in the pixel intensity histogram. The FLIM detectors were set to photon counting mode. FLIM acquisition mode was activated and 488 was selected from the filter supported white light laser lines. The frame repetitions were set to 100, the format at 512x512 and the speed at 400Hz. The gain remained on default setting at 100%. Auto range was used for the colour scale of the fluorescent lifetime.

#### **2.2.4.3 Image analysis**

Leica Application Suite X (LAS X) software was used to analyse the lifetimes of Flipper-TR, extracted from FLIM images by using the fit model n-Exponential Reconvolution using 3 exponential components. This fit model was used to enable the beginning of the decay curve for analysis, which improves the statistics of the data and enables a correct estimate of the relative amplitudes, i.e., the total number of photons detected at a specific time, from the sum of the exponential decay curves. Full images were used instead of choosing a region of interest to get the average Flipper-TR lifetime from all the cells present in the image.

### **2.2.5 Erythrocyte ROS production and PS detection using the fluorescent probe carboxy-H<sub>2</sub>DCFDA and annexin V, respectively.**

#### **2.2.5.1 Carboxy H<sub>2</sub>DCFDA and glucose treatment**

A 20 mM stock of carboxy-H<sub>2</sub>DCFDA was prepared in DMSO. After vortexing the mixture, aliquots of 50  $\mu$ L were made and stored at -20°C and a 1 mM carboxy-H<sub>2</sub>DCFDA then prepared by taking a 50  $\mu$ L aliquot (20 mM) and dissolving in 950  $\mu$ L DMSO. The total number of erythrocytes needed for each experiment were calculated approximately and taken from

the flask (approximately  $9 \times 10^7$ ). The cells were centrifuged at 500 G for 5 minutes, the media discarded, and PBS added, to obtain a final cell number of  $1 \times 10^6$  per 250  $\mu\text{L}$  (or  $4 \times 10^6$  per mL) and in order to remove the FBS in the media, as it contains esterases that can activate carboxy- $\text{H}_2\text{DCFDA}$  and can lead to a false positive result. A 48-well plate was used and 250  $\mu\text{L}$  containing  $1 \times 10^6$  added to the wells. Then  $1 \times 10^6$  erythrocytes in 250  $\mu\text{L}$  PBS were treated with a final concentration of 20 mM carboxy- $\text{H}_2\text{DCFDA}$  (5  $\mu\text{L}$  from 1 mM carboxy- $\text{H}_2\text{DCFDA}$  were added to the cells) for 30 minutes. The PBS was removed without disturbing the cells, and discarded to remove the dye that did not enter the cells. Subsequently, 225  $\mu\text{L}$  of fresh PBS was added to the cells. Next, 25  $\mu\text{L}$  of the X10 glucose stocks, 50 mM, 220 mM, and 1000 mM, were added to the cells to obtain a final glucose concentration of 5 mM, 22 mM, and 100 mM, respectively (performed in triplicate). Glucose treatment was carried out for 30 minutes, 1 and 4 hours on days 0, 2 and 4. Once treatment time was over, 200  $\mu\text{L}$  of cells were placed in a black non-binding 96 well plate put on ice. Hydrogen peroxide, prepared fresh each day at a final concentration of 10 mM, was used as a positive control and added to the cells immediately before fluorescent readings were taken. A x100 stock (1 mM) stock was prepared and 2.5  $\mu\text{L}$  added to the cells that were used as a positive control to obtain a final concentration of 10 mM. Mannitol was used as an osmotic control.

#### **2.2.5.2 Annexin V staining**

An Annexin V kit in which annexin V was conjugated with allophycocyanin (APC) was used to detect PS exposure in erythrocytes. Once glucose treatment was completed, the cells ( $1 \times 10^6$ ) were pipetted into 1.5 mL plastic reaction tubes and centrifuged at 500 g for five minutes. The PBS was removed and 50  $\mu\text{L}$  of 1X binding buffer, containing 10 mM HEPES, 140 mM NaCl, 25 mM  $\text{CaCl}_2$  and pH7.4, were added to the cells. The cells were pipetted into a 96-well plate and placed on ice.

#### **2.2.5.3 Flow cytometry**

The cells stained with carboxy- $\text{H}_2\text{DCFDA}$  and/or annexin V (APC conjugated) were analysed using a Beckman Coulter CytoFLEX S flow cytometer. Unstained erythrocytes were plotted according to their forward (FSC) and side scatter (SSC) profiles and then gated to exclude debris. Only erythrocytes were present, so a single main cell population appeared, and they were gated leaving out outlier events. Also unstained cells were gated below 2% on a single parameter histogram to allow identification of the percentage of positively stained RBCs. Each

sample was analysed using 10,000 cellular events, at a flow rate of less than 1000 events per second. The violet side scatter (V-SSC) cytometer detectors (405 nm) were used to increase resolution, reduce background noise from debris and enhance sensitivity allowing for more precise measurements of erythrocyte characteristics such as size and granularity. Carboxy-H<sub>2</sub>DCFDA was detected under blue-FITC channel (492/527 nm excitation/emission, respectively) and annexin V APC-conjugated was detected under red-APC channel (535/660 nm excitation/emission, respectively). The CytoFLEX allowed multiple stains on the cells to be detected in parallel using fluorescent probes that have different fluorescent emission wavelengths. For cells that were double stained with annexin V and carboxy-H<sub>2</sub>DCFDA, unstained cells were gated on the lower left quadrant of a dot plot with quadrants to allow identification of double positive cell populations. Data analysis was carried out using CytExpert software by looking at the percentage of positive cells as well as the mean fluorescence intensity (MFI).

### **2.2.6 Mass spectrometry analysis of erythrocyte lipids**

Mass spectrometry analysis of erythrocyte lipids was carried out at Aston University and AB Sciex laboratories in Manchester, UK.

#### **2.2.6.1 Erythrocyte lipid extraction**

Erythrocyte pellets, containing approximately  $1 \times 10^8$  cells, were washed with 250  $\mu$ L PBS and centrifuged for 5 minutes at 500 G. Then the pellet was subjected to hypotonic lysis by adding 250  $\mu$ L of cold low ionic strength buffer containing 5 mM sodium phosphate, 0.1 mM ethylenediaminetetraacetic acid (EDTA), pH8 (*Desrames et al., 2020*). The cells were centrifuged for 10 minutes at 500 G. Supplementary washes with cold low ionic strength buffer were carried out until the pellet was no longer red. This step was carried out to remove haemoglobin prior to lipid extraction and facilitate separation. The supernatant was discarded. To the cell pellet 300  $\mu$ L of methanol Optima LC/MS grade and 1 mL of tert-Butyl methyl ether (MTBE) were added followed by 1 minute of vortexing. The mixture was sonicated in a sonic bath for thirty seconds and then mixed thoroughly on a vortex mixer for 1 minute. The sonication and vortex steps were repeated three times. Then 200  $\mu$ L of MS grade water was added. The samples were mixed by vortex followed by centrifugation for 10 minutes at 1000 G. The upper lipid-containing phase were transferred into a glass collection vial and dried using nitrogen gas.

### 2.2.6.2 Lipid preparation prior to LC-MS analysis

Dried lipid extracts in a glass vial were resuspended in 100  $\mu\text{L}$  of 2:1:1 isopropanol, acetonitrile, and water, respectively (50  $\mu\text{L}$  isopropanol, 25  $\mu\text{L}$  acetonitrile and 25  $\mu\text{L}$  water). All solvents used were LC/MS grade. The lipid solvent mixture was vortexed for two minutes followed by a 1:10 dilution; 20  $\mu\text{L}$  of erythrocyte lipids were resuspended in 180  $\mu\text{L}$  containing isopropanol, acetonitrile and  $\text{H}_2\text{O}$ , at a ratio of 2:1:1; respectively with mass spectrometry analytical glass vials used. Quality control (QC) samples included adding 20  $\mu\text{L}$  from all the 1:10 diluted samples to a mass spectrometry analytical glass vial. All samples were vortexed and centrifuged for five minutes at 2000 G prior to LC-MS analysis.

### 2.2.6.3 Liquid chromatography (LC) conditions

The LC method was based on Cajka and Fiehn (*Cajka and Fiehn, 2016*). For positive ion mode a sample volume of 1  $\mu\text{L}$  was injected, whereas for negative ion mode 3  $\mu\text{L}$  were injected. Lipids were separated on an Acquity UPLC CSH C18 column (2.1x100mm; 1.7  $\mu\text{m}$ ) coupled to an Acquity UPLC CSH C18 VanGuard pre-column. The columns were maintained at 65°C at a flow rate of 0.6 mL/min. The separation was then conducted for 15 minutes, following the gradient shown in Table 2.2. For positive ion mode, the mobile phases consisted of (A) 60% Acetonitrile, 40%  $\text{H}_2\text{O}$ , 10 mM ammonium formate and 0.1% formic acid; and (B) 90% isopropanol and 10% acetonitrile containing 10 mM ammonium formate and 0.1% formic acid. For negative ion mode, the solvents consisted of (A) 60% acetonitrile and 40%  $\text{H}_2\text{O}$  containing 10 mM ammonium acetate; and (B) 90% isopropanol, 10% acetonitrile and 10 mM ammonium acetate. All solvents used were LC/MS grade.

Table 2. 2. LC method involving a flow rate of 0.6 mL/min with a total duration of 15 minutes. The gradient used involved at 0 minutes 15% (B); 0-2 minutes 30% (B); 2-2.5 minutes 48% (B); 2.5-11 minutes 82% (B); 11-11.5 minutes 99% (B); 11.5-12 minutes 99% (B); 12-12.1 minutes 15% (B) and 12.1-15 minutes 15% (B).

		Solvents	
Time (minutes)	Flow Rate mL/minute	A	B
0	0.6	85	15
2	0.6	70	30
2.5	0.6	52	48
11	0.6	18	82
11.5	0.6	1	99
12	0.6	1	99
12.1	0.6	85	15
15	0.6	85	15

#### 2.2.6.4 Mass Spectrometry

Mass spectrometry detection of lipids was performed on ZenoTOF 7600 Sciex system (Sciex) using Sciex OS software at AB Sciex facility in Manchester, UK with the workflow set to small molecules and the method duration to 15 minutes. Ionisation started from 0.5 minutes to 13 minutes, to help eliminate background noise from the beginning of the run. The source temperature was set to 550°C, and ion source gas 1 and 2 set to 50 and 70 psi, respectively. The experiment was set to IDA (Information Dependent Acquisition), which is equivalent to data dependent acquisition (DDA). The ion spray voltage was set to 5500 V and -4500 V for positive and negative ion modes, respectively. For positive ion mode, the mass range for TOF MS was set from 250 Da to 1800 Da, the collision energy set at 10 volts and the declustering potential at 50 volts. For TOF MSMS, the mass was set from 50 Da to 1800 Da and the collision energy set to 35 volts. For negative ion mode, the mass range for TOF MS was set from 150 Da to 1800 Da, the declustering potential to -50 volts and collision energy to -10 volts. The mass range for TOF MSMS was also set from 50 Da to 1800 Da and the collision energy to -35 volts. Zeno pulsing was enabled for ion intensities lower than 2000 cps. The instrument was calibrated using ESI negative, or positive, calibration solutions X500 from Sciex.

### 2.2.6.5 Data analysis

MS dial version 4.9 was used to look at raw data. Importing the data to MS dial involved selecting conventional LC/MS (data dependent MS/MS), centroid data for MS1 and MS/MS, lipidomics (under target omics) and choosing either negative or positive ion mode. For positive ion mode the adducts selected included  $[M+H]^+$ ,  $[M+NH_4]^+$  and  $[M+Na]^+$ . For negative ion mode the adducts selected included  $[M-H]^-$ ,  $[M-H_2O-H]^-$ ,  $[M+Cl]^-$ ,  $[M+FA-H]^-$  (formic acid) and  $[M+Hac-H]^-$  (acetic acid). The data were exported from MS dial by selecting the alignment results, followed by raw data matrix (area) and m/z matrix. Microsoft Excel was used to format the exported data according to the instructions in MetaboAnalyst. Once the data was accepted by MetaboAnalyst, the following parameters were used: normalisation by sum, log transformation under data transformation, and autoscaling.

### 2.2.7 Statistical analysis

GraphPad Prism was used for all data analysis, except from mass spectrometry data where MetaboAnalyst was used. Statistical tests used are detailed in the legend of the figures. Statistical significance was defined as  $P < 0.05$ . The P value approach was as follows:  $< 0.05$  (\*),  $< 0.005$  (\*\*),  $< 0.0005$  (\*\*\*) and  $< 0.0001$  (\*\*\*\*). Raw data is shown as mean values  $\pm$  SD.

# **Chapter 3**

**Effect of glucose and ageing, in the presence or absence of glyoxal and methylglyoxal, on erythrocyte membrane fluidity**

### 3.1 Introduction

Membrane fluidity refers to the freedom of movement of protein and lipid constituents within the cell membrane and is essential for the correct functioning of essential membrane proteins whose motion can be impaired when the membrane changes from liquid-crystalline to a gel phase (*Verde et al., 2016*). There are various techniques which allow membrane fluidity to be measured such as fluorescence spectroscopy, electron-spin resonance and nuclear magnetic resonance spectroscopy. Electron-spin resonance (ESR) can provide information about local dynamics of lipid molecules in the bilayer, such as lipid mobility, by the incorporation of spin-labels containing a free radical (*Chede et al., 2021, Dragicevic-Curic et al., 2011*). Phospholipid nitroxide derivatives are the most commonly used probes, and since these probes are similar to membrane components, they localise in the outer leaflet of the lipid bilayer. Changes in the motion of the spin label are used to identify changes in membrane fluidity (*Chede et al., 2021*). The information about the environment of the spin label is obtained from the recorded EPR spectra (*Yonar et al., 2019*).

In contrast, nuclear magnetic resonance (NMR) spectroscopy allows the detection of mobile fraction of lipids contained in the cells (*Quintero et al., 2007, Robinson and Cistola, 2014*). In NMR, the nuclei in a magnetic field absorb and re-emit electromagnetic energy (*Bottomley, 1984*). In the context of membrane fluidity, NMR can be used to measure the motion of hydrogen nuclei (protons) in lipid molecules. Measuring the relaxation times of these nuclei gives information about molecular dynamics and fluidity (*Robinson and Cistola, 2014*). Labelling in NMR is not typically required, although there are paramagnetic spin labels, such as deuterium-labelled lipids, which are used to assess membrane fluidity (*Munz et al., 2016, Davis, 1979, Seelig and Niederberger, 1973*). Electrons have a greater magnetic moment than nuclei, so ESR spectroscopy is more sensitive than NMR spectroscopy (*Dhanjal et al., 2003*).

Membrane fluidity can be measured indirectly by the use of polarity sensitive probes, whose emission spectra change with the polarity of the environment (*Amaro et al., 2017*). The fluorescent probe 2-dimethylamino-6-lauroylnaphthalene (laurdan), composed of a naphthalene molecule attached to the 12-carbon fatty acid lauric acid (Figure 3.1) has been extensively used in different membrane types such as vesicles, cells and organelles (*Jay and Hamilton, 2017*).

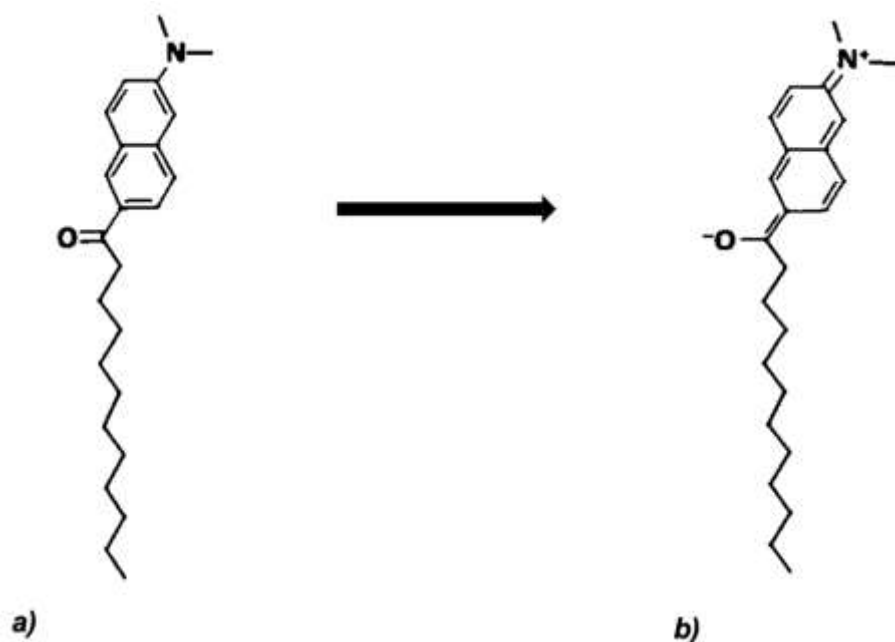


Figure 3. 1. Laurdan in the ground (a) and excited states (b). Image modified from (Jay and Hamilton, 2017), Permission granted from Springer Nature (5641860856750).

Laurdan is a solvochromatic probe that reports environmental changes. It can distinguish between the liquid ordered (*Lo*) and liquid disordered (*Ld*) membrane phases (Jay and Hamilton, 2017). In the gel or *Lo* phase it has a maximum emission of 440 nm, and in the liquid or *Ld* phase it has a maximum emission at 490 nm. The shift in emission between different states of membrane order is used to calculate the generalised polarisation (GP), a quantitative measure for lipid packing (Amaro *et al.*, 2017). Microscopy techniques using single and multi-photon excitation, as well as fluorescence spectroscopy, are standard approaches for measuring laurdan fluorescence (Jay and Hamilton, 2017); however, its photostability is low and fluorescence spectroscopy is predominantly used (Jay and Hamilton, 2017).

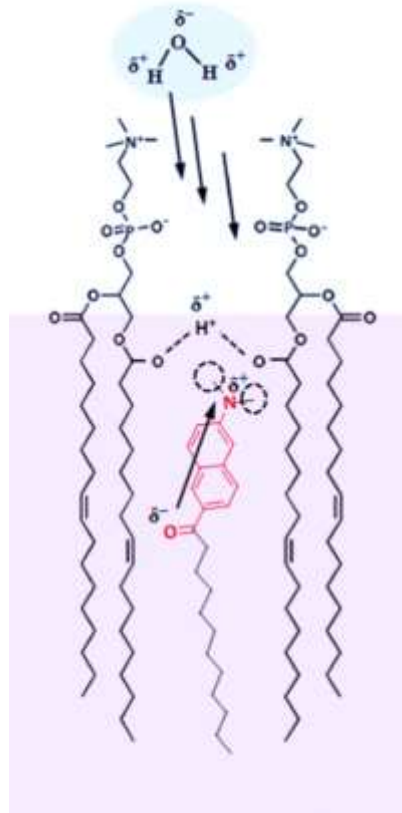


Figure 3. 2. Illustration of the polarization-like state of laurdan due to a weak interaction of the dimethylamino group of laurdan with the ester groups of DOPC. The laurdan fluorescent moiety localizes below the glycerol backbone of phospholipids. The interaction is strengthened when laurdan rises higher within the membrane (such as in Ld phase). Image taken from (Jay and Hamilton, 2017). Permission granted from Springer Nature (5641860856750).

It should be considered that laurdan does not measure fluidity directly, rather the accessibility of water around the lipid headgroups, which is strongly influenced by the phase of the membrane. There are drawbacks when using laurdan, including its low solubility in aqueous media, low fluorescence intensity and susceptibility to photo-bleaching (Kaiser *et al.*, 2009).

The level of hydration of the membrane is related to membrane fluidity (Parasassi *et al.*, 1997). Membrane fluidity is affected by various factors including the length and unsaturation of fatty acyl chains, the headgroups of phospholipids and cholesterol content: all these factors can affect the ability of water to penetrate the membrane.

Cholesterol is an essential component of cell membranes and modulates membrane fluidity (Vestergaard *et al.*, 2010). At lower temperatures, cholesterol is found between phospholipid tails, disrupting regular packing and lowering the freezing, or crystallisation, point of the

membrane (Cooper, 2000). On the other hand, at higher temperatures cholesterol reduces the mobility of the phospholipids, making it more difficult for them to transition from an ordered to a disordered state (Cooper, 2000). Hence, cholesterol, and its position in the membrane, affects the phase transition of the membrane and plays an important role in membrane fluidity, i.e., cholesterol near the surface restricts the passage of molecules by increasing the packing of phospholipids (decreasing membrane fluidity) (Subczynski et al., 2017).

Methyl- $\beta$ -cyclodextrin (MBCD) is a water-soluble oligosaccharide composed of seven glucose units, containing a hydrophobic cavity able to form a complex with cholesterol (Mahammad and Parmryd, 2015). MBCD is widely used to deplete cholesterol primarily from lipid rafts, where it strictly acts at the membrane surface (Lopez et al., 2011). The amount of cholesterol that MBCD can sequester depends on several factors, including MBCD concentration, treatment duration and cholesterol content in the membrane (Zidovetzki and Levitan, 2007). So, the maximum amount of cholesterol that can be sequestered by MBCD may vary under different experimental conditions. MBCD treatment (5 mM with an incubation period of one hour) on HeLa cells reduced the levels of cellular cholesterol by 90% compared to levels found in control untreated cells (Danthi and Chow, 2004). Moreover, 73% and 45% of membrane cholesterol from HL-60 (promyeloblasts) cells and neutrophils was sequestered by MBCD, respectively; MBCD concentrations ranged from 5-20 mM with an incubation period of 30 minutes. (Oh et al., 2009).

A study was carried out by Fernandez-Perez and co-workers, where they used MBCD to decrease cholesterol content in HEK-293 and primary rat hippocampal neurones. They also increased cholesterol content in cells by using MBCD/cholesterol complex (Fernandez-Perez et al., 2018). The results showed that membrane fluidity increased when cholesterol levels were reduced, and the membrane appeared more rigid when cholesterol levels were increased. (Fernandez-Perez et al., 2018). Cholesterol depletion by MBCD has also been shown to increase membrane tension and making cells prone to rupture (Biswas et al., 2019).

MBCD concentrations of 3 mM and 5 mM have been used on erythrocytes to deplete cholesterol from the membrane (Rodi et al., 2008, Ahiya et al., 2022). On the other hand, Bianchetti and colleagues used 10 mM MBCD and incubated RBCs for three hours to deplete them from cholesterol (Bianchetti et al., 2019). By using laurdan, they reported an increase in membrane fluidity in RBCs treated with MBCD.

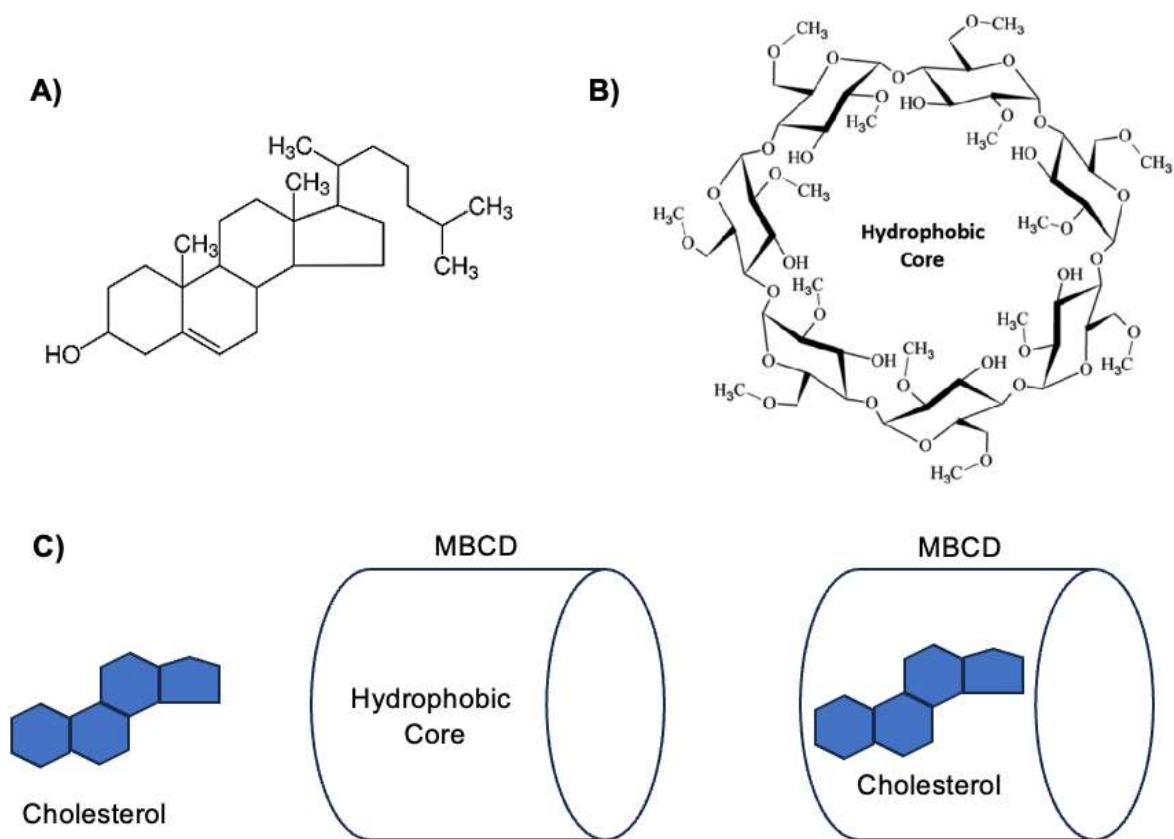


Figure 3. 3. Structure of cholesterol (A) and MβCD (B). Schematic representation of MβCD sequestering cholesterol (C). Adapted from: (Mahammad and Parmryd, 2015).

RBC membrane fluidity studies have reported inconsistent results. Increased membrane fluidity was reported in a study carried out by Maulucci and colleagues on patients suffering from type 1 diabetes mellitus; they also used laurdan to test fluidity (Maulucci et al., 2017). Bianchetti and colleagues studied membrane fluidity changes in RBCs from healthy, type 1 and type 2 diabetes mellitus subjects (Bianchetti et al., 2019). They reported an increase in membrane fluidity in subjects suffering from type 1 diabetes, whereas a decrease in membrane fluidity was observed in type 2 diabetes. It is important to highlight that the average laurdan GP was  $0.601 (\pm 0.017)$ ;  $0.558 (\pm 0.019)$  and  $0.636 (\pm 0.039)$  for control, type 1 and type 2 diabetic groups, respectively. The increase in membrane fluidity in the type 1 group was greater than the decrease observed in the type 2 group when compared to the control. Furthermore, other studies carried out on healthy, and type 2 diabetic individuals have shown a decrease in RBC membrane fluidity in diabetic subjects, with type 2 diabetes also being associated with hypercholesterolaemia (Waczulikova et al., 2002, Candiloros et al., 1995, Bianchetti et al., 2019, Gonzalez-Lleo et al., 2022, Harris, 1991).

High levels of glucose have been linked to increased oxidative stress, through various mechanisms such as increased lipid peroxidation, advanced glycation end products (AGEs) formation, activation of polyol pathway etc (*Giacco and Brownlee, 2010*). Glyoxal and methylglyoxal are intermediate breakdown products of glycation and lipid peroxidation (*Vistoli et al., 2013*). Typical concentrations of glyoxal and methylglyoxal in human plasma ranges from 50-150 nM, although it is very challenging to measure the exact amounts in the body due to these molecules being highly reactive and rapidly metabolised (*Rabbani et al., 2016*). However, these glycating compounds are known to be elevated in diabetes with plasma levels of methylglyoxal and glyoxal in diabetes reaching as high as 0.9  $\mu\text{M}$  and 1  $\mu\text{M}$ , respectively (*Kold-Christensen et al., 2019, Bierhaus et al., 2012, Han et al., 2007*). Intracellular levels of methylglyoxal have been reported to have reached 4  $\mu\text{M}$  (*Lai et al., 2022*). In the current investigation pathological, or higher, levels of glyoxal and methylglyoxal were used in the treatment of RBCs to simulate *in vivo* conditions and to make sure that the treatment reached the cells.

Experiments where high levels of glucose are used to treat cells often include an osmotic control. When working with high concentrations of glucose, it is important to have an osmotic control to ensure that any observed effects are specifically due to the presence of glucose and not simply due to changes in osmotic pressure. Having an osmotic control allows isolation of the effects of osmotic pressure from the effect of glucose. In the current investigation mannitol was used as an osmotic control for several reasons. It has a similar molecular weight to glucose which leads to comparable effects on osmotic pressure, it does not contain aldehyde groups (less reactive than glucose) and it is not metabolizable by RBCs.

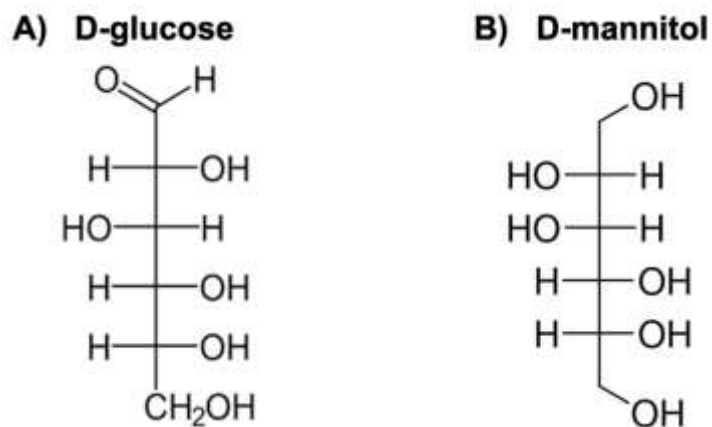


Figure 3. 4. Molecular structure of D-glucose (A) and D-mannitol (B). Glucose contains an aldehyde group (-CH=O) and has a molecular weight of 180.16 g/mol. Mannitol molecular weight is 182.12 g/mol.

### **Aim and objectives:**

The aim of this chapter was to investigate the effect of increasing glucose concentration on membrane fluidity in the presence or absence of pathological levels of glyoxal and methylglyoxal, with the intention of simulating *in vivo* conditions and ensuring cellular exposure to the treatments. The objectives included determining short- and long-term effects of glucose treatment to investigate whether the duration of glucose treatment had differential effects on membrane fluidity and to establish mannitol as an osmotic control in short term-glucose treatment to ensure that any observed changes in membrane fluidity during short-term glucose treatment were not solely due to osmotic effects. Additionally, the study sought to validate membrane fluidity measurements using laurdan and MBCD to confirm the reliability of the methods used for measuring membrane fluidity. The hypothesis was that increasing glucose concentrations would cause a decrease in membrane fluidity. To address the aim and objectives, blood was collected from healthy volunteers. Erythrocytes were isolated from whole blood and kept in glucose free RPMI media to which final concentrations of 5 mM, 11 mM, 22 mM, 50 mM and 100 mM glucose were added. During short-term treatment mannitol was used as osmotic control. Membrane fluidity was measured using the fluorescent probe laurdan and the presence of MBCD was used as a positive control.

### **3.2 Materials and Methods**

All materials and methods are described in Chapter 2. Details of membrane fluidity studies are found in section 2.2.3.

### 3.3 Results

#### 3.3.1 Short-term glucose treatment and its effect on erythrocyte membrane fluidity as the cells aged

The fluorescent probe laurdan was used to establish whether short-term glucose treatment causes a change in erythrocyte membrane fluidity (Figure 3.5). First, the cells were treated with 5 mM glucose for one hour on days 0 (the day blood was taken from the body) and 4, followed by measuring their membrane fluidity in the presence or absence of 5 mM MBCD, using 1  $\mu$ M laurdan (Figure 3.5A). The GP of cells treated with glucose did not change significantly on days 0 and 4. The presence of MBCD appeared to increase membrane fluidity, but no significant differences were found on days 0 and 4 despite an apparent decrease in the GP value of MBCD-treated cells. Mannitol was used as osmotic control at the same concentrations as glucose with the aim of isolating the effects of osmotic pressure from the effects of glucose (Figure 3.5B). The GP results from the mannitol treatment were similar to those obtained for glucose. No significant differences were found between the cells treated with 5 mM mannitol and those with 5 mM mannitol plus 5 mM MBCD, as for glucose treatment.

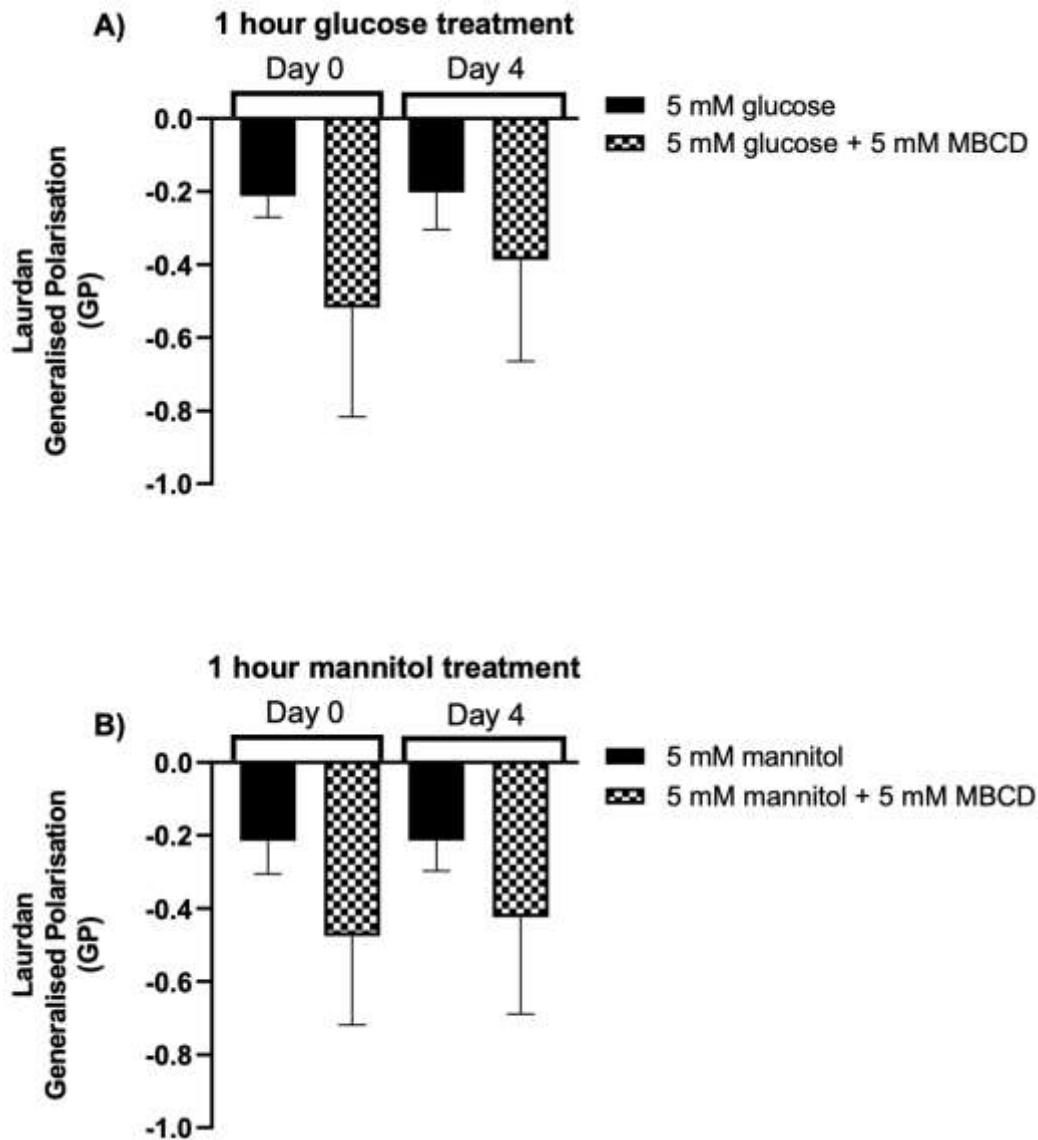


Figure 3. 5. GP of laurdan in erythrocytes treated for one hour with glucose (A) and mannitol (B) on days 0 and 4. Mannitol was used as osmotic control and 5 mM MBCD was used as membrane fluidising agent. Results are shown as means  $\pm$  SD.  $n=6$  for cells in 5mM glucose and mannitol, and  $n=4$  for cells treated with 5 mM glucose/mannitol and 5 mM MBCD. Significance was tested by two-way ANOVA followed by Tukey *post-hoc* test. Three technical replicates were carried out for each experimental condition for each participant.

The short-term effect of increasing glucose concentrations on RBC membrane fluidity was investigated by treating the cells on days 0 and 4 with various glucose concentrations. The erythrocytes were kept in media containing 5 mM glucose, which was changed every day until tests were carried out on day 4. The aim of this experiment was to treat erythrocytes with different glucose concentrations, ranging from physiological to pathological levels, for a short period of time using fresh and aged erythrocytes (in physiological levels of glucose) and evaluate the effect on membrane fluidity.

The GP results obtained for RBCs treated with glucose are shown in Figure 3.6A. On day 0, the GP appeared slightly more negative as the concentration of glucose increased (corresponding to increased membrane fluidity); except at 50 mM glucose, where a more positive GP was observed. However, no significant difference was found in glucose short-term treatment on RBC membrane fluidity. Furthermore, an anomaly in the 50 mM treatment (more positive GP and a larger error bar) was observed on day 4.

Results obtained when the cells were treated with mannitol (osmotic control) are shown in Figure 3.6B. An osmotic pressure can occur when high concentrations of glucose are used due to a difference in solute concentration across the membrane, and this can affect the morphology and function of cells. The GP values for 5 mM mannitol are similar to those obtained when the cells were treated with glucose, for both 0 and 4 days. However, no significant changes were observed when the cells were treated with mannitol. Furthermore, no significance was found between glucose and mannitol equivalent concentrations.

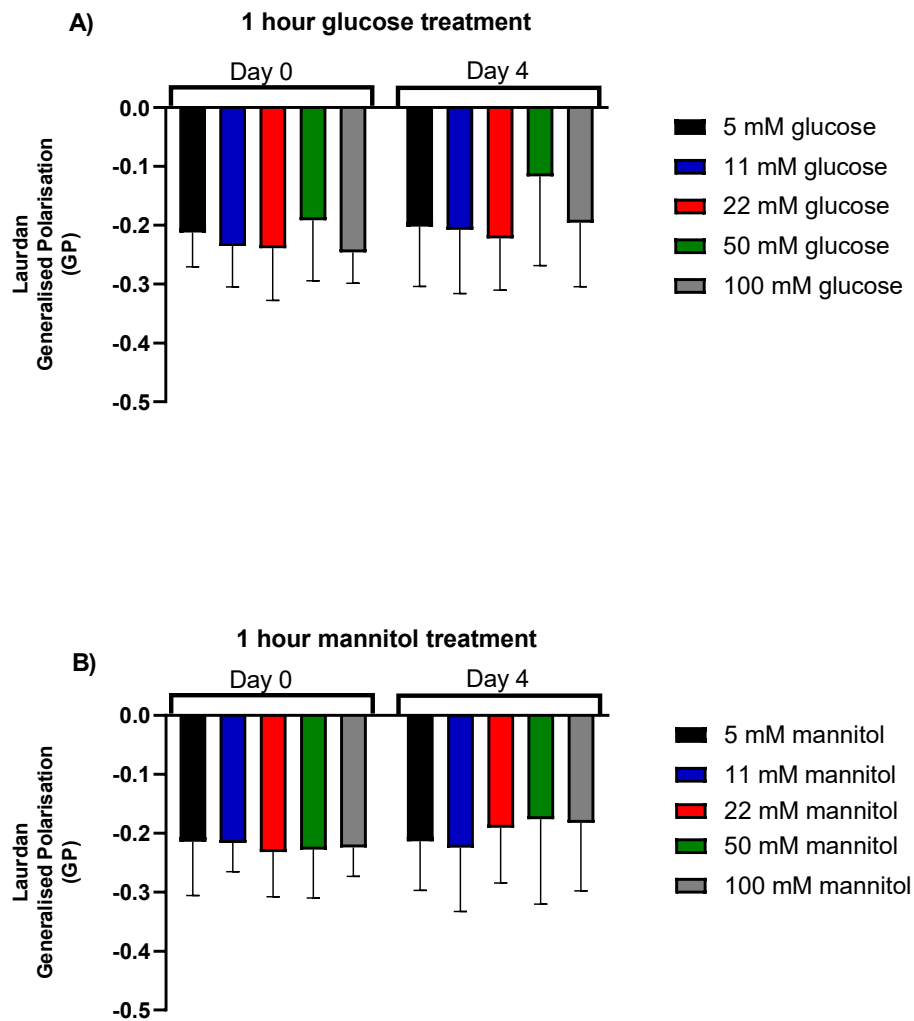


Figure 3. 6. Effect of short-term glucose treatment on erythrocyte membrane fluidity. RBCs were treated for one hour with glucose (A) and mannitol (B) on days 0 and 4. The solvchromatic probe laurdan was used at a concentration of 1  $\mu$ M to investigate membrane fluidity changes. Mannitol was used as osmotic control. Results are shown as means  $\pm$  SD,  $n=6$  for cells treated with 5 mM, 11 mM and 22 mM glucose or mannitol, and  $n=5$  for cells treated with 50 mM and 100 mM glucose or mannitol. Statistical analysis carried out by two-way ANOVA followed by *post-hoc* Tukey test.

### **3.3.2 Effect of increasing glucose concentrations on erythrocyte membrane fluidity as the cells aged *in vitro***

As no significant changes were observed with short-term glucose exposure on erythrocyte membrane fluidity, further work focused on the effect of long-term glucose exposure. Erythrocyte membrane fluidity was measured on days 0 (untreated), 2 and 4 (cells kept in 5 mM glucose), and MBCD was used as a positive control (Figure 3.7). No obvious effects on membrane fluidity were observed by ageing the cells in 5 mM glucose alone. No significant difference between untreated cells (day 0) and the positive control was found. Significant differences were found between the cells kept in 5 mM glucose and those treated with MBCD on days 2 and 4;  $P < 0.005$  and  $P = 0.001$  were obtained respectively. Furthermore, there were no significant differences between the positive controls on different days.

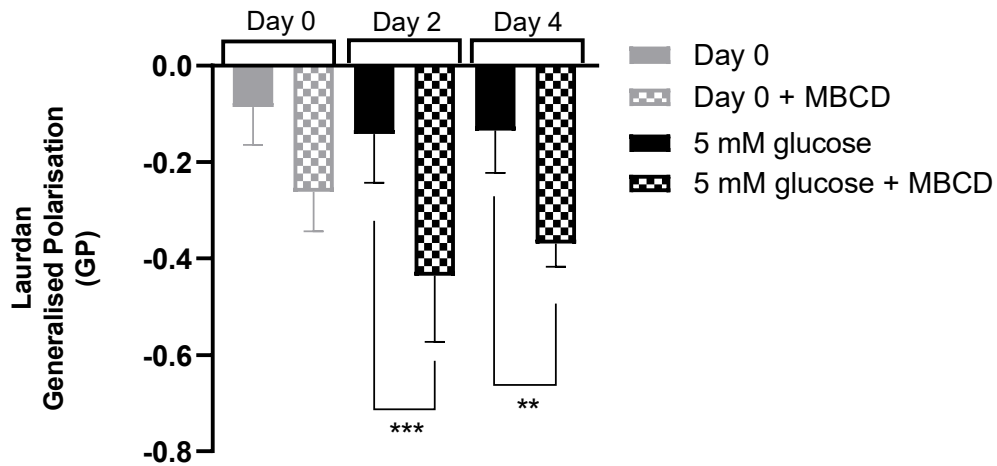


Figure 3. 7. Effect of long-term physiological levels of glucose exposure on erythrocyte membrane fluidity, measured by laurdan. Untreated RBCs are shown as day 0 (the day in which blood was taken), the cells were kept in 5 mM glucose, and media was changed every day. Membrane fluidity was tested on days 0; 2 and 4 with 5 mM MBCD used as membrane fluidising control. Results are shown as means  $\pm$  SD,  $n=6$  for day 0 and 5 mM glucose, and  $n=4$  for cells also treated with MBCD. Significance was tested by two-way ANOVA, and defined as  $p<0.05$ , to compare untreated cells (day 0) and those under 5 mM glucose at days 2 and 4, followed by Sidak's multiple comparison test.

To study the long-term effect of high levels of glucose on RBC membrane fluidity, the cells were kept under different glucose concentrations for five days (Figure 3.8). The results appeared to show a trend towards increasingly negative GP values as glucose concentration increased, although no significant differences were found.

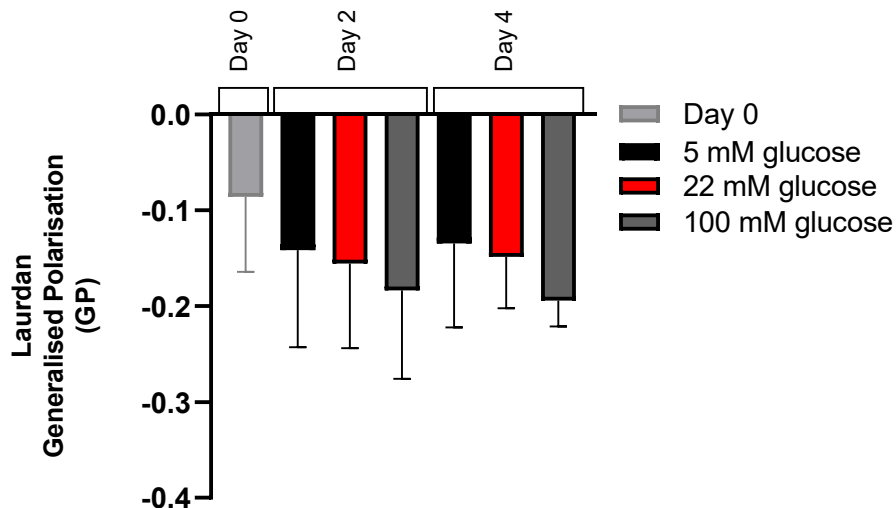


Figure 3. 8. Long term erythrocyte treatment under physiological and pathological levels of glucose. Untreated RBCs are shown as day 0 (the day in which blood was taken). GP values of cells kept in 5 mM, 22 mM, and 100 mM glucose. The media was changed every day. Membrane fluidity was tested on days 0; 2 and 4. Results are shown as means  $\pm$  SD;  $n=6$  for 5 mM and 22mM glucose for days 2 and 4 as well as for day 0; and  $n=5$  for 100 mM glucose for days 2 and 4. Significance was tested by one-way ANOVA, followed by *post-hoc* Tukey test for multiple comparisons.

Further analysis was carried out to examine the individual results for each participant. Table 3.1 summarises the changes in erythrocyte membrane fluidity for six participants following treatment with 5 mM, 22 mM, and 100 mM glucose for five days. Two participants showed no significant changes in membrane fluidity under any of the treatment conditions. In contrast, four participants showed significant differences in membrane fluidity. Among these, participant B displayed a decrease in membrane fluidity when erythrocytes were treated with 22 mM and 100 mM glucose. The remaining three participants showed an increase in membrane fluidity under similar conditions. Interestingly, only participant B presented significant differences in membrane fluidity between untreated and treated erythrocytes, whereas the other participants showed no significant differences between these groups.

Table 3. 1. Differences in erythrocyte membrane fluidity between participants.

<b>Participant</b>	<b>Significant difference</b>	<b>Untreated vs Day 4 5 mM glucose</b>	<b>Day 4 5 mM vs Day 4 22 mM glucose</b>	<b>Day 4 5 mM vs Day 4 100 mM glucose</b>
<b>A</b>	Yes	X	✓ (increased)	N/A
<b>B</b>	Yes	✓ (increased)	✓ (decreased)	✓ (decreased)
<b>C</b>	No	X	X	X
<b>D</b>	Yes	X	✓ (increased)	✓ (increased)
<b>E</b>	No	X	X	X
<b>J</b>	Yes	X	X	✓ (increased)

The table shows erythrocyte membrane fluidity treated with different glucose concentration. A total of six participants. For each treatment, the fluidity measurements were performed in triplicate

### 3.3.3 Effect of glucose in the presence or absence of methylglyoxal and glyoxal on erythrocyte membrane fluidity

Laurdan was used to establish whether long term exposure to high levels of glucose in the presence of glyoxal and methylglyoxal affects membrane fluidity in erythrocytes. Glyoxal and methylglyoxal are potent glycating agents and their presence is increased in diabetes mellitus. The cells were kept in media containing various concentrations of glucose. Glyoxal or methylglyoxal, at a concentration of 1  $\mu\text{M}$  or 5  $\mu\text{M}$ , respectively, were added daily once the media was changed. A significant increase in membrane fluidity was observed when the concentration of glucose was increased to 100 mM, compared to 5 mM glucose ( $P < 0.05$ ). Adding glyoxal increased membrane fluidity for 5 mM and 100 mM glucose. A significant difference ( $P < 0.05$ ) was found at 5 mM and 100 mM glucose between the cells that were treated with and without glyoxal. On the other hand, no significant effect on membrane fluidity was found for these two glucose concentrations when the cells were treated with methylglyoxal.

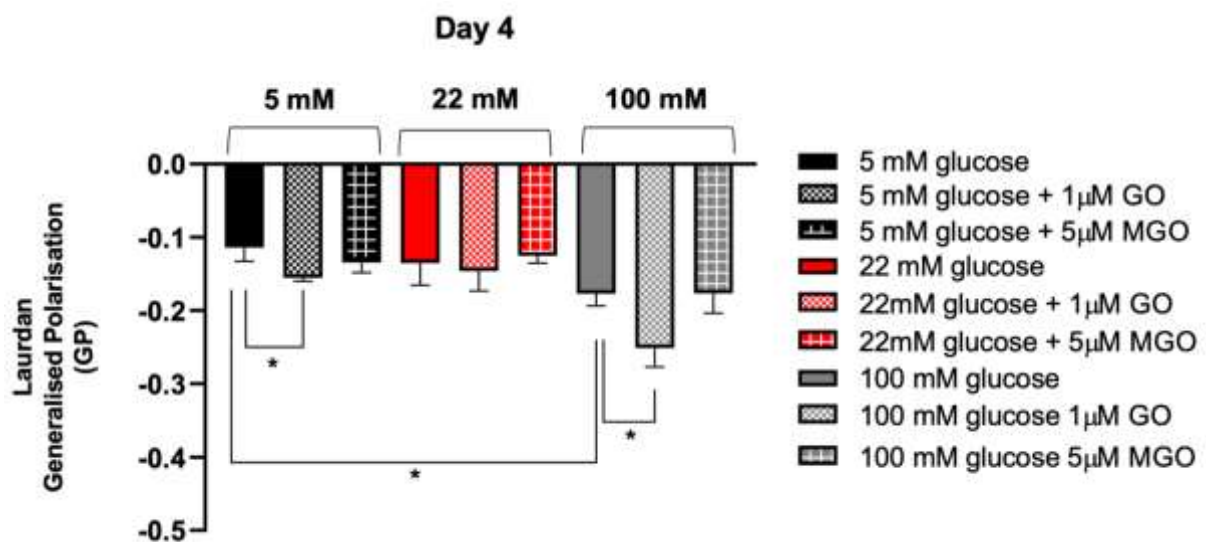


Figure 3. 9. Laurdan GP of erythrocytes, after the cells were kept for five days in different glucose concentrations (5 mM, 22 mM and 100 mM) in the presence or absence of glyoxal (1  $\mu\text{M}$ ) or methylglyoxal (5  $\mu\text{M}$ ). Results are shown as means  $\pm$  SD ( $n=3$ ). Significance was tested by one-way ANOVA followed by *post-hoc* Tukey test.

### 3.4 Discussion

This study was performed in order to evaluate the possible relationship between increasing concentrations of glucose and membrane fluidity on erythrocytes using the fluorescent probe laurdan, which is highly sensitive to the presence and mobility of water molecules within the membrane bilayer, yielding information on membrane micropolarity by a shift in its emission spectrum depending on the surrounding lipid phase state (*Bianchetti et al., 2019*). Short- and long-term glucose treatments were carried out to test the hypothesis that incubation of erythrocytes with increased glucose concentrations would cause decreased membrane fluidity. During these treatments, the cells were kept in media containing a range of concentrations based on physiological (5 mM) and pathological (11 mM, 22 mM, 50 mM, and 100 mM) glycemia (*Mathew et al., 2023*). No significant difference in membrane fluidity was found during short-term glucose treatments. Long-term treatment, where glucose was first used alone, showed no significant changes on membrane fluidity. However, when glyoxal and methylglyoxal were added to long-term glucose treatment significant differences were found between the controls, 5 mM and 100 mM glucose, where an increase in membrane fluidity was observed at 100 mM. Lastly, long-term treatments including the glycating agents showed significant changes on membrane fluidity, where the presence of glyoxal appeared to increase membrane fluidity for 5 mM and 100 mM glucose treatments. These results disagreed with the initial hypothesis that a decrease in membrane fluidity was expected at increasing glucose concentrations, as well as in the presence of glycating compounds.

MBCD was used as a positive control to show that laurdan was responsive to an agent known to affect membrane fluidity. When the RBCs were incubated with MBCD, the GP appeared considerably more negative, indicating increased membrane fluidity after cholesterol depletion. At lower temperatures, membranes tend to be more rigid and ordered, while at higher temperatures they become more fluid (*Los and Murata, 2004*). This transition temperature depends on lipid composition of the membrane and the removal of cholesterol by MBCD likely lowered the transition temperature making the membrane more fluid. So, decreasing cholesterol level at physiological temperature (37°C) likely increased the membrane water content and led to a decrease in the order of the membrane, hence augmenting membrane fluidity (*Fernandez-Perez et al., 2018*).

However, it appeared that the MBCD effect on membrane fluidity varied across incubation times, even though the glucose concentration remained the same (5 mM), i.e. the values

seemed variable. If no changes were taking place in the membrane, then the effect of MBCD would be expected to be the same each time, but it was not the case. This suggested that membrane properties might have been changing over time, possibly due to a combination of direct and indirect effects of glucose exposure and other factors associated with prolonged cell culture. MBCD is known to disrupt lipid rafts, which are cholesterol-rich microdomains in the cell membrane (*Korade and Kenworthy, 2008*). These lipid rafts play an important role in membrane organisation and fluidity (*Simons and Sampaio, 2011*). The effects of MBCD on membrane fluidity may vary depending on the cholesterol content, organisation of lipid rafts and phospholipid composition.

When erythrocytes were subjected to long-term glucose incubation, initial observations appeared to show an increase in membrane fluidity with increasing glucose concentration, although statistical significance was not reached. However, when the effects of glucose in the presence or absence of glyoxal and methylglyoxal were examined, a significance was observed between concentrations of 5 mM and 100 mM, with an increase in membrane fluidity evident. An interesting observation was that a larger sample size was available for the glucose-alone tests compared to the combined effect tests with glyoxal and methylglyoxal. It was noted that the larger sample exhibited more variation compared to the smaller sample.

Long term glucose incubation led to significant changes when the cells were treated with glucose in the presence or absence of glyoxal or methylglyoxal. The presence of glyoxal further increased membrane fluidity when compared to the cells that were only kept in glucose. Previous studies have treated erythrocytes with glyoxal and observed its conversion to oxalates, a metabolic waste product, by a glyoxalase system (*Knight et al., 2016*). This conversion is especially pronounced when intracellular glutathione levels are depleted, leading to oxalate accumulation, which is known to have detrimental effects on cell metabolism and redox homeostasis (*Kumar et al., 2021*). Despite the small sample size, the findings provide preliminary insights into the complex interactions between glucose, glyoxal and membrane fluidity in erythrocytes. The metabolic fate of glyoxal and its potential implications for cell metabolism and redox homeostasis, as indicated by the observed increase in membrane fluidity, highlight areas for future research. Isotope tracing is a technique that can be used to elucidate how glyoxal is metabolised within the cell and its downstream effects on cellular metabolism and redox status. To investigate the specific molecular mechanism underlying the observed increase in membrane fluidity associated with glyoxal exposure,

techniques such as proteomics and lipidomics could be employed to identify changes in proteins and lipid composition that could contribute to altered membrane fluidity.

Erythrocytes use glucose in the pentose phosphate pathway where NADPH is produced and then used to make glutathione (Wang *et al.*, 2021). This is an important antioxidant defence mechanism of RBCs, as glutathione helps neutralise reactive oxygen species and carbonyl compounds such as glyoxal and methylglyoxal (Meister and Anderson, 1983, Rahman and Adcock, 2006, Rabbani and Thomalley, 2008). In conditions of lower glucose availability, such as 5 mM, RBCs may have a reduced capacity to produce NADPH and glutathione than at higher glucose concentrations, such as 100 mM. However, it is important to note that 5 mM glucose is not considered a condition of low glucose availability for erythrocytes, as glucose enters the cell freely through GLUT1, and the  $K_m$  for hexokinase is typically less than 0.1 mM glucose, meaning the enzyme is fully saturated and operating at  $V_{max}$ . Therefore, glucose metabolism is not limited at this concentration (Aubert-Foucher *et al.*, 1984, Gerber *et al.*, 1970). A possible explanation of the reduced membrane fluidity observed at 5 mM in comparison to 100 mM glucose could be a decreased antioxidant capacity. So, lower glucose exposure may contribute to oxidative damage, protein glycation and alterations in membrane fluidity. This emphasised the importance of cellular energy metabolism and antioxidant defence mechanisms in maintaining membrane integrity and function under conditions of oxidative and carbonyl stress.

A recent investigation carried out by Thomas and colleagues found that RBCs contain fatty acid desaturases (FADs), suggesting a mechanism by which they could increase the amount of polyunsaturated fatty acids in the membrane. They were also able to show that fatty acid desaturation was triggered by oxidative stress (i.e. incubation with hydrogen peroxide). This could represent a compensatory mechanism to preserve membrane fluidity in the face of oxidant challenge to structural proteins and membrane lipids (Thomas *et al.*, 2021). This compensatory mechanism could be one explanation for the increased membrane fluidity observed in RBCs under high glucose concentrations. Exploring whether high glucose levels induce oxidative stress in the erythrocyte model could provide valuable insights into this phenomenon.

To test the hypothesis regarding fatty acid desaturation activity, several experimental approaches can be considered. Firstly, alterations in the composition of fatty acids in RBC membranes can be assessed using liquid chromatography (LC) coupled with mass

spectrometry (MS). By analysing the fatty acid profile of RBC membranes after exposure to different glucose concentrations or in individuals with different health statuses, such as healthy and diabetic, changes in the ratio of saturated to unsaturated fatty acids can indicate variations in desaturase activity. Additionally, the use of specific fatty acid desaturase inhibitors can help elucidate the role of FADs in regulating membrane lipid composition and fluidity. Stable isotope labelling techniques, such as employing  $^{13}\text{C}_{16}$  palmitate and  $^{13}\text{C}_{18}$  linoleate followed by mass spectrometry analysis, as utilized by Thomas and colleagues, offer a valuable means of tracing fatty acid metabolism and assessing desaturase activity in erythrocytes.

The increase in membrane fluidity observed after some treatments opposed the hypothesis that an increasing glucose concentration would decrease membrane fluidity. It also contrasted with the results from a study carried out by Tapia and colleagues; where they treated RBCs with glucose (5.5; 12.5 and 25 mM) for 24 hours and tested membrane fluidity using 1  $\mu\text{M}$  laurdan (incubation 1 hour at 37°C) (Tapia *et al.*, 2021). They showed significant differences between glucose physiological control (5.5 mM) and treatments (12.5 mM and 25 mM), where there was a decrease in membrane fluidity. However, they also saw that the GP reached a plateau at 12.5 mM glucose, with no further difference in GP from 12.5 mM and 25 mM glucose.

One explanation for this disparity lies in the difference in experimental temperatures between the two studies. Tapia and co-workers conducted their experiments at room temperature, while in the present study, the temperature was maintained at 37°C to match the physiological conditions of RBCs in the body. Membrane fluidity is closely linked to temperature, with higher temperatures generally promoting greater fluidity. At physiological temperatures, unsaturated fatty acids within the membrane become disorganized, leading to increased fluidity, while saturated fatty acids remain tightly packed (Leach and Cowen, 2014). Therefore, the discrepancy in results between the two studies could be attributed, at least in part, to the difference in experimental temperatures. Additionally, the differences observed in membrane fluidity in response to elevated glucose concentrations between the two studies may also suggest a potential interplay with cholesterol levels. One possibility is that at high glucose levels, through increased oxidative stress, may alter cholesterol distribution within the membrane. Since the effects of cholesterol on membrane fluidity differ below and above the transition temperature, these changes could impact membrane properties. At higher temperatures, cholesterol reduces the mobility of the phospholipids, making it more difficult for them to transition from an ordered to a disordered state (Cooper, 2000). Conversely, at

lower temperatures, cholesterol is found between phospholipid tails, disrupting regular packing, and lowering the freezing, or crystallization, point of the membrane (Cooper, 2000). Furthermore, conducting the experiments at 37°C helped simulate the *in vivo* conditions experienced by erythrocytes, which may have contributed to the observed increase in membrane fluidity in response to elevated glucose concentrations.

Furthermore, increased membrane fluidity in RBCs was observed by Bianchetti and colleagues, and these findings agree with some of the results obtained in the current investigation. They measured membrane fluidity similarly with laurdan in samples from patients suffering from type 1 diabetes mellitus. They observed an even greater increase in membrane fluidity when the patients also suffered from diabetic retinopathy (Bianchetti *et al.*, 2021).

Various concentrations of glucose were used to treat the cells during short- and long-term treatments. The concentrations ranged from physiological to pathological levels, although very high levels such as in the case of 50 mM and 100 mM glucose were used. Also, high concentrations of glucose such as 100 mM has been used previously by other researchers to treat RBCs (Viskupicova *et al.*, 2015). Nevertheless, it is important to validate findings from *in-vitro* with *in-vivo* studies to ensure that the observed *in-vitro* effects are relevant and meaningful in the context of living organisms. Sometimes treating the cells *in-vitro* means the conditions may not fully mimic the complexity of *in vivo* environment.

In summary, the results obtained in the present study done *in vitro* on the effect of several treatments of glucose on RBC membrane fluidity are not very clear. Short- and long-term treatments resulted in no obvious change in fluidity. However, the presence of glyoxal appeared to promote an increase in membrane fluidity, and the controls, 5 mM and 100 mM glucose containing no glycating compounds, showed significant difference with an increase in fluidity being observed at higher glucose levels. This highlights the complex and multifaceted nature of membrane dynamics.

Several parameters need to be taken into consideration in the current investigation. Pathological concentrations of glyoxal, or in the case of methylglyoxal substantially higher levels, were used to treat the cells. Media contained foetal bovine serum (FBS) which is known to contain antioxidants, so higher concentrations of glyoxal and methylglyoxal were used to ensure that the treatment reached the cells (Blank *et al.*, 2020). Mannitol was used as an osmotic control for short-term glucose treatment experiments and although it has been

extensively used for this purpose there are some factors to consider (*Hattori et al., 2000, El-Remessy et al., 2003*). Mannitol is often used to prevent haemolysis on RBCs, although the mechanism behind this is not well understood, and it can also present antioxidant properties by reducing levels of reactive oxygen species (ROS) (*Beutler and Kuhl, 1988, Antosik et al., 2018, Hess, 2006, Xu et al., 2019, Liu et al., 2010, El-Remessy et al., 2003, Karasu, 2000*). Nevertheless, mannitol has several properties which outweigh the disadvantages of its use, and these include its ability to cause osmotic stress; has similar molecular weight to glucose which leads to comparable effects on osmotic pressure; does not contain aldehyde groups (less reactive than glucose); and it is not metabolizable by RBCs. Besides mannitol, the cells were treated with 5 mM glucose, which was used as a physiological control representing basal glucose levels. For the long-term glucose treatment, where the cells were kept in increasing glucose concentrations for several days, no osmotic control was present. The main reason for this is that RBCs need glucose to produce ATP through the process of glycolysis and removing glucose was not possible. However, during long-term glucose treatment the cells were treated with glucose for a prolonged period of time and any acute osmotic change may have been diminished due to the cells adapting to changes in their environment.

It is important to mention that a limitation in the current study is the small sample size, and validation of the approach on a larger population is necessary. Also, during long-term glucose treatment the cells were kept in media for only five days; a longer glucose exposure would have been a better representation of the chronic ongoing hyperglycaemia observed in diabetes mellitus. However, in preliminary experiments, increased cell death was detected when RBCs were under high levels of glucose, as also reported in Chapter 6. It is important to mention that laurdan does not provide any information on what causes changes in membrane fluidity and therefore detailed studies of membrane composition, such as mass spectrometry analysis of membrane lipids, are needed.

Future work would need to include the analysis of erythrocytes from diabetic subjects, type 1, and type 2 diabetes mellitus, and comparing the results with those obtained *in-vitro*, which will also help validate *in-vitro* findings. The reason for including both types of diabetes is due to the possibility of differences in RBC membrane fluidity between subjects suffering from type 1 and type 2 diabetes mellitus. In the present study, membrane fluidity appeared to increase after RBCs were aged in very high glucose levels and even more so in the presence of glyoxal when compared to the control, which correlated with previous findings on RBCs from type 1 diabetic individuals. So, measuring the activity of fatty acid desaturases at increasing

concentrations of glucose *in-vitro*, and in samples from diabetic volunteers, as well as carrying out lipidomic analysis of RBCs will help with understanding the underlying complex mechanisms involved in the modulation of RBC membrane fluidity in diabetic conditions.

# Chapter 4

## ***In vitro* studies of the effect of glucose and ageing on erythrocyte membrane tension**

## 4.1 Introduction

Membrane tension is an important regulator of cellular processes such as membrane trafficking, cell spreading, phagocytosis and polarity (*Colom et al., 2018, Sitarska and Diz-Munoz, 2020*). There are three major forces that can act on cell membranes and generate membrane tension: (i) osmotic pressure between cytosol and the surrounding medium (ii) membrane interaction with cytoskeleton, and (iii) adhesion forces to surfaces or other cells (*Kozlov and Chernomordik, 2015*).

Various techniques have been used to measure membrane tension (Figure 4.1). The first measurements were performed on erythrocytes in the 1970s using micropipette aspiration and membrane tether pulling assays (*Evans, 1973*). Currently other techniques, such as atomic force microscopy and optical tweezers, are being used (*Pontes et al., 2017*). Optical tweezers use a highly focused laser beam where a coated bead is trapped. The bead is then attached to a cell and a membrane tether is extracted. The bead position is recorded over time and the force calculated (*Pontes et al., 2017*). Atomic force microscopy, with the use of coated cantilevers, is used to measure the force required to pull and hold membrane tethers (*Bergert and Diz-Munoz, 2023*). The force required to extend such tethers can be used to measure membrane tension (*Pradhan et al., 2022*). Creating membrane tethers has limitations; the tether radius and the force required to maintain the tether measurements, needed for the calculations of the tension, are complex to obtain. The formation of membrane tethers requires peeling the membrane away from the actin cortex; the adhesion energy of the membrane onto the actin cortex adds up to the membrane tension value (*Colom et al., 2018*). Also, tether force is dependent on membrane tension and bending rigidity, so measuring the force on individual cells does not allow an absolute estimation of the membrane mechanical parameters (*Pontes et al., 2017*).

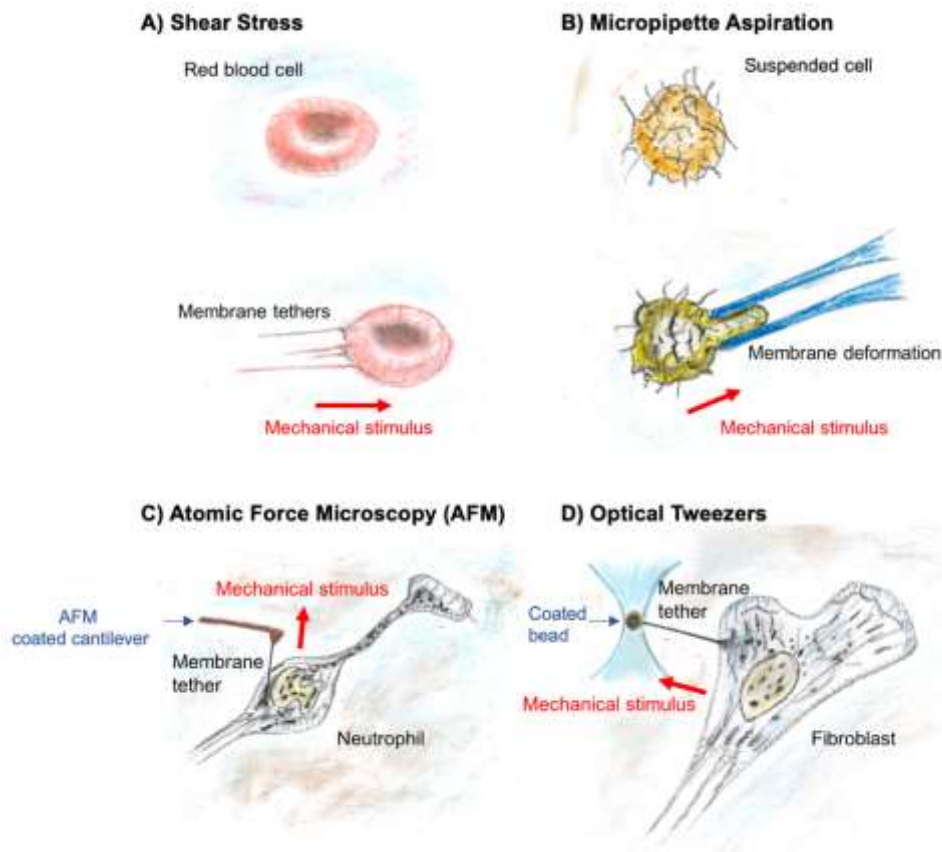


Figure 4. 1. Different illustrations of methods used to measure membrane tension. A) The erythrocytes attached onto coverslips subjected to fluid shear stress (flow channel assay). The cells deformed and membrane tethers begin to show. B) A portion of a cell aspirated into a small micropipette creating a tether. C) Atomic force microscopy (AFM) coated cantilever is used to pull and hold tethers D) A coated bead is trapped by optical tweezers (OT) and attached to a cell, the position of the bead is recorded over time and converted into force. *Reproduced from (Pontes et al., 2017) with permission granted from Elsevier. License no. 5647820490133.*

Recently, a non-invasive method was developed using fluorescent probes that allow membrane tension to be measured in living cells (Colom et al., 2018). The fluorescent probe Flipper-TR, also known as a fluorescent membrane tension reporter, is sensitive to lipid-packing and consists of two large dithienothiophene (DTT) moieties or flippers (Colom et al., 2018). Flipper-TR has a high photostability, does not disturb membrane order and can planarize upon increase of lateral pressure (Colom et al., 2018). Flipper-TR is mostly hydrophobic, but it has a hydrophilic head which helps the oriented insertion into the membrane. When the probe has inserted in the membrane, the hydrophobic forces that pack the lipids in the bilayer together exert pressure on the flipper probe and planarize it (Roffay et al., 2023). The planarization of the probe depends on the lipid composition; more ordered

membranes exert more force and provide more planarization than disordered membranes. In a non-confining environment, the two flippers are twisted out of co-planarity (Colom *et al.*, 2018).

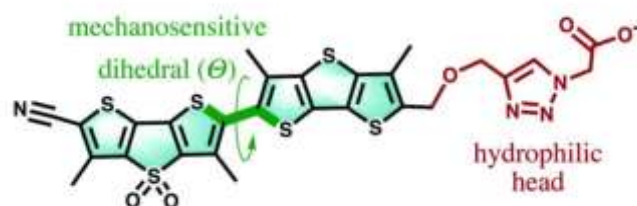


Figure 4. 2. Molecular structure of Flipper-TR, showing the two flippers and the mechanosensitive dihedral (Licari *et al.*, 2020). Licensed under a creative commons attribution-noncommercial 3.0 unported license (CC BY-NC 3.0).

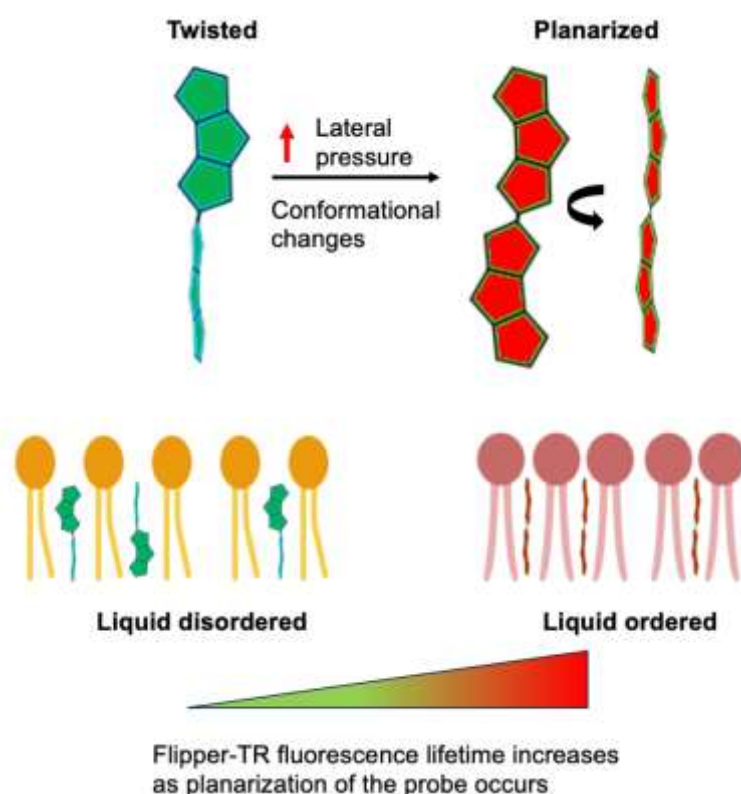


Figure 4. 3. Flipper TR and membrane tension. Pressure along the axis of the Flipper-Tr probe can planarize the two fluorescent groups, leading to changes in excitation and fluorescence lifetime (Colom *et al.*, 2018). Adapted from (Roffay *et al.*, 2023) and (Colom *et al.*, 2018). Springer Nature license number 5720221448262 for (Colom *et al.*, 2018) and CC BY-NC-ND 4.0 DEED for bioRxiv (Roffay *et al.*, 2023).

Flipper-TR design is a planarizable push-pull system, which means that the fluorophore can experience a complete charge transfer process from electron-donors to electron-acceptors upon excitation (*Assies et al., 2021*). Mechanical planarization is responsible for a spectrum of configurations from planar to twisted configuration, which affects the photo-physics and notably the lifetime of the probe. When the molecule is planarized, the photon emission efficiency is increased (*Roffay et al., 2023*). Lateral forces within the membrane directly set the twisting and therefore the photo-physics of the flipper probe. The high sensitivity of Flipper-TR allows it to report membrane tension variations by changes of the lifetime of their excited state (or fluorescence lifetime). Fluorescence lifetime is the best way to report conformational changes of flippers within the lipid bilayer. The lifetime of Flipper changes with lipid composition; in ordered membranes where lipid packing is higher, the acyl chains can exert more force on the probe and provide more planarization than disordered membranes (*Colom et al., 2018*). Ordered membranes are often made up of long saturated fatty acids, and present with less fluidity. The lifetime in the twisted state, is equivalent to highly disordered lipid membranes and can be as low as 2.3 ns, while in the planarized state or highly ordered membranes it can be 7 ns (*Roffay et al., 2023*). An experiment carried out by Goujon and co-workers measured Flipper-TR lifetime in ordered and disordered giant unilamellar vesicles (GUV) and reported increased membrane tension in ordered GUVs (*Goujon et al., 2019*).

Fluorescent lifetime imaging (FLIM) is a powerful technique to distinguish the molecular environment of fluorophores; and it is independent of fluorophore concentration (*Datta et al., 2020*). The fluorescent lifetime provides an absolute measurement which, compared to fluorescent intensity, is less susceptible to artefacts arising from scattered light, photobleaching, non-uniform illumination of the sample or excitation intensity variations (*Suhling, 2015*). However, fluorescence lifetime can be sensitive to temperature, fluorescence quenchers, polarity and pH (*Berezin and Achilefu, 2010*).

Fluorescence is a radiative process in which fluorophores decay to the ground state by emitting detectable photons. Fluorescence lifetime ( $\tau$ ) (Figure 4.4) can be defined as the average time a fluorophore remains in the excited state; and therefore it can be measured in the time-domain (*Datta et al., 2020*). During time-domain methods, a sample is excited using a pulsed laser and the decay is calculated from time-of-arrival of photons that are placed into a histogram. An advantage of using FLIM includes being able to distinguish between fluorophores with similar spectra using the fluorescence lifetime. A downside of the technique is a long acquisition time that may prevent visualisation of fast events (*Datta et al., 2020*).

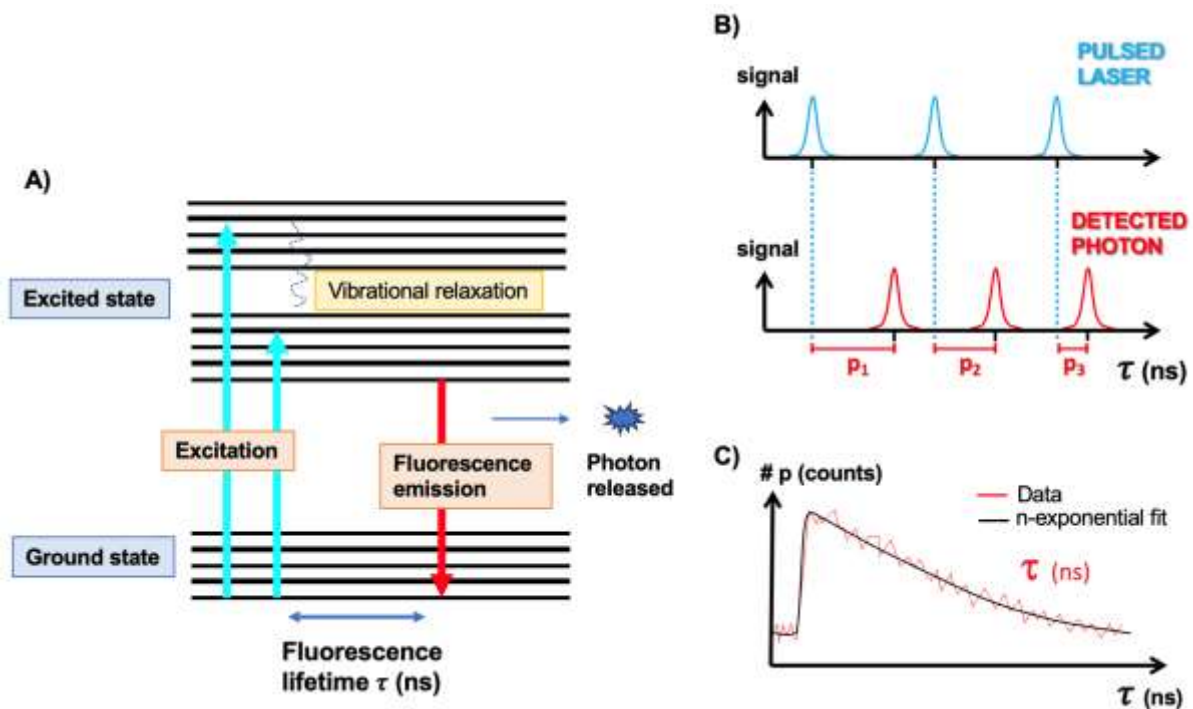


Figure 4. 4. Explanation of fluorescent lifetime imaging. A) A fluorophore in the ground state (low energy state) absorbs a photon, which takes the fluorophore to a higher energy state (excited state). The fluorophore returns to the ground state and emits a photon. When this happens, the light released is referred to as fluorescence emission. The emitted photon has lower energy than the absorbed photon, as some energy is lost through non-emitting processes (vibrational relaxation) leading to a red shift in the emission spectrum as compared to excitation (or absorption). The time it takes for the fluorophore to release the photon and return from the excited state to the ground state is called fluorescence lifetime. Fluorescence lifetime is obtained from a pool of molecules (all fluorophores within the confocal volume of observation), so the average time the molecules spend in the excited state is measured. B) Time-correlated single photon counting (TCSPC) allows the fluorescence lifetime to be measured. A pulsed laser is used to excite the fluorophores, and photons are detected using a sensitive detector capable of counting single photons. Then the time it takes for photons to be detected is measured. The photon arrival time is measured from a pool of molecules, so the average value of the arrival times is calculated, and this is referred to as FastFLIM. C) The distribution of the number of photons (counts) over time (in nanoseconds) can be fitted to an n-exponential decay model. The fit gives an estimation of the fluorescence lifetime properties of a sample. Then the information of the average photon arrival times can be assigned to every pixel and produce a FastFLIM image. Information adapted from Leica SP8 Falcon and (Luis A. J. Alvarez, 2019).

It is known that the mechanical properties of erythrocytes are altered by diabetes and increasing age (Wang *et al.*, 2021, Agrawal *et al.*, 2016). Erythrocyte membrane mechanical properties have been studied by haemolysis prediction (Faghih and Sharp, 2018), shear flow (Hochmuth *et al.*, 1973, Hochmuth and Evans, 1982), micropipette aspiration (Waugh and Evans, 1979), the use of fluorescent boron dipyrromethene (BODIPY) (which disappears from the membrane when tension increases) (D'Auria *et al.*, 2013), atomic force microscopy (Barns *et al.*, 2017) and optical tweezers (Zhu *et al.*, 2020). The latter method has been used to assess erythrocyte deformability in type 2 diabetes (Agrawal *et al.*, 2016). It is worth mentioning that measuring membrane tethers for a long period of time is challenging since actin polymerises inside the tethers within minutes and it may not be sufficient to resolve changes in fast and active processes (Pontes *et al.*, 2017). Furthermore, the processes by which membrane tension is regulated and propagated are still not well understood as methods to specifically measure it are currently limited (Sitarska and Diz-Munoz, 2020). Furthermore, Flipper-TR presents a reliable non-invasive method of measuring membrane tension in living cells (Colom *et al.*, 2018). The probe has been recently used on erythrocytes to measure membrane tension of cells infected with malaria parasite, Plasmodium (Kuehnel *et al.*, 2023). However, the *in vitro* effect of long-term glucose exposure on RBC membrane tension has not been investigated using the tension reporter probe or used on diabetic RBCs.

### **Aim and objectives:**

The aim of this chapter was to investigate the *in vitro* effect of increasing glucose concentration (in the presence or absence of glyoxal and methylglyoxal) and age on erythrocyte membrane tension. Glyoxal and methylglyoxal are known to be elevated in hyperglycaemia, and their excess formation can increase reactive oxygen species production and cause oxidative stress in the cells. They can react with proteins and lipids and are precursors of advanced glycation end products (AGEs). The hypothesis was based on the premise that erythrocyte membrane tension would increase as the cells aged in high glucose concentrations, and even more so in the presence of glyoxal and methylglyoxal. Flipper TR was used to measure membrane tension in fresh erythrocytes as well as erythrocytes aged in the presence of high glucose concentrations and glyoxal or methylglyoxal.

## 4.2 Materials and methods

All materials and methods are described in Chapter 2. Details of membrane tension studies are found in section 2.2.4.

## 4.3 Results

### 4.3.1 Assaying membrane tension of untreated erythrocytes, in the presence or absence of hypertonic and hypotonic treatments using Flipper-TR

Membrane tension of untreated cells (day 0) and their response to hypertonic and hypotonic treatments was investigated using the membrane tension reporter Flipper-TR. These controls were first used with the aim of cross checking if the probe worked as expected, i.e., increased Flipper TR lifetime in conditions that are estimated to increase membrane tension such as hypotonicity, and decreased lifetime in conditions expected to reduce membrane tension in such hypertonicity. The hypertonic control involved placing the erythrocytes in PBS containing 100 mM mannitol, while the hypotonic control involved placing the cells in a solution of 60% water and 40% PBS containing 5 mM glucose. Images acquired from each participant were analysed using LAS X software in order to obtain Flipper-TR fluorescence lifetime. Images from participant G are shown in Figure 5.5., which shows untreated cells (day 0, Figure 4.5A) and those under hypotonic (Figure 4.5B) and hypertonic (Figure 4.5C) solutions. The image of untreated cells showed several irregular shaped RBCs but most of the cells appeared green with a Flipper-TR average lifetime of 3.8 ns. Flipper-TR fluorescence lifetime can range, on average, from 2.8 to 7 ns, where a shorter lifetime is an indicative of less membrane tension. The cells under hypotonic condition showed a more uniformly round morphology, with more cells appearing yellow and red with an average lifetime of 4.5 ns. The increase in fluorescence lifetime indicated that planarization of the probe was taking place in the membrane, and hence an increase in erythrocyte membrane tension was observed. On the other hand, the cells under hypertonic condition appeared mostly green with an average lifetime Flipper-TR of approximately 3.6 ns and most RBCs showed echinocyte morphology.

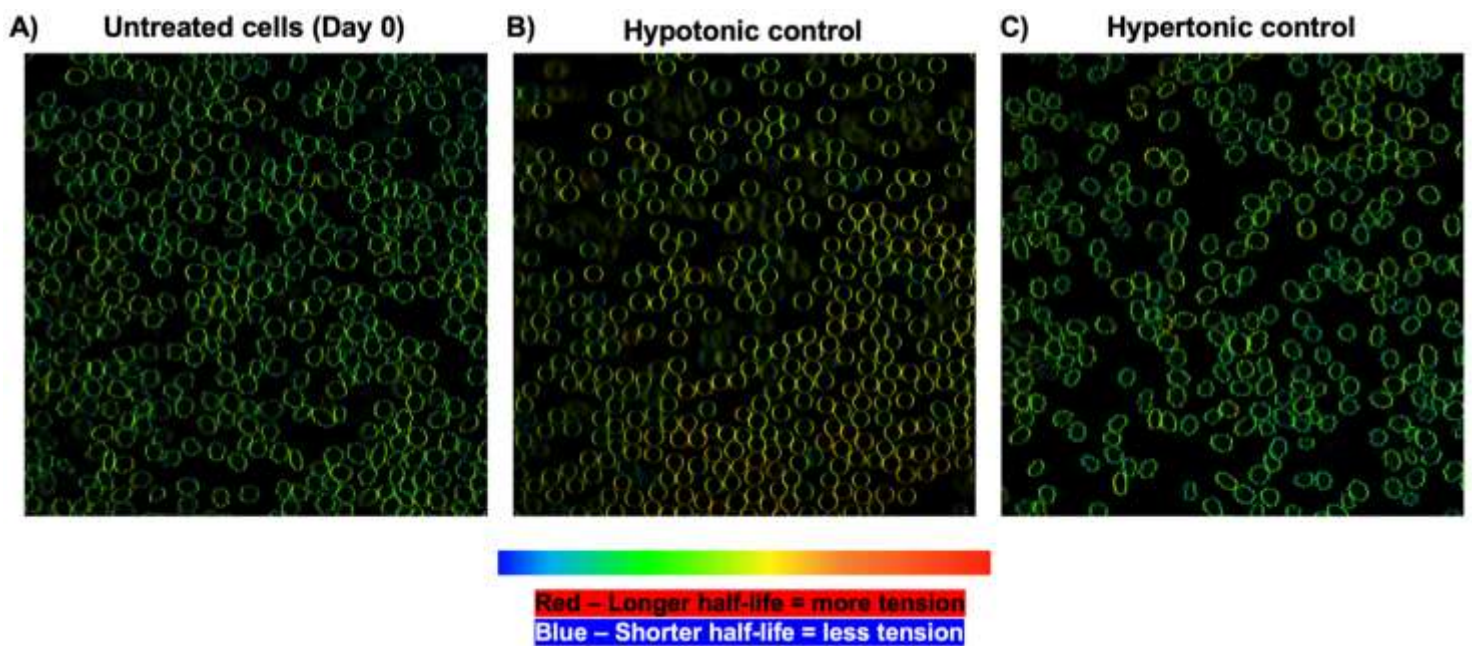


Figure 4. 5. Images acquired by FLIM of untreated erythrocytes and those under hypotonic and hypertonic conditions belonging to participant G. FastFLIM was used to obtain the images, which measured the photon arrival time from a group of molecules, so the average value of the arrival times was calculated, and the results interpreted as an array of pixels. The frame repetitions were set to 100, the format at 512x512 and the speed at 400Hz. The colour scale ranges from blue to red, where blue indicates less membrane tension (or shorter half-life) and red implies increased membrane tension (or longer half-life).

The next step was to analyse the results for each individual participant, which are shown in Figure 4.6. This was carried out with the aim of finding out if the same effect, after the cells were exposed to hypotonic and hypertonic solutions, was observed in each participant. Initially, untreated cells (day 0) were imaged and compared to hypotonic and hypertonic controls to test the range of the assay. The data showed significant differences between untreated cells and the hypotonic controls for all participants. Averaged values of 3.6 ns, 4.6 ns, 4.3 ns and 3.8 ns were obtained for untreated cells, whereas 5.7 ns, 5.2 ns and 4.6 ns were acquired for hypotonic controls for participants D, E, F and G, respectively. This confirmed that the hypotonic condition led to an increase in RBC membrane tension. On the other hand, a less apparent change was observed for cells in 100 mM mannitol (hypertonic control), values of 3.6 ns, 4.4 ns, 3.9 ns and 3.5 ns were obtained for participants D, E, F and G, respectively. Only participant G showed a significant change between untreated cells and

those in hypertonic solution. A significant difference was also observed between the two osmotic controls for all participants.

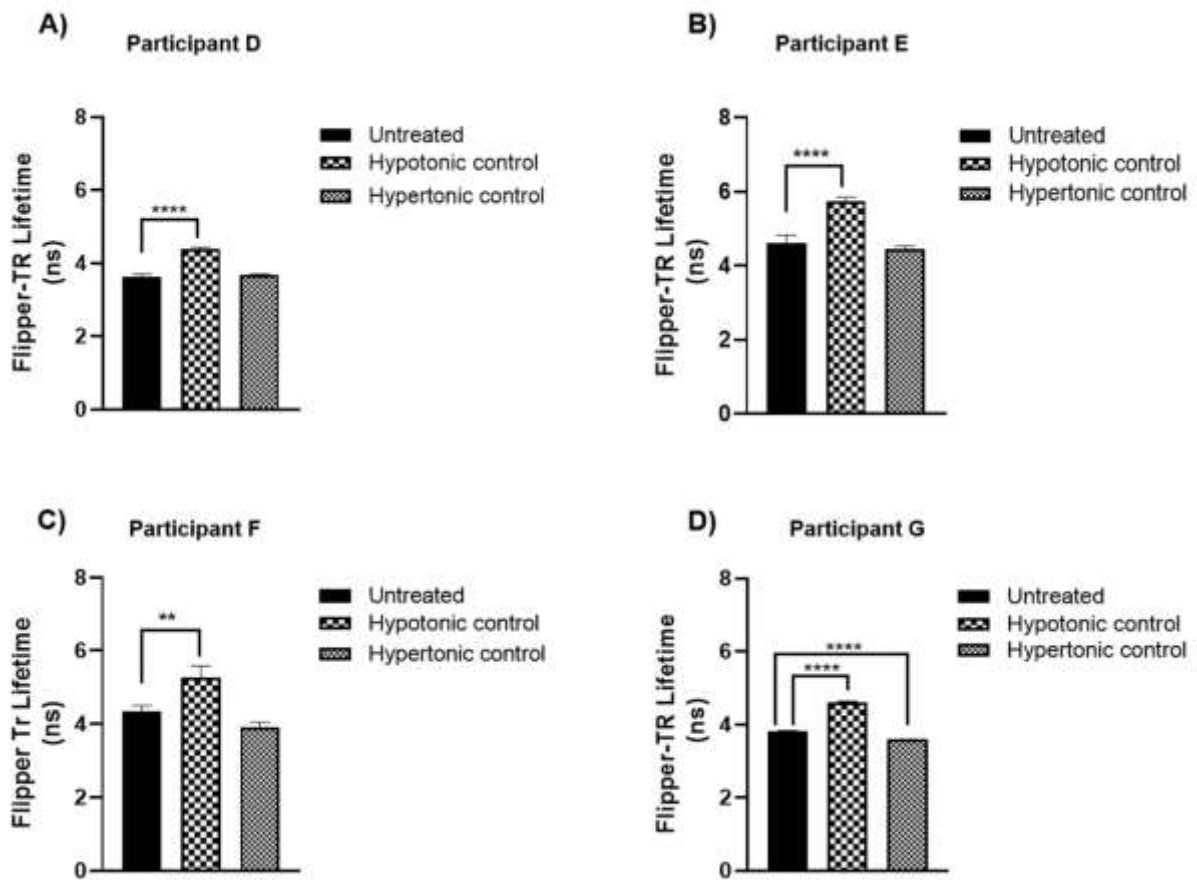


Figure 4. 6. Erythrocyte membrane tension assayed by Flipper-TR on untreated (day 0) and control cells per participant. Fluorescent lifetime measurements were taken by FLIM. A) participant D. B) participant E. C) participant F. D) participant G. Results shown as means  $\pm$  SD. Significance was defined by one-way ANOVA followed by Tukey's *post-hoc*. For participant D, a  $P$  value of  $<0.0001$  was obtained between the hypotonic control and untreated cells, as well as between the hypotonic and hypertonic controls. For participant E, a  $P$  value of  $<0.0001$  was obtained between untreated cells and hypotonic control, as well as between hypotonic and hypertonic controls. For participant F,  $P$  values of  $<0.005$  and  $<0.0001$  were obtained between untreated cells and hypotonic control, and between hypotonic and hypertonic controls, respectively. For participant G, a  $P$  value  $<0.0001$  was obtained between the hypotonic control and untreated cells, as well as between the hypotonic and hypertonic controls.

After analysing the results from each participant, the combined results were investigated with the aim of evaluating the averaged effect of hypotonic and hypertonic solutions on erythrocyte membrane tension. Figure 4.7 shows the combined data from four different participants. The hypotonic control appeared to increase the fluorescence lifetime. One-way ANOVA for matched subjects (repeated measures ANOVA) followed by Tukey *post hoc* test, which means that the same subjects are measured under different conditions, was used to compare untreated cells with hypotonic or hypertonic treatment. A significant difference was found between untreated cells (average Flipper-TR lifetime 4.0 ns) and the hypotonic control (average Flipper-TR lifetime 5.0 ns). Furthermore, significant differences were found between the hypertonic and hypotonic controls. However, the hypertonic control did not show any difference to the untreated sample (average Flipper-TR lifetime 3.9 ns).

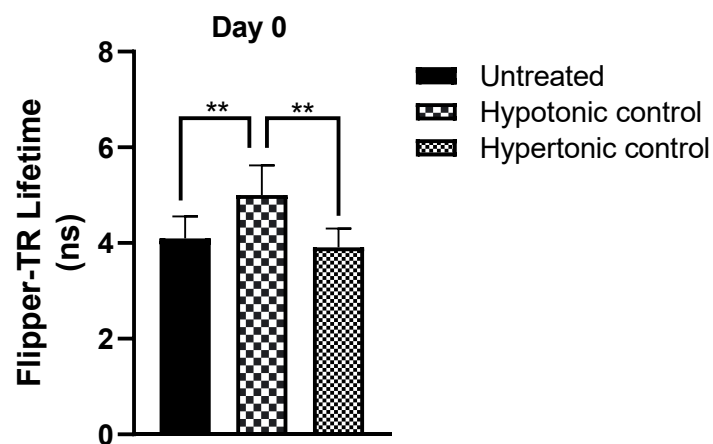


Figure 4. 7. Erythrocyte membrane tension assayed by Flipper-TR on untreated (day 0) cells ( $n=4$ ). Fluorescent lifetime measurements were taken by FLIM. The fluorescent probe Flipper-TR was used at a concentration of 1  $\mu\text{M}$ , and the hypotonic and hypertonic controls included 40% PBS containing 5 mM glucose plus 60% sterile water, and 100 mM mannitol, respectively. Results shown as means  $\pm$  SD of four biological samples corresponding to different participants (three technical replicates were also carried out). Significance was defined by one-way ANOVA for matched subjects (repeated measures ANOVA) followed by Tukey *post hoc* test. A  $P$  value of  $<0.005$  was obtained between untreated cells and the hypotonic control, and  $P<0.01$  between hypotonic and hypertonic controls.

#### **4.3.2 Effect of increasing glucose concentrations on erythrocyte membrane tension as the cells were aged *in vitro* for five days**

Once erythrocytes were isolated from whole blood and imaged on day 0, they were aged in media containing various glucose concentrations. Membrane tension was measured on day 4 using the probe Flipper-TR and the cells were imaged by FLIM. Images obtained from participant G on day 4 are shown in Figure 4.8. Cells that were kept in media containing 5 mM glucose (Figure 4.8A) looked mostly green (average lifetime of Flipper-TR in that image was 3.7 ns), although some cells looked red (shown in zoomed image) indicating higher membrane tension. Fewer RBCs showing red were observed for 22 mM glucose, which looked mostly green (Flipper-TR lifetime in the image was approximately 3.7 ns), although some of the cells appeared blue indicating low membrane tension in those cells. Echinocytes were present indicating membrane deformations (Figure 4.8B zoomed image). Thus, it appeared that membrane tension remained the same after the cells were aged in media containing 22 mM, although the morphology of the cells appeared different with more membrane deformations being observed at 22 mM. Echinocytes were less noticeable when the cells were kept in 100 mM and cells looked rounder with more yellow showing in the membranes (Flipper-TR fluorescent lifetime in the image 3.6 ns).

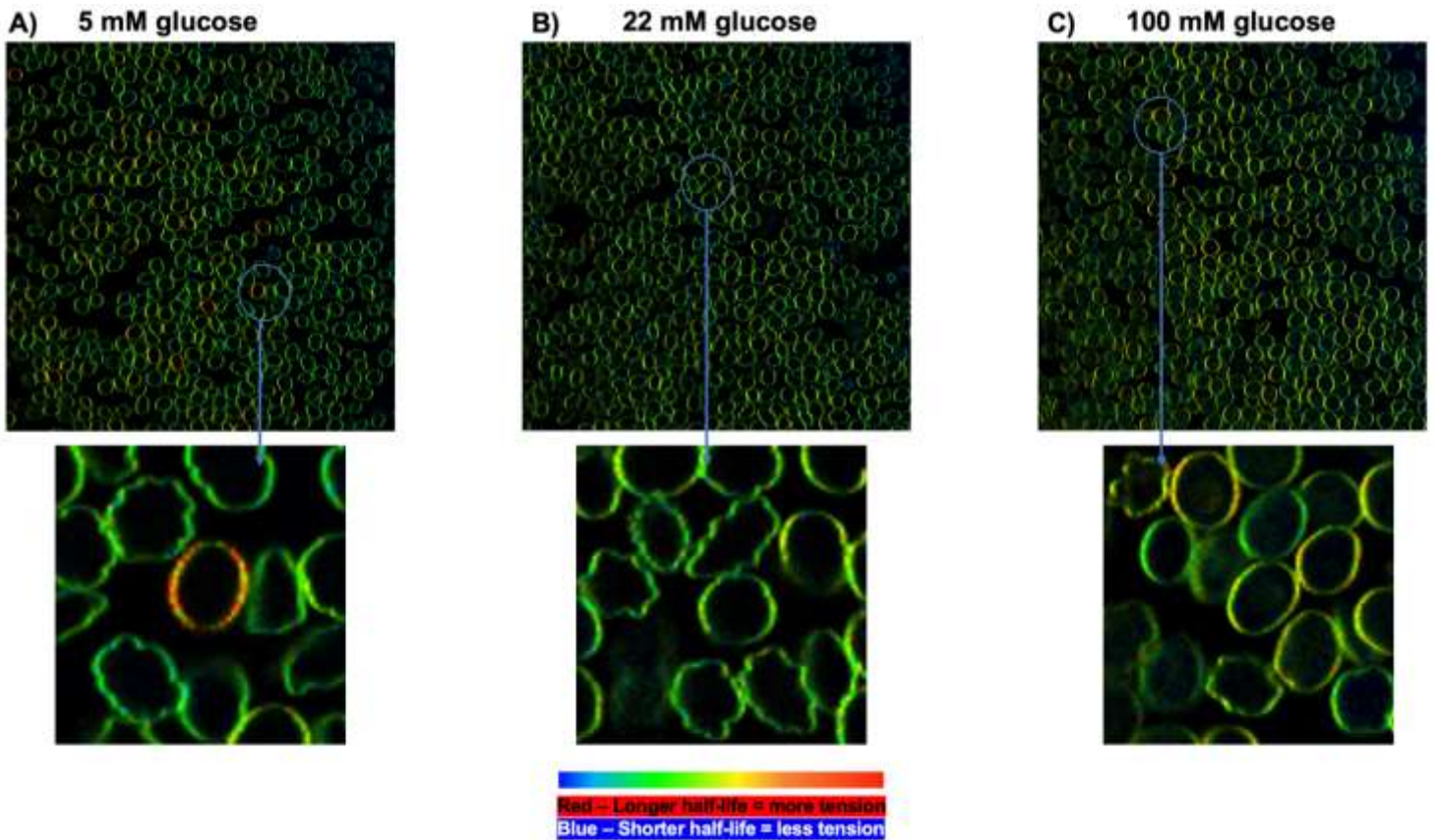


Figure 4. 8. Images of erythrocytes, aged in different glucose concentration (day 4), belonging to participant G. FastFLIM was used to obtain the images. The frame repetitions were set to 100, the format at 512x512 and the speed at 400Hz. The colour scale ranges from blue to red, where blue indicates less membrane tension (or shorter half-life) and red implies increased membrane tension (or longer half-life).

The experiments were carried out on other participants to determine whether this was a generalisable effect, and the data obtained for each participant is presented in Figure 4.9. Analysis of individual participants was carried out first in order to evaluate the effect of treatment on each subject. At this time the data corresponding to aged cells includes three participants, instead of four as for untreated cells. The reason for this is that cells from participant D did not survive being aged. The data from each participant was analysed and the results showed significant differences for all the participants between the physiological control and the pathological glucose concentrations used to age the RBCs *in vitro*. All the participants displayed an increase in membrane tension for the cells kept in 22 mM glucose, with participant G showing the smallest increase. Membrane tension increased when the cells were kept in 100 mM glucose for participant F. On the other hand, participant G had a lower Flipper-TR fluorescent lifetime at 100 mM than 5 mM glucose, showing the opposite effect to participants E and F. Another point to highlight is that Flipper-TR fluorescent lifetime from participants E and G under physiological glucose conditions was below 4 nanoseconds,

whereas it was above 4 nanoseconds for participant F, showing that membrane tension for participant F was slightly higher under physiological conditions. Furthermore, untreated cells (day 0) were compared with aged cells in 5 mM glucose for all participants and a significant difference was found only for participant E, where aged cells appeared to have a reduced membrane tension (Figure S9). For participants F and G no significance was found, although it is important to highlight that the trend in RBC membrane tension from each participant appeared different after being aged in 5 mM glucose, i.e., membrane tension seemed to increase for participant F and remained the same for participant G (Figures S11 and S13).

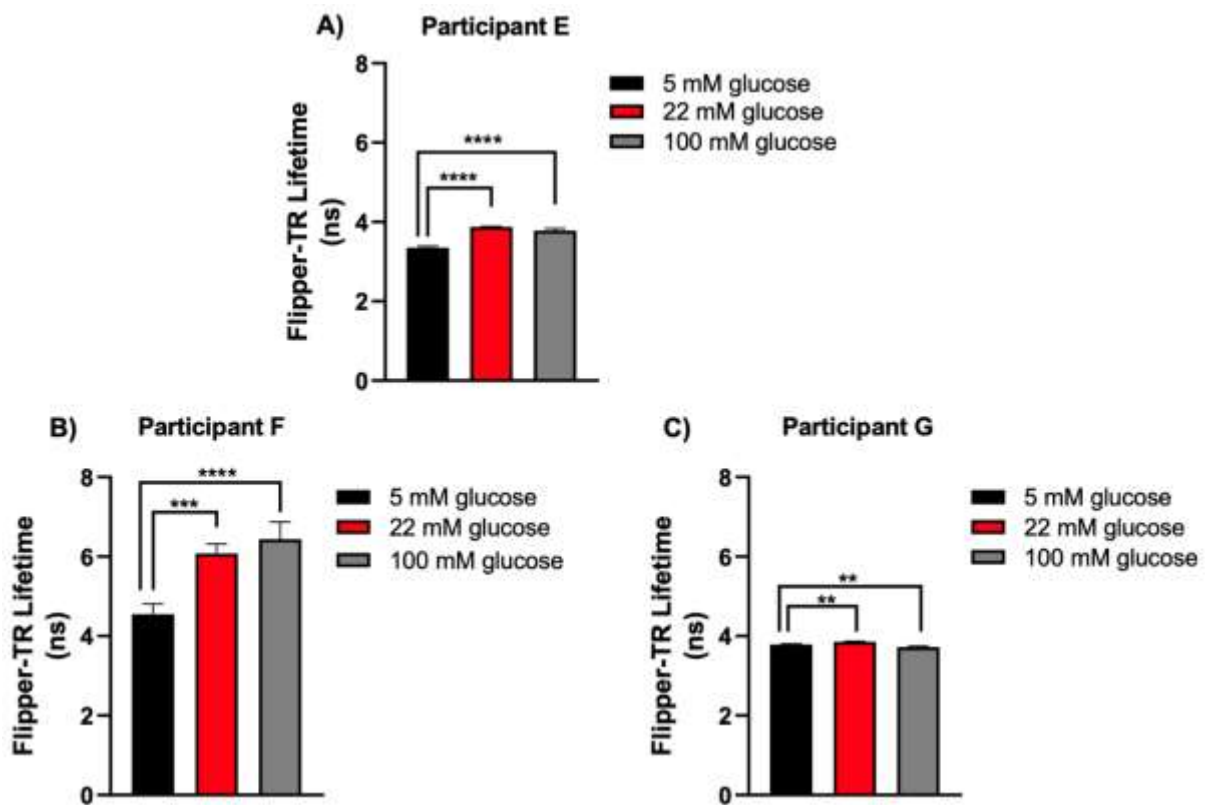


Figure 4. 9. Erythrocyte membrane tension assayed by Flipper-TR on erythrocytes aged in media containing different glucose concentrations. Fluorescent lifetime measurements were taken by FLIM. A) Participant E. B) Participant F. C) Participant G. Results shown as means  $\pm$  SD. Significance was determined by one-way ANOVA followed by Dunnett's *post-hoc*. For participant E, a  $P$  value of  $<0.0001$  was obtained between 5 mM and 22 mM, as well as between 5 mM and 100 mM. For participant F, a  $P$  value of  $<0.0005$  was observed between 5 mM and 22 mM,  $<0.0001$  for 5 mM and 100 mM. For participant G, a  $P$  value of  $<0.01$  was observed between 5 mM-22 mM, as well as for 5 mM-100 mM.

Further analysis was carried out to compare the differences between the osmotic controls on days 0 and 4 for each participant. A significant difference between hypotonic controls between days 0 and 4 was observed for participants E and F (Figures S10A and S12A). Flipper-TR fluorescence lifetime values of 5.7 ns and 4.2 ns were obtained for participant E and 5.2 ns and 6.1 ns for participant F for days 0 and 4, respectively. This showed that RBCs from the two participants had different responses to hypoosmotic conditions after being aged in media containing 5 mM glucose, as an increase in membrane tension was observed for one participant and a decrease for the other one.

After analysing the results from each participant individually, the combined data was analysed. The combined data for the controls on day 4 (Figure 4.10A) was analysed to investigate if untreated and aged cells behaved differently when exposed to osmotic changes. The average Flipper-TR fluorescence lifetime for day 4 was 5.0 ns and 3.4 ns for hypotonic and hypertonic controls, respectively. No significant differences were found between combined data on day 4 from cells aged in 5 mM glucose and the osmotic controls.

Further analysis was carried out to compare if there were differences between the combined data from the osmotic controls on days 0 and 4, and no significant difference was observed (Figures S16 A and 16B). Furthermore, no significant differences were found for the combined data after ageing the cells in media containing different glucose concentrations (Figure 4.10B). It seemed that membrane tension almost reached a plateau after 22 mM glucose. Also, no significant difference was found between the combined data from untreated (day 0) cells and those kept in media containing 5 mM glucose (Figure S15), although the trend shows a slight decrease after the cells were aged under physiological conditions (average Flipper-TR fluorescence lifetime of 4.0 ns and 3.8 ns for days 0 and 4, respectively).

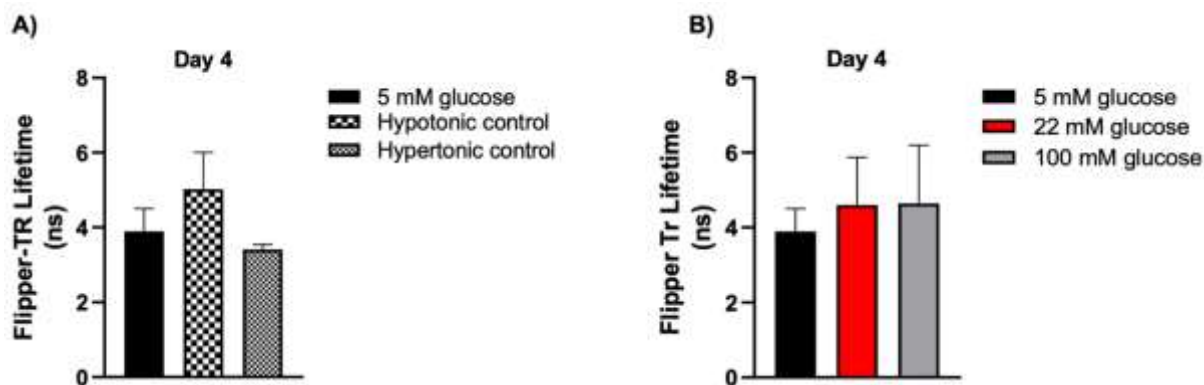


Figure 4. 10. Combined data of erythrocyte membrane tension measured by Flipper-TR fluorescent lifetime. The cells were kept in media containing 5 mM, 22 mM, and 100 mM glucose. Flipper-TR was used at a concentration of 1  $\mu$ M. The hypotonic control included placing the cells in 40% PBS containing 5 mM glucose, and 60% sterile water, whereas the hypertonic control included placing the cells in 100 mM mannitol. Data obtained for the controls are shown in Figure A, and those for glucose treatments are shown in Figure B. Results shown as means  $\pm$  SD of three biological samples corresponding to three different participants ( $n=3$ ). Significance was defined by one-way ANOVA for matched subjects (repeated measures ANOVA) followed by Tukey *post hoc* test.

### 5.3.3 Effect of increasing glucose concentrations in the presence of glyoxal and methylglyoxal on erythrocyte membrane tension as the cells were aged *in vitro* for five days

After investigating the effect of ageing erythrocytes in different glucose concentrations on membrane tension, the combined effect of glucose with glyoxal or methylglyoxal was investigated. Glyoxal and methylglyoxal are potent glycating agents found elevated in diabetes and can react with proteins and phospholipids in the membrane leading to structural alterations and changes in membrane activity. These changes may include increased rigidity, altered membrane fluidity, and disruption of normal protein functions, which can impair cellular processes. Pathological levels of glyoxal and methylglyoxal were used in the treatment of the cells. Erythrocytes from the same participants who took part in the study of the effect of glucose on membrane tension were used. Images from participant G are shown in Figure 4.11, which shows erythrocytes aged in 5 mM, 22 mM and 100 mM glucose being treated with 1  $\mu$ M glyoxal and 5  $\mu$ M methylglyoxal (Figures 4.11 A-F). Cells kept in 5 mM glucose treated with glyoxal (Figure 4.11A) appeared mostly green with some of the cells showing yellow, which would indicate an increase in membrane tension. The average lifetime of Flipper-TR in the image was 3.7 ns. Erythrocytes kept in 5 mM glucose but treated with methylglyoxal (Figure 4.11B) presented a mixture of colours ranging from blue, green, yellow and red. This

indicated a combination of different Flipper-TR lifetimes in the RBC membranes denoting different membrane tensions. However, the average Flipper-TR lifetime in the image was 3.6 ns.

RBCs kept in 22 mM glucose treated with glyoxal (Figure 4.11C) appeared green and yellow with some cells showing red around their membranes. The average fluorescence lifetime of Flipper-TR in the image was 3.6 ns. On the other hand, cells aged in 22 mM glucose treated with methylglyoxal (Figure 4.11D) appeared mostly yellow, with some cells showing red around the membranes indicating an increase in membrane tension. The average Flipper-TR fluorescence lifetime in the image was 3.8 ns.

Ageing cells in 100 mM glucose and treating them with glyoxal (Figure 4.11E) led to several cells showing red in their membrane, indicative of increased membrane tension. The average Flipper-TR fluorescence lifetime in the image was 3.9 ns. On the other hand, fewer cells appeared red when the cells kept in 100 mM glucose were treated with methylglyoxal (Figure 4.11F); the average fluorescence lifetime of Flipper-TR was 3.6 ns.

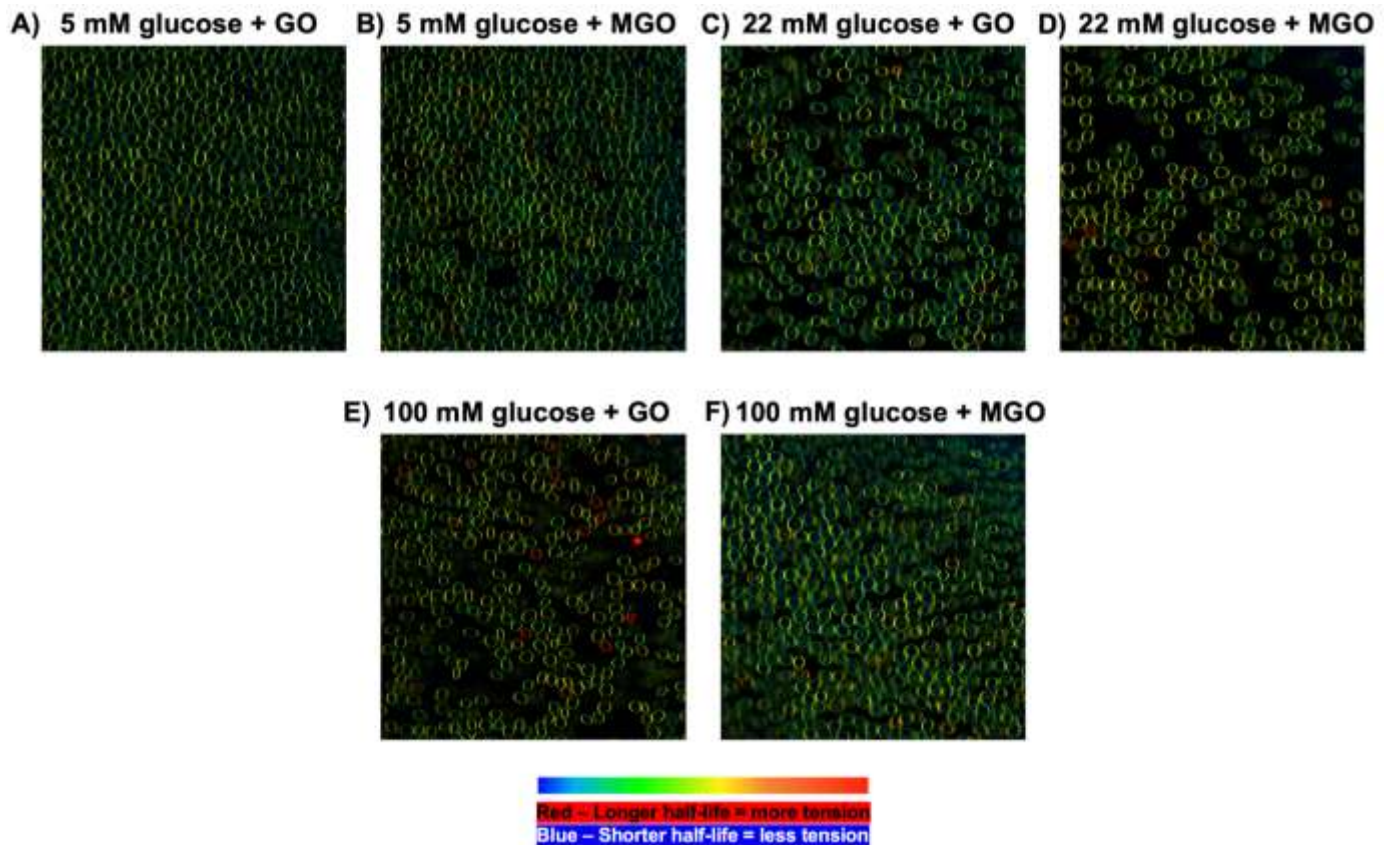


Figure 4. 11. Images of RBCs corresponding to participant G. The cells were aged in different glucose concentration (day 4) and treated with 1  $\mu$ M glyoxal or 5  $\mu$ M methylglyoxal. FastFLIM was used to obtain the images, measuring the photon arrival time from a group of molecules, so the average value of the arrival times was calculated, and the results interpreted as an array of pixels. The frame repetitions were set to 100, the format at 512x512 and the speed at 400Hz. The colour scale ranges from blue to red, where blue indicates less membrane tension (or shorter half-life) and red implies increased membrane tension (or longer half-life).

Further data analysis looking at individual results from each participant was carried out and variable results were observed. Figure 4.12 shows the results obtained for each participant when the cells were kept in 5 mM glucose, although the changes in membrane tension caused by the glycating agents were statistically significant for all participants, the effect on membrane tension were somewhat different between them. For participants E and F, the presence of glyoxal caused an increase in RBC membrane tension, whereas for participant G a decrease was observed. Similar results were detected for methylglyoxal, when comparing the results to the controls.

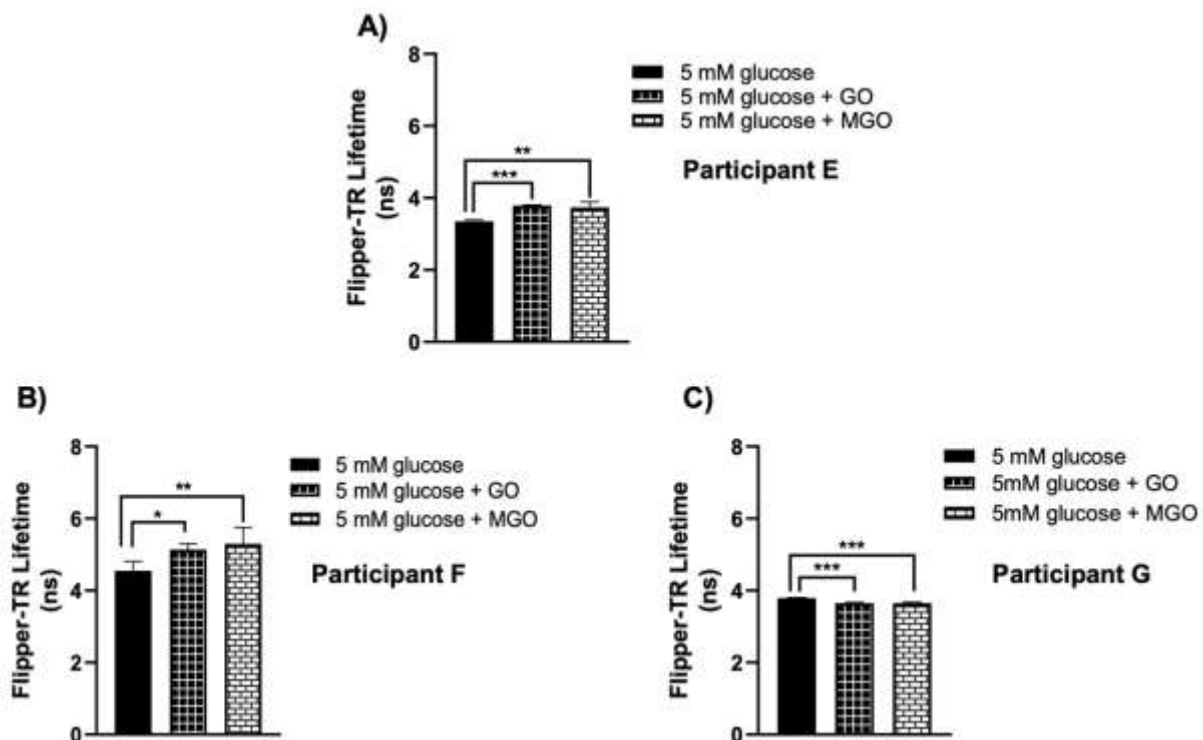


Figure 4. 12. Membrane tension assayed by Flipper-TR on erythrocytes aged in media containing 5 mM glucose in the presence or absence of glyoxal and methylglyoxal. Fluorescent lifetime measurements were taken by FLIM. A) Participant E. B) Participant F. C) Participant G. Results shown as means  $\pm$  SD of three technical replicates. Significance was defined by one-way ANOVA followed by Dunnett's *post-hoc* test. For participant E a  $P$  value of  $<0.0005$  and  $<0.005$  were obtained for glyoxal and methylglyoxal, respectively.  $P$  values of  $<0.05$  and  $<0.01$  were obtained for glyoxal and methylglyoxal for participant F. A  $P$  value of  $<0.0005$  was obtained for both, glyoxal and methylglyoxal, for participant G.

The effect of glyoxal and methylglyoxal in combination with pathological concentrations of glucose for each participant is shown in Figure 4.13. No significant changes were observed for the results from participant E when the cells were aged in 22 mM glucose and treated with glyoxal or methylglyoxal (Figure 4.13A). On the other hand, significance was obtained between cells kept in 100 mM glucose and those kept in 100 mM glucose in the presence of glyoxal, where a small increase in membrane tension was observed (Figure 4.13B). Data

obtained from participant F, where RBCs were incubated with 22 mM and 100 mM glucose showed a more consistent trend (Figures 4.13C and D). No significant difference was found for the cells kept in 22 mM glucose in the presence of glyoxal. However, a significant difference was found in the presence of methylglyoxal, where a decrease in membrane tension was observed. Adding glyoxal and methylglyoxal to cells aged in 100 mM glucose appeared to cause a decrease in membrane tension, with methylglyoxal causing the highest decrease. A significant difference was found for cells kept in 22 mM glucose in the presence of glyoxal for participant G (Figure 4.13E), showing a decrease in membrane tension. Methylglyoxal also caused a significant change, in this case also a decreased membrane tension. Furthermore, cells from participant G kept in 100 mM glucose (Figure 4.13F) show no significant changes in membrane tension in the presence of either glyoxal or methylglyoxal. The effect of the glycating compounds detected for participant G was similar to that observed for participant E.

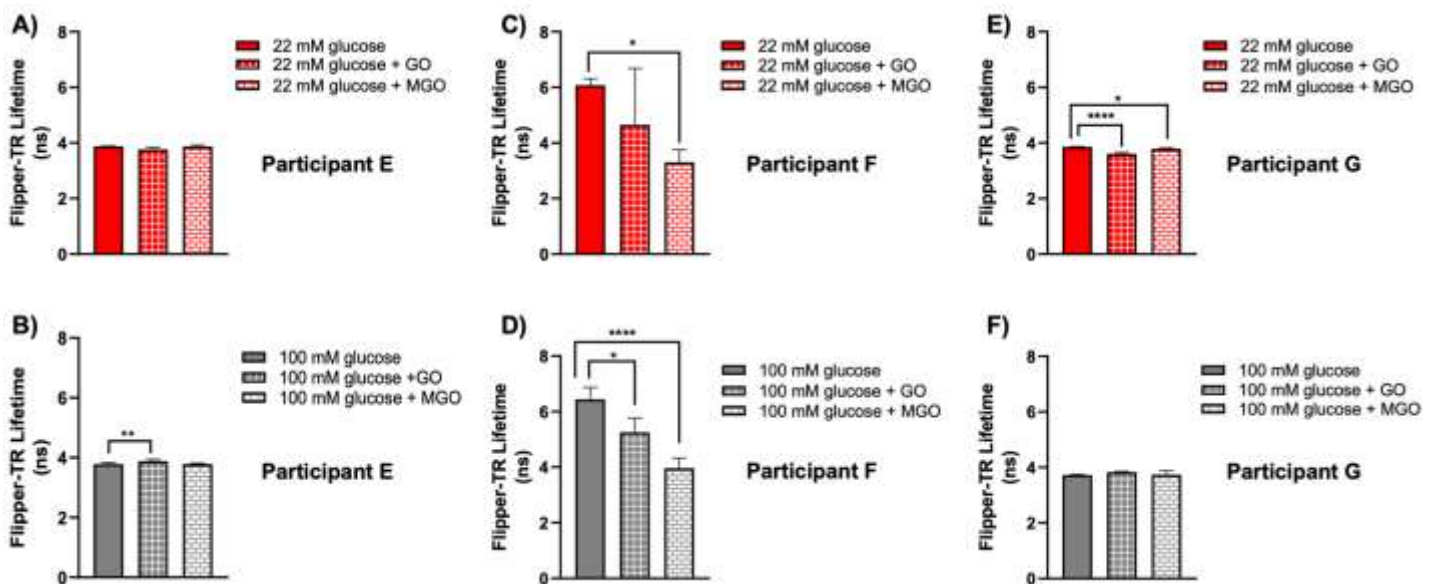


Figure 4. 13. Membrane tension assessed by Flipper-TR on erythrocytes aged in media containing 22 mM and 100 mM glucose and treated with 1  $\mu$ M glyoxal and 5  $\mu$ M methylglyoxal. Fluorescent lifetime measurements were taken by FLIM. A) Participant E, cells aged in 22 mM glucose (+/- GO or MGO). B) Participant E, cells kept in 100 mM glucose (+/- GO or MGO). C) Participant F, cells aged in 22 mM glucose (+/- GO or MGO). D) Participant F, cells aged in 100 mM glucose (+/- GO or MGO). E) Participant G, cells aged in 22 mM glucose (+/- GO or MGO). F) Participant G, cells kept in 100 mM glucose (+/- GO or MGO). Results shown as means  $\pm$  SD of three technical replicates. Significance was defined by one-way ANOVA followed by Dunnett's *post hoc* test. Significance was found for participant E between 100 mM-100mM/GO, with a *P* value of <0.005. For participant F, *P* values of <0.05, <0.05 and <0.0001 were obtained between 22 mM-22 mM/MGO, 100 mM-100 mM/GO and 100 mM-100 mM/MGO, respectively. Significance for participant G at 22 mM treatment included *P* values of <0.0001 and <0.05 for 22 mM-22mM/GO and 22 mM-22 mM/MGO, respectively.

After analysing individual results for each participant and observing some significant changes in membrane tension, the combined results were investigated (Figure 4.14). Physiological levels of glucose in the presence of glycating compounds appeared to cause an increase in Flipper-TR fluorescence lifetime, whereas Flipper-TR lifetime at pathological levels of glucose in the presence of glycating compounds appeared to decrease, although no significant changes in membrane tension were observed for the cells aged in 5 mM, 22 mM and 100 mM glucose in the presence of glyoxal and methylglyoxal.

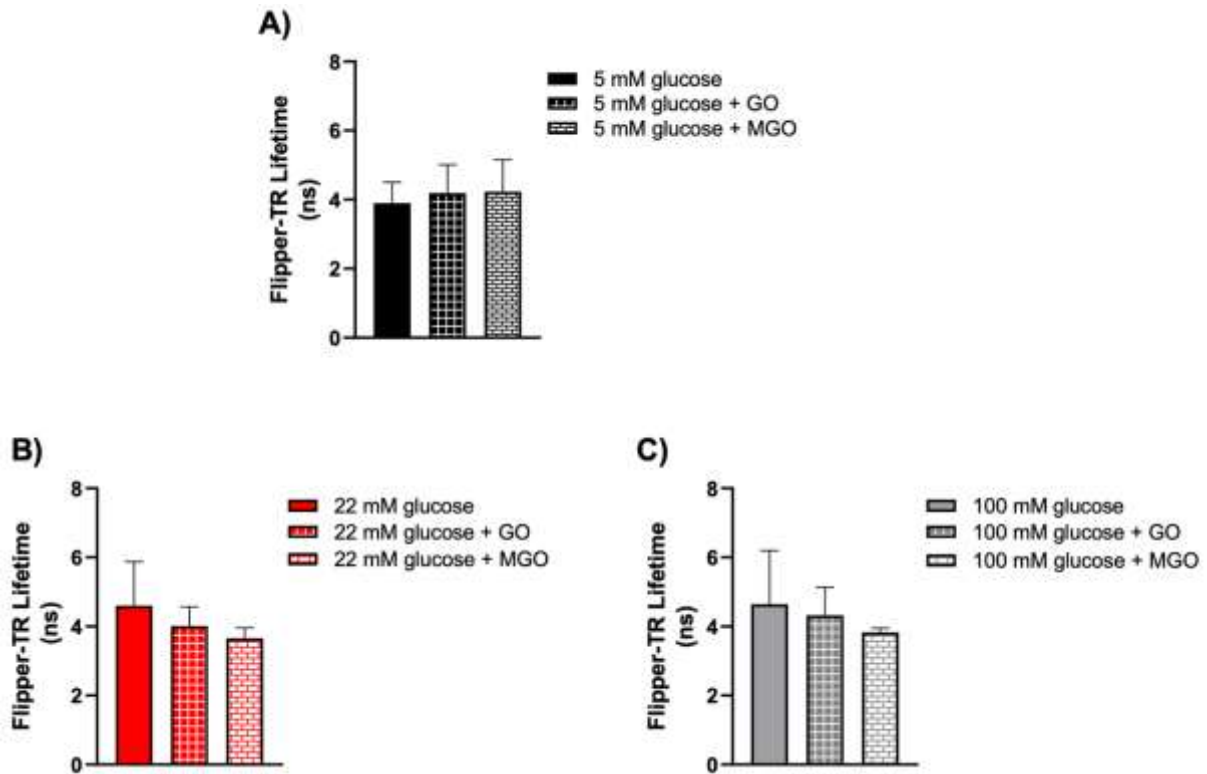


Figure 4. 14. Combined erythrocyte membrane tension data from three different participants ( $n=3$ ). RBC membrane tension was measured by using the fluorescent probe Flipper-TR at a concentration of  $1 \mu\text{M}$  and imaging was carried out by using FLIM. The cells were kept in media containing 5 mM (A), 22 mM (B), and 100 mM glucose (C). The cells were also treated with  $1 \mu\text{M}$  glyoxal and  $5 \mu\text{M}$  methylglyoxal. Results shown as means  $\pm$  SD. Significance was defined by one-way ANOVA for matched subjects (repeated measures ANOVA) followed by Tukey post hoc test.

## Discussion

Membrane tension plays a number of important roles in the physiological functions and physicochemical properties of the membrane such as membrane trafficking and cell polarity. The current investigation was performed to assess the possible relationship between increasing concentrations of glucose, *in vitro* ageing of erythrocytes and membrane tension using the fluorescent probe Flipper-TR, which is highly sensitive to lipid-packing. Flipper-TR fluorescence lifetime increases as planarization of the probe occurs, corresponding to increased membrane tension. It is worth mentioning that Flipper-TR was commercialised in 2018, and very little work has been carried out in erythrocytes using this probe (Chen *et al.*, 2023).

Lipid membranes are viscoelastic bilayers separating cells from their environment. They are easy to bend but resistant to stretching: their lysis tension (the tension at which they lyse), is high, which protects the cells against lysis upon processes that stretch the cell membrane, but it cannot protect from the high stretch generated by hypotonic shocks (Roffay *et al.*, 2021). Incubation of RBCs in hypotonic solutions causes cells to take up water and swell, which is expected to lead to an increase in membrane tension. On the other hand, cells placed in a hypertonic solution, such as pathological levels of glucose, containing a higher concentration of solute compared with the solution inside the cells causes the cytoplasmic volume to decrease through water expulsion, leading to a decrease of plasma membrane tension (Mercier *et al.*, 2020). The hypotonic and hypertonic tests were carried out to check that the probe behaved as expected and the results confirmed it worked as predicted, although the range was quite small. Significant differences were found for all participants between the hypotonic and hypertonic controls, hypotonic controls and untreated cells, as well as those cells kept under physiological levels of glucose (5 mM) and hypotonic controls. The hypotonic shock induced on the RBCs had a higher impact at increasing membrane tension than the hypertonic shock at decreasing it. This can be observed by the hypotonic effect on membrane tension across all the participants was significant in causing an increase in tension, whereas the hypertonic effect was not always significant, and the change observed was normally small. This variability observed between participants under hypertonic conditions could be due to individual differences in erythrocyte membrane composition and cytoskeletal integrity. Factors such as variations in lipid composition, levels of membrane proteins, and the overall health of the erythrocytes can influence how the cells respond to hypertonic stress.

A study carried out by Assies and colleagues measured membrane tension following induced hyperosmotic stress in HeLa cells using Flipper-TR and reported a decrease in fluorescence lifetime; values of 4.8 ns and 4.2 ns were obtained for the cells in isotonic and hypertonic solutions respectively (Assies *et al.*, 2021). Overall, HeLa cells seemed to have a slightly more elevated membrane tension when compared to RBCs (values of 4.1 ns and 3.8 ns were obtained for untreated cells and those aged in physiological levels of glucose, respectively). This difference could be attributed to the fact that HeLa cells are adherent, and RBCs were kept in suspension. It has been shown that membrane tension increases with higher adhesion (Lieber *et al.*, 2013). On the other hand, a higher reduction in membrane tension was observed in HeLa cells when placed in a hypertonic solution than RBCs (values of 3.9 ns and 3.4 ns were obtained on days 0 (untreated) and 4 (5 mM), respectively).

Also, in the case of erythrocytes, the hypertonic control seemed to be more effective when the cells were tested on day 4 than on day 0. Interestingly, the hypotonic control remained the same on days 0 and 4 for combined participant data (5.0 ns), increasing membrane tension to a critical magnitude, and could lead to pore formation, causing lysis of the cells and inducing leakage (efflux) of their internal contents (Alam Shibly *et al.*, 2016). Furthermore, two participants showed significant differences in membrane tension when the effect of hypotonicity was compared between untreated cells and those aged in 5 mM glucose, although opposite changes were observed i.e., an increase in membrane tension for older cells when exposed to hypotonic changes in one participant, and a decrease in membrane tension for the other one.

Results from individual participants showed significant changes in membrane tension, i.e., an increase, as the cells were aged in increasing glucose concentrations (except for one of three participants at 100 mM glucose). These results agree with the initial hypothesis that ageing the cells in increasing glucose concentrations would lead to an increase in membrane tension. Significant changes were also found for all the participants when the cells were in physiological levels of glucose in the presence of glyoxal and methylglyoxal. The changes observed in the presence of the glycating agents varied among different participants, i.e., increase or decrease in membrane tension. Keeping the cells under pathological levels of glucose and adding glyoxal or methylglyoxal provided less reliable results. However, statistically significant changes were observed for some of the participants, and these indicated a reduction in membrane tension.

Cells aged in physiological levels of glucose showed no significant changes from those untreated. However, a significant difference was found between untreated cells and those aged in 5 mM glucose for one participant where a reduction in tension was observed in aged cells. Recently, Kuehnel and co-workers measured membrane tension in erythrocytes and reported an average Flipper-TR fluorescence lifetime of just above 3 ns, which is lower than the average lifetime for untreated cells in the present study (just below 4 ns). (*Kuehnel et al., 2023*). This indicates that in the current investigation membrane tension in erythrocytes was higher.

Keeping erythrocytes in media containing increasing concentrations of glucose led to an increase in membrane tension as the glucose concentration increased. All participants showed an increase in membrane tension after the cells were kept in 22 mM glucose. Keeping the cells in 100 mM glucose showed an increase in membrane tension for two participants and a decrease for one. The results acquired contrast with the results obtained by *Tapia et al.*, where they incubated RBCs with 5.5 mM, 12.5 mM and 25 mM glucose for 24 hours. They reported a decrease in membrane tension as glucose increased, although there was a difference in incubation time between the two studies. In the current investigation, erythrocytes were aged in media for five days to try and simulate the chronic glucose exposure present in diabetes mellitus, and this same treatment time was used in Chapter 3 (Erythrocyte membrane fluidity studies) because in earlier work no differences were observed following short term incubations.

A recent study carried out by *Bravo and colleagues* investigated how foetal erythrocytes were affected by gestational diabetes mellitus (GDM). In the study they obtained erythrocytes from the placenta after delivery, and reported that foetal RBCs from GDM had higher membrane tension when compared to healthy foetal RBCs (*Bravo et al., 2023*). The increase in membrane tension found in GDM foetal RBCs agrees with the results obtained in the present study. One possible explanation for the increase in tension observed can be due to increased lipid peroxidation, glycation, and lower antioxidant activity which is often observed in RBCs from patients that suffer from diabetes. Lipid peroxidation, which leads to modifications of lipid composition and the asymmetry of the bilayer, can contribute to increased membrane stiffness and reduced membrane deformability (*Buys et al., 2013*).

An important question is how and why an increase in membrane tension occurs. An explanation includes alterations of the cytoskeletal proteins that connect the bilayer and the spectrin network, which can impact erythrocyte membrane integrity, when encountering shear

stress (*Buys et al., 2013*). The erythrocyte membrane-cytoskeleton linkage depends on molecular interactions between spectrin and band 3-ankyrin (*Blanc et al., 2010*). Band 3 is plasma membrane integral protein whose expression is decreased in RBCs from diabetic patients. Also, spectrin, band 3, and ankyrin have been reported to be highly susceptible to post-translational modifications associated with oxidative stress and glycation. So, another possible cause for the increase in membrane tension observed may be due to a link between oxidative stress and glycation (as a result of hyperglycaemia) causing mechanical alterations of the RBC membrane, affecting its function (*Tapia et al., 2021*).

It is thought that an increase in membrane tension can lead to dispersion in the hydrophobic chains reducing lipid packing and increasing fluidity (*Reddy et al., 2012*). Lipid composition also plays an important role, the physical properties of the individual lipid domains guide the local changes required for adapting to a change in tension. Lateral movement, rotation and flipping of lipids between the leaflets of the plasma membrane are physical changes that work together to allow the fluid membrane to adapt to changes in membrane tension (*Horn and Jaiswal, 2019*). Recently it has been shown that increased oxidation of membrane lipids can cause increased membrane tension, activation of the Piezo1 channel and depressed activity of the Na<sup>+</sup>/K<sup>+</sup> ATPase (*Hirata et al., 2023*). Piezo1 is a mechanosensitive ion channel that opens in response to mechanical stimuli, allowing positively charged ions, including calcium, to flow into the cell (*Ridone et al., 2019, Wu et al., 2017*).

Glyoxal and methylglyoxal are two potent glycating agents known to be elevated in diabetes with plasma levels of methylglyoxal and glyoxal in diabetes as high as 0.9  $\mu\text{M}$  and 1  $\mu\text{M}$ , respectively (*Kold-Christensen et al., 2019, Bierhaus et al., 2012, Han et al., 2007*). Both agents can cause changes to the membrane by increasing lipid peroxidation and glycation of protein and amino containing phospholipids accelerating the formation of advanced glycation end products. Pathological levels of these treatments were added to cells aged in different glucose concentrations to evaluate the change in membrane tension. Due to lower reactivity of methylglyoxal compared to glyoxal, a higher concentration of methylglyoxal (5  $\mu\text{M}$ ) was used to account for factors such as dilution effects, while 1  $\mu\text{M}$  glyoxal was used to reflect its greater reactivity. Several studies have previously reported how different factors can affect RBC membrane tension including a malaria parasite, different types of haemoglobin, osmotic changes and glucose (*Alimohamadi and Rangamani, 2023, Tapia et al., 2021, Frohlich et al., 2019, Betz et al., 2009*). However, the effects of these glycating agents in combination with glucose have not been investigated on ageing RBCs before. Adding glyoxal or methylglyoxal to RBCs kept in physiological levels of glucose showed slightly different results across

participants. For two participants an increase in membrane tension was observed, whereas the other participant showed a decrease. Increasing glucose concentrations to pathological levels and adding glyoxal or methylglyoxal did not cause a major change in membrane tension for two participants; a decrease in membrane tension at 22 mM glucose in the presence of glyoxal and methylglyoxal was observed for one, and an increase in membrane tension at 100 mM glucose in the presence of glyoxal for the other one. However, for the remaining participant a decreased membrane tension was also observed, especially at 100 mM glucose. A possible explanation for the decrease in membrane tension in the presence of high glucose and glyoxal and methylglyoxal, could be related to increased oxidative stress leading to cytoskeletal dynamic impairment and detachment from the bilayer. Hyperglycaemia, as well as glucose degradation products such glyoxal and methylglyoxal, can cause oxidative stress in RBCs and lead to the activation of protein kinase C (PKC) (*Giri et al., 2018*). It has been shown that overactivation of PKC can lead to a decrease in membrane tension. PKC phosphorylates 4.1R protein, resulting in an increased dissociation of the spectrin network. Protein 4.1R is a multifunctional protein essential for maintaining RBC shape and mechanical properties through interactions with spectrin and actin (*Takakuwa, 2000*).

Membrane tension is dynamic and heterogenous, reflecting the complex interplay of mechanical, biochemical and biophysical factors that modulate cellular membrane properties. Images of erythrocytes treated with glyoxal, and methylglyoxal displayed a mixture of colours indicating different Flipper-TR lifetimes in the erythrocyte membranes and thus denoting different membrane tensions. Membrane tension can occur and change dynamically when various processes are taking place in the membrane such as membrane protein activity (*Yan et al., 2024*). A recent study carried out in human fibroblasts reported that indentation and aspiration increased tension locally, indicating that tension does not propagate across the cell membrane (*Luchtefeld et al., 2024*). In contrast, when the perturbation directly involved the underlying cell cortex and the membrane, a global change in membrane tension was sensed throughout HL-60 cells, a lymphocyte-derived cell line (*De Belly et al., 2023*). Conversely, in lipid vesicles or cellular membrane lacking a cortex in-plane membrane tension can propagate globally (*Sitarska and Diz-Munoz, 2020, Luchtefeld et al., 2024*). Plasma membrane tension in cells can be greater and more local than in pure lipid vesicles due to factor such as peripheral protein binding, the presence of transmembrane proteins and interactions with the cytoskeleton. These factors provide additional resistance to membrane area changes and can constrain such changes to a localised area of the cell (*Sitarska and Diz-Munoz, 2020*).

It has been reported that erythrocytes from diabetes mellitus patients present low deformability and high mechanical fragility (*Lippi et al., 2012*). This can be an indication of increased membrane tension in RBCs, making the cells more prone to lysis when under mechanical or osmotic stress. Furthermore, a study carried out by Agrawal and colleagues where the deformability of RBCs from diabetic individuals was studied, reported significantly swollen RBCs in the diabetic group in comparison to age matched healthy controls (*Agrawal et al., 2016*). This may imply metabolic disturbances in diabetes affecting RBCs size and hence, membrane tension (as swollen RBCs would generally have higher membrane tension).

There are several factors to take into consideration that can influence the lifetime of Flipper-TR. These include changes in pH, temperature, the fluidity of the membrane and membrane lipid composition. Low pH can cause protonation of phospholipid headgroups leading to decreased membrane fluidity, whereas an increase in pH can lead to deprotonation of headgroups (increasing the negative charge on the headgroups) leading to electrostatic repulsion between neighbouring lipids resulting in greater separation between lipid molecules and increased membrane fluidity (*Furuike et al., 1999, Ghazvini et al., 2018, Angelova et al., 2018*). The temperature used to incubate erythrocytes in the present study was 37°C; at this temperature the membrane is expected to be fluid. Fluid membranes exert less pressure on Flipper-TR than more rigid membranes so less planarization can occur, which will yield a lower lifetime value. Lipid membrane composition also plays an important role; ordered membranes, such as lipid rafts and cholesterol content, exert more pressure on Flipper-TR causing planarization and an increase in fluorescence lifetime. So, there are several factors other than the cytoskeleton influencing the results, which highlight the complex and multifaceted nature of membrane dynamics.

There were various limitations in this study including the small sample size, which would require validation on a larger population. In the present study the cells were aged in media containing various glucose concentrations for five days. A longer glucose exposure would have been a better representation of the chronic ongoing hyperglycaemia observed in diabetes mellitus. It is important to mention that some cells did not survive being exposed to the high glucose concentrations during the five-day treatment, so increasing the number of days of treatment might not be possible. Erythrocytes need glucose to survive and produce ATP through the process of glycolysis, which means that having the right osmotic control for long-term glucose treatments is challenging. To have the appropriate osmotic controls, the cells will need to undergo short term glucose treatment, which will allow for the right controls to be present; and these studies can be carried out in the future. This will allow a comparison

of long and short-term glucose exposure on RBC membrane tension. However, in the present study RBCs were treated with glucose for a prolonged period of time and any acute osmotic change may have diminished due to the cells adapting to changes in their environment. An important limitation is that it was all observational changes, no experiments were carried out to investigate how the changes occurred. After validating the current results on a larger number of samples, the next step would be to measure membrane tension on RBCs from diabetic individuals. This will allow a comparison of the *in vitro* and *in vivo* studies and get a better understanding of membrane tension changes in cells that are constantly exposed to ongoing increased glycaemia.

Furthermore, investigating the role of the cytoskeleton, which involves assessing the structural integrity of key cytoskeletal proteins like spectrin and actin, along with other factors such as lipid composition, oxidative stress, protein glycation would provide valuable insights into the mechanisms underlying changes in membrane tension. Techniques such as co-immunoprecipitation and co-localization studies could be used to investigate protein-protein interactions, while mass spectrometry could be employed to analyse lipid and protein modifications. Additionally, super-resolution microscopy could provide detailed insights into the spatial organisation of these molecular components within the erythrocyte membrane.

In conclusion, the participants included in this study showed that ageing RBCs *in vitro* with increasing glucose concentrations can lead to changes in membrane tension. The presence of glyoxal and methylglyoxal can also alter erythrocyte membrane tension, and as these studies have not been carried out before, they are expected to serve as the basis for future research. However, further work is required to understand the underlying mechanisms leading to such changes in membrane tension. Lipid peroxidation and glycation due to elevated glucose concentrations seem to play a crucial role on RBC deformability and are increased in diabetes and ageing. Understanding the exact changes taking place in the bilayer (lipid changes), and the cytoskeleton may help comprehend the increase in membrane tension, and the fluctuations observed when the glycating compounds were elevated.

# Chapter 5

***In vitro* studies of the effect of glucose and ageing on erythrocyte reactive oxygen species (ROS) production and phosphatidylserine (PS) exposure on outer membrane leaflet**

## 5.1 Introduction

Hyperglycaemia can enhance glycation and the generation of ROS, and that weakens the antioxidant power causing oxidative damage in erythrocytes (Qasim *et al.*, 2023). Oxidative stress, induced by an increase of ROS or failure in the antioxidant mechanism, is the cause of many pathologies, including diabetes (Nowotny *et al.*, 2015). The accumulation of ROS within erythrocytes can affect membrane structure and function leading to membrane integrity deficiency, low deformability and phosphatidylserine (PS) exposure (Wang and Zennadi, 2021).

PS is located in the inner leaflet of the membrane, but its translocation to the outer membrane serves as a signal (Bever and Williamson, 2016). PS exposure is a hallmark of erythrocyte ageing and senescence, marking cells for clearance by macrophages (Lutz and Bogdanova, 2013). This process ensures the removal of aged and potentially dysfunctional erythrocytes from circulation. Additionally, PS exposure is associated with eryptosis, a form of programmed cell death in erythrocytes, triggered by stress conditions such as oxidative stress (Lutz and Bogdanova, 2013). This marker is particularly relevant to diabetes because elevated blood glucose levels lead to increase oxidative stress, which can induce eryptosis in erythrocytes (Obeagu, 2024).

Chemiluminescence, fluorescence-based assays, electron paramagnetic resonance spectroscopy and amplex red assay can all be used to measure reactive oxygen species production (Kalyanaraman *et al.*, 2012). Chemiluminescence technique measures oxidative end products between ROS and certain reagents such as luminol (reacts with superoxide anion, hydroxyl radical and hydrogen peroxide), the reaction causes light to be emitted, which is measured by a luminometer (Agarwal *et al.*, 2004). Electron paramagnetic resonance, also known as electron spin resonance, can detect the interaction between electromagnetic radiation and unpaired electrons in paramagnetic species (Rana *et al.*, 2010, Kevan, 2003). ROS such as superoxide radicals, hydroxyl radicals and other oxygen centred radicals, possess unpaired electrons, which give rise to their paramagnetism (He *et al.*, 2014). When subjected to a magnetic field and microwave radiation, the unpaired electrons in ROS can undergo a transition between energy levels, resulting in the absorption or emission of electromagnetic radiation at specific frequencies (Suzen *et al.*, 2017). Spin traps, such as 5,5,-dimethylpyrro- line N-oxide (DMPO), are used to trap and stabilised free radicals, including those that are ROS (He *et al.*, 2014). They contain a functional group that reacts with the radical species, forming a more stable radical adduct and allowing them to be detected by

electron spin resonance (*He et al., 2014*). The amplex red assay is based on the oxidation of amplex red (10-acetyl-3,7-dihydroxypenoxazine) which is catalysed by horseradish peroxidase in the presence of hydrogen peroxide to produce a fluorescent oxidation product called resorufin (*Karakuzu et al., 2019*). Furthermore, the most widely used method for ROS assay is fluorometry and there are several fluorescent dyes which have been used extensively to quantify ROS, for example dihydroethidium (DHE) or dichlorodihydrofluorescein diacetate (DCFH-DA, also commonly known as DCF-DA) and its derivatives (*Wang and Zou, 2018, Pasciu et al., 2023*).

Other techniques that allow intracellular ROS production, and also PS exposure, to be measured in the cells include flow cytometry and microscopy (*Tetz et al., 2013, Pasciu et al., 2023*). These require the use of sensitive and specific fluorescent probes (*Winterbourn, 2014*). Microscopy can provide information of the effects of ROS on cell morphology and cell adhesion, whereas flow cytometry is an effective and quick method to detect and quantify intracellular ROS (*Wu and Yotnda, 2011*). The principle of this technique involves the analysis of each cell for visible light scatter and or multiple fluorescence parameters (Figure 5.1) (*McKinnon, 2018*). Visible light scatter is measured in two different directions (Figure 5.2): the forward direction (FSC or forward scatter) suggesting the relative size of the cell or particle, and the side scatter (SSC) which indicates the internal granularity of the cell. Light scatter is independent of fluorescence (*McKinnon, 2018*). One key advantage of flow cytometry is that, unlike other methods, intracellular levels of ROS can be studied on a cell-by-cell basis (*Luo et al., 2002*).

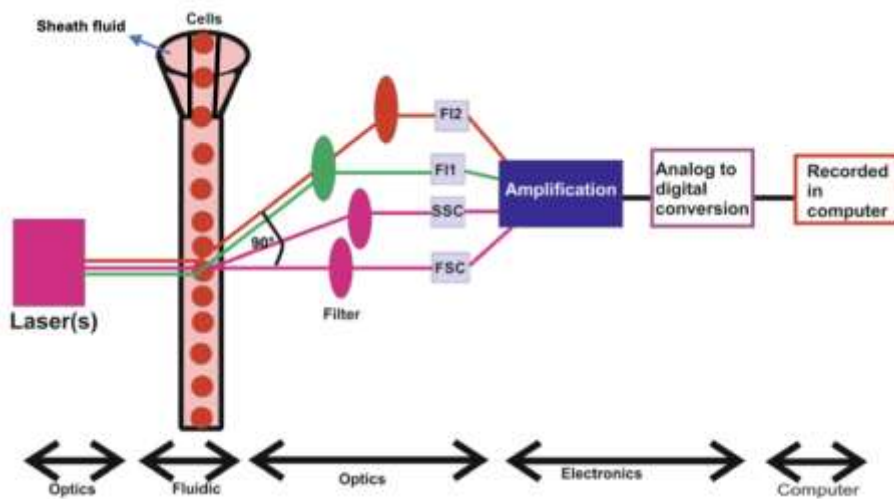


Figure 5. 1. A flow cytometer has three main systems: optics, fluidics, and electronics. Flow cytometry works on the principle of light scattering and fluorescence emission by the specific fluorescent probe-labelled cells as they pass through a laser beam. Various physical characteristics of cells are analysed such as cell size (FSC), granularity (SSC) and fluorescence intensity. These characteristics are determined using an optical to electronic system which records how the cell scatters light and emits fluorescence. Diagram taken from: (Dey and SpringerLink (Online service), 2021). Permission granted from Springer Nature (5614750964686).

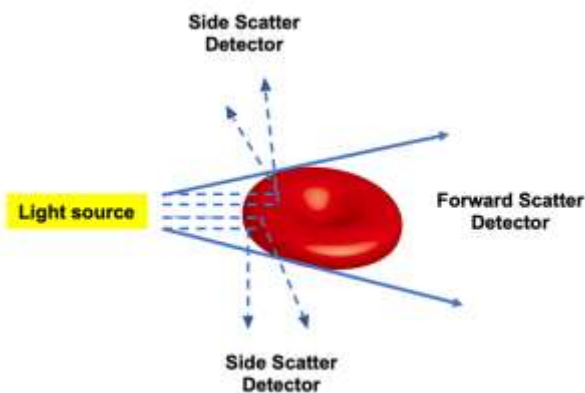


Figure 5. 2. Light scattering properties of a cell. Light scattering takes place when a cell deflects light. The extent to which this occurs depends on the physical properties of the cell, i.e. size and internal complexity. Factors affecting light scattering include the cell membrane, any granular material inside the cells and cell shape. Forward scatter gives information about the cell size and the side scatter (SSC) the internal complexity or granularity.

Intracellular ROS can be measured using carboxy-2',7'-dichlorodihydrofluorescein diacetate (carboxy-H<sub>2</sub>DCF-DA). This molecule is colourless and lipophilic (*Shehat and Tigno-Aranjuez, 2019*). Once it enters the cell, esterases cleave the acetate groups resulting in the formation of carboxy-2',7'-dichlorodihydrofluorescein (carboxy-H<sub>2</sub>DCF) (Figure 5.3). Intracellular ROS oxidise carboxy-H<sub>2</sub>DCF, yielding the fluorescent product, carboxy-2',7'-dichlorofluorescein (carboxy-DCF), which is cell impermeable (*Pasciu et al., 2023*). Carboxy-H<sub>2</sub>DCF-DA differs from DCF-DA in that it contains additional carboxyl groups, which make the molecule more negatively charged, and therefore enhancing its retention within cells. This probe is frequently used assuming it is detecting hydrogen peroxide, but it is not specific to hydrogen peroxide; although oxidation of carboxy-H<sub>2</sub>DCF can occur by reaction with hydrogen peroxide providing a catalyst is present, such as a haem (*Wrona and Wardman, 2006, Winterbourn, 2014*). Though it is a commonly used probe for detecting ROS, its use comes with some disadvantages such as the inability to specifically identify what ROS is being detected (*Kalyanaraman et al., 2012, Winterbourn, 2014*). The main route from H<sub>2</sub>DCF to DCF is through a reaction between H<sub>2</sub>DCF radical and oxygen that generates superoxide, which can amplify the signal (*Winterbourn, 2014, Dikalov and Harrison, 2014*). Carboxy-H<sub>2</sub>DCF-DA was chosen for this study because it is a good and simple assay which can provide information about disturbances in the redox state of cells. Additionally, it has better retention within cells than other derivatives, ensuring a more reliable measure of intracellular ROS levels.

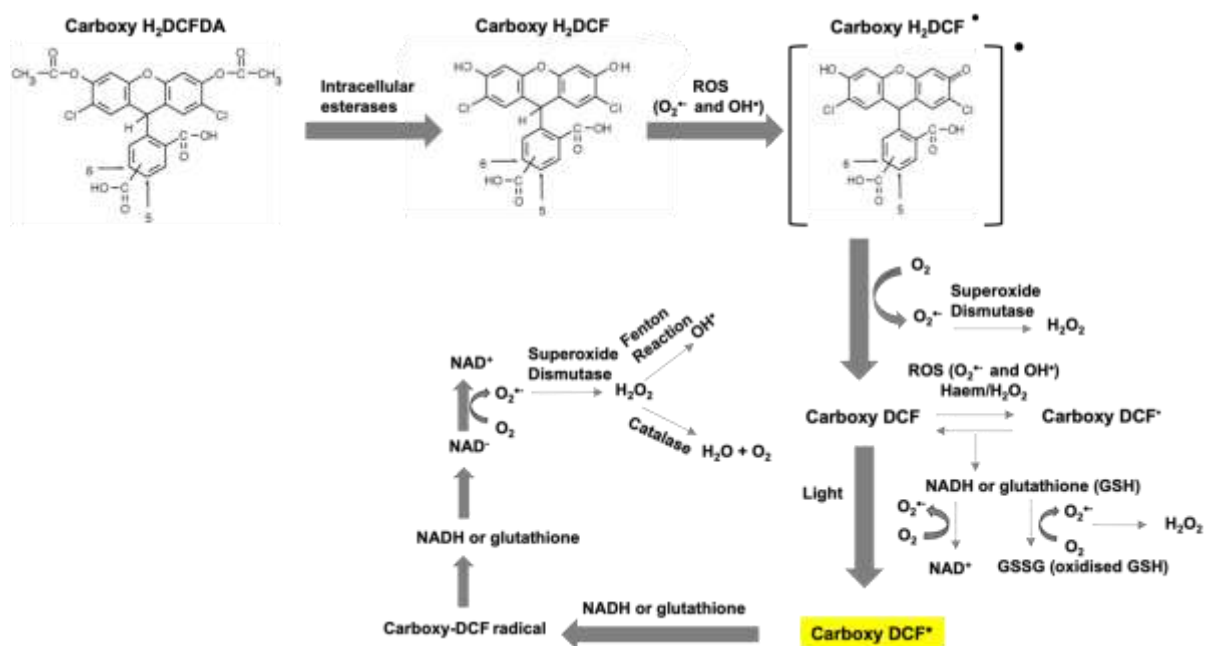


Figure 5. 3. The complex redox chemistry of carboxy-H<sub>2</sub>DCFDA. Carboxy-H<sub>2</sub>DCFDA enters the cells and intracellular esterases cleave the acetate groups forming carboxy-H<sub>2</sub>DCF. Upon reaction with oxidising species, carboxy-H<sub>2</sub>DCF is converted to carboxy-H<sub>2</sub>DCF radical which reacts with oxygen and forms carboxy-DCF which is highly fluorescent. In the process superoxide is generated and converted to H<sub>2</sub>O<sub>2</sub> by superoxide dismutase. Carboxy-DCF can be converted to carboxy-DCF radical by oxidising species. This is a reversible reaction; NADH or GSH can reduce the radical back to its fluorescent form, but in the process superoxide and H<sub>2</sub>O<sub>2</sub> (which can enter the Fenton reaction and lead to production of hydroxyl radical) are formed. Information for this diagram was taken from (Dikalov and Harrison, 2014, Kalyanaraman et al., 2012).

Intracellular ROS production in erythrocytes was measured by flow cytometry using DHE by Turpin and colleagues (Turpin et al., 2020). Erythrocytes were incubated with 0, 5, 25 and 137 mM glucose and then were treated with annexin V for 30 minutes. A subpopulation of cells appeared at high concentrations of glucose corresponding to glycated positive erythrocytes that become predominant when erythrocytes were incubated with increasing concentrations of glucose. Intracellular ROS production increased as glucose concentration increased. PS exposure also increased as glucose concentration increased (Turpin et al., 2020).

Erythrocytes from diabetic mice have shown an increase in ROS when compared to wildtype (Yang et al., 2018). On the other hand, Zhou and colleagues incubated healthy erythrocytes with glucose and found that ROS production did not change, although increased ROS was observed in diabetic erythrocytes when compared to cells from healthy subjects (Zhou et al., 2018). Perpetuation of ROS production, under hyperglycaemic conditions, can severely suppress antioxidant enzymes and non-enzymatic antioxidants, further exacerbating oxidative

stress (Ighodaro, 2018). Furthermore, PS exposure has been shown to increase for erythrocytes incubated with 48 mM and 100 mM glucose for 48 hours (Kucherenko *et al.*, 2010).

## **Aim and objectives**

The aim was to investigate the effect of increasing glucose concentration and ageing on erythrocyte ROS production and PS exposure. The objectives included assessing how different levels of glucose affect the generation of ROS and PS exposure in fresh and aged erythrocytes, as well as examining changes in ROS production and PS exposure over time by treating fresh and aged erythrocytes with various glucose concentrations at different timepoints. The hypothesis was that erythrocyte production of ROS and PS exposure would rise with increasing glucose concentration and ageing cells. To address the aim, blood was collected from healthy volunteers. Erythrocytes were isolated from whole blood and kept in RPMI media to which a final concentration of 5 mM glucose was added. The cells were treated for 30 minutes, 1 and 4 hours using 5 mM, 22 mM and 100 mM glucose. ROS were measured by flow cytometry using the fluorescent probe carboxy-H<sub>2</sub>DCFDA and PS exposure using annexin V.

## **5.2 Materials and Methods**

All materials and methods are described in Chapter 2. Details of erythrocyte ROS production and PS exposure are found in section 2.2.5.

## **5.3 Results**

### **5.3.1 Effect of glucose on the production of reactive oxygen species (ROS) as erythrocytes aged**

The fluorescent probe carboxy-H<sub>2</sub>DCFDA was used to establish whether increasing glucose concentrations causes a change in ROS production in erythrocytes. The cells were treated for 30 minutes, 1 and 4 hours on days 0 (the day they were taken from the body) and 4 with various concentrations of glucose (Figure 5.4 A-C). ROS production, measured by flow cytometry, did not change significantly as glucose concentration increased. A similar trend was observed for the three different time points carried out and glucose concentrations used. The presence of H<sub>2</sub>O<sub>2</sub>, used as a positive control, increased ROS production in the cells, significant differences were found after a thirty-minute treatment for both days, as well as on day 0 after a four-hour treatment. H<sub>2</sub>O<sub>2</sub> can increase the production of reactive hydroxyl radical via the

Fenton reaction, and even more so in erythrocytes as they contain high levels of iron in haemoglobin (*Paul et al., 2023, Chen et al., 2024, Orrico et al., 2023*). Statistical analysis (two-way ANOVA followed by Tukey *post hoc* test) showed no significant effect of glucose on ROS production. However, a significant difference ( $P < 0.05$ ) was found in the overall ROS produced between day 0 and 4 when the cells were treated for 1 hour (Figure 5.4B). Looking closely at the data shown in Figure 5.4B, it can be observed that the pattern was similar, but the ROS concentration appeared to be slightly higher at day 0 vs day 4.

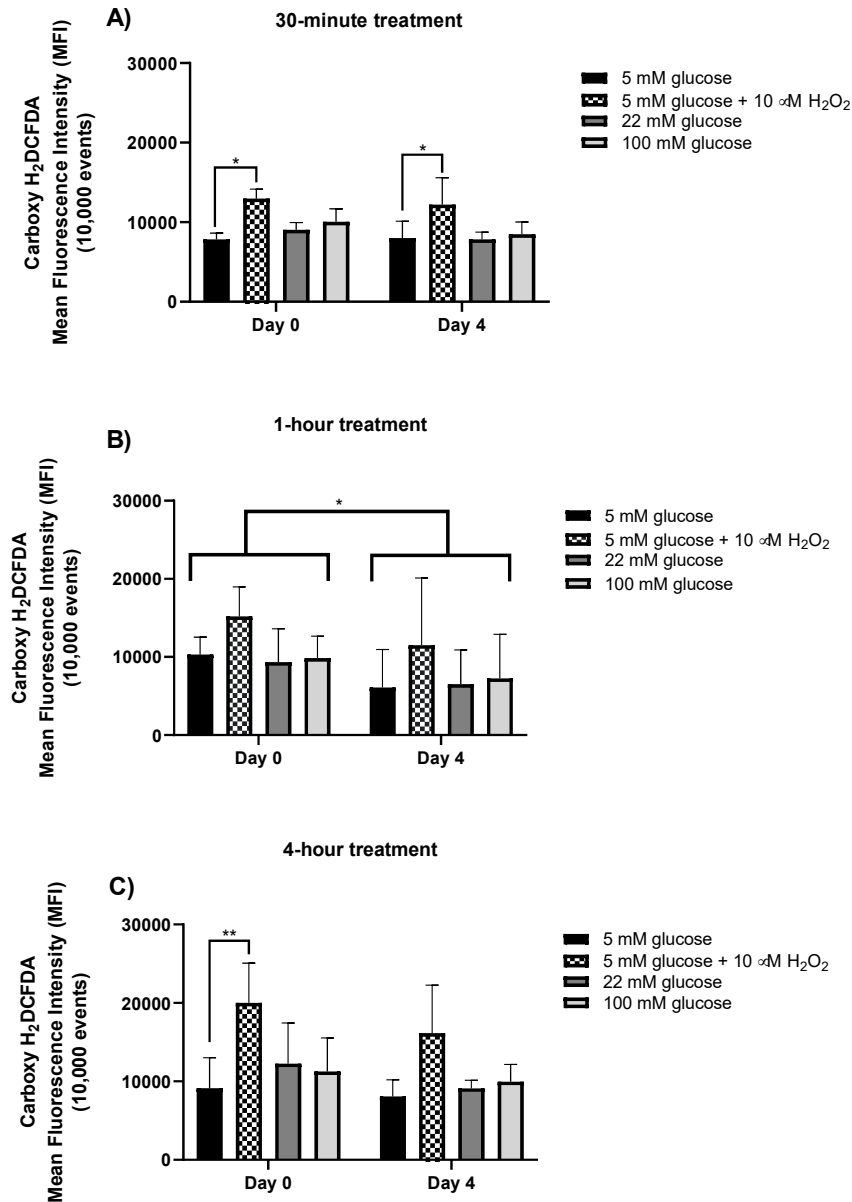


Figure 5. 4. ROS production of erythrocytes treated with 5 mM, 22 mM, and 100 mM glucose for 30 minutes (A) (n=3), 1 hour (B) (n=4), and 4 hours (C) (n=4) on days 0 and 4. The fluorescent probe Carboxy-H<sub>2</sub>DCFDA was used at a concentration of 20  $\mu$ M, and 10  $\mu$ M H<sub>2</sub>O<sub>2</sub> was used as a positive control. ROS production was measured by flow cytometry. Results shown as means  $\pm$  SD of three biological samples corresponding to three (30-minute treatment) or four (1- and 4-hour treatment) different participants (three technical replicates were also carried out for each glucose concentration measuring 10,000 events each time for every participant). Significance was defined by two-way ANOVA followed by Tukey's *post hoc* comparing treatments and days. A significant difference (P<0.05) was found between days 0 and 4 after 1 hour glucose treatment. During the 30-minute treatment, significant differences were found between 5 mM glucose in the presence or absence of H<sub>2</sub>O<sub>2</sub>, P values of <0.05 were obtained for days 0 and 4. After a 4-hour glucose treatment, a significant difference between 5 mM glucose and the positive control (H<sub>2</sub>O<sub>2</sub>) was observed, P<0.01.

Additional analysis corresponding to the 1-hour glucose treatment on day 0 and 4 for each participant was carried out (Figure 5.5 A-D). Figures 5.5A and 5.5B show data obtained on day 0, for glucose and the osmotic control (mannitol), respectively. Data obtained on day 4 is shown in Figures 5.5C and 5.5D for glucose and mannitol, respectively. ROS production for each participant under different glucose treatments had nearly the same trend, except from participant D, which showed a significant difference between 5 mM and 22 mM glucose on day 0 and showed very low ROS production on day 4, when compared to other participants. The presence of H<sub>2</sub>O<sub>2</sub> appeared to cause an increase in carboxy-H<sub>2</sub>DCFDA fluorescence in all participants. Significant differences were found between 5 mM glucose in the presence or absence of H<sub>2</sub>O<sub>2</sub> for participants G, H and I on day 0, and participants G and I for day 4. It is important to mention that although H<sub>2</sub>O<sub>2</sub> increased ROS production, some participants had a much larger response than others.

Significant differences in ROS production were found between the participants. These differences showed that glucose effects on ROS production in erythrocytes varied from person to person and suggested that this difference is not dependent on glucose concentration. This can be clearly observed as only participant D showed a significant difference ( $P < 0.005$ ) between glucose concentrations, at 5 mM and 22 mM on day 0 (Figure 5.5A), whereas the rest of the participants showed no significant effect of glucose on ROS production on either day.

Figures 5.5B and 5.5D show cells treated with mannitol for each participant (corresponding to 1-hour treatment on day 0 and 4, respectively), which was used as osmotic control. Mannitol was used to deliver the same osmolarity stress as under conditions of high glucose concentrations, to the erythrocytes. A similar trend to glucose was found for mannitol (for ROS production) for all the participants, although sometimes carboxy-H<sub>2</sub>DCFDA mean fluorescence intensity was lower in the presence of mannitol when compared to that of glucose e.g., participant I on day 0. The presence of H<sub>2</sub>O<sub>2</sub> also appeared to increase ROS production when the cells were treated with mannitol. Significant differences were found on day 0 between 5 mM glucose and the positive control for participants D ( $P < 0.01$ ) and G ( $P < 0.0001$ ). On day 4, significant differences were also observed between 5 mM glucose and the positive control for participants G ( $P < 0.0001$ ), H ( $P < 0.0001$ ) and I ( $P < 0.001$ ). Differences between participants were also observed. On day 0, there was significant difference observed between participant D and the rest of the participants ( $P < 0.0001$ ). This significance was the result of less ROS being produced by the erythrocytes belonging to participant D in comparison to the rest of the participants and not dependent on glucose concentration. On the other hand, further

differences between the participants were observed on day 4; significant differences between participants D and G ( $P<0.0001$ ), D and H ( $P<0.0001$ ), D and I ( $P<0.0001$ ), G and H ( $P<0.0001$ ), G and I ( $P<0.0001$ ) and H and I ( $P<0.0001$ ).

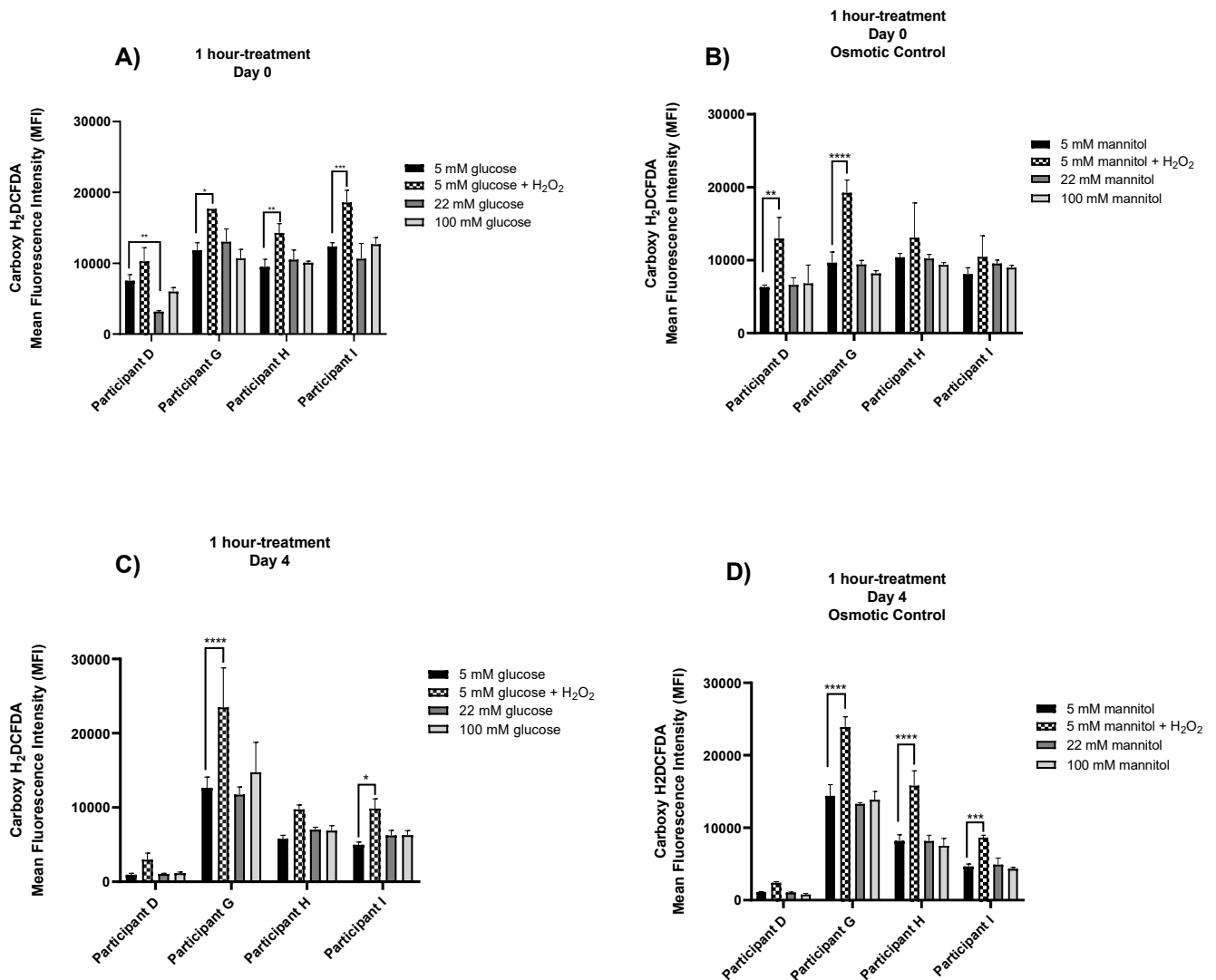


Figure 5.5. Figure 4.5. ROS production of erythrocytes for each participant treated with glucose (A and C) and mannitol (B and D) for 1 hour on days 0 and 4, respectively. Three technical replicates were present for each participant ( $n=3$ ), except from participant G at 5mM glucose + H<sub>2</sub>O<sub>2</sub>  $n=1$ . Results are shown as means  $\pm$  SD. Significance was determined by two-way ANOVA followed by Tukey's *post-hoc* comparing treatments and participants. Significant differences between participants on day 0 ( $P<0.0001$ ) and 4 ( $P<0.0001$ ) were found. For cells treated with glucose, a significant difference between participant D and G ( $P<0.0001$ ), D and H ( $P<0.0001$ ), D and I ( $P<0.0001$ ), G and H ( $P<0.05$ ) and H and I ( $P=0.05$ ) was found on day 0. No significant difference was found between participants G and I on day 0. A significant difference was also found between participants D and G ( $P<0.0001$ ), D and H ( $P<0.0001$ ), D and I ( $P<0.0001$ ), G and H ( $P<0.0001$ ), and G and I ( $P<0.0001$ ) on day 4. No significant difference was found between participants H and I on day 4. For cells treated with mannitol, significant differences were found on day 0 between 5 mM glucose and the positive control for participants D ( $P<0.01$ ) and G ( $P<0.0001$ ). On day 4, significant differences were also observed between 5 mM glucose and the positive control for participants G ( $P<0.0001$ ), H ( $P<0.0001$ ) and I ( $P<0.001$ ). A significant difference between participant D and the rest of the participants ( $P<0.0001$ ) was observed on day 0. Significant differences between participants D and G ( $P<0.0001$ ), D and H ( $P<0.0001$ ), D and I ( $P<0.0001$ ), G and H ( $P<0.0001$ ), G and I ( $P<0.0001$ ) and H and I ( $P<0.0001$ ) were observed on day 4.

Further analysis, using CytEXpert, was carried out to understand the significance observed in participant D between 5mM and 22 mM glucose after 1 hour glucose treatment on day 0, which was the only significance found between glucose concentrations and seemed to be an outlier. Results are shown in Figures 5.6 A-E. First, an SSC-FSC plot (Figure 5.6A) was observed to make sure the cells were gated correctly. The histogram, Figure 5.6B, shows the event count and the fluorescence intensity for unstained cells under 5 mM glucose treatment, and stained cells, under 5 mM and 22 mM glucose. The histogram confirms that the stained cells in 22 mM glucose had lower fluorescence intensity than those in 5 mM, i.e., the peak belonging to 5 mM had a higher shift to the right than that of 22 mM. Further analysis using dot plots showed unstained cells (Figure 5.6C), stained cells treated with 5 mM (Figure 5.6D) and 22 mM (Figure 5.6E) glucose. Unstained cells appeared in the lower left quadrant, whereas stained cells with carboxy-H<sub>2</sub>DCFDA in 5 mM shifted to the lower right quadrant (99.96%). On the other hand, the majority of cells (97%) treated with 22 mM glucose exhibited fluorescence, indicating the presence of intracellular ROS. However, a small portion of cells (2.68%) did not show fluorescence. This observation suggests two possible scenarios, the dye was retained inside the cells but did not fluoresce due to the absence or lower levels of ROS, or the dye was not retained within this small subset of cells. The lack of fluorescence could imply either insufficient ROS production or the presence of two distinct cell populations, one of which is less active in terms of esterase activity required for the dye to be trapped intracellularly. The latter scenario might be due to less active esterases, which could result in less efficient cleavage of acetate groups from carboxy-H<sub>2</sub>DCFDA, thereby reducing its retention and subsequent oxidation to a fluorescent product.

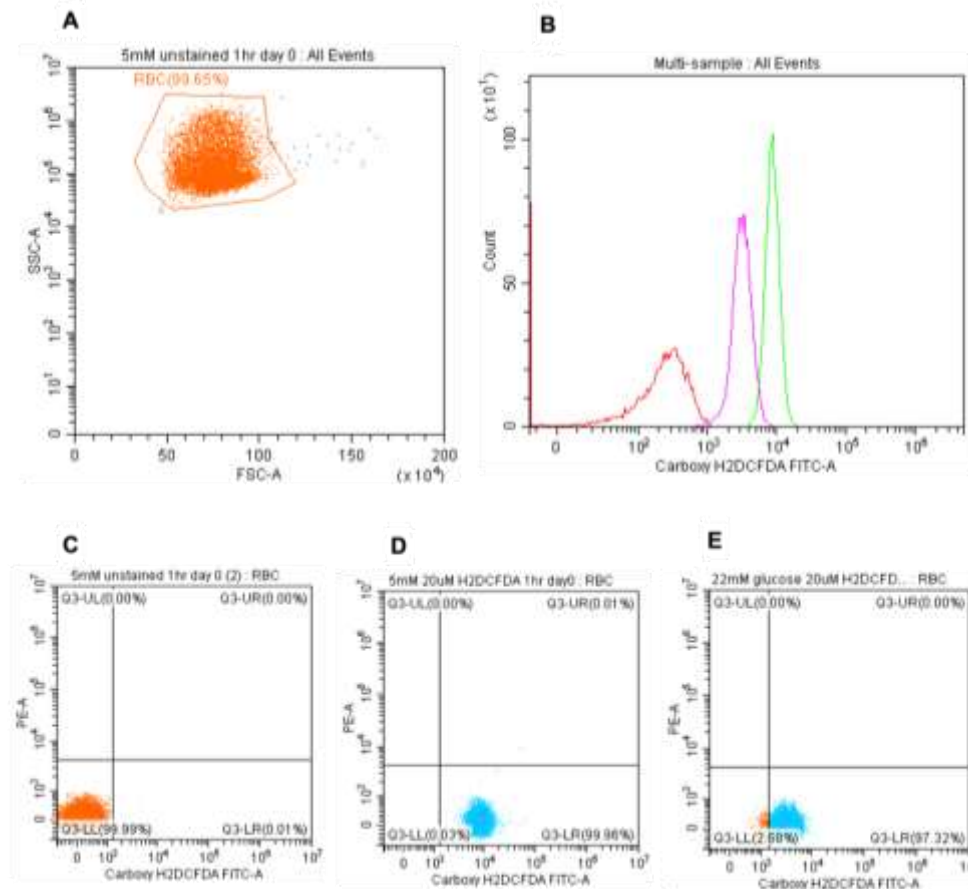


Figure 5. 6. Shows data belonging to participant D on day 0 at 1 hour treatment between 5 mM and 22 mM glucose. The FSC and SSC of unstained RBCs and how these were gated (A), a histogram indicating the fluorescence results for cells treated with 5 mM glucose unstained (red), stained with carboxy-H2DCFDA at 5 mM (green) and 22 mM (pink) glucose (B), and dot plots of: unstained cells under 5 mM glucose treatment (C); stained cells with carboxy- H2DCFDA under 5 mM A (D) and 22 mM A (E) glucose.

### 5.3.2 Effect of glucose on phosphatidylserine (PS) exposure as erythrocytes aged

Elevated oxidative stress can cause phosphatidylserine (PS) to translocate from the inner leaflet to the outer leaflet of the erythrocyte plasma membrane. Annexin V conjugated to APC, with excitation and emission of 650 nm/660 nm, respectively, was used to detect PS externalisation in erythrocytes as a marker of early apoptosis, following glucose treatments of 5 mM, 22 mM and 100 mM for 30 minutes, and 1 and 4 hours on days 0 and 4. Erythrocyte externalisation of PS was measured by flow cytometry, where data shown in Figure 5.7 represents the mean  $\pm$  SD of three biological samples corresponding to three different participants. Erythrocytes belonging to the same participants who took part in the study of the effect of glucose on ROS production were used, except from participant D. It appeared that PS detection increased as glucose concentration increased and was observed for all treatments except on day 0 at 1 hour treatment for cells treated with 22 mM, but owing to large standard errors no statistical significance was found. Also, it seemed that more PS was detected on day 4 than on day 0, especially for 30-minute and 4-hour treatments, although a significant difference ( $P < 0.05$ ) was only observed between day 0 and 4 following a 4-hour treatment. This significance was related to differences between the overall mean values of days 0 and 4, excluding glucose concentration groupings. Furthermore, although it appeared that more PS was detected when the cells were treated with 100 mM glucose for both days (0 and 4) at all treatment times, this was not found to be statistically significant.

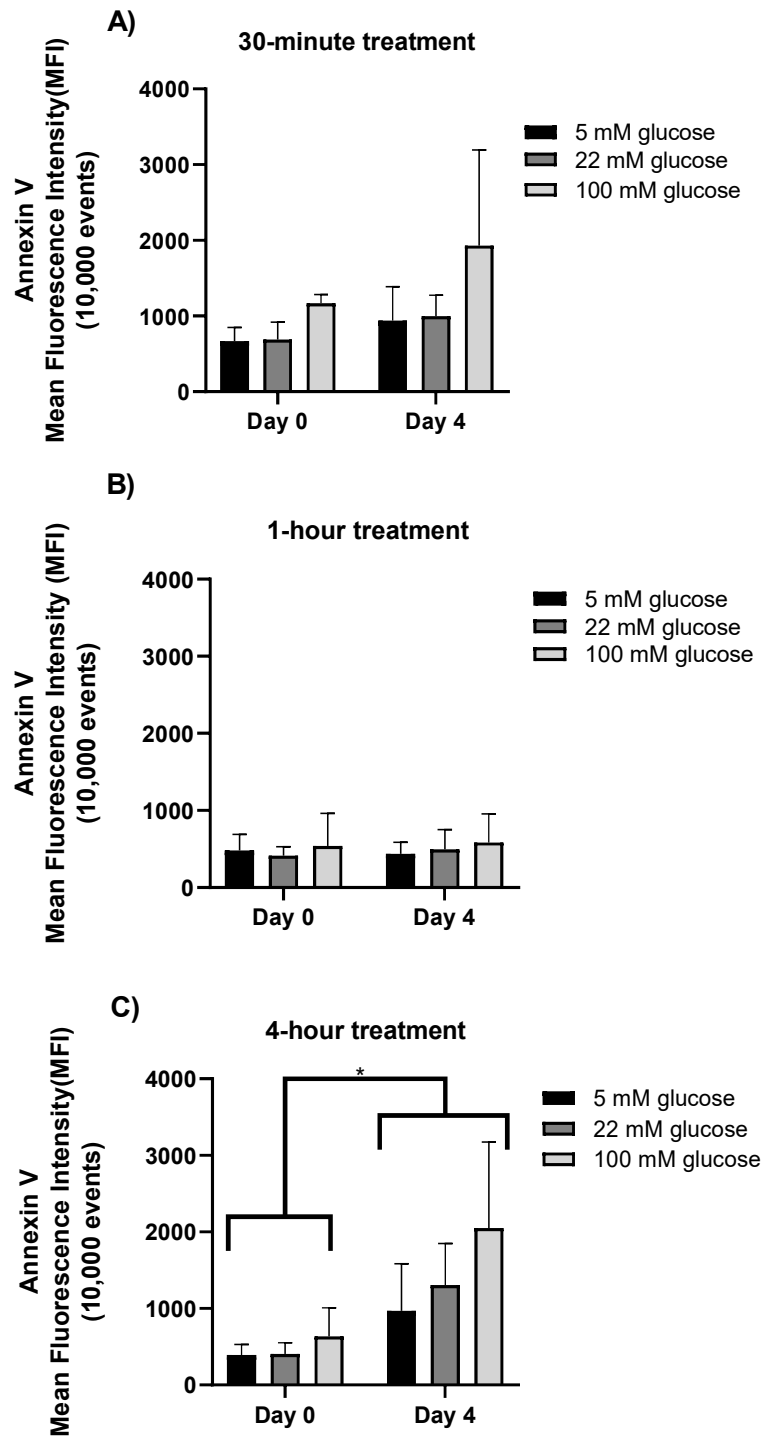


Figure 5. 7. Annexin V used to detect PS exposure on erythrocyte as a marker of apoptosis. RBCs were treated with 5 mM, 22 mM, and 100 mM glucose for 30 minutes (A) ( $n=3$ ), 1 hour (B) ( $n=4$  for day 0 and  $n=3$  for day 4), and 4 hours (C) ( $n=4$  for day 0 and  $n=3$  for day 4) on days 0 and 4. Results are shown as means  $\pm$  SD. Significance was defined by two-way ANOVA followed by Tukey's *post-hoc* comparing treatments and days. A significant difference ( $P < 0.05$ ) was observed between day 0 and 4 following a 4-hour treatment.

Further analysis corresponding to the 4-hour glucose treatment on days 0 and 4 for each participant is shown on Figures 5.8A and B, respectively. For most participants on day 0, PS exposure did not really change as the glucose concentration increased, except from participant G at 100 mM glucose. More PS was detected, as a higher MFI was observed (Figure 5.8A-B), on day 4 than on day 0. There appeared to be a difference in PS exposure as glucose concentration increased for all participants on day 4, but it was only significant for participant G. Statistical analysis showed significant differences between participants H and I ( $P<0.0001$ ), and H and G ( $P<0.0001$ ) for day 0; and there was also a significant difference between participant H and G ( $P<0.0001$ ), and I and G ( $P<0.0001$ ) on day 4. This shows that the effect of glucose on erythrocyte PS exposure varied from person to person.

In addition, only participant G showed a significant difference in PS exposure between glucose treatments. The dot plots (Figures 5.8C-F) correspond to data obtained from participant G on days 0 (C-D) and 4 (E-F), where the cells were stained with annexin V and carboxy- $H_2DCFDA$ . Figure 5.8D shows that on day 0, around 95% of the cells were stained with  $H_2DCFDA$  and about 4.8% were double stained with  $H_2DCFDA$  and Annexin V. On the other hand, on day 4, approximately 79% of the cells were stained with  $H_2DCFDA$  and about 20% were double stained. This shift in the percentage of the cells which were double stained indicates that more cells were dying on day 4 after the treatment than on day 0. In this case, more PS was detected when the cells were treated with 100 mM glucose, especially on day 4.

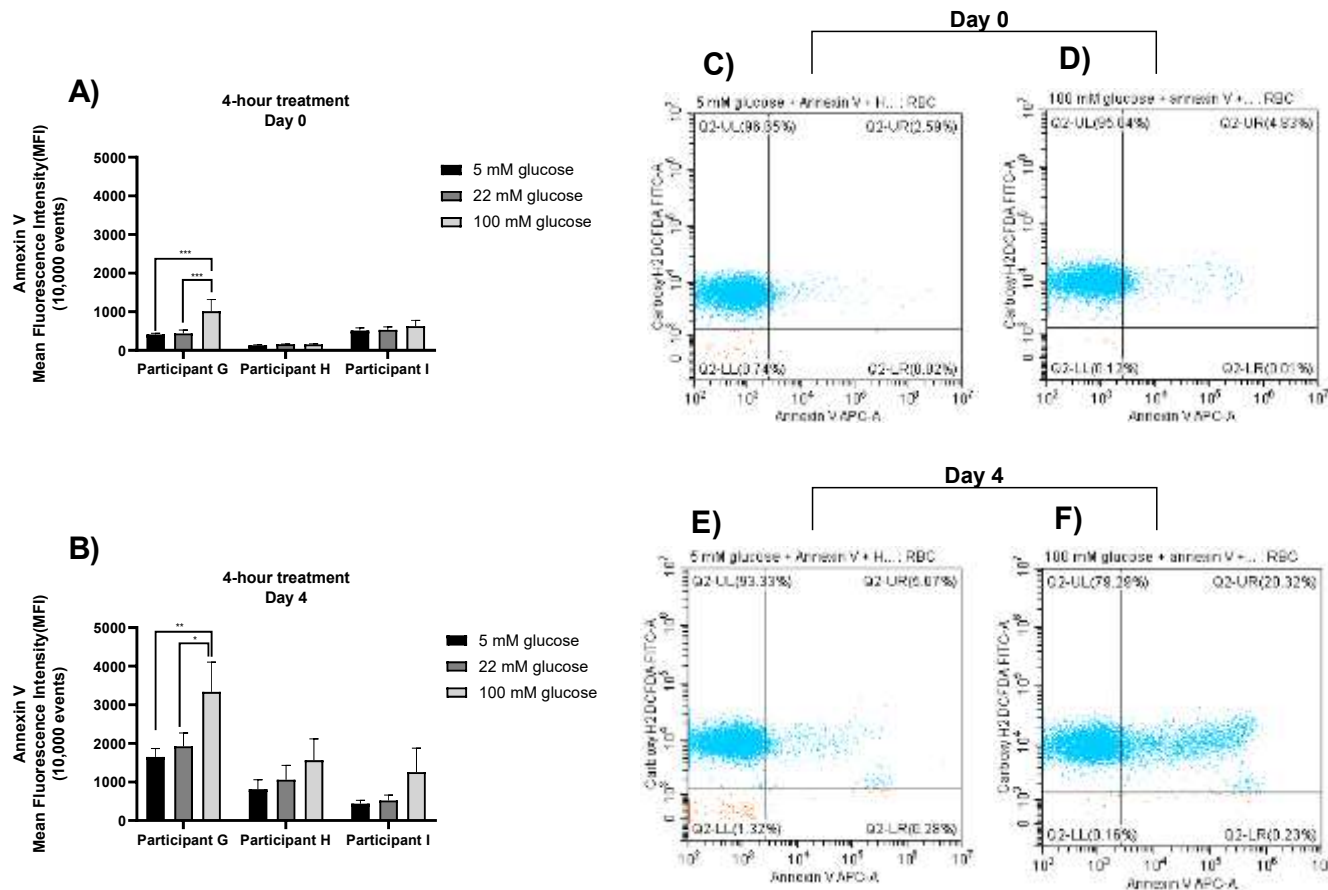


Figure 5. 8. Annexin V used to detect PS exposure on erythrocytes as a marker of apoptosis for each participant on days 0 (A) and 4 (B) after 4-hour glucose treatment. RBCs were treated with 5 mM, 22 mM, and 100 mM glucose ( $n=3$  – three technical replicates for each participant). Results shown as means  $\pm$  SD. Significance was defined by two-way ANOVA followed by Tukey's post-hoc comparing treatments and days. C- F are dot plots representing RBCs from participant G treated with 5 mM (C and E) and 100 mM (D and F) glucose on days 0 and 4 respectively. P values of 0.0002; 0.0003; 0.0037 and 0.0187 were obtained for days 0 and 4 between 5 mM and 100 mM, and 22 mM and 100 mM glucose, respectively for participant D. Significances between participants were observed; H and I ( $P<0.0001$ ), and H and G ( $P<0.0001$ ) for day 0, and participants H and G ( $P<0.0001$ ), and I and G ( $P<0.0001$ ) on day 4.

## 5.4 Discussion

In the present study the effect of increasing glucose concentration on ROS production and PS exposure in fresh and aged erythrocytes was investigated. The cells were treated for 30 minutes, 1- and 4-hours using glucose levels that ranged from physiological (5 mM) to pathological (22 mM and 100 mM). The fluorescent probes carboxy-H<sub>2</sub>DCFDA and annexin V were used to measure ROS and PS exposure reflecting apoptosis, respectively. The results showed that ROS production did not change significantly as glucose concentration increased in both fresh and aged cells. The presence of hydrogen peroxide, which was used as a positive control, appeared to increase ROS production in the cells, although only significant differences were found after a 30-minute treatment for days 0 and 4, as well as on day 0 after a 4-hour treatment. When comparing individual participants, it is important to mention that although hydrogen peroxide appeared to increase ROS production in most cases, some participants had a much larger response than others. Differences between the overall ROS production among participants were observed and this highlighted that ROS production differed from person to person. In terms of PS exposure, increasing glucose concentration appeared to increase the PS detected by annexin V, although no significant difference was observed. However, a significant difference was observed between day 0 and 4 after a 4-hour glucose treatment, where PS exposure was higher on day 4. Furthermore, only one participant showed a significant difference in PS exposure as glucose concentration increased.

Adding hydrogen peroxide to fresh and aged cells (5 mM glucose) appeared to increase ROS production significantly for most participants. Carboxy-H<sub>2</sub>DCFDA does not measure hydrogen peroxide levels directly; instead it mostly measures the presence of hydroxyl radical and superoxide, although it can also react with other ROS (Cohn *et al.*, 2008). The presence of hydrogen peroxide can cleave the haem ring of haemoglobin and release free redox reactive iron, making haemoglobin a major factor initiating oxidative stress within the erythrocytes (Belcher *et al.*, 2010, Gwozdziński *et al.*, 2021). Both, hydrogen peroxide and free reactive iron (Fe<sup>2+</sup>) can participate in the Fenton and Haber-Weiss reactions, exacerbating the production of hydroxyl radical, and hence the increase observed in carboxy-H<sub>2</sub>DCFDA fluorescence in the presence of hydrogen peroxide.

The initial hypothesis was that erythrocyte production of ROS would increase as glucose concentration increased, as well as cells aged. While occasionally a trend indicating an increased ROS production with increasing glucose concentrations was observed, there were no significant changes in ROS production post-treatments. Most studies, where ROS

production was measured in erythrocytes, and other cells such as myocytes, after glucose treatments have shown an increase in ROS (Turpin *et al.*, 2020, Yang *et al.*, 2018, Lu *et al.*, 2020). A recent study carried out by Qasim and colleagues treated erythrocytes *in vitro* with 5 mM, 15 mM, 30 mM and 45 mM glucose for 24 hours and they found an increase in ROS generation using DCFH and DHE probes (Qasim *et al.*, 2023). On the other hand, results obtained in the present study agreed with results obtained by Zhou and colleagues where incubation of healthy erythrocytes with glucose did not change ROS production. (Zhou *et al.*, 2018). Both studies used erythrocytes from multiple donors, which highlights the importance of considering inter-donor variability in ROS responses to glucose.

Furthermore, it appeared that the cells generated more ROS following treatment on day 0 compared to day 4, although a significant change was observed only after a 1-hour treatment. This observation was counterintuitive as aged cells are often associated with increased oxidative stress and ROS production (Maldonado *et al.*, 2023). On day 0 the cells were freshly collected and may have experienced stress due to the isolation process, including centrifugation and separation from whole blood. This stress could have triggered cellular responses, including ROS production, as the cells adapted to their new environment. In contrast, cells that were aged in media for several days may have adapted to culture conditions and exhibited reduced stress responses, leading to lower ROS levels. Also, freshly collected cells may have been in a different metabolic state compared to aged cells. The metabolic activity of cells can influence ROS production, where higher metabolic rates are often associated with increased ROS generation (Balaban *et al.*, 2005, Quijano *et al.*, 2016). In the case of erythrocytes, glucose is used in the pentose phosphate pathway to produce NADPH, which is then used by NADPH oxidase to produce superoxide free radical and hydrogen peroxide by transferring one electron to oxygen from NADPH (Skonieczna *et al.*, 2017).

Increased ROS production has been associated with increased PS exposure in erythrocytes (Wang and Zennadi, 2020). In the current study, PS translocation to the outer membrane leaflet was measured, using annexin V, on fresh and aged cells. No significant differences were found between PS translocation and increased glucose concentration on days 0 and 4. The results obtained contrast with studies carried out on erythrocytes, treated *in vitro* with glucose and isolated from diabetic individuals, which have presented an increase in PS translocation to the outer membrane (Muhlberger *et al.*, 2021, Turpin *et al.*, 2020). Recently, a study where oral glucose tolerance testing was carried out on prediabetic subjects found that

the glucose load increased PS exposure in RBCs from prediabetic patients (*Eligini et al., 2022*).

Furthermore, it appeared that PS exposure was higher on day 4, although a significant difference was only found after the 4-hour treatment. This could suggest that the duration of glucose exposure may be a critical factor in inducing changes in PS exposure. It is possible that a longer glucose treatment exacerbated oxidative stress leading to PS exposure. Furthermore, the significance in PS exposure between fresh and aged erythrocytes after the 4-hour glucose treatment could also imply that the age of the RBCs may influence their response to glucose induced stress. Aged erythrocytes may be more susceptible to oxidative damage or other metabolic changes induced by glucose, leading to PS exposure compared to fresh erythrocytes.

Further analysis carried out on individual participants after the 4-hour treatment showed significant changes in response to changed glucose concentrations for only one participant, on both days. This highlighted the considerable inter-participant variability in the response of erythrocytes to glucose treatment. Factors such as genetic variations and age of erythrocytes could have contributed to this variability. Increased PS exposure is often associated with the formation of membrane blebs (*Kirov et al., 2012*). Membrane blebbing occurs due to the dissociation of the plasma membrane and the cytoskeleton network (*Manakova et al., 2016*). Spectrin is the major component of the erythrocyte membrane cytoskeleton and plays a crucial role in maintaining membrane stability and shape (*Blanc et al., 2010*). Spectrin molecules form a lattice like structure that supports the lipid bilayer, and is known to have binding sites for PS (*An et al., 2004*). Glycation of spectrin, which can take place during high levels of glucose, such as 100 mM, can cause the dissociation of PS from its binding sites in spectrin and destabilise the membrane-cytoskeleton interaction, leading to membrane blebbing and externalisation of PS on the cells surface (*Manno et al., 2010, Viskupicova et al., 2015*).

Several aspects need to be taken into consideration. The cells were treated with carboxy-H<sub>2</sub>DCFDA before being treated with different glucose concentrations. Preloading the cells with the dye first ensured that the dye was already inside the cells before glucose treatment. This meant that any changes in ROS levels induced by glucose would directly affect the fluorescence of the dye. Other studies have used this approach to measure ROS production in cells (*Aranda et al., 2013*).

Treating the cells *in vitro*, i.e. outside of their natural environment, may require using higher concentrations of treatment to compensate for dilution effect, ensuring that the treatment

reaching the cells produces a detectable effect. Sometimes treating the cells *in vitro* means the conditions may not fully mimic the complexity of an *in vivo* environment. So, various concentrations of glucose were used to treat the cells, and these ranged from physiological to pathological levels, although very high levels such as in the case of 100 mM glucose was used. Furthermore, 100 mM glucose has been used previously by other researchers to treat erythrocytes (*Viskupicova et al., 2015*).

A concentration of 10  $\mu$ M hydrogen peroxide was used as a positive control, surpassing the physiological range (1-5  $\mu$ M) commonly found in blood, to induce oxidative stress and validate experimental setups (*Forman et al., 2016, Gaikwad et al., 2021*). Furthermore, other studies have used much higher hydrogen peroxide to treat RBCs ranging from 45  $\mu$ M to 1 mM (*Hale et al., 2011, Nagababu et al., 2000, Masuoka et al., 2020, Snyder et al., 1985*). However, in the current study 10  $\mu$ M was sufficient to produce an increase in ROS levels compared to controls.

Mannitol was used as an osmotic control and although it has been extensively used for this purpose there are some factors to consider (*Hattori et al., 2000, El-Remessy et al., 2003*). At times it appeared that erythrocytes treated with mannitol showed less ROS than those treated with glucose. Mannitol is often used to prevent haemolysis of erythrocytes, although the mechanism behind this is not well understood, and can also present antioxidant properties by reducing levels of ROS and scavenging hydroxyl radicals (*Beutler and Kuhl, 1988, Antosik et al., 2018, Hess, 2006, Xu et al., 2019, Liu et al., 2010, El-Remessy et al., 2003, Karasu, 2000*). Nevertheless, mannitol has several properties which outweigh the disadvantages of its use, and these include its ability to cause osmotic stress; it has similar molecular weight to glucose which leads to comparable effects on osmotic pressure; does not contain aldehyde groups (less reactive than glucose); and it is not metabolizable by erythrocytes, at least not through glycolysis.

Some limitations need to be considered in the study, such as a small sample size, which needs validation in a larger population. Another consideration was the age of erythrocytes at the time of collection, which could have influenced the response to glucose treatment and ROS production. Erythrocyte populations in the circulation are heterogenous in terms of their age, with a mix of newly produced (reticulocytes) and older erythrocytes. The age distribution of erythrocytes can vary among individuals and may change over time due to factors such as erythropoiesis rate, erythrocyte turnover, and clearance from circulation. The age of the cells can influence their metabolic activity, membrane properties, and susceptibility to oxidative

stress. For example, younger erythrocytes may have higher metabolic rates and antioxidant capacity, while older erythrocytes may be more susceptible to oxidative damage and membrane alterations.

Inter-volunteer variability was observed in this study, a theme that recurred throughout the analyses. Such variability among participants can be attributed to a range of factors, including genetic differences, varying health conditions and individual responses to glucose exposure. This variability served as a confounding factor, complicating the interpretation of data derived from a small participant group. Addressing this variability in future studies by increasing the sample size and incorporating more controlled variables (such as sex, diet, medication use) will be crucial for obtaining more reliable and generalisable findings.

Future work would involve validating the findings from *in vitro* with *in vivo* studies to ensure that the observed *in vitro* effects are relevant and meaningful in the context of living organisms. Samples from diabetic subjects could help to assess the effects of hyperglycaemia on erythrocytes in terms of oxidative stress markers and membrane alterations. This could provide valuable insights into the long-term implications of glucose-induced oxidative stress on erythrocytes.

# **Chapter 6**

## **Lipidomic analysis of erythrocyte phospholipids**

## 6.1 Introduction

### 6.1.1 Lipid composition of erythrocyte membranes

Lipids are complex and play a key role in many biological functions such as acting as a structural scaffold for the cell membrane, serving as energy storage and participating in signalling pathways (*Addepalli and Mullangi, 2021*). Lipid classification is described by LIPID MAPS and can be divided into eight main categories: fatty acids (FA), glycerolipids, glycerophospholipids, sphingolipids, sterol lipids, prenol lipids, saccharolipids and polyketides (*Addepalli and Mullangi, 2021*).

The complete profile of lipids within a cell is referred to as lipidome (*Wu et al., 2020*). The study of lipid profiles within biological systems, also known as lipidomics, combines lipid specific isolation methods with mass spectrometry-based profiling methods (*Wu et al., 2020, Saini et al., 2021*). The isolation and identification of all the lipids is a challenging task, requiring large-scale studies using suitable methods for lipid isolation and analytical methods.

The membrane of mammalian cells, including erythrocytes, is comprised of a cytoskeleton and a lipid bilayer tethered together. The lipid bilayer includes various types of phospholipids, sphingolipids, cholesterol and integral membrane proteins such as band 3 (*Li and Lykotrafitis, 2014*). The lipid bilayer of the erythrocyte membrane is approximately 45% cholesterol and 55% phospholipids where about 29% are phosphatidylcholines (PCs), 27% phosphatidylethanolamines (PEs), 25% sphingomyelins (SMs) and 15% phosphatidylserines (PSs) (*Dodge and Phillips, 1967, Melzak et al., 2020*). Other phospholipids including phosphatidylinositol (PI), phosphatidic acid (PA) and phosphatidylglycerol (PG) are found in lesser quantities.

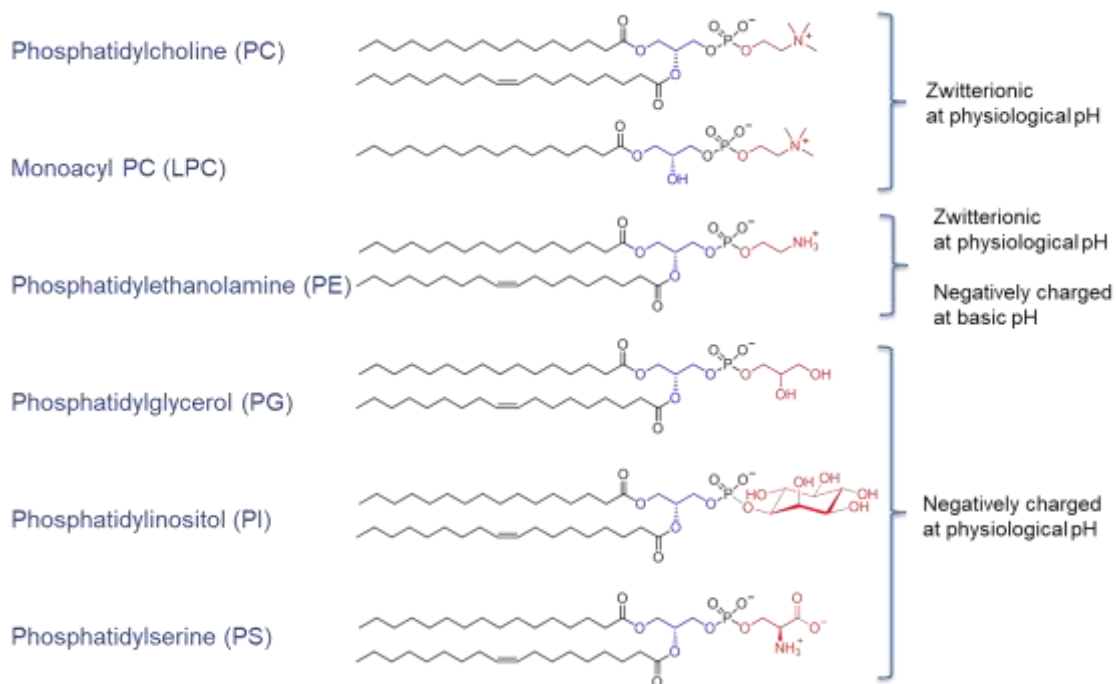


Figure 6. 1. Chemical structure of phospholipids. The molecular structure of phospholipids comprises a glycerol backbone which is esterified in *sn1* and *sn2* positions with fatty acids, and with phosphate in *sn3* position. Depending on the polar region of the phospholipid and pH of the medium, PE and PC are zwitterionic and have a neutral charge at pH 7. A phospholipid may have two esterified fatty acids, known as diacyl-phospholipids, whereas a phospholipid with one fatty acid is called monoacyl-phospholipid or lyso-phospholipid. Reproduced from (Hoogevest *et al.*, 2021) with permission from John Wiley and Sons (lic. # 5700720584823).

Sphingomyelin (SM) is a dominant sphingolipid in the erythrocyte membrane, which is mainly found in the outer leaflet of the membrane, together with PC, while the inner leaflet is known to mainly consist of amino-phospholipids such as PE and PS (Vahedi *et al.*, 2020). A recent lipidomic study of the asymmetry of erythrocyte plasma membrane was carried out by Lorent and colleagues, where they reported that the outer leaflet of erythrocytes is composed of SM, PC and small amounts of PS, while the inner leaflet primarily consists of PE, PS, PC and small amounts of SM (Lorent *et al.*, 2020). Erythrocytes were the first cells in which membrane asymmetry was revealed and are particularly suitable for studies on membrane lipid composition given that they lack internal organelles and therefore the majority of their lipids can be attributed to the membrane (Vahedi *et al.*, 2020).

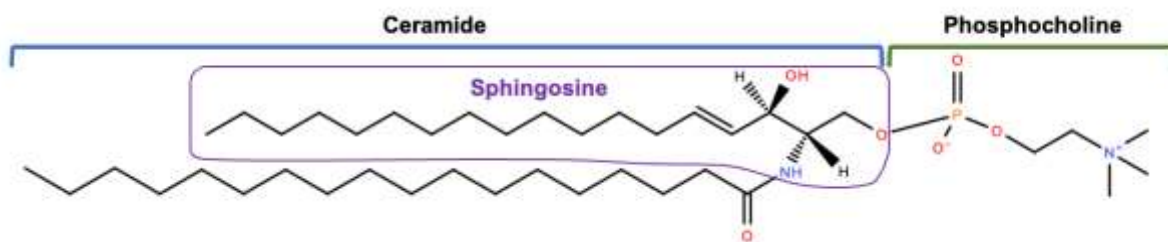


Figure 6. 2. Structure of sphingomyelin, which consists generally of a sphingosine base with 18-carbon chain and a double bond at position 4, a fatty acid joined by an amide bond and phosphocholine head group (*Chiu et al., 2003*). In other words, a ceramide attached to phosphocholine. The example given corresponds to SM 36:1 (18:1, 18:0).

Traditional techniques for the analysis of lipids, such as thin layer chromatography (TLC), enable differentiation between lipid classes but lack the resolving power to study unique and complex lipid species. Besides chromatography-based methods, other analytical techniques have been applied to lipid analysis such as nuclear magnetic resonance and mass spectrometry. While each method has its advantages and disadvantages, mass spectrometry has emerged as the most powerful tool for the analysis of all lipids (*Lerno et al., 2010*).

### Mass spectrometry methods

Mass spectrometry-based methods involve measuring the mass to charge ratio ( $m/z$ ) of ions, which are then manipulated by electrical and magnetic fields (*Spickett et al., 2011, Urban, 2016, Olshina and Sharon, 2016*). Historically, sector instruments utilized magnetic fields for ion manipulation. However, in modern times, this practice is primarily associated with Fourier-transform ion cyclotron resonance mass spectrometry (*Barrow et al., 2005*).

A mass spectrometer consists of three main components: the ion source, wherein ionisation of the sample takes place; the mass analyser (e.g. a quadrupole (FIGURE 6.3) or time of flight (TOF)), where the ions are sorted based on their mass-to-charge ratio; and the detector, where ions are measured and then displayed on the mass spectrum graph (*Garg and Zubair, 2023*). Electrospray ionisation (ESI), whereby ions from a solution are transferred into the gaseous phase before mass spectrometry analysis, is one of the most popular and powerful technologies used to identify and quantify lipid species; it allows the formation of intact lipid ions with little to no fragmentation and has high sensitivity and compatibility with liquid chromatography (*Yang and Han, 2011, Randolph et al., 2020*). Mass analysers can be combined to perform tandem mass spectrometry (MS/MS), where two mass analyses occur in series, often with a fragmentation step in between (*Thomas et al., 2022*). Examples of MS/MS include combining two or more identical analyser series such as triple quadrupoles analysers or combining two (or more) types of analysers to create hybrid instruments such as

a quadrupole and TOF to create a Q-TOF analyser. An example of a Q-TOF can be observed in FIGURE 6.4; the Zeno TOF 7600 mass spectrometer which is made up of quadrupoles, ion trap (Zeno trap) and a TOF chamber.

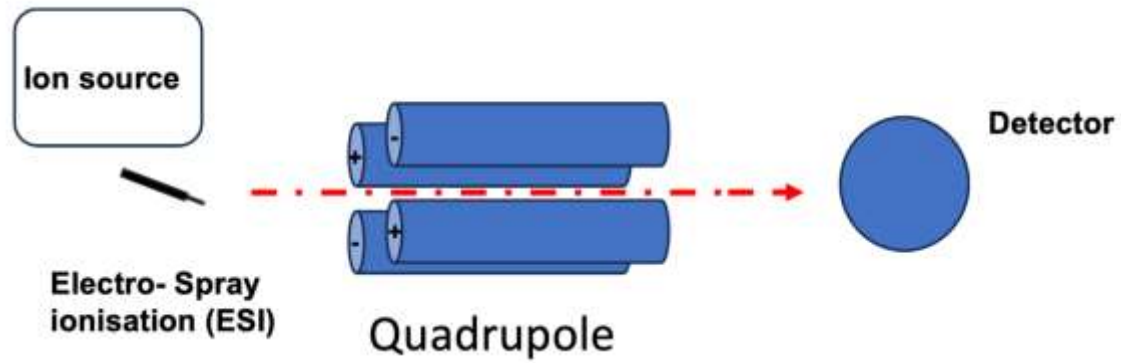


Figure 6. 3. Quadrupole mass analyser contain four parallel conducting rods (quadrupole) spaced about a central axis along which ions are conducted. Quadrupoles separate ions based on the stability of their flight trajectories through an oscillating electric field.

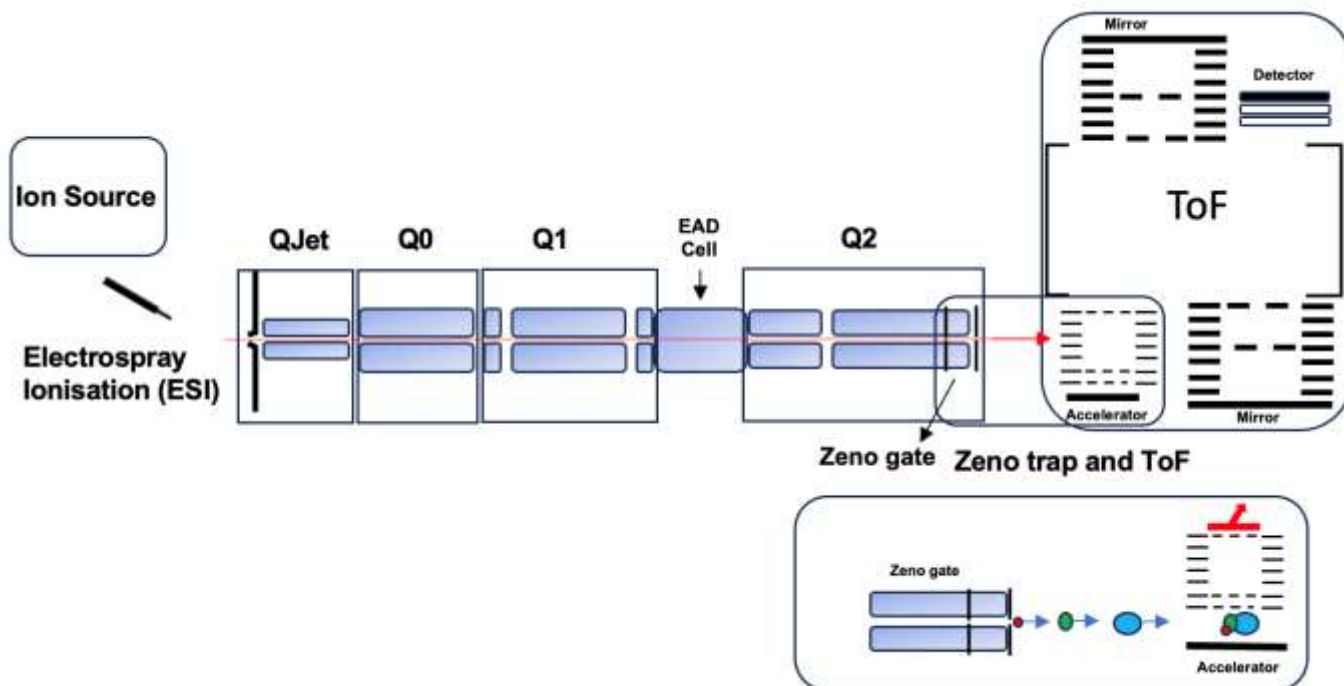


Figure 6. 4. Diagram of Zeno TOF 7600 mass spectrometer, showing the assembly of ion rail components, through which ions flow from left to right. The ion source charges the ions so they can accelerate through the mass spectrometer. Electro spray ionisation (ESI) uses electrical energy to assist the transfer of ions from solution into the gaseous phase before they are subjected to mass spectrometric analysis. The QJet ion guide allows the use of a larger orifice from the source into the mass spectrometer, and a smaller aperture leading into the Q0 chamber. This reduces gas load on following stages and improves sensitivity. The rods in the Q0 do not act as mass filters but allow guiding the ions into the mass spectrometer. Ions are selected for product analysis in Q1. Ions leave Q1 and enter the EAD cell, which can trap and fragment ions or transfer precursor ions to Q2 for collision induced dissociation (CID)-based fragmentation. The higher the collision energy, the greater the fragmentation. Fragment ions enter the Zeno trap, where they are collected and sent to the TOF accelerator in a mass dependent manner. High molecular weight ions are scanned out first and are followed by lower molecular weight ions so that they all arrive at the TOF accelerator at the same time.

Liquid chromatography coupled to tandem mass spectrometry (LC-MS/MS) is often used in lipidomic analysis and aids the separation of analytes, improving sensitivity and specificity by being able to separate isobaric and isomeric compounds that cannot be differentiated by the mass spectrometer alone (*Thomas et al., 2022*). Reverse phase liquid chromatography is also frequently used in lipid analysis. This type of chromatography involves a non-polar stationary phase, and relatively polar mobile phases are used for the separation of lipids. The more hydrophobic the lipid components are, the longer they are retained in the system.

There are two main mass spectrometry approaches being used in lipidomics, which are untargeted and targeted analysis. Untargeted analysis involves the analysis of all detectable lipids in a sample, whereas targeted measures specific classes or species of lipid (*Lee and*

Yokomizo, 2018). Untargeted mass spectrometry approach provides the most appropriate route to detect unexpected changes in metabolite concentrations.

Table 6. 1. Diagnostic ions of major phospholipids found in erythrocytes (Leidl et al., 2008, Spickett et al., 2011)

Headgroup	Positive ion	Negative ion
Phosphatidylcholine	Precursor ion m/z 184 Da	-
Phosphatidylethanolamine	Neutral loss m/z 141 Da	-
Phosphatidylserine	Neutral loss m/z 185 Da	Neutral loss m/z 87 Da
Sphingomyelin	Precursor ion m/z 184 Da	-
Phosphatidylinositol	-	Precursor ion m/z 241 Da

### Sample preparation

Sample preparation is critical for successful mass spectrometry analysis (Garg and Zubair, 2023). There are various methods in which lipids can be extracted and these include the Folch lipid extraction method, the Bligh-Dyer and methyl tert-butyl ether (MTBE). The Folch method is the oldest and most widely used method for lipid extraction, which involves mixing chloroform, methanol and water, and it has high sensitivity for the extraction of phospholipids. The Bligh-Dyer method is an adaptation of the Folch method, also using a chloroform methanol and water mixture. However, this method is ideal for lipid isolation from cell pellets (Wu et al., 2020). The main difference between these two methods is the ratio of chloroform, methanol and water, which is 2:1:0.75 in Folch and 1:1:0.9 in Bligh-Dyer. Also, the volume of the solvent system is 20 times the sample in Folch, and four times in Bligh-Dyer (Saini et al., 2021). Lastly, the MTBE method allows the extraction of lipids without the use of toxic chloroform and involves the use of MTBE, methanol and water. MTBE has a lower density than water, and so the organic phase containing the lipids is formed at the top, simplifying the extraction and reducing the risk of contamination from the aqueous phase (Wu et al., 2020). Lipid extraction is the major limiting factor to analyse the complete set of lipids in biological systems. Lipid classes display a large variety of polarities, and in consequence none of the current protocols are efficient in extracting all lipid classes simultaneously (Aldana et al., 2020).

Lipidomics research has captured increased attention due to well recognised roles of lipids in numerous human diseases, including diabetes (*Hu et al., 2009*). The identification of pathogenic lipid metabolites, characterization of pathogenic lipid profiles and their correlation to clinical outcomes are essential for the development of the next generation of prevention, therapy and/or intervention strategies (*Wu et al., 2020*).

### **Lipidomics of erythrocytes**

Several lipidomics studies have been carried out on erythrocytes. In 2008, Leidl and colleagues carried out an investigation involving mass spectrometric analysis of lipid species of human circulating blood cells, including erythrocytes from healthy donors (*Leidl et al., 2008*). Samples from nine participants (male and females) were used and it was found that PC and SM were the most abundant phospholipids, followed by PE and PS. The PC species of PC 34:2, PC 34:1, PC 36:2 and PC 36:3 were found to be highly profuse. Also, PC 36:4 and PC O-36:4 were detected but in lesser quantities. Some lyso-PC species were also found to be high in erythrocytes and these included LPC 16:0, LPC 18:0, LPC 18:1 and LPC 18:2. Abundant PE species identified included PE 34:1, PE 38:4, PE 38:5, PE 36:4. Lastly, PS species included PS 38:4, PS 40:6, PS 40:5 and PS 40:4. This study gave an insight into the different phospholipid species which are commonly abundant in erythrocytes. An investigation carried out later, in 2020, by Vahedi and collaborators also reported that PC and SM were the most abundant phospholipids found in erythrocytes, with PC 34:1 and SM 34:1 being the most abundant species (*Vahedi et al., 2020*).

In 2014, Koehrer and colleagues looked at erythrocyte phospholipids and polyunsaturated fatty acids in diabetic retinopathy (*Koehrer et al., 2014*). The most striking difference they found between controls and diabetic patients (with or without retinopathy) was a relative decrease in the amounts of docosahexaenoic acid (DHA, C22:6  $\omega$ -3) and arachidonic acid (C20:4  $\omega$ -6) and an increase in saturated fatty acids (C16:0, C18:0 and 20:4) in the diabetic group when compared to controls (*Koehrer et al., 2014*). Modifications were observed for PE species, which were largely altered in all diabetic patients (with or without retinopathy). These changes were observed on PE species esterified with arachidonic acid and/or DHA and included PE 20:4/22:6, PE 18:0/22:6, PE 18:1/22:6, PE 18:2/20:4 and PE 16:0/22:6. These alterations led to a decrease in the total number of PE species esterified with DHA in all diabetic patients. Diabetic subjects without retinopathy showed specific modifications in PCs, which consisted in significantly increased levels of PC esterified with saturated and/or monounsaturated fatty acids (namely PC 16:0/16:1, PC 16:0/16:0, PC 16:0/18:1, PC 18:1/18:1 and PC 18:0/18:1).

No major changes were found in individual PC species, except from PC 18:0/22:6 which was found to be lowered in patients suffering from diabetic retinopathy.

In 2020, Melzak and colleagues looked at lipid ratios as a marker for erythrocyte storage quality; they assessed lipid composition on erythrocytes on weeks 1 and 5, and the results showed that extracted POPC (16:0/18:1) remained constant but that the extracted SM (18:1/16:0) was decreased (*Melzak et al., 2020*). An explanation for this could be that sphingomyelins are hydrolysed by sphingomyelinases producing ceramides which have been linked to a form of erythrocyte death that is equivalent to apoptosis (*Melzak et al., 2020*).

Hyperglycaemia is known to induce oxidative stress, inflammation, and the formation of advanced glycation end products (AGEs), all of which are mechanisms implicated in cellular ageing (*Nowotny et al., 2015*). However, little is known about how hyperglycaemia influences age-related changes in the lipid composition of erythrocytes. It is also important to study individual factors to determine their specific contributions, as diabetes involves various changes beyond just hyperglycaemia including insulin resistance and altered metabolic pathways. Understanding the interplay between hyperglycaemia and ageing in erythrocyte lipid metabolism is crucial for elucidating the molecular mechanisms underlying age-related alterations in erythrocyte and their implications for health and disease.

### **Aim and objectives**

Thus, there is evidence that hyperglycaemia and ageing can cause changes in the erythrocyte lipidome, but there have been relatively few studies. Moreover, the combined effect of age and high levels of glucose on erythrocyte phospholipids has not yet been explored. Therefore, the aim of this study was to investigate the changes in erythrocyte phospholipid composition, after ageing the cells *in vitro* for five days using 5 mM, 22 mM and 100 mM glucose. The key research questions guiding this investigation included: How did ageing affect the phospholipid of erythrocytes? Did incubation in high glucose concentrations alter erythrocyte phospholipid profiles, and what were the differences in lipid profiles among participants? The objectives included assessing changes in erythrocyte phospholipid profiles after subjecting the cells to *in vitro* ageing and investigating the influence of different glucose concentrations on erythrocyte phospholipid composition during the ageing process. Lipid extraction using the MTBE method was used, followed by an untargeted lipidomics approach using the Zeno TOF 7600. Erythrocytes from the participants used in this investigation were also used in membrane fluidity studies.

## 6.2 Materials and methods

All materials and methods are described in Chapter 2. Details of mass spectrometry analysis of erythrocyte lipids are found in section 2.2.6.

## 6.3 Results

### 6.3.1 Effect of ageing on erythrocyte phospholipids

Lipid extracts from erythrocytes obtained from four different individuals were analysed using liquid chromatography tandem mass spectrometry. The samples were processed and analysed as a batch to ensure consistency and comparability of results. Mass spectrometry data were acquired in both positive and negative ion modes to characterise the lipid composition of the samples. The raw data was processed using MS-DIAL software to identify features. Results from the quality control (QC) are shown in the supplementary data (Figures S1-S5), demonstrating the consistency and reliability of the mass spectrometry analysis. These results confirmed that the QCs met the required standards for accuracy and reproducibility. In positive ion mode, a total of 2054 features were identified, while in negative ion mode, 4709 features were identified. Based on exact precursor mass and fragmentation data, 341 lipid species were identified in positive ion mode, and 677 in negative ion mode. The data was exported and imported into MetaboAnalyst for further statistical analysis. In MetaboAnalyst, the samples were normalised by the sum, meaning that the intensity values for each lipid feature within a sample were divided by the total sum of intensities for all lipid features in that sample. This normalisation method helped correct for differences in total ion intensity between samples, allowing more accurate comparison. The data were then transformed by log transformation (base 10), which involved taking a logarithm of the intensity values. Log transformation helped to stabilise variance across the data and achieved a more symmetrical distribution, making the data more suitable for statistical analysis. Finally, under data scaling, autoscaling was used, where the intensity values for each lipid feature were mean centred and divided by the standard deviation of that variable. Autoscaling ensured that each lipid feature contributed equally to the analysis by removing differences in scale and variance, facilitating the detection of patterns and differences between samples.

To address the first question, 'how did ageing affect the phospholipid of erythrocytes?' volcano plots were generated with the aim of visualising and identifying statistically significant differences in lipid abundance between untreated (day 0) and aged (day 4, 5 mM) cells (Figure 6.5). The fold change and *P* value thresholds were set to 2.0 and 0.05, respectively. The x-

axis shows the log<sub>2</sub> fold change and the y axis the statistical significance, represented as negative logarithm (base 10) of the *P* value obtained from a *t*-test. The log<sub>2</sub> fold change represented the ratio between untreated and treated cells under 5 mM glucose on a logarithmic scale with base 2. This is different from log<sub>10</sub> transformation, which was used initially to normalise the data, which helped compressed the wide range of values to make patterns more visible. Using a fold change threshold of 2.0 emphasised changes in abundance that were at least twofold higher or lower between experimental conditions. This helped filter out smaller and less meaningful differences. By using these thresholds, the features in the volcano plot were prioritised by substantial changes in abundance and statistically significant differences between the conditions. Figure 6.5A illustrates the results obtained in positive ion mode, indicating that out of 341 lipids analysed, 329 were found to be not significant, while 11 were found to be statistically significant. Among these, 7 were elevated on day 0, while 4 were increased on day 4 under 5 mM glucose. In contrast, Figure 6.5B shows the results obtained in negative ion mode, revealing that out of 677 lipids, 613 were not statistically significant, while 64 were significant. Among the significant lipids, 61 lipids were elevated on day 0, while 3 were increased on day 4 at 5 mM glucose.

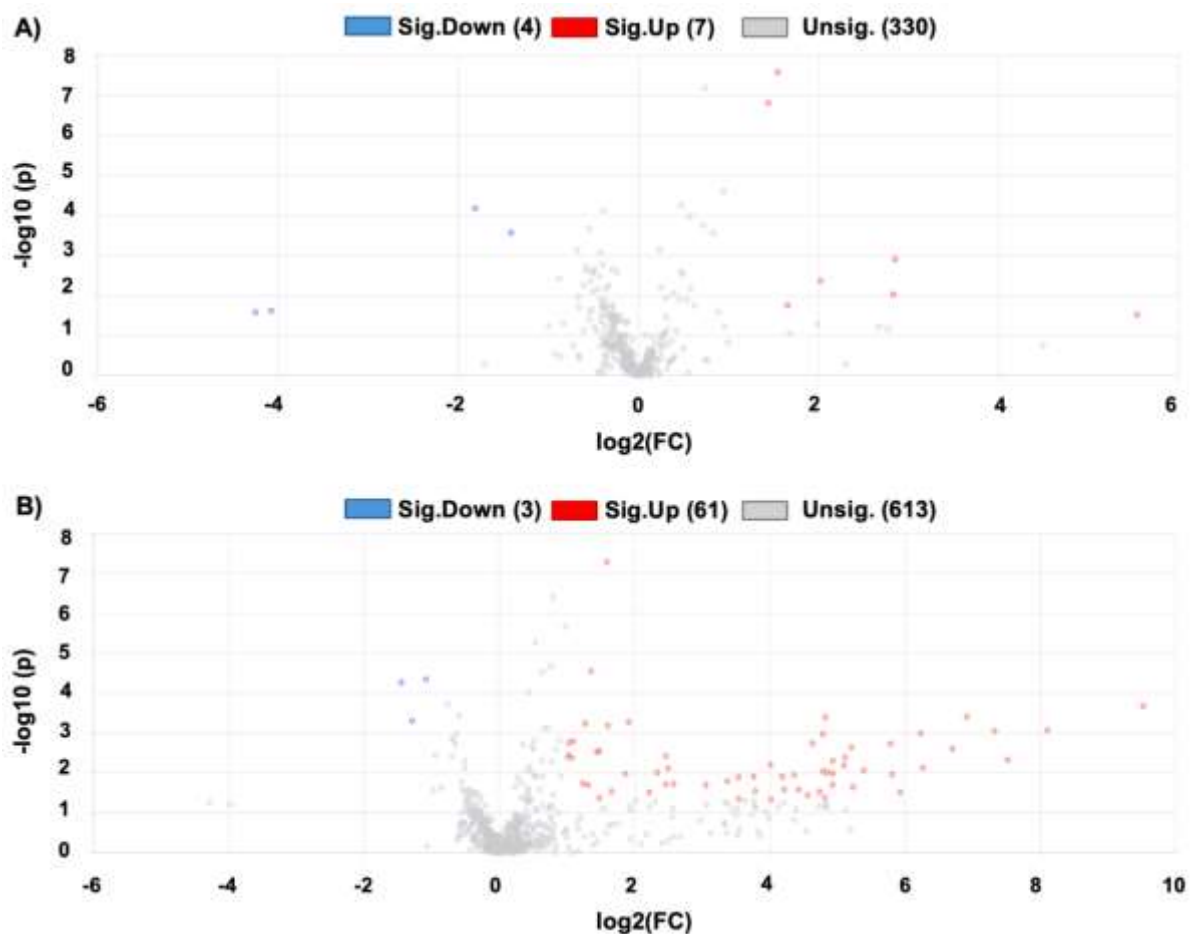


Figure 6. 5. Volcano plots were used to compare untreated and treated cells under 5 mM glucose. MetaboAnalyst V 6.0 was used to generate the plots. The direction of comparison was established based on untreated/aged in 5mM glucose, so significance up (sig. up) means that it was elevated on day 0, whereas significant down (sig. down) means a reduction on day 0. The fold change and *P* value thresholds were set to 2.0 and 0.05, respectively. The log<sub>2</sub> fold change represents the ratio between untreated and treated cells under 5 mM glucose on a logarithmic scale with base 2 with a formula:  $\text{Log}_2 \text{ fold change} = \log_2 (\text{untreated}/\text{treated with 5 mM glucose})$ . The plots represent the data obtained in positive (A) and negative (B) ion modes. In positive ion mode 341 lipids were identified and analysed, where 11 were found to be significantly different. The data represents the results obtained from 4 different participants ( $n=4$ ). For each participant, lipid extraction and mass spectrometry analysis were performed in triplicate, except for one participant on day 0 in positive ion mode, which was carried out in duplicate.

A total of 75 lipids, acquired during positive and negative ion mode, were found to be significantly different between untreated and treated cells under physiological levels of glucose. The list was refined to include lipids with mass errors of 5 parts per million (ppm) or less. Mass error refers to the difference between the measured mass of an ion and its expected (theoretical) mono-isotopic mass. A total of 44 lipids were identified including one fatty acid, four lysophospholipids (including PC, PE and PS), eighteen PCs (including ether

and oxidised PCs), sixteen PEs (including ether and oxidised PEs), three PSs and one SM. These were separated by non-oxidised and oxidised lipids and are shown in Tables 6.2 and 6.3, respectively. Twenty-four lipids were identified as non-oxidised with common adducts such as acetate ( $[M+CH_3COO]^-$ ), formate ( $[M+HCOO]^-$ ) and the loss of a hydrogen ( $[M-H]^-$ ) in negative ion mode. In positive ion mode, the adducts included the addition of hydrogen ( $[M+H]^+$ ) and sodium ( $[M+Na]^+$ ). Not all identified phospholipids had information about fatty acyl chains; instead, only the total number of carbons and double bonds were shown, such as PC 36:4, PC 40:6 and PC 32:2. This is because the mass spectrometry analysis sometimes cannot match all the fragments necessary to determine the exact fatty acyl composition. Most of these phospholipids had sodium adducts, which are generally more stable than protonated ions and require more energy to fragment. This results in less predictable and complex fragmentation patterns making the identification of phospholipids more challenging. Lyso-phospholipids, such as LPC 18:2, LPS 18:0 and LPE 16:0, eluted earlier than other phospholipids, between 1.35-1.84 minutes. These phospholipids only contain one fatty acid chain, which leads to weaker interactions with the hydrophobic stationary phase leading to faster elution times. PC 36:4|PC 18:2\_18:2 was the phospholipid identified with the lowest *P* value (raw), a fold change of 2.9, higher on day 0 and had a retention time of 5.347 minutes. On the other hand, PC O-36:4 |PC O-14:0\_22:4, an ether phospholipid, eluted last having a retention time of 6.197 minutes, the ether linkage might have resulted in a stronger interaction with the stationary phase. PC 28:0|PC 14:0\_14:0, PC 28:0, PC 40:6 and PC 40:6|PC 18:1\_22:5 were elevated on day 4 under 5 mM glucose treatment, the rest of the lipids were higher on day 0.

Table 6. 2. Significantly different lipids found between untreated (day 0) and treated cells under physiological glucose levels (day 4, 5 mM).

Identified lipids	Formula	Retention Time (mins)	Measured mass (m/z)	Expected mass (m/z)	Mass Error (ppm)	Adduct	FC	log2(FC)	Raw P value	-log10 (P value)	Highest
FA 20:5	C20H30O2	2.293	301.2172	301.2173	-0.432	[M-H] <sup>-</sup>	2.780	1.475	4.26E-02	1.371	Day 0
LPC 18:2	C26H50NO7P	1.35	578.3461	578.3463	-0.415	[M+CH3COO] <sup>-</sup>	2.410	1.269	5.74E-04	3.241	Day 0
LPE 16:0	C21H44NO7P	1.662	452.2780	452.2783	-0.597	[M-H] <sup>-</sup>	3.152	1.656	2.90E-02	1.537	Day 0
LPE 18:1	C23H46NO7P	1.84	478.2937	478.2939	-0.502	[M-H] <sup>-</sup>	2.098	1.069	4.21E-03	2.375	Day 0
LPS 18:0	C24H48NO9P	1.56	524.2997	524.2994	0.687	[M-H] <sup>-</sup>	5.955	2.574	1.88E-02	1.725	Day 0
PC 28:0	C36H72NO8P	4.857	700.4891	700.48877	0.528	[M+Na] <sup>+</sup>	0.059	-4.079	2.38E-02	1.623	Day 4, 5mM
PC 28:0 PC 14:0_14:0	C36H72NO8P	4.853	678.5067	678.50677	-0.088	[M+H] <sup>+</sup>	0.052	-4.253	2.59E-02	1.587	Day 4, 5mM
PC 32:2	C40H76NO8P	5.105	752.5209	752.52008	1.143	[M+Na] <sup>+</sup>	4.050	2.018	4.31E-03	2.365	Day 0
PC 33:2	C41H78NO8P	4.013	788.5424	788.5447	-2.866	[M+HCOO] <sup>-</sup>	159.450	7.317	8.96E-04	3.048	Day 0
PC 34:3	C42H78NO8P	4.066	756.5529	756.55377	-1.203	[M+H] <sup>+</sup>	7.093	2.826	9.30E-03	2.031	Day 0
PC 36:4	C44H80NO8P	5.345	804.5520	804.55139	0.758	[M+Na] <sup>+</sup>	2.711	1.439	1.52E-07	6.819	Day 0
PC 36:4 PC 18:2_18:2	C44H80NO8P	5.347	782.5690	782.5694	-0.511	[M+H] <sup>+</sup>	2.920	1.546	2.56E-08	7.592	Day 0
PC 40:6	C48H84NO8P	5.776	856.5819	856.5827	-0.992	[M+Na] <sup>+</sup>	0.285	-1.813	6.61E-05	4.180	Day 4, 5mM
PC 40:6 PC 18:1_22:5	C48H84NO8P	5.784	834.6014	834.60071	0.875	[M+H] <sup>+</sup>	0.375	-1.417	2.66E-04	3.575	Day 4, 5mM

<b>PC O-36:4 PC O-14:0_22:4</b>	C44H82NO7P	6.197	826.5947	826.5967	-2.432	[M+CH3COO] <sup>-</sup>	2.135	1.095	1.64E-03	2.785	Day 0
<b>PE 21:1 PE 6:0_15:1</b>	C26H50NO8P	2.182	534.3181	534.3201	-3.893	[M-H] <sup>-</sup>	18.48 6	4.208	2.63E-02	1.580	Day 0
<b>PE 26:3</b>	C31H56NO8P	2.79	600.3671	600.3671	-0.100	[M-H] <sup>-</sup>	16.03 2	4.003	6.26E-03	2.204	Day 0
<b>PE 34:2 PE 16:0_18:2</b>	C39H74NO8P	5.031	714.5059	714.5079	-2.813	[M-H] <sup>-</sup>	3.762	1.912	5.31E-04	3.275	Day 0
<b>PE 35:2 PE 16:0_19:2</b>	C40H76NO8P	5.404	728.5214	728.5236	-3.020	[M-H] <sup>-</sup>	2.481	1.311	2.03E-02	1.693	Day 0
<b>PE 35:2 PE 17:1_18:1</b>	C40H76NO8P	5.368	728.5212	728.5236	-3.349	[M-H] <sup>-</sup>	2.718	1.443	2.99E-03	2.525	Day 0
<b>PE 36:2 PE 18:1_18:1</b>	C41H78NO8P	5.391	742.5383	742.5392	-1.145	[M-H] <sup>-</sup>	3.639	1.863	1.06E-02	1.973	Day 0
<b>PE 38:4 PE 18:0_20:4</b>	C43H78NO8P	5.254	766.5382	766.5392	-1.265	[M-H] <sup>-</sup>	2.557	1.355	2.83E-05	4.548	Day 0
<b>PE 40:5 PE 18:0_22:5</b>	C45H80NO8P	5.426	792.5526	792.5549	-2.852	[M-H] <sup>-</sup>	2.792	1.481	2.87E-03	2.543	Day 0
<b>SM 32:2;O2 SM 17:0;O2 15:2</b>	C37H73N2O6P	4.133	731.5350	731.5345	0.670	[M+CH3COO] <sup>-</sup>	2.035	1.025	3.64E-03	2.439	Day 0

The table shows 24 lipids with an error mass of 5 parts per million (ppm) or less. The error mass was calculated following the formula:  $((\text{measured mass} - \text{expected mass}) / \text{expected mass}) * 10^6$ . The lipids were arranged based on lipid type. The data represents the results obtained from 4 different participants ( $n = 4$ ). For each participant, lipid extraction and mass spectrometry analysis were performed in triplicate, except for one participant on day 0 in positive ion mode, which was carried out in duplicate. FC represents the fold change.

The phospholipid PC 36:4 has previously been identified in erythrocytes. In the current study, PC 36:4|PC 18:2\_18:2 was found to differ significantly between untreated (day 0) and treated (aged in 5 mM glucose) samples, with a fold change of 2.9, being higher on day 0. Figure 6.6 shows the information on PC 36:4|PC 18:2\_18:2, which was obtained using positive ion mode. Figure 6.6A illustrates the MS<sup>2</sup> data, and the fragments detected. The m/z of 782.569 corresponds to PC 36:4 in positive ion mode and the matching fragments of m/z 184; 502 and 520 were also observed. One of these fragments is the precursor of PC, m/z 184, which is a diagnostic for the presence of choline containing phospholipids, and hence confirmed the phospholipid species. The m/z 502 fragment corresponded to the loss of linoleic acid (C18:2), and m/z 520 to the loss of linoleic acyl group (excluding the carboxyl group). Further analysis was carried out to look at the extracted ion chromatogram (EIC) of 782.569 (PC 36:4) (Figure 6.6B) where a large and a small peak were observed. The retention time of the larger peak was below six minutes and for the smaller peak it was just above six minutes. The larger peak corresponds to m/z 782.569 and the smaller peak is likely an isomer, which refers to a molecule that has the same molecular formula, but its atoms are arranged in a different order or configuration. Isomers can arise when a double bond in one or both fatty acyl chains is located at different positions along the carbon chain or when the fatty acids in the sn1 and sn2 positions are switched. The overall structure of PC 36:4| PC 18:2\_18:2 and where fragmentation likely occurred is shown in Figure 6.5C. The position of double bonds is not certain and is represented only to indicate their presence in the carbon chain. This is because the analytical technique used (LC-MS/MS) to determine the composition of phospholipids does not provide information about the exact positions of the double bonds. The fragmentation patterns observed can only identify the lengths and saturation levels of the fatty acids. Fatty acids can have multiple positional isomers, meaning they have the same number of carbon atoms and double bonds, but with the double bonds in different positions. These extra steps carried out, allowed to further investigate, and verify this specific phospholipid by looking at the MS<sup>2</sup> data.

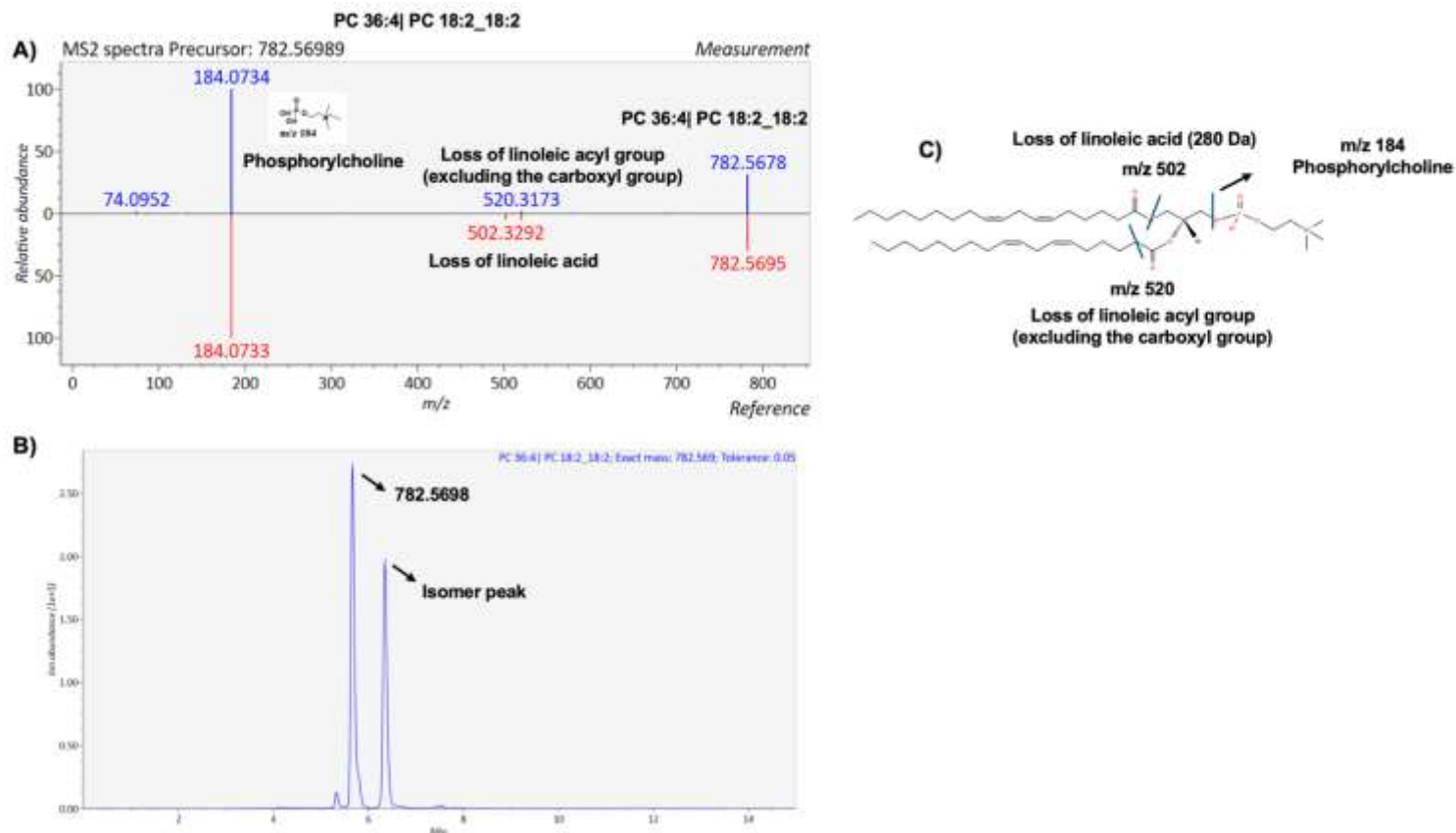


Figure 6. 6. Information on PC 36:4| PC 18:2\_18:2 obtained using positive ion mode. The adduct present was  $[M+H]^+$ . A) MS<sup>2</sup> spectra showing the matching fragments for m/z 782.569. Precursor ion m/z 184, corresponds to phosphorylcholine. Fragment m/z 502 correspond to the loss of linoleic acid (18:2). Fragment m/z 520 corresponds to the loss of linoleic acid excluding the carboxyl group. B) Extracted ion chromatogram showing the retention time (minutes) of PC 36:4| PC 18:2\_18:2 and a tolerance mass of 0.05. C) Overall composition PC 36:4| PC 18:2\_18:2 and where fragmentation likely occurred. The position of double bonds is not certain.

All oxidised phospholipids were found to be elevated on day 0 and in negative ion mode, such as PC O-36:5;O|PC O-20:5\_16:0;O and PC 34:1;O2|PC 16:0\_18:1;O2, which had a fold change of 3 and 103, respectively. Common adducts found in oxidised phospholipids were acetate ( $[M+CH_3COO]^-$ ), formate ( $[M+HCOO]^-$ ) and the loss of a hydrogen ( $[M-H]^-$ ) in negative ion mode. In positive ion mode, the adducts included the addition of hydrogen ( $[M+H]^+$ ) and sodium ( $[M+Na]^+$ ). Long chain oxidised ether phospholipids such as PC O-36:5;O|PC O-20:5\_16:0;O and PE O-40:7;O2|PE O-18:1\_22:6;O2 appeared to elute last, with retention times of 5.261 and 5.548 minutes, respectively. On the other hand, PE O-38:5;O4|PE O-18:1\_20:4;O4 and PE O-36:3;O3|PE O-18:2\_18:1;O3 had retention times of 4.008 and 4.011 minutes, respectively. These differences in retention times can be attributed to the varying lengths and degrees of saturation of the fatty acid chains, as well as the number of oxidized groups present. In reverse-phase chromatography, longer fatty acid chains increase hydrophobic interactions with the stationary phase, resulting in longer retention times. Conversely, phospholipids with higher degrees of unsaturation and oxidation tend to have stronger interactions with the mobile phase due to increased polarity, leading to shorter retention times. This balance of hydrophobic interactions with the stationary phase and polarity effects with the mobile phase explains why long chain, less oxidized lipids elute later than shorter chain, highly oxidized lipids. PS 25:0;O|PS 18:0\_7:0;O had the highest fold change (119.910) and PC O-36:5;O|PC O-20:5\_16:0;O the lowest (3.008). A fold change of 119.910 suggests that PS 25:0;O|PS 18:0\_7:0;O was highly abundant in untreated cells, possibly indicating a process that might be diminished or affected by aging, such as a signalling pathway. On the other hand, the low fold change of 3.008 for PC O-36:5;O|PC O-20:5\_16:0;O suggests it underwent less significant alteration, perhaps indicating it is less involved in the aging process or more stable under stress conditions. Lastly, PS 25:0;O|PS 18:0\_7:0;O and PC 25:1;O|PC 10:0\_15:1;O were the first oxidised lipids to elute with retention times of 1.919 and 2.684 minutes, respectively. This early elution can be attributed to their structural properties. Typically, shorter chain lengths elute earlier due to less interaction with the stationary phase and the presence of oxidation increases polarity, further reducing the retention times.

Table 6. 3. Significantly different oxidised phospholipids found between untreated (day 0) and treated cells under physiological glucose levels (day 4, 5 mM).

Identified lipids	Formula	Retention Time (mins)	Measured mass (m/z)	Expected mass (m/z)	Mass Error (ppm)	Adduct	FC	log2(FC)	Raw P value	-log10 (P value)	Highest
PC 25:1;O PC 10:0_15:1; O	C33H64NO9P	2.684	708.4442	708.4457	-2.075	[M+CH3COO] <sup>-</sup>	27.454	4.779	1.07E-03	2.972	Day 0
PC 34:1;O2 PC 16:0_18:1; O2	C42H82NO10P	4.394	850.5798	850.5815	-1.940	[M+CH3COO] <sup>-</sup>	103.460	6.693	2.48E-03	2.605	Day 0
PC 34:2;O2 PC 16:0_18:2; O2	C42H80NO10P	4.013	848.5616	848.5658	-4.973	[M+CH3COO] <sup>-</sup>	23.531	4.557	3.64E-02	1.439	Day 0
PC 34:2;O3 PC 16:0_18:2; O3	C42H80NO11P	3.569	864.5612	864.5608	0.497	[M+CH3COO] <sup>-</sup>	30.390	4.926	1.03E-02	1.987	Day 0
PC 34:3;O PC 16:0_18:3; O	C42H78NO9P	4.209	830.5552	830.5553	-0.072	[M+CH3COO] <sup>-</sup>	13.739	3.780	2.86E-02	1.544	Day 0
PC 36:3;O2 PC 18:1_18:2; O2	C44H82NO10P	4.069	874.5778	874.5815	-4.185	[M+CH3COO] <sup>-</sup>	28.009	4.808	4.15E-02	1.382	Day 0
PC 36:4;O2 PC 16:0_20:4; O2	C44H80NO10P	4.542	872.5634	872.5658	-2.728	[M+CH3COO] <sup>-</sup>	21.420	4.421	2.63E-02	1.580	Day 0

PC O- 36:5;O PC O- 20:5_16:0; O	C44H80NO8P	5.261	840.5718	840.5760	-5.008	[M+CH3COO] <sup>-</sup>	3.008	1.589	5.25E-08	7.280	Day 0
PE 35:3;O PE 18:2_17:1; O	C40H74NO9P	4.659	742.5027	742.5028	-0.162	[M-H] <sup>-</sup>	5.489	2.457	1.93E-02	1.715	Day 0
PE 36:2;O PE 18:1_18:1; O	C41H78NO9P	5.137	758.5326	758.5341	-2.017	[M-H] <sup>-</sup>	5.513	2.463	3.76E-03	2.425	Day 0
PE 36:4;O2 PE 16:0_20:4; O2	C41H74NO10P	4.272	770.4946	770.4978	-4.192	[M-H] <sup>-</sup>	20.529	4.360	1.14E-02	1.943	Day 0
PE 36:4;O3 PE 16:0_20:4; O3	C41H74NO11P	3.489	786.4894	786.4927	-4.196	[M-H] <sup>-</sup>	11.586	3.534	4.48E-02	1.349	Day 0
PE 40:4;O4 PE 18:0_22:4; O4	C45H82NO11P	4.147	842.5544	842.5553	-1.021	[M-H] <sup>-</sup>	10.343	3.371	1.61E-02	1.792	Day 0
PE O- 36:3;O3 PE O- 18:2_18:1; O3	C41H78NO10P	4.011	774.5271	774.5291	-2.595	[M-H] <sup>-</sup>	37.474	5.228	2.27E-02	1.645	Day 0
PE O- 38:5;O4 PE O- 18:1_20:4; O4	C43H78NO11P	4.008	814.5208	814.5240	-3.978	[M-H] <sup>-</sup>	34.482	5.108	4.15E-03	2.382	Day 0

<b>PE O-40:7;O2 PE O-18:1_22:6;O2</b>	C45H78NO9P	5.548	806.5312	806.5341	-3.633	[M-H] <sup>-</sup>	28.692	4.843	9.66E-03	2.015	Day 0
<b>PS 25:0;O PS 18:0_7:0;O</b>	C31H60NO11P	1.919	652.3809	652.3831	-3.372	[M-H] <sup>-</sup>	119.910	6.906	3.94E-04	3.404	Day 0
<b>PS 38:4;O2 PS 18:0_20:4;O2</b>	C44H78NO12P	4.079	842.5147	842.5189	-4.997	[M-H] <sup>-</sup>	16.163	4.015	4.65E-02	1.333	Day 0
<b>PS 38:4;O4 PS 18:0_20:4;O4</b>	C44H78NO14P	3.479	874.5089	874.5087	0.206	[M-H] <sup>-</sup>	60.535	5.920	3.06E-02	1.514	Day 0
<b>PS 40:6;O2 PS 18:0_22:6;O2</b>	C46H78NO12P	4.272	866.5186	866.5189	-0.346	[M-H] <sup>-</sup>	30.341	4.923	1.99E-02	1.701	Day 0

The table shows 20 lipids with an error mass of 5 parts per million (ppm) or less. The error mass was calculated following the formula:  $((\text{measured mass} - \text{expected mass}) / \text{expected mass}) * 10^6$ . The lipids were arranged based on lipid type. The data represents the results obtained from 4 different participants ( $n = 4$ ). For each participant, lipid extraction and mass spectrometry analysis were performed in triplicate, except for one participant on day 0 in positive ion mode, which was carried out in duplicate. FC represents the fold change.

The oxidized phospholipid PC 34:2;O2|PC 16:0\_18:2;O2 was found to differ significantly between untreated (day 0) and treated (aged in 5 mM glucose) samples, with a fold change of 23, being higher on day 0. Figure 6.6 shows detailed information on PC 34:2;O2|PC 16:0\_18:2;O2, which was obtained using negative ion mode. Figure 6.7A illustrates the MS<sup>2</sup> data, highlighting the fragments detected. The m/z value of 848 corresponds to PC 34:2;O2 in negative ion mode. The m/z 774 represents a neutral loss of 74 Da, which is indicative of the PC head group. Additionally, matching fragments at m/z 255 and 311 were observed. The m/z 255 corresponds to palmitic acid (C16:0), a saturated fatty acid. The m/z 311 corresponds to linoleic acid (C18:2) containing two hydroxyl groups. In negative ion mode, the m/z of linoleic acid is typically 279, and the addition of two hydroxyl groups adds a mass of 32 (16 Da for each hydroxyl group), resulting in a new m/z of 311. Figure 6.7B shows the structure of PC 34:2;O2|PC 16:0\_18:2;O2, highlighting the palmitic acid and linoleic acid containing two double bonds and two hydroxyl groups. Figure 6.7C shows the extracted ion chromatogram of PC 34:2;O2|PC 16:0\_18:2;O2, with a mass of 848.5616, which had a retention time of around 4 minutes.

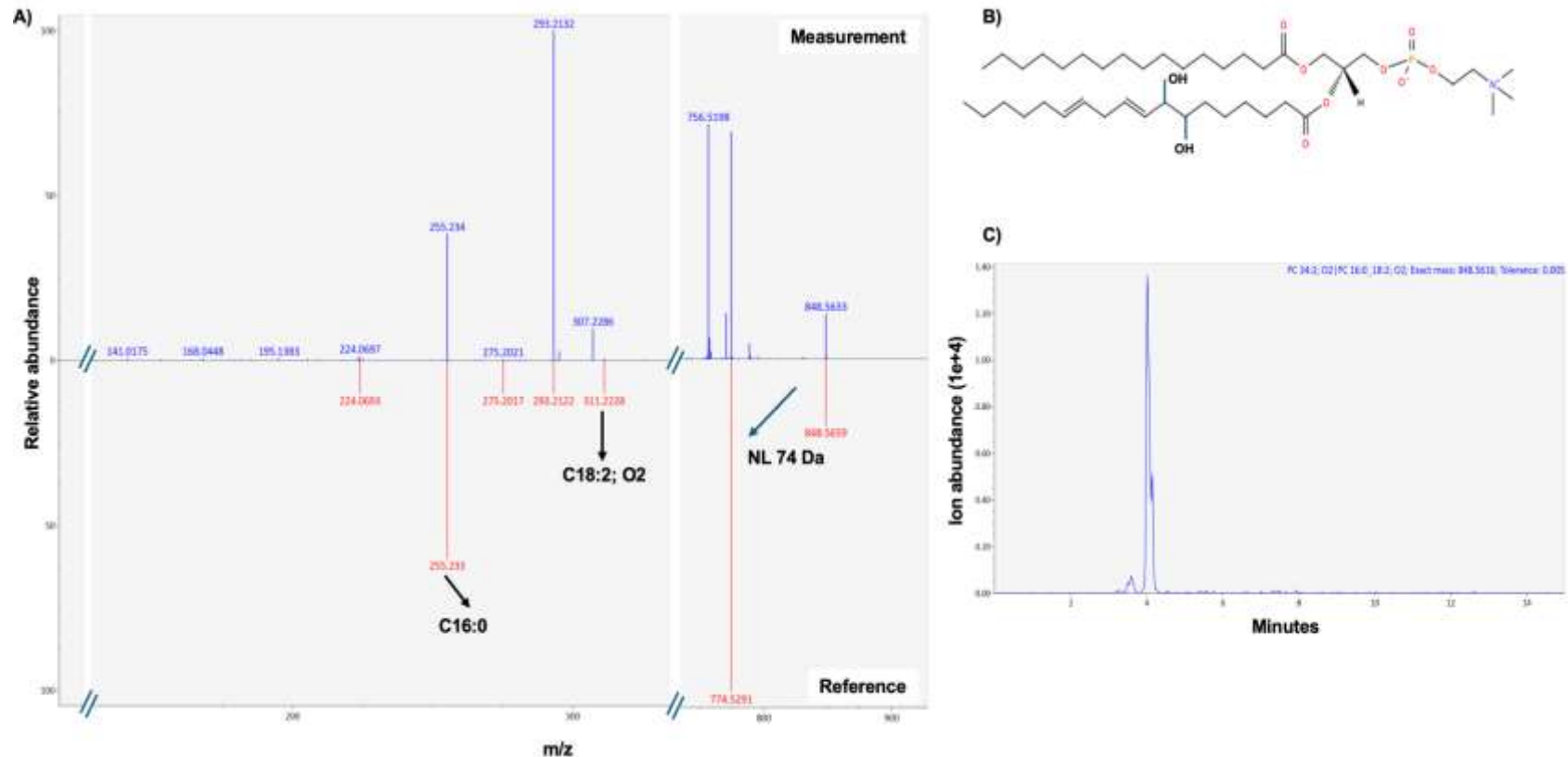


Figure 6. 7. Information on PC 34:2;O2|PC 16:0\_18:2; O2 obtained using negative ion mode. The adduct present was  $[M+CH_3COO]^-$ . A) MS<sup>2</sup> spectra showing the matching fragments for 848.5616 m/z. A neutral loss of 74 Da corresponds to the presence of phosphorylcholine. Fragment m/z 255 correspond to palmitic acid (C16:0). Fragment m/z 311 corresponds to linoleic acid containing two hydroxyl molecules. B) Overall composition PC 34:2;O2|PC 16:0\_18:2; O2. The position of double bonds and hydroxyl groups not certain, it is just a representation to show the presence of them in the phospholipid. C) Extracted ion chromatogram showing the retention time (minutes) of PC 34:2| PC 16:0\_18:2;O2 and a tolerance mass of 0.005.

### 6.3.2 Effect of glucose treatments on erythrocyte phospholipids

To address the second question, 'did incubation in high glucose concentrations alter erythrocyte phospholipid profiles?', volcano plots were generated with the aim of visualising and identifying statistically significant differences in phospholipid abundance between 5-22 mM and 5-100 mM glucose. Figure 6.8 shows volcano plots for the data acquired between 5 mM and 22 mM glucose during positive (Figure 6.8A) and negative ion modes (Figure 6.8B). Few differences were found between the cells kept in media containing 5 mM and 22 mM. In positive ion mode two phospholipids were found to be elevated at 5 mM and one at 22 mM glucose. In negative ion mode one lipid was found elevated in erythrocytes kept in media containing 5 mM glucose and six phospholipids were found to be increased after 22 mM glucose treatment.

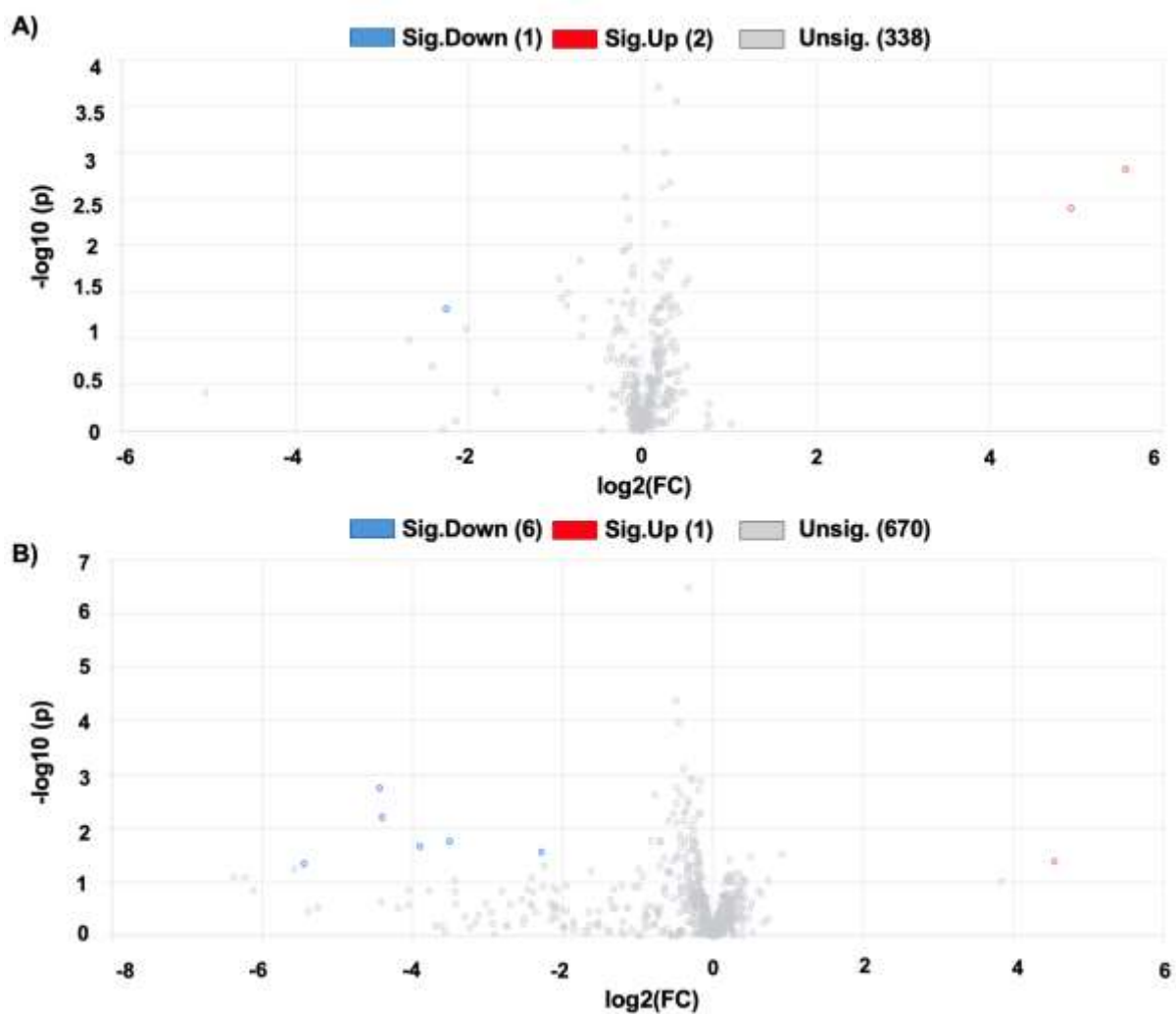


Figure 6. 8. Volcano plots used to compare lipids extracted from erythrocytes under 5 mM and 22 mM glucose. MetaboAnalyst V 6.0 was used to generate the plots. The direction of comparison was established based on 5mM/22mM glucose, so significance up (sig. up) means that it was elevated on day 4 under 5 mM glucose treatment, whereas significant down (sig. down) means a reduction. The fold change and  $P$  value thresholds were set to 2.0 and 0.05, respectively. The plots represent the data obtained in positive (A) and negative (B) ion mode. The data represents the results obtained from 4 different participants ( $n= 4$ ). For each participant, lipid extraction and mass spectrometry analysis were performed in triplicate.

A total of ten lipids, acquired during positive and negative ion mode, were found to be significantly different between cells kept in media containing 5 mM and 22 mM glucose. The list was refined to include only phospholipids with mass errors of 5 parts per million (ppm) or less. Table 6.4 shows seven phospholipids, including four PCs (including one oxidised PC), two PEs (one ether and one oxidised PE), and one oxidised PS. Common adducts found were acetate ( $[M+CH_3COO]^-$ ) and the loss of a hydrogen ( $[M-H]^-$ ) in negative ion mode. In positive ion mode, the adducts included the addition of hydrogen ( $[M+H]^+$ ) and sodium ( $[M+Na]^+$ ). In erythrocytes exposed to 5 mM glucose, PC 28:0|PC 14:0\_14:0 and PC 28:0 showed elevated levels, with PC 28:0|PC 14:0\_14:0 showing the lowest *P* value among all phospholipids in the table. When treated with 22 mM glucose, five phospholipids, including two oxidised forms (PC 25:1;O|PC 10:0\_15:1;O and PS 25:0;O|PS 18:0\_7:0;O) were increased. PC 28:0|PC 14:0\_14:0 had the highest fold change, being higher at 5 mM glucose (fold change of 47).

Table 6. 4. Significantly different lipids found between cells kept in media containing 5 mM and 22 mM glucose.

Identified lipids	Formula	Retention Time (mins)	Measured mass (m/z)	Expected mass (m/z)	Mass Error (ppm)	Adduct	FC	log2(FC)	Raw P value	-log10 (P value)	Highest
PC 25:1;O PC 10:0_15:1;O	C33H64NO9P	2.684	708.4442	708.4457	-2.075	[M+CH3COO] <sup>-</sup>	0.046	-4.437	1.77E-03	2.751	22 mM
PC 28:0	C36H72NO8P	4.857	700.4891	700.4888	0.471	[M+Na] <sup>+</sup>	30.717	4.941	3.98E-03	2.400	5 mM
PC 28:0 PC 14:0_14:0	C36H72NO8P	4.853	678.5067	678.5068	-0.103	[M+H] <sup>+</sup>	47.474	5.569	1.51E-03	2.820	5 mM
PC 34:3	C42H78NO8P	4.066	756.5529	756.5538	-1.150	[M+H] <sup>+</sup>	0.208	-2.262	4.86E-02	1.314	22 mM
PE 41:7 PE 19:2_22:5	C46H78NO8P	4.740	802.5351	802.5392	-5.084	[M-H] <sup>-</sup>	0.067	-3.902	2.17E-02	1.664	22 mM
PE O-38:5 PE O-18:1_20:4	C43H78NO7P	5.433	750.5421	750.5443	-2.931	[M-H] <sup>-</sup>	0.205	-2.284	2.76E-02	1.560	22 mM
PS 25:0;O PS 18:0_7:0;O	C31H60NO11P	1.919	652.3809	652.3831	-3.372	[M-H] <sup>-</sup>	0.047	-4.404	6.21E-03	2.207	22 mM

The table shows seven phospholipids with an error mass of 5 ppm or less. The error mass was calculated following the formula:  $((\text{measured mass} - \text{expected mass}) / \text{expected mass}) * 10^6$ . The lipids were arranged based on lipid type. The data represents the results obtained from 4 different participants ( $n=4$ ). For each participant, lipid extraction and mass spectrometry analysis were performed in triplicate.

The oxidized phospholipid PS 18:0\_7:0;O was found to be significantly different between cells cultured in 5 mM and 22 mM glucose, with higher levels observed in the 22 mM glucose condition. Figure 6.8 provides detailed information, including the MS<sup>2</sup> spectra (Figures 6.9A and 6.9B) and the proposed structure of PS 25:0;O|PS 18:0\_7:0;O (Figure 6.9C). In the MS<sup>2</sup> data (Figure 6.9A), the precursor ion at m/z 652 corresponds to PS 18:0\_7:0;O in negative ion mode. The fragment at m/z 565 indicates a neutral loss of 87 Da, which is characteristic of the PS head group. Additionally, fragments at m/z 283 and 145 were detected, corresponding to stearic acid (C18:0) and heptanoic acid (C7:0) with one hydroxyl group, respectively. The molecular formula for heptanoic acid is C<sub>7</sub>H<sub>14</sub>O<sub>2</sub>, and adding a hydroxyl group changes it to C<sub>7</sub>H<sub>14</sub>O<sub>3</sub>, giving a mass of 146 Da. In negative ion mode, the deprotonated ion ([M-H]<sup>-</sup>) results in a m/z of 145. The structure of PS 18:0\_7:0;O is shown in Figure 6.8C. The exact position of the hydroxyl group on the heptanoic acid chain is not certain based on the fragmentation data alone. Additionally, there is a possibility that the fatty acid chains could be reversed in the sn1 and sn2 positions, as this detail cannot be definitively determined from the current MS<sup>2</sup> data.

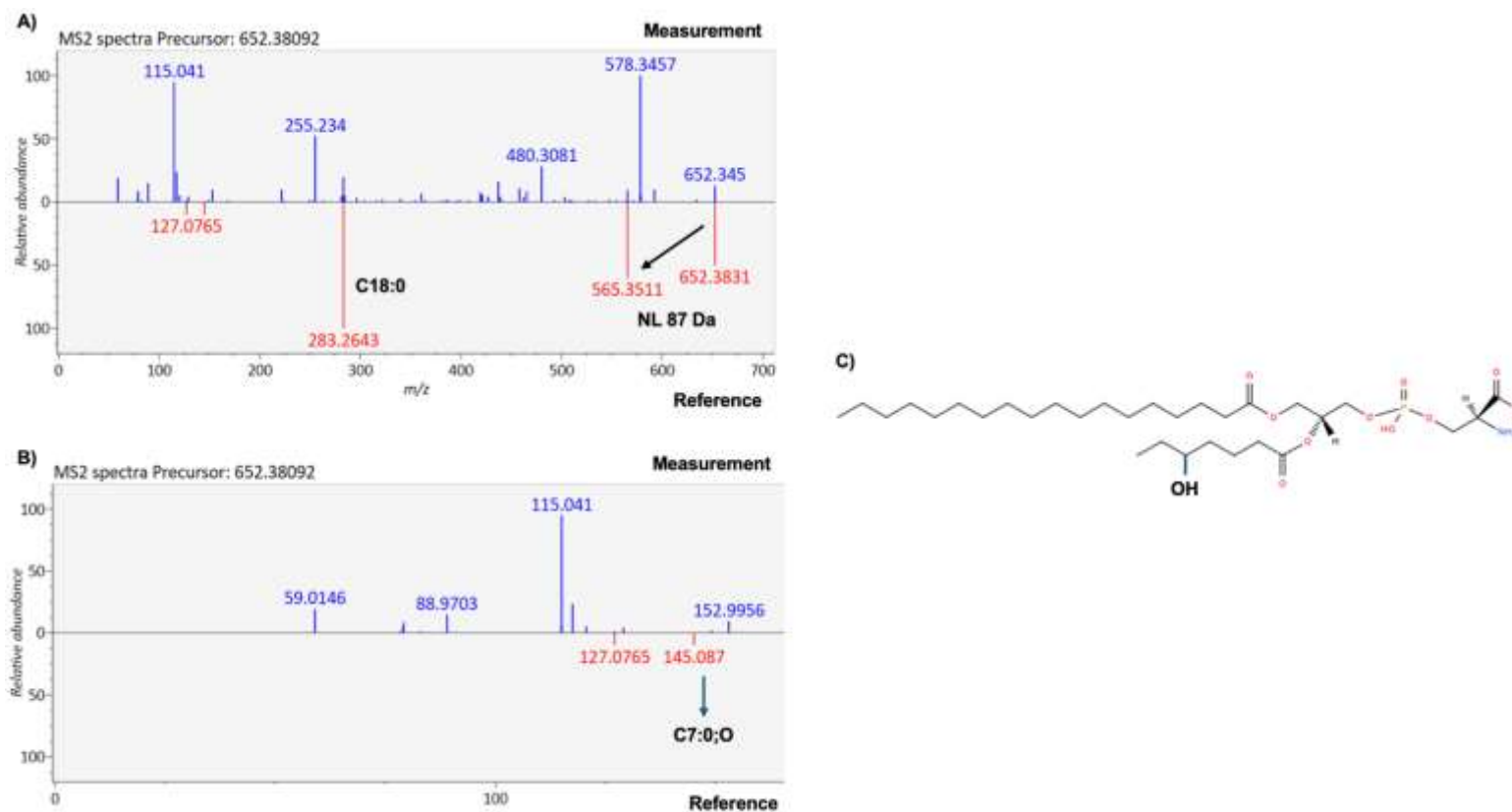


Figure 6. 9. Information on PS 25:0;O|PS 18:0<sub>7:0</sub>;O obtained using negative ion mode with [M-H]<sup>-</sup> adduct. A) MS<sup>2</sup> spectra showing the matching fragments for 652.3809 m/z. A neutral loss of 87 Da corresponds to the presence of phosphatidylserine. The fragment at m/z 283 corresponds to stearic acid (C18:0). B) Zoomed-in MS<sup>2</sup> spectra showing fragment at m/z 145, which corresponds to heptanoic acid and one hydroxyl group. (C7:0;O). C) Overall composition of PS 25:0;O|PS 18:0<sub>7:0</sub>;O. The position of the hydroxyl group in the C7:0 fatty acyl chain not certain, it is represented to indicate its presence in the phospholipid.

Volcano plots were generated to evaluate differences between erythrocyte lipid composition after 5 mM and 100 mM glucose treatments. Figure 6.10 shows volcano plots for the data acquired between 5 mM and 100 mM glucose during positive (Figure 6.10A) and negative ion mode (Figure 6.10B). In positive ion mode two phospholipids were found to be significantly different and were increased at 5 mM glucose. On the other hand, in negative ion mode five phospholipids were significantly different. Among these, one was found increased in erythrocytes kept in 5 mM glucose and four in 100 mM glucose.

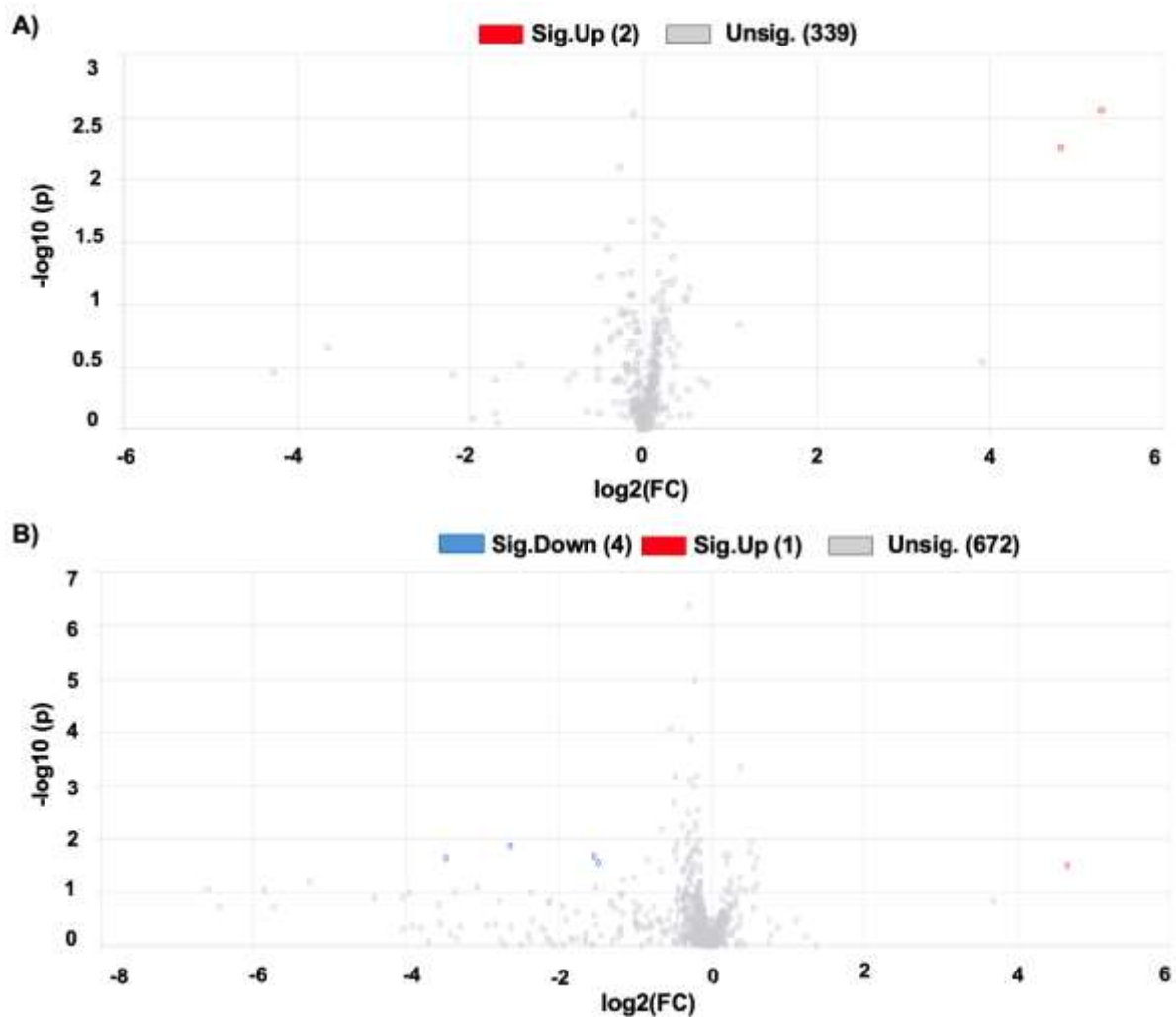


Figure 6. 10. Volcano plots used to compare lipids extracted from erythrocytes under 5 mM and 100 mM glucose. Plots were generated by MetaboAnalyst V 6.0. The direction of comparison was established based on 5mM/100mM glucose, so significance up (sig. up) means that it was elevated on day 4 under 5 mM glucose treatment, whereas significant down (sig. down) means a reduction. The fold change and P value thresholds were set to 2.0 and 0.05, respectively. The data represents the results obtained from 4 different participants (n= 4). For each participant, lipid extraction and mass spectrometry analysis were performed in triplicate.

Seven lipids, acquired during positive and negative ion modes, exhibited significant differences between erythrocytes kept in media containing 5 mM and 100 mM glucose. To ensure accuracy, phospholipids with mass errors exceeding 5 parts per million (ppm) were excluded from further analysis. Table 6.5 shows five phospholipids, including two PCs and three PEs. The repetition of PE 34:1|PE 16:0\_18:1 in the table is due to its detection at different retention times, likely due to the presence of structural isomers or isobaric compounds, which can exhibit distinct chromatographic behaviours resulting in varying elution times. In negative ion mode, the predominant adduct observed was the loss of a hydrogen ( $[M-H]^-$ ), whereas positive ion mode revealed the addition of hydrogen ( $[M+H]^+$ ) and sodium ( $[M+Na]^+$ ). Erythrocytes exposed to 5 mM glucose showed increased levels of shorter chain PCs, such as PC 28:0|PC 14:0\_14:0 and PC 28:0, with PC 28:0|PC 14:0\_14:0 showing the lowest *P* value among all phospholipids in the table. Conversely, when treated with 100 mM glucose, longer chain PEs were observed to increase. The phospholipids PC 28:0|PC 14:0\_14:0 and PC 28:0 both have the same total number of carbons. However, they differ in terms of their adducts and the information that can be derived from their fragmentation patterns. PC 28:0|PC 14:0\_14:0, which has a proton ( $H^+$ ) adduct, allows clearer interpretation of the individual fatty acid chains. The fragmentation pattern of this molecule provides distinct peaks corresponding to the two C14 fatty acid chains. This detailed fragmentation makes it easier to confirm that the molecule consists of two 14-carbon chains. On the other hand, PC 28:0 with a sodium ( $Na^+$ ) adduct presents a different challenge. Sodium adducts often produce different fragment ions compared to protonated phospholipids and the fragmentation data does not provide sufficient information to determine the specific composition of the carbon chains. As a result, the exact distribution of carbon atoms between the fatty acid chains cannot be determined as easily. Therefore, while it is known that the total carbon number is 28, the specific composition of the carbon chains (e.g., whether it is composed of two C14 chains or another combination) remains unclear.

Table 6. 5. Significantly different phospholipids found between cells kept in media containing 5 mM and 100 mM glucose.

Identified lipids	Formula	Retention Time (mins)	Measured mass (m/z)	Expected mass (m/z)	Mass Error (ppm)	Adduct	FC	log2(FC)	Raw <i>P</i> value	-log10 ( <i>P</i> value)	Highest
<b>PC 28:0 PC 14:0_14:0</b>	C36H72NO8P	4.853	678.5067	678.5068	-0.088	[M+H] <sup>+</sup>	39.021	5.286	2.75E-03	2.560	5 mM
<b>PC 28:0</b>	C36H72NO8P	4.857	700.4891	700.4888	0.528	[M+Na] <sup>+</sup>	28.282	4.822	5.54E-03	2.257	5 mM
<b>PE 41:7 PE 19:2_22:5</b>	C46H78NO8P	4.740	802.5351	802.53918	-5.084	[M-H] <sup>-</sup>	0.161	-2.632	1.34E-02	1.873	100 mM
<b>PE 34:1 PE 16:0_18:1</b>	C39H76NO8P	5.155	716.52087	716.52362	-3.838	[M-H] <sup>-</sup>	0.345	-1.535	2.10E-02	1.677	100 mM
<b>PE 34:1 PE 16:0_18:1</b>	C39H76NO8P	5.111	716.52252	716.52362	-1.535	[M-H] <sup>-</sup>	0.360	-1.475	2.76E-02	1.559	100 mM

The table shows five phospholipids with an error mass of 5 ppm or less. The error mass was calculated following the formula:  $((\text{measured mass} - \text{expected mass}) / \text{expected mass}) * 10^6$ . The phospholipids were arranged based on lipid type. The data represents the results obtained from 4 different participants ( $n=4$ ). For each participant, lipid extraction and mass spectrometry analysis were performed in triplicate.

The phospholipid PC 28:0|PC 14:0\_14:0 was found to be significantly different between cells cultured in 5 mM and 100 mM glucose, with higher levels observed in the 5 mM glucose treatment. Figure 6.11 provides detailed information, including the MS<sup>2</sup> spectra (Figure 6.11A), the extracted ion chromatogram (Figure 6.11B) and the structure of PC 28:0|PC 14:0\_14:0 (Figure 6.11C). In the MS<sup>2</sup> data, the precursor ion at m/z 184 corresponds to PC headgroup in positive ion mode. The fragment at m/z 450 indicates the loss of C14:0. Figure 6.11B shows the extracted ion chromatogram of PC 28:0|PC 14:0\_14:0, with a mass of 678.5067, which had a retention time just below five minutes. Figure 6.11C shows the structure of PC 28:0|PC 14:0\_14:0, highlighting myristic acids as the carbon chains.

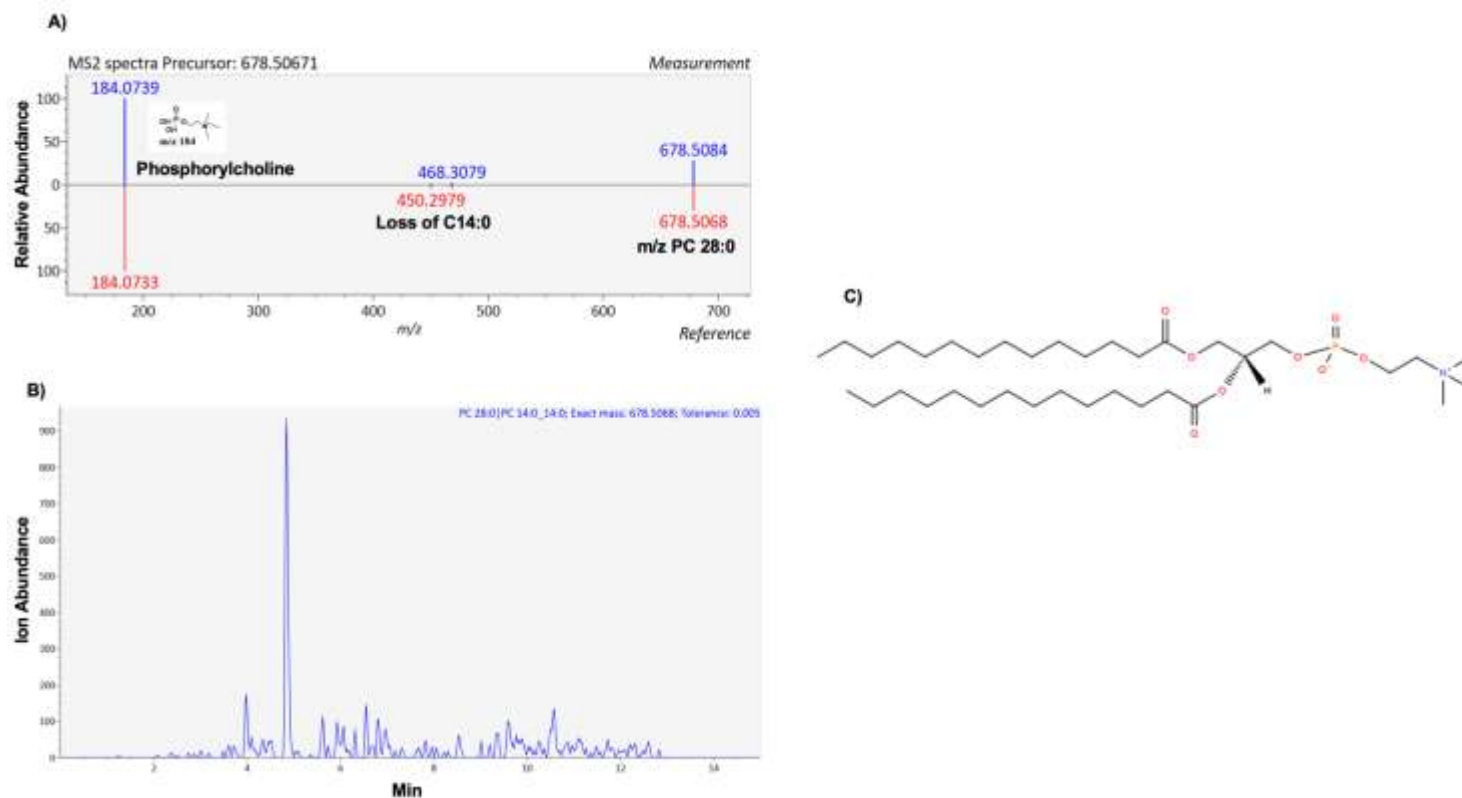


Figure 6. 11. Information on PC 28:0|PC 14:0\_14:0 obtained using positive ion mode with  $[M-H]^+$  adduct. A) MS<sup>2</sup> spectra showing the matching fragments for 678.5067 m/z. A precursor ion of 184 Da corresponds to the presence of phosphatidylcholine. The fragment at m/z 450 corresponds to myristic acid (C14:0). B) Extracted ion chromatogram of PC 28:0|PC 14:0\_14:0. C) Overall composition of PC 28:0|PC 14:0\_14:0.

The phospholipid PE 34:1|PE 16:0\_18:1 was elevated at 100 mM treatment. Figure 6.12 shows the MS<sup>2</sup> spectra (6.12A) and the proposed structure of the phospholipid (6.12B). The m/z 716 corresponds to the deprotonated molecular ion of PE 34:1 [M-H]<sup>-</sup>, indicating a total of 34 carbons and one double bond. The fragments m/z 281 and 255 correspond to oleic acid (C18:1) and palmitic acid (C16:0), respectively. Based on the fragmentation data alone the exact position of the double bond is not certain. Additionally, there is a possibility that the fatty acid chains could be reversed in the sn1 and sn2 positions, as this detail cannot be definitively determined from the current MS<sup>2</sup> data.

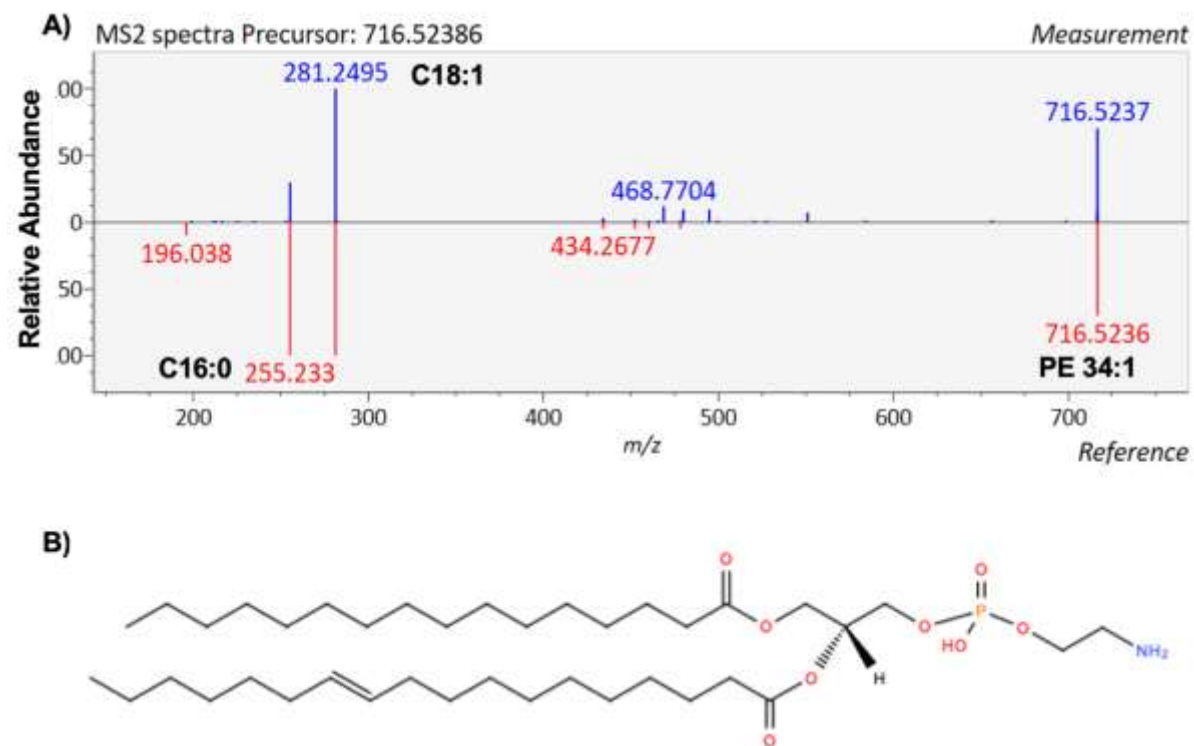


Figure 6. 12. Information on PE 34:1|PE 16:0\_18:1 obtained using negative ion mode with  $[M-H]^-$  adduct. A) MS<sup>2</sup> spectra showing the matching fragments for 716.5225 m/z. The fragments at m/z 281 and 255 correspond to oleic acid (C18:1) and palmitic acid (16:0). B) Overall structure of PE 34:1|PE 16:0\_18:1. The position of the double bond in the acyl chain is not certain, it is represented to indicate its presence in the phospholipid.

### 6.3.3 Differences in lipid profiles between participants

To address the question regarding the differences in lipid profiles among participants, principal component analysis (PCA) plots (Figure 6.13) were generated for the data acquired in both positive (Figure 6.13A) and negative ion modes (Figure 6.13B). PCA plots were employed to analyse lipid profiles derived from untreated erythrocytes obtained from different participants. The aim of this analysis was to characterise the variability in lipid composition among individuals and to identify any potential clustering or separation patterns that may exist based on these lipid profiles. Data analysis in MetaboAnalyst requires the use of triplicate samples. However, it is important to note that for participant D, only two samples were available for the analysis using mass spectrometry during positive ion mode. As a result, the data acquired for participant D during positive ion mode was omitted from the analysis, as MetaboAnalyst was unable to process it. However, the data acquired during negative ion mode was retained and included in the analysis. In the PCA plots generated, distinct clusters corresponding to each participant can be readily identified, with no observed overlap. Figure 6.13A illustrates that clusters for participants B and C were positioned on the positive side of the principal component 1 axis, while clusters for participant A were located on the negative side. This suggested that there were similarities in lipid profiles between participants B and C, while participant A appeared to have a more distinct profile. Similarly, Figure 6.13B shows that clusters for participants B and C were situated on the positive side of the principal component 1 axis, whereas participants A and D were located on the negative side. While the clusters belonging to each participant were clearly separated, indicating differences among samples, some similarities can be observed between the lipid profiles of participants B and C, as well as between participants A and D.

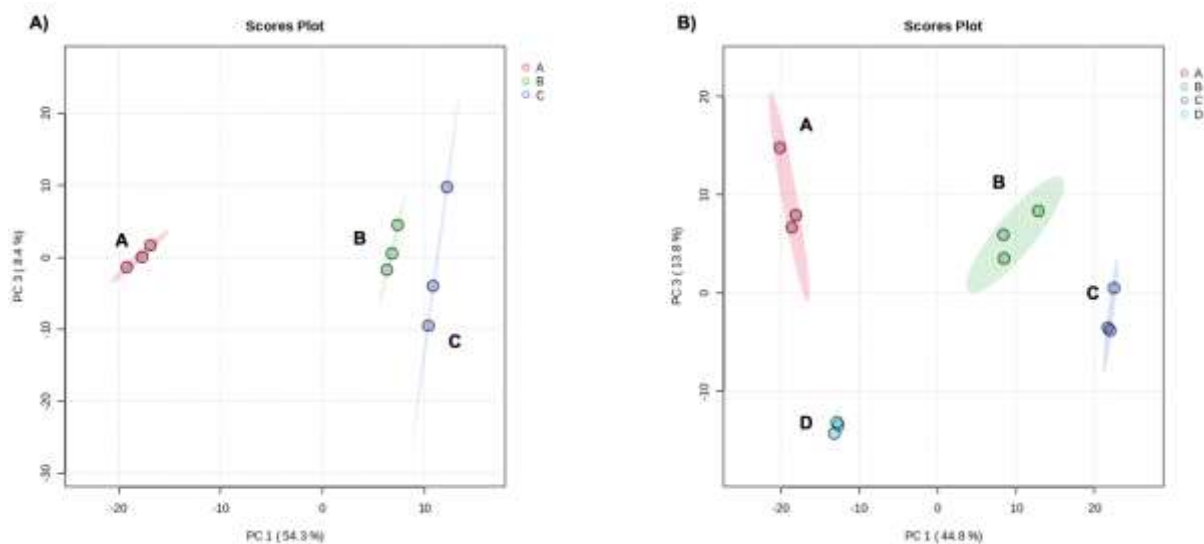


Figure 6. 13. Principal component analysis (PCA) plots, labelled (A) for positive ion mode and (B) for negative ion mode, were generated using samples from different participants through MetaboAnalyst.  $n=3$  for positive ion mode and  $n=4$  for negative ion mode.

To evaluate variations in lipid profiles among untreated erythrocytes from different participants, a one-way ANOVA (Figure 6.14) was conducted separately for data obtained in positive (Figure 6.14A) and negative (Figure 6.14B) ion modes. The Tukey's honestly significant difference (HSD) *post hoc* test, with a raw  $P$ -value threshold of 0.05, was applied to identify specific group differences. In positive ion mode, 228 lipids were found to be significantly different, while 113 were deemed insignificant. Conversely, in negative ion mode, 487 lipids were identified as significantly different among the participants. These results underscored the heterogeneity of lipid profiles among individuals and highlighted the importance of considering individual variability in lipidomic studies.



Figure 6. 14. One-way ANOVA was performed on the data obtained from different participants in positive (A) and negative (B) ion modes. A significance level of 0.05 was used for the ANOVA test. Subsequently, Tukey's honestly significance difference (HSD) post hoc test was applied with a raw  $P$ -value threshold of 0.05 to identify specific group differences.  $n=$  for positive ion mode and  $n=4$  for negative ion mode. The data represents the results obtained from 3 and 4 different participants for positive ( $n=3$ ) and negative ( $n=4$ ) ion modes, respectively. For each participant, lipid extraction and mass spectrometry analysis were performed in triplicate.

The results obtained from the one-way ANOVA followed by Tukey HSD post hoc test were exported for both positive and negative ion mode data. Subsequently, the analysis focused on diacyl phospholipids that exhibited significant differences among all participants and had a mass error of 5 ppm or less to streamline the presentation of the results. Diacyl phospholipids are among the most abundant and well-characterised species in erythrocytes, and by concentrating on them, the analysis provided a clearer and more concise insight into the differences observed among participants. This refinement led to the identification of 49 phospholipids comprising 15 distinct PCs (including 2 LPCs), 15 PEs (including 4 LPEs), 11 SMs, 3 PSs and 5 oxidised phospholipids. Table 6.6 shows the significantly different diacyl phospholipids identified among untreated erythrocytes from different participants, excluding

oxidised phospholipids. Among the identified phospholipids, PE 40:6|PE 18:0\_22:6 and PE 38:6|PE 16:0\_22:6 emerged as the first two species with the lowest *P*-values, respectively. LPE 22:4 appears twice in the table due to two distinct retention times: 1.743 and 1.867 minutes. LPE 22:4 with a retention time of 1.743 minutes was found higher in participant A and lower in participant C. Conversely, LPE 22:4 that eluted at 1.867 minutes was higher in participant B and lower in participant C. Similarly, the phospholipid PE 40:6|PE 18:0\_22:6 also appears twice with different retention times of 6.268 and 5.431 minutes. PE 40:6|PE 18:0\_22:6 that eluted at 6.268 minutes was higher in participant A and lower in participant C, whereas the one with a retention time of 5.431 minutes was higher in participant D and lower in participant C. The occurrence of the same phospholipid at different retention times can be attributed to the presence of isomers, molecules with the same molecular formula but different structural arrangements. In the case of lysolipids, isomers could arise from different positions of the acyl chain (sn1 versus sn2 positions). Also, variations could be due to differences in the positions of double bonds within the fatty acid chains or the combination of different acyl chains in the sn1 and sn2 positions. These structural variations can affect the retention times during chromatography, leading to differences in retention times for the same molecular species. Odd chain fatty acids such as PE 35:2|PE 17:1\_18:1 and SM 33:1;O2|SM 17:1;O2/16:0 (highest A and lowest C) were identified as significantly different among the participants. PE 35:2|PE 17:1\_18:1 was highest in participant B and lowest in participant C, whereas SM 33:1;O2|SM 17:1;O2/16:0 was highest in participant A and lowest in participant C.

Table 6. 6. Significantly different diacyl phospholipids identified among untreated erythrocytes from different participants.

Lipids Identified	Formula	Retention Time (mins)	Measured Mass (m/z)	Expected Mass (m/z)	Mass Error (ppm)	Adduct	Raw P value	-log10 (P value)	Tukey's HSD	Highest	Lowest
LPC 16:0	C24H50NO 7P	1.721	496.3403	496.3398	0.987	[M+H] <sup>+</sup>	6.54E-08	7.184	B-A; C-A; C-B	C	B
LPC 18:0	C26H54NO 7P	2.436	524.3706	524.3711	-0.915	[M+H] <sup>+</sup>	5.85E-05	4.233	B-A; C-A; C-B	C	A
LPE 18:1	C23H46NO 7P	1.840	478.2937	478.2939	-0.502	[M-H] <sup>-</sup>	1.87E-06	5.728	B-A; C-A; D-A; C-B; D-B; D-C	D	C
LPE 20:4	C25H44NO 7P	1.252	500.2788	500.2783	0.919	[M-H] <sup>-</sup>	1.98E-09	8.703	B-A; C-A; D-A; C-B; D-B; D-C	A	C
LPE 22:4	C27H48NO 7P	1.743	528.3099	528.3096	0.587	[M-H] <sup>-</sup>	1.28E-07	6.893	B-A; C-A; D-A; C-B; D-B; D-C	A	C
LPE 22:4	C27H48NO 7P	1.867	528.3114	528.3096	3.464	[M-H] <sup>-</sup>	4.60E-06	5.338	B-A; C-A; D-A; C-B; D-B; D-C	B	A
LPE 22:6	C27H44NO 7P	1.274	524.2781	524.2783	-0.458	[M-H] <sup>-</sup>	3.47E-06	5.460	B-A; C-A; D-A; C-B; D-B; D-C	B	A
PC 32:0 PC 16:0_16:0	C40H80NO 8P	6.298	734.5682	734.5694	-1.579	[M+H] <sup>+</sup>	1.69E-06	5.771	B-A; C-A; C-B	A	C

<b>PC 34:0 PC 16:0_18:0</b>	C42H84NO 8P	7.049	762.6004	762.6007	-0.407	[M+H] <sup>+</sup>	6.27E-06	5.203	B-A; C-A; C-B	A	C
<b>PC 34:1 PC 16:0_18:1</b>	C42H82NO 8P	6.384	760.5848	760.5851	-0.394	[M+H] <sup>+</sup>	9.33E-07	6.030	B-A; C-A; C-B	A	C
<b>PC 36:0 PC 18:0_18:0</b>	C44H88NO 8P	7.755	790.6324	790.6320	0.468	[M+H] <sup>+</sup>	1.04E-07	6.984	B-A; C-A; C-B	C	A
<b>PC 36:1 PC 18:0_18:1</b>	C44H86NO 8P	7.119	788.6167	788.6164	0.393	[M+H] <sup>+</sup>	1.34E-06	5.874	B-A; C-A; C-B	A	C
<b>PC 36:2 PC 18:1_18:1</b>	C44H84NO 8P	6.555	786.6007	786.6007	-0.076	[M+H] <sup>+</sup>	4.20E-06	5.377	B-A; C-A; C-B	A	C
<b>PC 36:4 PC 18:2_18:2</b>	C44H80NO 8P	5.347	782.5690	782.5694	-0.473	[M+H] <sup>+</sup>	6.00E-05	4.222	B-A; C-A; C-B	C	B
<b>PC 36:5</b>	C44H78NO 8P	5.239	802.5348	802.5357	-1.146	[M+Na] <sup>+</sup>	1.66E-04	3.779	B-A; C-A; C-B	B	A
<b>PC 36:5 PC 16:0_20:5</b>	C44H78NO 8P	5.236	780.5525	780.5538	-1.640	[M+H] <sup>+</sup>	4.11E-05	4.387	B-A; C-A; C-B	B	A
<b>PC 38:3 PC 18:0_20:3</b>	C46H86NO 8P	6.750	812.6154	812.6164	-1.268	[M+H] <sup>+</sup>	5.31E-06	5.275	B-A; C-A; C-B	C	A
<b>PC 38:5 PC 16:0_22:5</b>	C46H82NO 8P	5.744	808.5844	808.5851	-0.829	[M+H] <sup>+</sup>	1.49E-04	3.826	B-A; C-A; C-B	B	A
<b>PC 38:6</b>	C46H80NO 8P	5.252	828.5510	828.5514	-0.519	[M+Na] <sup>+</sup>	1.98E-05	4.704	B-A; C-A; C-B	C	A
<b>PC 40:4</b>	C48H88NO 8P	6.928	860.6146	860.6140	0.709	[M+Na] <sup>+</sup>	3.43E-04	3.465	B-A; C-A; C-B	C	A
<b>PE 32:0 PE 16:0_16:0</b>	C37H74NO 8P	6.335	690.5046	690.5079	-4.765	[M-H] <sup>-</sup>	1.10E-08	7.960	B-A; C-A; D-A; C-B; D-B; D-C	D	C

<b>PE 34:0 PE 16:0_18:0</b>	C39H78NO 8P	6.205	718.5360	718.5392	-4.495	[M-H]-	1.07E-06	5.972	B-A; C-A; D-A; C-B; D-B; D-C	D	C
<b>PE 34:2 PE 16:0_18:2</b>	C39H74NO 8P	5.857	714.5043	714.5079	-5.038	[M-H]-	1.41E-07	6.851	B-A; C-A; D-A; C-B; D-B; D-C	A	C
<b>PE 35:2 PE 17:1_18:1</b>	C40H76NO 8P	5.368	728.5212	728.5236	-3.349	[M-H]-	5.63E-09	8.250	B-A; C-A; D-A; C-B; D-B; D-C	B	C
<b>PE 36:2 PE 18:1_18:1</b>	C41H78NO 8P	6.495	742.5360	742.5392	-4.350	[M-H]-	6.93E-07	6.159	B-A; C-A; D-A; C-B; D-B; D-C	A	C
<b>PE 36:3 PE 18:1_18:2</b>	C41H76NO 8P	6.034	742.5375	742.5381	-0.741	[M+H]+	1.36E-04	3.866	B-A; C-A; C-B	B	A
<b>PE 38:4 PE 18:0_20:4</b>	C43H78NO 8P	6.467	766.5357	766.5392	-4.527	[M-H]-	2.91E-08	7.536	B-A; C-A; D-A; C-B; D-B; D-C	A	C
<b>PE 38:6 PE 16:0_22:6</b>	C43H74NO 8P	5.548	762.5057	762.5079	-2.793	[M-H]-	6.12E-10	9.213	B-A; C-A; D-A; C-B; D-B; D-C	A	C
<b>PE 40:6 PE 18:0_22:6</b>	C45H78NO 8P	6.268	790.5360	790.5392	-4.010	[M-H]-	2.16E-11	10.665	B-A; C-A; D-A; C-B; D-B; D-C	A	C
<b>PE 40:6 PE 18:0_22:6</b>	C45H78NO 8P	5.431	790.5369	790.5392	-2.846	[M-H]-	3.13E-06	5.505	B-A; C-A; D-A; C-B; D-B; D-C	D	C

<b>PE P-38:4 PE P-18:0_20:4</b>	C43H78NO 7P	6.923	752.5578	752.5589	-1.462	[M+H] <sup>+</sup>	1.02E-07	6.989	B-A; C-A; C-B	A	B
<b>PS 36:1 PS 18:0_18:1</b>	C42H80NO 10P	6.367	790.5578	790.5593	-1.935	[M+H] <sup>+</sup>	1.15E-04	3.941	B-A; C-A; C-B	A	C
<b>PS 38:3 PS 18:0_20:3</b>	C44H80NO 10P	6.001	814.5592	814.5593	-0.160	[M+H] <sup>+</sup>	1.59E-06	5.799	B-A; C-A; C-B	C	A
<b>PS 40:5 PS 18:0_22:5</b>	C46H80NO 10P	5.737	838.5573	838.5593	-2.480	[M+H] <sup>+</sup>	5.10E-07	6.292	B-A; C-A; C-B	B	A
<b>SM 32:1;O2 SM 16:1;O2/16:0</b>	C37H75N2 O6P	4.671	733.5492	733.5501	-1.254	[M+CH3C OO] <sup>-</sup>	1.90E-09	8.721	B-A; C-A; D-A; C-B; D-B; D-C	A	C
<b>SM 32:1;O2 SM 16:1;O2/16:0</b>	C37H75N2 O6P	4.757	675.5436	675.5436	0.089	[M+H] <sup>+</sup>	3.70E-07	6.432	B-A; C-A; C-B	A	C
<b>SM 33:1;O2 SM 17:1;O2/16:0</b>	C38H77N2 O6P	5.135	689.5584	689.5592	-1.146	[M+H] <sup>+</sup>	1.84E-05	4.736	B-A; C-A; C-B	A	C
<b>SM 36:1;O2</b>	C41H83N2 O6P	6.274	753.5879	753.5881	-0.239	[M+Na] <sup>+</sup>	7.32E-05	4.136	B-A; C-A; C-B	A	C
<b>SM 36:1;O2 SM 18:1;O2/18:0</b>	C41H83N2 O6P	6.272	731.6047	731.6062	-2.078	[M+H] <sup>+</sup>	1.97E-08	7.705	B-A; C-A; C-B	A	C
<b>SM 36:2;O2 SM 18:2;O2/18:0</b>	C41H81N2 O6P	5.607	729.5898	729.5905	-0.932	[M+H] <sup>+</sup>	4.94E-08	7.306	B-A; C-A; C-B	A	C
<b>SM 38:2;O2</b>	C43H85N2 O6P	6.363	757.6200	757.6218	-2.415	[M+H] <sup>+</sup>	1.61E-06	5.793	B-A; C-A; C-B	A	C
<b>SM 38:2;O2 SM 18:2;O2/20:0</b>	C43H85N2 O6P	6.389	757.6211	757.6218	-0.977	[M+H] <sup>+</sup>	1.36E-06	5.867	B-A; C-A; C-B	A	C
<b>SM 40:1;O2 SM 18:1;O2/22:0</b>	C45H91N2 O6P	7.777	787.6678	787.6688	-1.308	[M+H] <sup>+</sup>	5.08E-07	6.294	B-A; C-A; C-B	A	C

<b>SM 40:2;O2</b>	C45H89N2 O6P	7.141	785.6519	785.6531	-1.476	[M+H] <sup>+</sup>	1.07E- 04	3.971	B-A; C-A; C-B	A	C
<b>SM 42:2;O2 SM 18:1;O2/24:1</b>	C47H93N2 O6P	7.741	813.6835	813.6844	-1.057	[M+H] <sup>+</sup>	6.65E- 04	3.178	B-A; C-A; C-B	A	B

Significance was determined by one-way ANOVA followed by Tukey' HSD post hoc test with a *P*-value threshold of 0.05. The table shows diacyl phospholipids with an error mass of 5 ppm or less. The error mass was calculated following the formula: ((measured mass-expected mass)/expected mass)\*10<sup>6</sup>. The phospholipids were arranged based on lipid type. The Tukey's HSD column shows the difference between participants; *n*=3 for positive ion mode and *n*=4 for negative ion mode.

Five oxidised phospholipids are shown in Table 6.7. PE 36:3;O2|PE 16:0\_20:3;O2, showed variations among participants, with participant D showing the highest levels and participant B the lowest. Additionally, PS 25:0;O|PS 18:0\_7:0;O was highest in participant D and lowest in participant C, indicative of individual specific differences in oxidative stress. Furthermore, PC 36:4;O2|PC 16:0\_20:4;O2, PC 34:2;O2|PC 16:0\_18:2;O2, PC 36:4;O2|PC 16:0\_20:4;O2 and PE 36:4;O4|PE 16:0\_20:4;O4 displayed varying levels across participants, with participant A exhibiting higher levels compared to participant C. These results showed the interindividual variability in oxidative stress in lipid metabolism, with participants A and D exhibiting higher levels of oxidised phospholipids compared to participant B and C, particularly C.

Table 6. 7. Significantly different oxidised diacyl phospholipids identified among untreated erythrocytes from different participants.

Lipids Identified	Formula	Retention Time (mins)	Measured Mass (m/z)	Expected Mass (m/z)	Mass Error (ppm)	Adduct	Raw <i>P</i> value	-log <sub>10</sub> (P value)	Tukey's HSD	Highest	Lowest
PC 34:2;O2 PC 16:0_18:2;O2	C42H80NO10P	4.013	848.5616	848.5658	-4.973	[M+CH3COO]-	1.72E-08	7.765	B-A; C-A; D-A; C-B; D-B; D-C	A	C
PC 36:4;O2 PC 16:0_20:4;O2	C44H80NO10P	4.542	872.5634	872.5658	-2.728	[M+CH3COO]-	1.25E-08	7.902	B-A; C-A; D-A; C-B; D-B; D-C	A	C
PE 36:3;O2 PE 16:0_20:3;O2	C41H76NO10P	3.701	772.5126	772.5134	-1.036	[M-H]-	8.60E-10	9.065	B-A; C-A; D-A; C-B; D-B; D-C	D	B
PE 36:4;O4 PE 16:0_20:4;O4	C41H74NO12P	3.481	802.4838	802.4876	-4.710	[M-H]-	6.96E-08	7.158	B-A; C-A; D-A; C-B; D-B; D-C	A	C
PS 25:0;O PS 18:0_7:0;O	C31H60NO11P	1.919	652.3809	652.3831	-3.372	[M-H]-	3.13E-09	8.504	B-A; C-A; D-A; C-B; D-B; D-C	D	C

Significance was determined by one-way ANOVA followed by Tukey' HSD post hoc test with a *P*-value threshold of 0.05. The table shows oxidised phospholipids with an error mass of 5 ppm or less. The error mass was calculated following the formula: ((measured mass-expected mass)/expected mass)\*10<sup>6</sup>. The phospholipids were arranged based on lipid type. The Tukey's HSD column shows the difference between participants; *n*=3 for positive ion mode and *n*=4 for negative ion mode.

## 6.4 Discussion

The aim of this study was to investigate the effect of ageing and increasing glucose concentration on erythrocyte membrane phospholipids. The results revealed differences between fresh and aged cells at physiological glucose levels, with increased levels of oxidised phospholipids observed in untreated cells. Treatment with various glucose concentrations led to the elevation of PC 28:0|PC 14:0\_14:0 and PC 28:0 in cells aged in 5 mM glucose. In the 22 mM glucose treatment, two oxidised phospholipids, PC 25:1;O|PC 10:0\_15:1;O and PS 25:0;O|PS 18:0\_7:0;O, were increased compared to the physiological control. Additionally, longer chain phospholipids with a high number of double bonds, such as PE 41:7|PE 19:2\_22:5, PE O-38:5|PE O-18:1\_20:4 and PC 34:3 were elevated. In the 100 mM glucose treatment, long chain PEs (PE 41:7|PE 19:2\_22:5 and PE 34:1|PE 16:0\_18:1) were found to be elevated. Significant differences among participants were also observed when data from untreated erythrocytes were compared, highlighting the interindividual variability in oxidative stress and lipid metabolism.

The observation of differences between fresh and aged erythrocytes revealed insights into lipid composition variations. PC 36:4, previously noted for its abundance in erythrocytes by Leidl and colleagues, showed elevated levels in untreated and unaged cells, while PC 40:6 showed increased abundance in aged cells (*Leidl et al., 2008*). Most other PC species were elevated on day 0, with exceptions of PC 28:0|PC 14:0\_14:0 and PC 28:0, which were elevated in aged cells. Fold changes of 0.06 and 0.05 were found for PC 28:0 and PC 28:0|PC 14:0\_14:0, respectively. These fold changes indicated a significant decrease on day 0 compared to cells aged in 5 mM glucose. One possible explanation for this shift is the stability of certain phospholipids. PC species such as PC 28:0 and PC 14:0\_14:0 might be more stable and resistant to degradation over time compared to other PCs. This increased stability could result in their relative accumulation in aged cells. More stable phospholipids may play a crucial role in maintaining membrane integrity and cellular function as cells age.

The presence of saturated fatty acids, as in the case of PC 28:0|PC 14:0\_14:0 and PC 28:0 observed in aged cells, is known to make the membrane more rigid. This increased rigidity is due to the enhanced van der Waals interactions between the phospholipid acyl chains, leading to greater membrane stiffness. Conversely, the presence of double bonds, as in PC 40:6 found elevated in aged cells, can lead to increased membrane fluidity. The fatty acyl chains with unsaturated double bonds introduce kinks into the hydrocarbon chains, making it more difficult for the lipids in the membrane to pack closely together. From a structural perspective, the

presence of double bonds increases the interchain distance between fatty acids, diminishing intermolecular van der Waals forces within the phospholipid bilayer. This results in increased flexibility and decreased rigidity of the membrane, hence increasing membrane fluidity (*Kostara et al., 2021*).

Lyso-phospholipids, such as LPC 18:2, LPS 18:0 and LPE 16:0, eluted earlier than other phospholipids. These phospholipids only contain one fatty acid chain, which leads to weaker interactions with the hydrophobic stationary phase leading to faster elution times. Also, when using a hydrophobic C<sub>18</sub> column, the hydrophobic C<sub>18</sub> groups interact with the hydrophobic fatty acid chains of phospholipids. As a result, phospholipids with longer fatty acid chains possess greater solute hydrophobicity, and retention times are decreased as the number of double bonds on fatty acid chains is increased (*Pati et al., 2016*).

In the present study, LPC 18:2 was found to be elevated in untreated cells compared to aged cells. A study carried out in blood plasma by Mapstone and colleagues found that levels of LPC 18:2 progressively decreased with age (*Mapstone et al., 2014*). LPCs, which are synthesised from PC through the action of phospholipase A<sub>2</sub>, have demonstrated a significant correlation with insulin resistance (*Makki and Rahman, 2023*). Reduced levels of LPC species, specifically LPC 18:2, have been suggested as an early prognostic indicator for type 2 diabetes mellitus, with lipidomics analyses confirming reduced plasma LPC levels in type 2 diabetic groups (*Suvitaival et al., 2018, Wang-Sattler et al., 2012, Barber et al., 2012*). On the other hand, LPCs, including LPC 18:2, have been found significantly increased in type 1 diabetes mellitus (*Barranco-Altirriba et al., 2024*). These findings highlight the distinct lipidomic signatures associated with different types of diabetes.

The observed reduction of LPC 18:2 in aged cells align with the observed decrease in LPC 18:2 with ageing and its correlation with type 2 diabetes. This reduction could reflect early metabolic changes associated with insulin resistance and type 2 diabetes. On the other hand, elevated LPC 18:2 in untreated cells might correlate with the findings in type 1 diabetes, where increased levels are noted. This dual aspect of LPC 18:2 levels being associated differently with type 1 and type 2 diabetes underlines the complexity of lipid metabolism and its role in different types of diabetes.

PE species which have been previously found abundant in erythrocytes included PE 38:4, PE 40:5 and PE 36:2 (*Leidl et al., 2008*). In the current study these were found elevated in fresh cells. Some studies have shown that PE contents change with age (*Delion et al., 1997, Dai et al., 2021*). PE species, such as PE 38:4 decreased significantly in the kidney of old mice Y. Pantoja Estrada, PhD Thesis, Aston University, 2024

(Braun *et al.*, 2016). Also, a decrease in PE has been observed in aged nematodes, the brain of old mice and in the liver of type 2 diabetic mice (Gao *et al.*, 2017, Braun *et al.*, 2016, Dai *et al.*, 2021, Lin *et al.*, 2016, Xu *et al.*, 2023). Changes in the membrane PE composition, such as a reduction, can lead to an increase in membrane fluidity (Dawaliby *et al.*, 2016). It is known that the presence of PE decreases fluidity and this is because it has a relatively smaller headgroup resulting in a larger area of fatty acyl chains relative to the headgroup (Fajardo *et al.*, 2011). Therefore, the reduction of PE species in aged cells could contribute to increased membrane fluidity, which might affect membrane stability and cellular functions such as the enzyme activity of membrane proteins.

All the PS identified as significantly different between fresh and aged cells showed signs of oxidation, with the exception of LPS 18:0. These oxidised PS species included PS 25:0;O|PS 18:0\_7:0;O, PS 40:6;O2|PS 18:0\_22:6;O2, PS 38:4;O4|PS 18:0\_20:4;O4 and PS 38:4;O2|PS 18:0\_20:4;O2 and were all increased in fresh cells. The observed decrease in oxidised PS levels as erythrocytes aged aligns with findings from previous studies. These studies have reported similar declines in PS levels in ageing erythrocytes, as well as erythrocytes from type 1 and type 2 diabetic patients, and in kidney cells of diabetic rats (Minetti *et al.*, 2023, Xiao and Chang, 2023, Labrousche *et al.*, 1996). However, it is important to note that the declines reported in these studies were in total PS levels, not specifically in oxidized PS species.

The PSs identified, except for PS 25:0;O|PS 18:0\_7:0;O, contained unsaturated fatty acyl chains in their structure rendering them vulnerable to attack by reactive oxygen species. This susceptibility leads to lipid peroxidation and the subsequent formation of oxidised products. Moreover, the predominant location of PS in the inner leaflet of the membrane exposes them to reactive oxygen species within the cell, further increasing their susceptibility to oxidation. Thus, the presence of oxidised PS species could be attributed to the inherent vulnerability of PSs to oxidation and the oxidative stress condition during the experimental procedures. Additionally, oxidative stress associated with apoptosis results in the selective oxidation of PS, followed by translocation of oxidised PS to the surface of the apoptotic cells (Matsura, 2014).

Not all the phospholipids identified had information about fatty acyl chains; instead, only the total number of carbons and double bonds were shown, such as PC 36:4, PC 40:6 and PC 32:2. This is because the mass spectrometry analysis sometimes cannot match all the fragments necessary to determine the exact fatty acyl composition. The process of identifying each fatty acid within a phospholipid molecule can be complex, and the fragmentation patterns may not always provide complete information for each component. Additionally, the presence

of sodium adducts in various phospholipids such as PC 36:4, PC 40:6 and PC 32:2 can complicate the fragmentation patterns in the mass spectrometer. Sodium, as well as formate, adducts can lead to more complex mass spectrum (*Al-Saad et al., 2003*). These adducts can alter the fragmentation patterns and make it more challenging to accurately interpret the data and determine the exact fatty acyl composition of phospholipids (*Kerwin et al., 1994*). The presence of these adducts can lead to variations in ionisation efficiency and fragmentation, resulting in incomplete data regarding the structure of the phospholipid.

Furthermore, fresh erythrocytes displayed higher levels of oxidised phospholipids than aged ones. While several experimental parameters remained constant, including sample workup, volume of extract injected in column and the number cells, it is also important to acknowledge the possibility of experimental errors, such as those occurring during lipid extraction and cell pellet handling. Additionally, the high levels of haemoglobin present in erythrocytes could have contributed to oxidative stress during lipid extraction, as free haemoglobin may catalyse the Fenton reaction, generating hydroxyl radicals that oxidise membrane components, including phospholipids. This could have been prevented by the usage of reducing agents such as butylated hydroxyanisole.

While experimental errors cannot be ruled out, there are biological mechanisms that plausibly explain the higher levels of oxidised phospholipids observed in fresh cells compared to aged cells. Fresh cells may have higher metabolic rate than aged cells and consequently generate more ROS as byproducts, leading to increased oxidation of phospholipids. Additionally, aged cells may later form protein adducts or break down further, reducing detectable oxidized phospholipids. Another possible explanation is that fresh cells may experience higher levels of oxidative stress due to factors such as exposure to environmental stressors. The process of collecting blood samples can expose erythrocytes to mechanical stress, and temperature changes, which may trigger oxidative stress potentially leading to the oxidation of phospholipids. Also, erythrocytes may undergo changes in response to the altered environment outside the body, including changes in pH, osmolarity and exposure to reagents using during sample preparation.

Treating erythrocytes with increasing glucose levels resulted in changes in phospholipid composition. Specifically, increasing glucose levels to 22 mM led to a decrease in PC 28:0|PC 14:0\_14:0 and PC 28:0, while these lipids remained elevated at 5 mM. During ageing, changes in phospholipid composition occur, often leading to increased saturation levels (*Dai et al., 2021, Albouery et al., 2019*). Increased fatty acid saturation in erythrocytes, however, is often

observed in diabetes mellitus. Myristic acid (C14:0), and also palmitic acid (C16:0), are associated with diabetes risk and have been found elevated in type 2 diabetics patients (*Patel et al., 2010, Bykhovets, 2020, Koehrer et al., 2014*). This appears to contradict the data from the current study, where PC 28:0|PC 14:0\_14:0 decreased with higher glucose levels. An explanation for this discrepancy could be that the acute exposure, five days, to high glucose in the present study triggered metabolic adaptations to maintain cellular homeostasis, unlike the chronic high glucose exposure in diabetic patients, which leads to long-term metabolic changes. The observed decrease in saturated phospholipids could also be an adaptive response to maintain membrane fluidity.

Two oxidised phospholipids, PC 25:1;O|PC 10:0\_15:1;O and PS 25:0;O|PS 18:0\_7:0;O, were increased in cells treated with 22 mM glucose. This observation aligns with the association between high glucose levels and increased lipid peroxidation (*Jain, 1989, Viskupicova et al., 2015, Suryawanshi et al., 2006*). Glucose-induced lipid peroxidation can occur through various mechanisms (*Ayala et al., 2014, Wang et al., 2021*). Firstly, auto-oxidation of glucose and activation of the polyol pathway can generate reactive oxygen species, initiating lipid peroxidation processes (*Juan et al., 2021, Wang et al., 2021*). Glucose can undergo non-enzymatic glycation reactions with phospholipids, forming advanced glycation end products that promote oxidative stress and lipid peroxidation by further reactive oxygen species generation (*Wang et al., 2021, Mengstie et al., 2022*). These mechanisms collectively can contribute to the observed alterations in oxidised phospholipid levels with increasing glucose concentrations.

Additionally, three longer-chain phospholipids, including PE 41:7|PE 19:2\_22:5, PE O-38:5|PE O-18:1\_20:4 and PC 34:3 were elevated under 22 mM glucose condition. These phospholipids had higher degree of desaturation compared to those in the control group. An increase in erythrocyte fatty acid desaturation has been reported in response to ageing and disease related to increased oxidative stress, such as type 1 diabetes (*Ali et al., 2023, Nono Nankam et al., 2020, Sobczak et al., 2021, Thomas et al., 2021*). Fatty acid desaturases have been recently found to be present and active in mature erythrocytes and are responsible for the conversion of saturated fatty acids into unsaturated fatty acids (*Thomas et al., 2021*). It has been observed that the activity of fatty acid desaturases in mature erythrocytes appeared to be sensitive to increased oxidant stress. One hypothesis regarding the activation of erythrocyte fatty acid desaturases included a compensatory mechanism to preserve membrane fluidity when structural proteins and membrane lipids face oxidant challenge.

The presence of increased myristoyl (C14:0) containing species at 5 mM and the observed decrease of these saturated species at higher glucose levels might be due to the action of fatty acid desaturases and elongases (known to be present in erythrocytes as well), which convert them into more unsaturated fatty acids and longer-chains, respectively (*Minic et al., 2023*). To test the hypothesis that fatty acid desaturases are upregulated in response to increased glucose levels, and consequently increased oxidative stress, the activity levels of these enzymes in erythrocytes under varying glucose conditions can be measured using enzyme activity assays and fluorescent-based assays. For example, the enzyme activity of stearoyl-CoA desaturase, which converts palmitic acid (C16:0) to palmitoleic acid (C16:1), can be assessed by measuring the ratio of the product to the concentration of the precursor. In terms of fluorescent assays, BODIPY (boron-dipyrromethene)-labelled fatty acids can be used. BODIPY conjugates of fatty acids can serve as fluorescent substrates; when incorporated into cells, the action of desaturases can alter the fluorescent properties, which can be measured using a fluorometer. This can be followed by lipidomic analysis to quantify the levels of saturated and unsaturated fatty acids in erythrocytes under these conditions and help elucidate the metabolic adaptations in response to glucose-induced oxidative stress.

The phospholipid PC 34:3 was elevated at 22 mM glucose treatment. A lipidomics study conducted in China, involving 667 patients with type 2 diabetes mellitus, revealed that 38 lipid species in serum associated with heightened risk of developing new onset type 2 diabetes. Among the identified lipids, PC 34:3 was associated with this increased risk (*Lu et al., 2019*). This finding in blood serum aligns with the current study in erythrocytes, suggesting that elevated levels of PC 34:3 might serve as a biomarker for metabolic disturbances linked to high glucose conditions.

In the 100 mM glucose treatment, long chain PEs (PE 41:7|PE 19:2\_22:5, PE 34:1|PE 16:0\_18:1) were found to be elevated. In a recent study, PE 16:0\_18:1 has been associated with the development of diabetes (*Villasanta-Gonzalez et al., 2023*). The phospholipid PE 41:7|PE 19:2\_22:5, which was also found elevated at 22 mM, likely enhanced membrane fluidity due to its high number of double bonds, resulting in increased spacing and flexibility of its acyl chains. Increased membrane fluidity was observed in Chapter 3 between 5 mM and 100 mM glucose.

In contrast to the findings of the present study, Kostara and colleagues reported a reduction in unsaturation in erythrocyte membranes in type 2 diabetes, potentially attributed to decreased activity of desaturase enzymes responsible for the synthesis of  $\omega$ -3 and  $\omega$ -6

polyunsaturated fatty acids (*Kostara et al., 2021*). This reduction in unsaturation may have implications for membrane fluidity and functionality in diabetic individuals.

The presence of polyunsaturated fatty acids such as arachidonic acid (C20:4) and docosapentaenoic acid (C22:5), found in phospholipids like PE O-38:5|PE O-18:1\_20:4 and PE 41:7|PE 19:2\_22:5, have been shown to effectively reduce cell fragility under osmotic shock conditions (*Kadri et al., 2021*). This effect may be related to the role of polyunsaturated fatty acids in increasing membrane fluidity, which enhances the ability of the cell membrane to deform and adapt to stress (*Stillwell and Wassall, 2003*).

The presence of ether linkage in phospholipids, such as in PE O-38:5|PE O-18:1\_20:4, however, alters membrane physical properties (*Dean and Lodhi, 2018*). Ether-linked phospholipids lack the carbonyl oxygen that facilitates stronger hydrogen bonding between headgroups. This characteristic allows them to have better alignment in the membrane and form tighter packing, resulting in decreased membrane fluidity and increased rigidity (*Dean and Lodhi, 2018*). Furthermore, polyunsaturated fatty acids can decrease the thickness of the membrane due to their kinked structure, which disrupts the packing of adjacent phospholipid molecules (*Baccouch et al., 2023*). The reduction in membrane thickness is often associated with increased membrane tension, as there is less surface area to distribute internal and external pressure (*Reddy et al., 2012*). Increased membrane tension was observed in Chapter 5 for each participant when the cells were kept in 22 mM glucose and compared to the physiological control.

Variations in lipid profiles were identified among all participants. Differences were observed in lyso-phospholipids, including LPE 22:6, which has also been found to be increased in the serum of diabetic individuals (*Ha et al., 2012*). Other lyso-PEs species, such as LPE 20:4, LPE 22:4 and LPE 18:1 also showed significant differences among all participants. An increase in lyso-phospholipids is often associated with a more permeable membrane leading to an increase in fluidity. One possible explanation for an increase in lyso-phospholipid could be attributed to variations in erythrocyte age within the blood sample, as different erythrocyte may have experienced varying levels of oxidative stress over time. In response to such damage, the repair mechanism for phospholipids in the erythrocyte membrane involves diacylation and re-acylation processes facilitated by enzymes such as phospholipases, acyl-CoA lyso-phospholipid acyltransferases and carnitine (*Arduini et al., 1992, Bogdanova et al., 2013*). Under conditions of increased oxidative stress, there may be an upregulation of diacylation process and a reduction in the reacylation process, leading to an increase in lyso-

phospholipids in the erythrocyte membrane. Also, the observed variations in lysophospholipids among participants could be influenced by different activities or physiological states of the participants.

Odd chain fatty acids, such as PE 35:2|PE 17:1\_18:1 and SM 33:1;O2|SM 17:1;O2/16:0 were identified as significantly different among the participants. The presence of odd chain fatty acids is uncommon in mammalian cells and might be attributed to dietary intake, especially from ruminant fats such as dairy and meat. Additionally, gut microbiota can also contribute to the presence of these fatty acids (*Ampong et al., 2022, Venn-Watson et al., 2020*).

PE 40:6|PE 18:0\_22:6 emerged as the phospholipid with the lowest *P* value among all the participants, followed by PE 38:6|PE 16:0\_22:6, PE 36:3;O2|PE 16:0\_20:3;O2 and SM 32:1;O2|SM 16:1;O2/16:0. These phospholipids, characterised by long polyunsaturated fatty acyl chains also contained palmitic acid (C16:0). Palmitic acid, along with stearic acid (C18:0) and oleic acid (C18:1), were the most common fatty acids esterified with PCs, PEs, PSs, and SMs. Studies have shown that the fatty acid pattern of erythrocyte phospholipids is strongly linked with the incidence of type 2 diabetes mellitus (*Qureshi et al., 2019, Barranco-Altirriba et al., 2024*).

This study had several limiting factors, which included a small sample size, lack of information on dietary and other clinical/demographic data from the participants and glycaemic control (no fasting was required). Another limiting factor was that cells were aged in media containing serum, and it is known that the erythrocytes can take up free fatty acids from plasma/serum. However, it was not possible to eliminate serum because many cells died after being aged in serum-free medium for five days under high glucose conditions. Future work should be focused on increasing the study sample size to achieve a greater statistical power. Also, it will be very interesting to work with erythrocyte from diabetic patients and compare *in vitro* and *in vivo* results.

In summary, this study demonstrated that ageing erythrocytes and treating them with increasing glucose levels *in vitro* can induce alterations in phospholipid composition. High glucose concentrations led to increased desaturation, while ageing was associated with increased saturation. Moreover, variations in erythrocyte lipid profiles were observed among participants. These variations could stem from individual differences in genetics and underlying health conditions. Such variability can complicate the interpretation of results. The findings of this study are expected to serve as the basis for future research. While this study provides valuable observational data, it lacked direct mechanistic testing to uncover the

pathways driving the observed changes. To address this, future studies would include experiments designed to uncover the underlying mechanisms. For example, measuring the activity levels of key enzymes involved in lipid metabolism, such as fatty acid desaturases and elongases, through enzyme activity assays could reveal how these enzymes are regulated under varying glucose conditions. Future work would also need to include the analysis of erythrocytes from diabetic subjects and comparing the results with those obtained *in vitro*, which will also help validate *in vitro* findings. It would also be interesting to conduct a comparative analysis of the lipid profiles of erythrocytes from individuals with type 1 and type 2 diabetes. Previous studies have highlighted variations in membrane fluidity, indicating an increase in membrane fluidity in type 1 diabetes and a decrease in type 2 diabetes. A comparative examination of these lipids could shed further light on the underlying mechanisms and implications for cellular function in both diabetic conditions. Moreover, a detailed characterisation of erythrocyte lipid composition will aid in identifying the lipid alterations and changes, providing vital information regarding cellular homeostasis and disease pathogenesis.

# Chapter 7

## General Discussion

The aim of the study was to explore the relationship between the production of ROS, membrane fluidity, membrane tension, and lipid composition changes in erythrocytes after being aged or treated with various glucose concentrations. The cells were aged in media containing 5 mM glucose or treated with 5 mM, 22 mM, and 100 mM glucose for up to five days. Various tests were then carried out to measure membrane fluidity using laurdan, membrane tension using Flipper-TR, ROS production using carboxy-H<sub>2</sub>DCFDA, and mass spectrometry analysis of membrane phospholipids. A summary of the results corresponding to age and glucose treatments is shown in Figures 7.1 and 7.2, respectively.

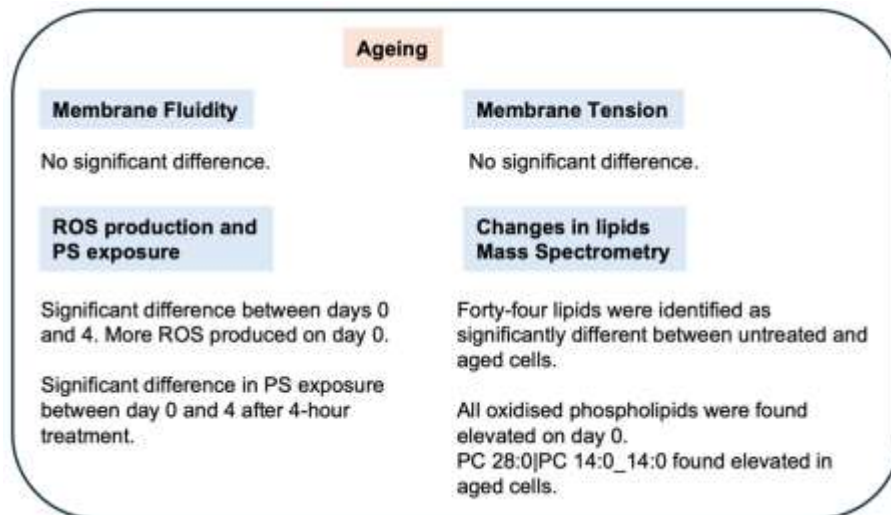


Figure 7. 1. Summary of results investigating the effect of ageing on erythrocytes.

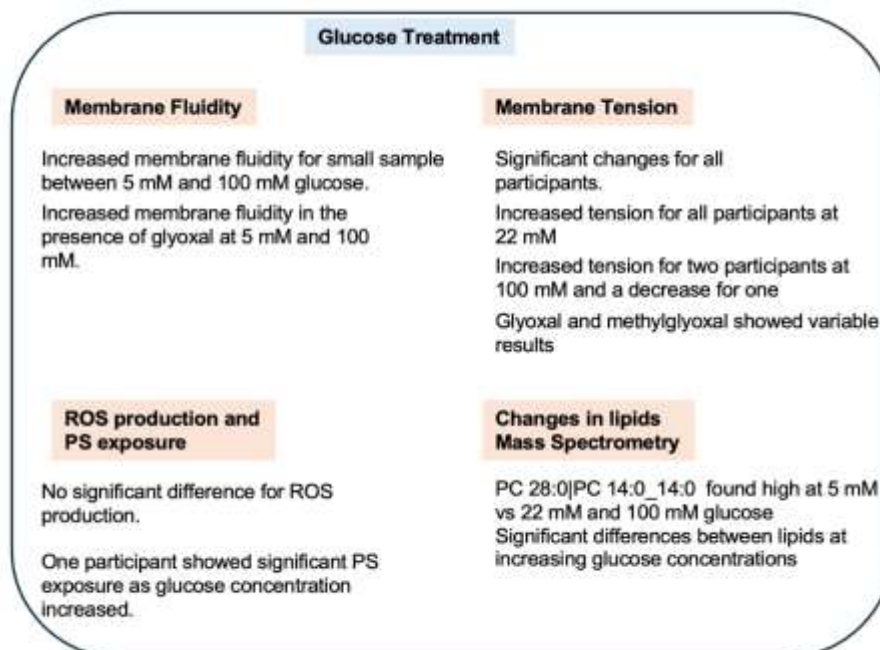


Figure 7. 2. Summary of results investigating the effect of glucose on erythrocytes.

Short-term glucose treatments did not alter membrane fluidity, and long-term exposure to glucose alone also showed no significant changes. This finding aligns with previous studies indicating that incubation of erythrocytes with glucose alone may not significantly impact membrane fluidity (*Zavodnik et al., 1997*). However, during the smaller sample testing (when glycating compounds were being examined), a significant increase in membrane fluidity was observed between 5 mM and 100 mM glucose. Additionally, the presence of glyoxal also increased membrane fluidity for both 5 mM and 100 mM glucose treatments. The larger sample available for glucose-alone tests exhibited more variation compared to the smaller sample used for testing the combined effects of glucose and glyoxal or methylglyoxal. Interestingly, this increase in erythrocyte membrane fluidity was not expected, as type 2 diabetics often show a decrease in membrane fluidity (*Waczulikova et al., 2002, Candiloros et al., 1995, Bianchetti et al., 2019*). The presence of glycating compounds was anticipated to reduce membrane fluidity due to their ability to form adducts and crosslinks. Glyoxal, a well-known glycating agent, promotes AGE formation, which typically cross-links membrane proteins and lipids, thereby stiffening the cell and decreasing fluidity. However, the increase in membrane fluidity aligns with results reported by Maulucci and Bianchetti on subjects suffering from type 1 diabetes (*Maulucci et al., 2017, Bianchetti et al., 2019*).

The observed increase in fluidity could potentially be influenced by the *in vitro* conditions under which the erythrocytes were incubated. Unlike the *in vivo* environment, where multiple factors such as insulin resistance, chronic inflammation (closely linked to obesity and metabolic syndrome), and hyperlipidaemia play a crucial role in type 2 diabetes, the *in vitro* setting isolates the cells from these systemic influences (*Pearson, 2019, Galicia-Garcia et al., 2020*). This isolation may have resulted in a different response to glucose and glycating agents, resembling the response seen in type 1 diabetes. Consequently, the lack of complex metabolic interactions in the *in vitro* system might have contributed to the unexpected increase in membrane fluidity.

Membrane tension results were consistent across all participants, showing an increase after exposure to 22 mM glucose. This finding aligns with previous studies that have indicated that hyperglycaemia can enhance membrane tension (*Bravo et al., 2023*). However, at 100 mM glucose, two participants exhibited increased membrane tension while one showed a decrease. The addition of glyoxal or methylglyoxal to RBCs in physiological glucose levels produced mixed results, with some participants showing increased membrane tension and others showing a decrease. Elevated glucose levels and the presence of glycating compounds are typically associated with the formation of AGEs, which are known to cross-link proteins

Y. Pantoja Estrada, PhD Thesis, Aston University, 2024

and alter membrane properties. While early-stage of glycation might increase membrane tension by forming initial cross-links, extensive glycation can lead to more complex effects. In erythrocytes, AGEs of cytoskeletal proteins like spectrin can cause cytoskeletal detachment, which often results in a decrease in membrane tension due to the structural integrity of the membrane being compromised. This detachment can lead to PS exposure on the outer membrane, contributing to the observed decrease in membrane tension (An *et al.*, 2004). One possible explanation for these mixed results could be the variability in the extent of glycation and the subsequent formation of AGEs. Different participants might have different metabolic profiles, affecting how their erythrocytes respond to glycation. For example, some individuals may have more robust antioxidant defences that mitigate effects of glycation, leading to less pronounced increase in membrane tension. The mixed results might also reflect the limitations of the experimental setup, which isolated erythrocytes from systemic influences.

High levels of glucose were expected to increase ROS production in erythrocytes. Oxidative stress is a critical factor influencing membrane characteristics such as fluidity and tension, particularly under high glucose conditions. In this study oxidative stress was assessed using the fluorescent probe carboxy-H<sub>2</sub>DCFDA, but no significant changes were observed with increasing glucose concentrations in either fresh or aged cells. However, there were differences between days 0 and 4, with aged cells producing less detectable ROS than fresh cells after one hour of treatment. Despite the lack of direct evidence for increased oxidative stress, the observed alterations in membrane fluidity, tension and lipid composition may still be related to subtle oxidative mechanisms that were not captured by this method. For a more comprehensive assessment of oxidative stress, future studies could employ additional methods, such as measuring glutathione levels, lipid peroxidation assays (e.g. malondialdehyde levels), or detecting protein carbonylation.

Externalization of PS to the outer leaflet of the erythrocyte membrane was also significant between days 0 and 4, with aged cells showing increased PS exposure after a four-hour treatment. The observed increase in PS exposure over time may reflect the progression of cellular ageing and accumulation of stress factors that compromise membrane integrity. The increased PS exposure after a four-hour treatment may suggest that the treatment induced cellular stress related to ageing, leading to signs of eryptosis.

Lipidomic analysis revealed significant differences between fresh and aged cells at physiological glucose levels, with increased levels of oxidized phospholipids in untreated cells. Various glucose treatments led to the elevation of specific phospholipids, including PC

28:0|PC 14:0\_14:0 in cells aged in 5 mM glucose, and longer chain phospholipids with multiple double bonds such as PE 41:7|PE 19:2\_22:5 in cells treated with 22 mM glucose. In the 100 mM glucose treatment, long chain PEs (PE 41:7|PE 19:2\_22:5 and PE 34:1|PE 16:0\_18:1) were found to be elevated.

The presence of increased myristoyl (C14:0) containing species at 5 mM glucose, along with the observation of longer chains with increased unsaturation at 100 mM glucose, likely contributed to the increased membrane fluidity observed at 100 mM glucose in the smaller sample. In a recent study, Bianchetti reported no significant differences in total amount of PUFA among the groups which included controls versus diabetics with and without cardiovascular history and they also reported that increased membrane fluidity was associated with higher cardiovascular risk in subjects with type 2 diabetes, where they also used laurdan to measure membrane fluidity, (*Bianchetti et al., 2024*). These findings highlight the complex relationship between lipid composition and membrane dynamics.

Membrane fluidity is linked to membrane tension and studies suggest a positive relationship between the two (*Li et al., 2018*). Experimental evidence has indicated that the fluidity of the lipid bilayer increases with rising membrane tension (*Reddy et al., 2012, Muddana et al., 2011, Li et al., 2018*). This correlation was supported by the results of the current study, where membrane tension and fluidity increased with higher glucose concentrations. Conversely, Tapia and colleagues reported different findings, noting decreased membrane tension and fluidity as glucose increased in erythrocytes (*Tapia et al., 2021*). An increase in membrane tension can lead to dispersion in the hydrophobic chains, reducing lipid packing and subsequently increasing fluidity (*Reddy et al., 2012*). Lipid composition plays an important role in this process, as the physical properties of the individual lipid domains guide the local changes required for adapting to a change in tension. Lateral movement, rotation, and flipping of lipids between the leaflets of the plasma membrane are physical changes that work together to allow the fluid membrane to adapt to changes in membrane tension (*Reddy et al., 2012*).

Significant changes in lipid composition within cell membranes, was observed in cells treated with 22 mM and 100 mM glucose. This alteration in lipid profiles subsequently impacts membrane characteristics such as fluidity and tension. Additionally, the presence of unsaturated lipids, which have a kinked structure preventing tight packing, further increases membrane fluidity. Interestingly, studies using giant unilamellar vesicles have shown that membrane tension slows down lipid mixing compared to tension-free conditions (*Shendrik et al., 2023*). This observation suggests that the physical state of the membrane can influence

the behaviour of its lipid components, with higher tension restricting the mixing of lipids. This shows the complex interaction between oxidative stress, lipid composition, and membrane properties.

The activity of desaturases may have contributed to the increased level of unsaturation in membrane lipids, potentially explaining the observed increase in membrane fluidity under conditions of elevated glucose and glycation compounds. It has been reported that fatty acid desaturation can be triggered by oxidant stress (i.e. incubation with hydrogen peroxide) and it is thought that it could represent a compensatory mechanism to preserve membrane fluidity in the face of an oxidant challenge to structural proteins and membrane lipids (*Thomas et al., 2021*). This was not measured in the present study, but using stable isotope labelling techniques, like employing  $^{13}\text{C}_{16}$  palmitate and  $^{13}\text{C}_{18}$  linoleate followed by mass spectrometry analysis could help investigate their action.

The presence of glyoxal at 5 mM and 100 mM increased membrane fluidity, while varied results in terms of membrane tension were observed among participants. Some participants showed increased membrane tension with higher glucose levels, whereas others showed a decrease, indicating a heterogeneous response dependent on individual reactions to glucose and glycation agents. The observed decrease in membrane tension in the presence of glycation compounds could be attributed to cytoskeletal detachment. To investigate this hypothesis, the use of fluorescence microscopy with specific dyes such as phalloidin, which targets actin, or antibodies against spectrin, would be required to visualise the integrity and organisation of the cytoskeleton in erythrocytes under different treatment conditions.

Also, hyperglycaemia, as well as glucose degradation products such glyoxal and methylglyoxal, can cause oxidative stress in erythrocytes and lead to the activation of protein kinase C (PKC) (*Giri et al., 2018*). It has been shown that overactivation of PKC can lead to a decrease in membrane tension. PKC phosphorylates 4.1R protein (interacts with spectrin and actin), resulting in an increased dissociation of the spectrin network.

Mass spectrometry analysis revealed a higher presence of oxidised phospholipids in fresh cells compared to aged cells, with aged cells exhibiting increased levels of PC 28:0|PC 14:0\_14:0. On the other hand, in a study carried out in plasma reported an increased linoleic oxidised derivatives in transfusion blood of 42 days (*D'Alessandro et al., 2019b*). The increase in oxidised phospholipids could be due to experimental errors such as those occurring during lipid extraction, or due to biological mechanisms such as fresh cells having a higher metabolic

rate generating more ROS as byproducts, leading to increased oxidation of phospholipids. However, since all samples were subjected to the same extraction procedures, it is less likely that this increase in oxidised lipids in untreated cells is due solely to technical artifacts. While fresh cells may have a higher metabolic rate, it is important to note that erythrocytes do not have mitochondria, which are typically major sources of ROS in other cell types. However, other ROS-generating processes, such as the activity of NADPH oxidase, haemoglobin autoxidation, and the Fenton reaction, could contribute to increased ROS production in RBCs (George *et al.*, 2013). These processes can generate ROS as byproducts, potentially leading to oxidative stress and the observed biological effects. Fresh cells also showed increased ROS production after 1 hour of glucose treatment when compared to aged cells. Despite these changes in lipid composition, membrane fluidity studies showed no significant differences between fresh and aged cells when treated with 5 mM glucose. In terms of membrane tension, the results were inconsistent, with only one participant showing a significant difference between fresh and aged cells, with a decrease in membrane tension in aged cells. However, older cells showed more PS exposure compared to fresh cells after a four-hour treatment. This finding indicates a potential shift in membrane stability and cell ageing mechanisms.

The media used in this study contained FBS, which has lipids. Erythrocytes are incapable of *de novo* synthesis of fatty acids (Arduini *et al.*, 1992). The major metabolic pathway for membrane phospholipid fatty acid turnover in human erythrocytes is confined to the deacylation of membrane phospholipids and their subsequent reacylation by the Land's cycle (Arduini *et al.*, 1992). However, it has been reported that erythrocytes have a low turnover rate of phospholipids due to minimal activity of phospholipases and acyltransferases (Quinn *et al.*, 2009). The relatively slow turnover of membrane phospholipids in mature erythrocytes, ensures a stable long-term homeostasis that can be reliably characterised through lipidomic analysis (Quinn *et al.*, 2009). Given this, it is possible that the ageing of erythrocytes could affect their ability to take up and incorporate lipids from the FBS. As erythrocytes age, their membrane becomes less flexible and more prone to oxidative damage, which could impair lipid transport mechanisms and the efficacy of the Land's cycle. A reduction in lipid uptake might contribute to alterations in membrane composition and function.

In conclusion, results have shown that the presence of high levels of glucose, with or without glycation agents, can lead to changes in the erythrocyte membrane, including fluidity, tension and changes in lipid composition. The study showed that the membrane is dynamic and heterogeneous with a complex interaction of mechanical, biochemical and biophysical factors that modulate cellular membrane properties. These findings highlight the complex interaction

between glucose levels, ageing and erythrocyte membrane properties, emphasising the need for further research to fully understand the mechanisms.

The most convincing and important finding from the study was the mass spectrometry analysis of erythrocyte phospholipids, which revealed significant differences between fresh and aged cells, as well as changes corresponding to increasing glucose concentrations. This provided clear evidence of how aging and glucose exposure affect erythrocyte membrane composition. Additionally, while membrane tension results did not show significance when combined across all participants (likely due to the small sample size,  $n=3$ ), individual participant analyses did reveal significant changes, highlighting the potential variability in response and the need for a larger sample size to draw more definitive conclusions.

The investigation faced limitations primarily attributed to its small sample size, which posed challenges in the interpretation of results. This was largely attributed to the technical complexity and time-consuming nature of the experiments, which limited the number of samples that could be processed. The observed interindividual variability in oxidative stress markers showed the complex relationship between membrane properties and glucose treatment. Another limitation of the study was the use of different blood samples from different participants for various tests. Ideally, blood from the same individual should have been used for all tests, including fluidity, tension, ROS, and lipidomic studies, to ensure consistency and accuracy in the results. However, obtaining repeated samples from the same participants proved difficult, as some individuals were unwilling to undergo frequent blood draws. Treating the erythrocytes with high levels of glucose for five days was also a limitation, as it does not fully replicate the prolonged hyperglycaemic conditions experienced by individuals with diabetes. Additionally, access to samples from individuals with diabetes was not feasible due to ethical constraints. Recruiting diabetic subjects would have required additional ethical approval and clinical partnerships, which were not possible to address within the timeframe of the study. Future work should include larger cohorts, as well as samples from diabetic participants, which could provide deeper insights into these complex interactions, potentially offering more robust conclusions.

# Chapter 8

## References

- ADDEPALLI, R. V. & MULLANGI, R. 2021. A concise review on lipidomics analysis in biological samples. *ADMET DMPK*, 9, 1-22.
- AGARWAL, A., ALLAMANENI, S. S. & SAID, T. M. 2004. Chemiluminescence technique for measuring reactive oxygen species. *Reprod Biomed Online*, 9, 466-8.
- AGRAWAL, R., SMART, T., NOBRE-CARDOSO, J., RICHARDS, C., BHATNAGAR, R., TUFAIL, A., SHIMA, D., P, H. J. & PAVESIO, C. 2016. Assessment of red blood cell deformability in type 2 diabetes mellitus and diabetic retinopathy by dual optical tweezers stretching technique. *Sci Rep*, 6, 15873.
- AHIYA, A. I., BHATNAGAR, S., MORRISEY, J. M., BECK, J. R. & VAIDYA, A. B. 2022. Dramatic Consequences of Reducing Erythrocyte Membrane Cholesterol on *Plasmodium falciparum*. *Microbiol Spectr*, 10, e0015822.
- AL-SAAD, K. A., SIEMS, W. F., HILL, H. H., ZABROUSKOV, V. & KNOWLES, N. R. 2003. Structural analysis of phosphatidylcholines by post-source decay matrix-assisted laser desorption/ionization time-of-flight mass spectrometry. *J Am Soc Mass Spectrom*, 14, 373-82.
- ALAM SHIBLY, S. U., GHATAK, C., SAYEM KARAL, M. A., MONIRUZZAMAN, M. & YAMAZAKI, M. 2016. Experimental Estimation of Membrane Tension Induced by Osmotic Pressure. *Biophys J*, 111, 2190-2201.
- ALBOUERY, M., BUTEAU, B., GREGOIRE, S., CHERBUY, C., PAIS DE BARROS, J. P., MARTINE, L., CHAIN, F., CABARET, S., BERDEAUX, O., BRON, A. M., ACAR, N., LANGELLA, P. & BRINGER, M. A. 2019. Age-Related Changes in the Gut Microbiota Modify Brain Lipid Composition. *Front Cell Infect Microbiol*, 9, 444.
- ALDANA, J., ROMERO-OTERO, A. & CALA, M. P. 2020. Exploring the Lipidome: Current Lipid Extraction Techniques for Mass Spectrometry Analysis. *Metabolites*, 10.
- ALI, S., AIELLO, A., ZOTTI, T., ACCARDI, G., CARDINALE, G., VITO, P., CALABRO, A., LIGOTTI, M. E., INTRIERI, M., CORBI, G., CARUSO, C., CANDORE, G., SCAPAGNINI, G. & DAVINELLI, S. 2023. Age-associated changes in circulatory fatty acids: new insights on adults and long-lived individuals. *Geroscience*, 45, 781-796.
- ALIMOHAMADI, H. & RANGAMANI, P. 2023. Effective cell membrane tension protects red blood cells against malaria invasion. *PLoS Comput Biol*, 19, e1011694.
- ALROUJI, M., AL-KURAIISHY, H. M., AL-GAREEB, A. I., ALEXIOU, A., PAPADAKIS, M., SAAD, H. M. & BATIHA, G. E. 2023. The potential role of human islet amyloid polypeptide in type 2 diabetes mellitus and Alzheimer's diseases. *Diabetol Metab Syndr*, 15, 101.
- AMARO, M., REINA, F., HOF, M., EGGELING, C. & SEZGIN, E. 2017. Laurdan and Di-4-ANEPPDHQ probe different properties of the membrane. *J Phys D Appl Phys*, 50, 134004.
- AMPONG, I., JOHN IKWUOBE, O., BROWN, J. E. P., BAILEY, C. J., GAO, D., GUTIERREZ-MERINO, J. & GRIFFITHS, H. R. 2022. Odd chain fatty acid metabolism in mice after a high fat diet. *Int J Biochem Cell Biol*, 143, 106135.
- AN, X., GUO, X., WU, Y. & MOHANDAS, N. 2004. Phosphatidylserine binding sites in red cell spectrin. *Blood Cells Mol Dis*, 32, 430-2.
- ANGELOVA, M. I., BITBOL, A. F., SEIGNEURET, M., STANEVA, G., KODAMA, A., SAKUMA, Y., KAWAKATSU, T., IMAI, M. & PUFF, N. 2018. pH sensing by lipids in membranes:

- The fundamentals of pH-driven migration, polarization and deformations of lipid bilayer assemblies. *Biochim Biophys Acta Biomembr*, 1860, 2042-2063.
- ANTONELOU, M. H., KRIEBARDIS, A. G. & PAPASSIDERI, I. S. 2010. Aging and death signalling in mature red cells: from basic science to transfusion practice. *Blood Transfus*, 8 Suppl 3, s39-47.
- ANTOSIK, A., CZUBAK, K., CICHON, N., NOWAK, P. & ZBIKOWSKA, H. 2018. Vitamin E Analogue Protects Red Blood Cells against Storage-Induced Oxidative Damage. *Transfus Med Hemother*, 45, 347-354.
- ARANDA, A., SEQUEDO, L., TOLOSA, L., QUINTAS, G., BURELLO, E., CASTELL, J. V. & GOMBAU, L. 2013. Dichloro-dihydro-fluorescein diacetate (DCFH-DA) assay: a quantitative method for oxidative stress assessment of nanoparticle-treated cells. *Toxicol In Vitro*, 27, 954-63.
- ARDUINI, A., MANCINELLI, G., RADATTI, G. L., DOTTORI, S., MOLAJONI, F. & RAMSAY, R. R. 1992. Role of carnitine and carnitine palmitoyltransferase as integral components of the pathway for membrane phospholipid fatty acid turnover in intact human erythrocytes. *J Biol Chem*, 267, 12673-81.
- ARIVAZHAGAN, L., LOPEZ-DIEZ, R., SHEKHTMAN, A., RAMASAMY, R. & SCHMIDT, A. M. 2022. Glycation and a Spark of ALEs (Advanced Lipoxidation End Products) - Igniting RAGE/Diaphanous-1 and Cardiometabolic Disease. *Front Cardiovasc Med*, 9, 937071.
- ASSIES, L., GARCIA-CALVO, J., PIAZZOLLA, F., SANCHEZ, S., KATO, T., REYMOND, L., GOUJON, A., COLOM, A., LOPEZ-ANDARIAS, J., STRAKOVA, K., MAHECIC, D., MERCIER, V., RIGGI, M., JIMENEZ-ROJO, N., ROFFAY, C., LICARI, G., TSEMPEROULI, M., NEUHAUS, F., FURSTENBERG, A., VAUTHEY, E., HOOGENDOORN, S., GONZALEZ-GAITAN, M., ZUMBUEHL, A., SUGIHARA, K., GRUENBERG, J., RIEZMAN, H., LOEWITH, R., MANLEY, S., ROUX, A., WINSSINGER, N., SAKAI, N., PITSCH, S. & MATILE, S. 2021. Flipper Probes for the Community. *Chimia (Aarau)*, 75, 1004-1011.
- AUBERT-FOUCHER, E., FONT, B. & GAUTHERON, D. C. 1984. Rabbit heart mitochondrial hexokinase: solubilization and general properties. *Arch Biochem Biophys*, 232, 391-9.
- AUGUSTINE, J., TROENDLE, E. P., BARABAS, P., MCALEESE, C. A., FRIEDEL, T., STITT, A. W. & CURTIS, T. M. 2020. The Role of Lipoxidation in the Pathogenesis of Diabetic Retinopathy. *Front Endocrinol (Lausanne)*, 11, 621938.
- AYALA, A., MUNOZ, M. F. & ARGUELLES, S. 2014. Lipid peroxidation: production, metabolism, and signaling mechanisms of malondialdehyde and 4-hydroxy-2-nonenal. *Oxid Med Cell Longev*, 2014, 360438.
- BACCOUCH, R., SHI, Y., VERNAY, E., MATHÉLIE-GUINLET, M., TAIB-MAAMAR, N., VILLETTE, S., FEUILLIE, C., RASCOL, E., NUSS, P., LECOMTE, S., MOLINARI, M., STANEVA, G. & ALVES, I. D. 2023. The impact of lipid polyunsaturation on the physical and mechanical properties of lipid membranes. *Biochim Biophys Acta Biomembr*, 1865, 184084.
- BALABAN, R. S., NEMOTO, S. & FINKEL, T. 2005. Mitochondria, oxidants, and aging. *Cell*, 120, 483-95.

- BARBER, M. N., RISIS, S., YANG, C., MEIKLE, P. J., STAPLES, M., FEBBRAIO, M. A. & BRUCE, C. R. 2012. Plasma lysophosphatidylcholine levels are reduced in obesity and type 2 diabetes. *PLoS One*, 7, e41456.
- BARNS, S., BALANANT, M. A., SAURET, E., FLOWER, R., SAHA, S. & GU, Y. 2017. Investigation of red blood cell mechanical properties using AFM indentation and coarse-grained particle method. *Biomed Eng Online*, 16, 140.
- BARRANCO-ALTIRRIBA, M., ALONSO, N., WEBER, R. J. M., LLOYD, G. R., HERNANDEZ, M., YANES, O., CAPELLADES, J., JANKEVICS, A., WINDER, C., FALGUERA, M., FRANCH-NADAL, J., DUNN, W. B., PERERA-LLUNA, A., CASTELBLANCO, E. & MAURICIO, D. 2024. Lipidome characterisation and sex-specific differences in type 1 and type 2 diabetes mellitus. *Cardiovasc Diabetol*, 23, 109.
- BARROW, M. P., BURKITT, W. I. & DERRICK, P. J. 2005. Principles of Fourier transform ion cyclotron resonance mass spectrometry and its application in structural biology. *Analyst*, 130, 18-28.
- BELCHER, J. D., BECKMAN, J. D., BALLA, G., BALLA, J. & VERCELLOTTI, G. 2010. Heme degradation and vascular injury. *Antioxid Redox Signal*, 12, 233-48.
- BEREZIN, M. Y. & ACHILEFU, S. 2010. Fluorescence lifetime measurements and biological imaging. *Chem Rev*, 110, 2641-84.
- BERGERT, M. & DIZ-MUNOZ, A. 2023. Quantification of Apparent Membrane Tension and Membrane-to-Cortex Attachment in Animal Cells Using Atomic Force Microscopy-Based Force Spectroscopy. *Methods Mol Biol*, 2600, 45-62.
- BETZ, T., LENZ, M., JOANNY, J. F. & SYKES, C. 2009. ATP-dependent mechanics of red blood cells. *Proc Natl Acad Sci U S A*, 106, 15320-5.
- BEUTLER, E. & KUHL, W. 1988. Volume control of erythrocytes during storage. The role of mannitol. *Transfusion*, 28, 353-7.
- BEVERS, E. M. & WILLIAMSON, P. L. 2016. Getting to the Outer Leaflet: Physiology of Phosphatidylserine Exposure at the Plasma Membrane. *Physiol Rev*, 96, 605-45.
- BIANCHETTI, G., CEFALO, C. M. A., FERRERI, C., SANSONE, A., VITALE, M., SERANTONI, C., ABELTINO, A., MEZZA, T., FERRARO, P. M., DE SPIRITO, M., RICCARDI, G., GIACCARI, A. & MAULUCCI, G. 2024. Erythrocyte membrane fluidity: A novel biomarker of residual cardiovascular risk in type 2 diabetes. *Eur J Clin Invest*, 54, e14121.
- BIANCHETTI, G., DI GIACINTO, F., PITOCOCO, D., RIZZI, A., RIZZO, G. E., DE LEVA, F., FLEX, A., DI STASIO, E., CIASCA, G., DE SPIRITO, M. & MAULUCCI, G. 2019. Red blood cells membrane micropolarity as a novel diagnostic indicator of type 1 and type 2 diabetes. *Anal Chim Acta X*, 3, 100030.
- BIANCHETTI, G., VITI, L., SCUPOLA, A., DI LEO, M., TARTAGLIONE, L., FLEX, A., DE SPIRITO, M., PITOCOCO, D. & MAULUCCI, G. 2021. Erythrocyte membrane fluidity as a marker of diabetic retinopathy in type 1 diabetes mellitus. *Eur J Clin Invest*, 51, e13455.
- BICALHO, B., HOLOVATI, J. L. & ACKER, J. P. 2013. Phospholipidomics reveals differences in glycerophosphoserine profiles of hypothermally stored red blood cells and microvesicles. *Biochim Biophys Acta*, 1828, 317-26.
- BIERHAUS, A., FLEMING, T., STOYANOV, S., LEFFLER, A., BABES, A., NEACSU, C., SAUER, S. K., EBERHARDT, M., SCHNOLZER, M., LASITSCHKA, F., NEUHUBER, W. L., KICHKO, T. I., KONRADE, I., ELVERT, R., MIER, W., PIRAGS, V., LUKIC, I. K., Y. Pantoja Estrada, PhD Thesis, Aston University, 2024

- MORCOS, M., DEHMER, T., RABBANI, N., THORNALLEY, P. J., EDELSTEIN, D., NAU, C., FORBES, J., HUMPERT, P. M., SCHWANINGER, M., ZIEGLER, D., STERN, D. M., COOPER, M. E., HABERKORN, U., BROWNLEE, M., REEH, P. W. & NAWROTH, P. P. 2012. Methylglyoxal modification of Nav1.8 facilitates nociceptive neuron firing and causes hyperalgesia in diabetic neuropathy. *Nat Med*, 18, 926-33.
- BISWAS, A., KASHYAP, P., DATTA, S., SENGUPTA, T. & SINHA, B. 2019. Cholesterol Depletion by MbetaCD Enhances Cell Membrane Tension and Its Variations-Reducing Integrity. *Biophys J*, 116, 1456-1468.
- BLANC, L., SALOMAO, M., GUO, X., AN, X., GRATZER, W. & MOHANDAS, N. 2010. Control of erythrocyte membrane-skeletal cohesion by the spectrin-membrane linkage. *Biochemistry*, 49, 4516-23.
- BLANK, M. H., SILVA, V. C., RUI, B. R., NOVAES, G. A., CASTIGLIONE, V. C. & GARCIA PEREIRA, R. J. 2020. Beneficial influence of fetal bovine serum on in vitro cryosurvival of chicken spermatozoa. *Cryobiology*, 95, 103-109.
- BOGDANOVA, A., MAKHRO, A., WANG, J., LIPP, P. & KAESTNER, L. 2013. Calcium in red blood cells-a perilous balance. *Int J Mol Sci*, 14, 9848-72.
- BOGGS, J. M. 1987. Lipid intermolecular hydrogen bonding: influence on structural organization and membrane function. *Biochim Biophys Acta*, 906, 353-404.
- BOSCH, F. H., WERRE, J. M., ROERDINKHOLDER-STOELWINDER, B., HULS, T. H., WILLEKENS, F. L. & HALIE, M. R. 1992. Characteristics of red blood cell populations fractionated with a combination of counterflow centrifugation and Percoll separation. *Blood*, 79, 254-60.
- BOTTOMLEY, P. A. 1984. NMR in medicine. *Comput Radiol*, 8, 57-77.
- BRAUN, F., RINSCHEN, M. M., BARTELS, V., FROMMOLT, P., HABERMANN, B., HOEIJMAKERS, J. H., SCHUMACHER, B., DOLLE, M. E., MULLER, R. U., BENZING, T., SCHERMER, B. & KURSCHAT, C. E. 2016. Altered lipid metabolism in the aging kidney identified by three layered omic analysis. *Aging (Albany NY)*, 8, 441-57.
- BRAVO, N., TORRES, J., GONZALEZ-ORTIZ, M. & STAFORELLI-VIVANCO, J. P. 2023. Flickering of fetal erythrocytes membrane under gestational diabetes observed with dual time resolved membrane fluctuation spectroscopy. *Biochem Biophys Rep*, 36, 101556.
- BROWN, M. F. 2012. Curvature forces in membrane lipid-protein interactions. *Biochemistry*, 51, 9782-95.
- BRYSEWSKA, M. & SZOSLAND, K. 1988. Association between the glycation of erythrocyte membrane proteins and membrane fluidity. *Clin Biochem*, 21, 49-51.
- BRYSEWSKA, M., WATALA, C. & TORZECKA, W. 1986. Changes in fluidity and composition of erythrocyte membranes and in composition of plasma lipids in type I diabetes. *Br J Haematol*, 62, 111-6.
- BUKOWIECKA-MATUSIAK, M., BURZYNSKA-PEDZIWIATR, I., SANSONE, A., MALACHOWSKA, B., ZURAWSKA-KLIS, M., FERRERI, C., CHATGILIALOGLU, C., OCHEDALSKI, T., CYPRYK, K. & WOZNIAK, L. A. 2018. Lipid profile changes in erythrocyte membranes of women with diagnosed GDM. *PLoS One*, 13, e0203799.
- BURTON, N. M. & BRUCE, L. J. 2011. Modelling the structure of the red cell membrane. *Biochem Cell Biol*, 89, 200-15.

- BURZYNSKA-PEDZIWIATR, I., DUDZIK, D., SANSONE, A., MALACHOWSKA, B., ZIELENIAK, A., ZURAWSKA-KLIS, M., FERRERI, C., CHATGILIALOGLU, C., CYPRYK, K., WOZNIAK, L. A., MARKUSZEWSKI, M. J. & BUKOWIECKA-MATUSIAK, M. 2022. Targeted and untargeted metabolomic approach for GDM diagnosis. *Front Mol Biosci*, 9, 997436.
- BUTLER, P. J., NORWICH, G., WEINBAUM, S. & CHIEN, S. 2001. Shear stress induces a time- and position-dependent increase in endothelial cell membrane fluidity. *Am J Physiol Cell Physiol*, 280, C962-9.
- BUYS, A. V., VAN ROOY, M. J., SOMA, P., VAN PAPENDORP, D., LIPINSKI, B. & PRETORIUS, E. 2013. Changes in red blood cell membrane structure in type 2 diabetes: a scanning electron and atomic force microscopy study. *Cardiovasc Diabetol*, 12, 25.
- BYKHOVETS, M. 2020. Studying fatty acid content in red blood cell membranes in diabetic retinopathy of type 2 diabetes patients.
- BYRNES, J. R. & WOLBERG, A. S. 2017. Red blood cells in thrombosis. *Blood*, 130, 1795-1799.
- CAJKA, T. & FIEHN, O. 2016. Increasing lipidomic coverage by selecting optimal mobile-phase modifiers in LC-MS of blood plasma.
- CANDILOROS, H., MULLER, S., ZEGHARI, N., DONNER, M., DROUIN, P. & ZIEGLER, O. 1995. Decreased erythrocyte membrane fluidity in poorly controlled IDDM. Influence of ketone bodies. *Diabetes Care*, 18, 549-51.
- CAPRARI, P., SCUTERI, A., SALVATI, A. M., BAUCO, C., CANTAFORA, A., MASELLA, R., MODESTI, D., TARZIA, A. & MARIGLIANO, V. 1999. Aging and red blood cell membrane: a study of centenarians. *Exp Gerontol*, 34, 47-57.
- CATAN, A., TURPIN, C., DIOTEL, N., PATCHE, J., GUERIN-DUBOURG, A., DEBUSSCHE, X., BOURDON, E., AH-YOU, N., LE MOULLEC, N., BESNARD, M., VEERAPEN, R., RONDEAU, P. & MEILHAC, O. 2019. Aging and glycation promote erythrocyte phagocytosis by human endothelial cells: Potential impact in atherothrombosis under diabetic conditions. *Atherosclerosis*, 291, 87-98.
- CHANG, H. Y., LI, X. & KARNIADAKIS, G. E. 2017. Modeling of Biomechanics and Biorheology of Red Blood Cells in Type 2 Diabetes Mellitus. *Biophys J*, 113, 481-490.
- CHATZINIKOLAOU, P. N., MARGARITELIS, N. V., PASCHALIS, V., THEODOROU, A. A., VRABAS, I. S., KYPAROS, A., D'ALESSANDRO, A. & NIKOLAIDIS, M. G. 2024. Erythrocyte metabolism. *Acta Physiol (Oxf)*, 240, e14081.
- CHAUDHURI, J., BAINS, Y., GUHA, S., KAHN, A., HALL, D., BOSE, N., GUGLIUCCI, A. & KAPAHI, P. 2018. The Role of Advanced Glycation End Products in Aging and Metabolic Diseases: Bridging Association and Causality. *Cell Metab*, 28, 337-352.
- CHEDE, L. S., WAGNER, B. A., BUETTNER, G. R. & DONOVAN, M. D. 2021. Electron Spin Resonance Evaluation of Buccal Membrane Fluidity Alterations by Sodium Caprylate and L-Menthol. *Int J Mol Sci*, 22.
- CHEN, X., SUN, D., HE, Z., KANG, S., MIAO, Y. & LI, Y. 2024. Ferrite bismuth-based nanomaterials: From ferroelectric and piezoelectric properties to nanomedicine applications. *Colloids Surf B Biointerfaces*, 233, 113642.

- CHEN, X. X., BAYARD, F., GONZALEZ-SANCHIS, N., PAMUNGKAS, K. K. P., SAKAI, N. & MATILE, S. 2023. Fluorescent Flippers: Small-Molecule Probes to Image Membrane Tension in Living Systems. *Angew Chem Int Ed Engl*, 62, e202217868.
- CHIU, S. W., VASUDEVAN, S., JAKOBSSON, E., MASHL, R. J. & SCOTT, H. L. 2003. Structure of sphingomyelin bilayers: a simulation study. *Biophys J*, 85, 3624-35.
- CLIFTON, P. M. & NESTEL, P. J. 1998. Relationship between plasma insulin and erythrocyte fatty acid composition. *Prostaglandins Leukot Essent Fatty Acids*, 59, 191-4.
- COHEN, A. E. & SHI, Z. 2020. Do Cell Membranes Flow Like Honey or Jiggle Like Jello? *Bioessays*, 42, e1900142.
- COHEN, R. M., FRANCO, R. S., KHERA, P. K., SMITH, E. P., LINDSELL, C. J., CIRAOLO, P. J., PALASCAK, M. B. & JOINER, C. H. 2008. Red cell life span heterogeneity in hematologically normal people is sufficient to alter HbA1c. *Blood*, 112, 4284-91.
- COHEN, R. M., HOLMES, Y. R., CHENIER, T. C. & JOINER, C. H. 2003. Discordance between HbA1c and fructosamine: evidence for a glycosylation gap and its relation to diabetic nephropathy. *Diabetes Care*, 26, 163-7.
- COHN, C. A., SIMON, S. R. & SCHOONEN, M. A. 2008. Comparison of fluorescence-based techniques for the quantification of particle-induced hydroxyl radicals. *Part Fibre Toxicol*, 5, 2.
- COLOM, A., DERIVERY, E., SOLEIMANPOUR, S., TOMBA, C., MOLIN, M. D., SAKAI, N., GONZALEZ-GAITAN, M., MATILE, S. & ROUX, A. 2018. A fluorescent membrane tension probe. *Nat Chem*, 10, 1118-1125.
- COOPER, G. M. 2000. Structure of the Plasma Membrane. *The Cell: A Molecular Approach. 2nd edition*. 2nd edition ed. Sunderland (MA): Sinauer Associates.
- D'ALESSANDRO, A., HANSEN, K. C., EISENMESSER, E. Z. & ZIMRING, J. C. 2019a. Protect, repair, destroy or sacrifice: a role of oxidative stress biology in inter-donor variability of blood storage? *Blood Transfus*, 17, 281-288.
- D'ALESSANDRO, A., REISZ, J. A., ZHANG, Y., GEHRKE, S., ALEXANDER, K., KANIAS, T., TRIULZI, D. J., DONADEE, C., BARGE, S., BADLAM, J., JAIN, S., RISBANO, M. G. & GLADWIN, M. T. 2019b. Effects of aged stored autologous red blood cells on human plasma metabolome. *Blood Adv*, 3, 884-896.
- D'AURIA, L., FENAUX, M., ALEKSANDROWICZ, P., VAN DER SMISSEN, P., CHANTRAIN, C., VERMYLEN, C., VIKKULA, M., COURTOY, P. J. & TYTECA, D. 2013. Micrometric segregation of fluorescent membrane lipids: relevance for endogenous lipids and biogenesis in erythrocytes. *J Lipid Res*, 54, 1066-76.
- DAI, Y., TANG, H. & PANG, S. 2021. The Crucial Roles of Phospholipids in Aging and Lifespan Regulation. *Front Physiol*, 12, 775648.
- DALLE-DONNE, I., ROSSI, R., GIUSTARINI, D., MILZANI, A. & COLOMBO, R. 2003. Protein carbonyl groups as biomarkers of oxidative stress. *Clin Chim Acta*, 329, 23-38.
- DANTHI, P. & CHOW, M. 2004. Cholesterol removal by methyl-beta-cyclodextrin inhibits poliovirus entry. *J Virol*, 78, 33-41.
- DAS, U. N. 2021. "Cell Membrane Theory of Senescence" and the Role of Bioactive Lipids in Aging, and Aging Associated Diseases and Their Therapeutic Implications. *Biomolecules*, 11.

- DATTA, R., HEASTER, T. M., SHARICK, J. T., GILLETTE, A. A. & SKALA, M. C. 2020. Fluorescence lifetime imaging microscopy: fundamentals and advances in instrumentation, analysis, and applications. *J Biomed Opt*, 25, 1-43.
- DAVIS, J. H. 1979. Deuterium magnetic resonance study of the gel and liquid crystalline phases of dipalmitoyl phosphatidylcholine. *Biophys J*, 27, 339-58.
- DAWALIBY, R., TRUBBIA, C., DELPORTE, C., NOYON, C., RUYSSCHAERT, J. M., VAN ANTWERPEN, P. & GOVAERTS, C. 2016. Phosphatidylethanolamine Is a Key Regulator of Membrane Fluidity in Eukaryotic Cells. *J Biol Chem*, 291, 3658-67.
- DE BELLY, H., YAN, S., BORJA DA ROCHA, H., ICHBIAH, S., TOWN, J. P., ZAGER, P. J., ESTRADA, D. C., MEYER, K., TURLIER, H., BUSTAMANTE, C. & WEINER, O. D. 2023. Cell protrusions and contractions generate long-range membrane tension propagation. *Cell*, 186, 3049-3061 e15.
- DE JONG, K., RETTIG, M. P., LOW, P. S. & KUYPERS, F. A. 2002. Protein kinase C activation induces phosphatidylserine exposure on red blood cells. *Biochemistry*, 41, 12562-7.
- DE KROON, A. I., RIJKEN, P. J. & DE SMET, C. H. 2013. Checks and balances in membrane phospholipid class and acyl chain homeostasis, the yeast perspective. *Prog Lipid Res*, 52, 374-94.
- DE OLIVEIRA, S. & SALDANHA, C. 2010. An overview about erythrocyte membrane. *Clin Hemorheol Microcirc*, 44, 63-74.
- DEAN, J. M. & LODHI, I. J. 2018. Structural and functional roles of ether lipids. *Protein Cell*, 9, 196-206.
- DELION, S., CHALON, S., GUILLOTEAU, D., LEJEUNE, B., BESNARD, J. C. & DURAND, G. 1997. Age-related changes in phospholipid fatty acid composition and monoaminergic neurotransmission in the hippocampus of rats fed a balanced or an n-3 polyunsaturated fatty acid-deficient diet. *J Lipid Res*, 38, 680-9.
- DESRAMES, A., GENETET, S., DELCOURT, M. P., GOOSSENS, D. & MOURO-CHANTELOUP, I. 2020. Detergent-free isolation of native red blood cell membrane complexes. *Biochim Biophys Acta Biomembr*, 1862, 183126.
- DEY, P. & SPRINGERLINK (ONLINE SERVICE) 2021. Diagnostic Flow Cytometry in Cytology. 1st ed.
- DHANJAL, N. S., COX, I. J. & TAYLOR-ROBINSON, S. D. 2003. In vivo electron spin resonance spectroscopy: what use is it to gastroenterologists?
- DI MEO, S. & VENDITTI, P. 2020. Evolution of the Knowledge of Free Radicals and Other Oxidants. *Oxid Med Cell Longev*, 2020, 9829176.
- DIKALOV, S. I. & HARRISON, D. G. 2014. Methods for detection of mitochondrial and cellular reactive oxygen species. *Antioxid Redox Signal*, 20, 372-82.
- DINKLA, S., WESSELS, K., VERDURMEN, W. P., TOMELLERI, C., CLUITMANS, J. C., FRANSEN, J., FUCHS, B., SCHILLER, J., JOOSTEN, I., BROCK, R. & BOSMAN, G. J. 2012. Functional consequences of sphingomyelinase-induced changes in erythrocyte membrane structure. *Cell Death Dis*, 3, e410.
- DIZ-MUNOZ, A., FLETCHER, D. A. & WEINER, O. D. 2013. Use the force: membrane tension as an organizer of cell shape and motility. *Trends Cell Biol*, 23, 47-53.
- DODGE, J. T. & PHILLIPS, G. B. 1967. Composition of phospholipids and of phospholipid fatty acids and aldehydes in human red cells. *J Lipid Res*, 8, 667-75.

- DRAGICEVIC-CURIC, N., FRIEDRICH, M., PETERSEN, S., SCHEGLMANN, D., DOUROUMIS, D., PLASS, W. & FAHR, A. 2011. Assessment of fluidity of different invasomes by electron spin resonance and differential scanning calorimetry. *Int J Pharm*, 412, 85-94.
- DUNMORE, S. J., AL-DERAWI, A. S., NAYAK, A. U., NARSHI, A., NEVILL, A. M., HELLWIG, A., MAJEBI, A., KIRKHAM, P., BROWN, J. E. & SINGH, B. M. 2018. Evidence That Differences in Fructosamine-3-Kinase Activity May Be Associated With the Glycation Gap in Human Diabetes. *Diabetes*, 67, 131-136.
- EL-REMESSY, A. B., ABOU-MOHAMED, G., CALDWELL, R. W. & CALDWELL, R. B. 2003. High glucose-induced tyrosine nitration in endothelial cells: role of eNOS uncoupling and aldose reductase activation. *Invest Ophthalmol Vis Sci*, 44, 3135-43.
- ELIGINI, S., PORRO, B., WERBA, J. P., CAPRA, N., GENOVESE, S., GRECO, A., CAVALCA, V. & BANFI, C. 2022. Oxidative Stress and Arginine/Nitric Oxide Pathway in Red Blood Cells Derived from Patients with Prediabetes. *Biomedicines*, 10.
- EMAM, S. N., AR; NAKHJAVANI, M; & ESTEGHAMATI, AR 2008. Erythrocyte membrane fluidity in ageing, type 2 diabetes and stroke patients. *International Journal of Endocrinology and Metabolism*.
- ERMAK, G. & DAVIES, K. J. 2002. Calcium and oxidative stress: from cell signaling to cell death. *Mol Immunol*, 38, 713-21.
- ERMILOVA, I. & LYUBARTSEV, A. P. 2018. Cholesterol in phospholipid bilayers: positions and orientations inside membranes with different unsaturation degrees. *Soft Matter*, 15, 78-93.
- ESPINOSA, G., LOPEZ-MONTERO, I., MONROY, F. & LANGEVIN, D. 2011. Shear rheology of lipid monolayers and insights on membrane fluidity. *Proc Natl Acad Sci U S A*, 108, 6008-13.
- EVANS, E. A. 1973. New membrane concept applied to the analysis of fluid shear- and micropipette-deformed red blood cells. *Biophys J*, 13, 941-54.
- FAGHIH, M. & SHARP, M. K. 2018. Characterization of erythrocyte membrane tension for hemolysis prediction in complex flows. *Biomech Model Mechanobiol*, 17, 827-842.
- FAJARDO, V. A., MCMEEKIN, L. & LEBLANC, P. J. 2011. Influence of phospholipid species on membrane fluidity: a meta-analysis for a novel phospholipid fluidity index. *J Membr Biol*, 244, 97-103.
- FERNANDEZ-PEREZ, E. J., SEPULVEDA, F. J., PETERS, C., BASCUNAN, D., RIFFO-LEPE, N. O., GONZALEZ-SANMIGUEL, J., SANCHEZ, S. A., PEOPLES, R. W., VICENTE, B. & AGUAYO, L. G. 2018. Effect of Cholesterol on Membrane Fluidity and Association of Abeta Oligomers and Subsequent Neuronal Damage: A Double-Edged Sword. *Front Aging Neurosci*, 10, 226.
- FORMAN, H. J., BERNARDO, A. & DAVIES, K. J. 2016. What is the concentration of hydrogen peroxide in blood and plasma? *Arch Biochem Biophys*, 603, 48-53.
- FRANCO, R. S., PUCHULU-CAMPANELLA, M. E., BARBER, L. A., PALASCAK, M. B., JOINER, C. H., LOW, P. S. & COHEN, R. M. 2013. Changes in the properties of normal human red blood cells during in vivo aging. *Am J Hematol*, 88, 44-51.
- FROHLICH, B., JAGER, J., LANSCH, C., SANCHEZ, C. P., CYRKLAFF, M., BUCHHOLZ, B., SOUBEIGA, S. T., SIMPORE, J., ITO, H., SCHWARZ, U. S., LANZER, M. & TANAKA, Y. Pantoja Estrada, PhD Thesis, Aston University, 2024

- M. 2019. Hemoglobin S and C affect biomechanical membrane properties of *P. falciparum*-infected erythrocytes. *Commun Biol*, 2, 311.
- FURUIKE, S., LEVADNY, V. G., LI, S. J. & YAMAZAKI, M. 1999. Low pH induces an interdigitated gel to bilayer gel phase transition in dihexadecylphosphatidylcholine membrane. *Biophys J*, 77, 2015-23.
- GABREANU, G. R. & ANGELESCU, S. 2016. Erythrocyte membrane in type 2 diabetes mellitus. *Discoveries (Craiova)*, 4, e60.
- GAIKWAD, R., THANGARAJ, P. R. & SEN, A. K. 2021. Direct and rapid measurement of hydrogen peroxide in human blood using a microfluidic device. *Sci Rep*, 11, 2960.
- GALICIA-GARCIA, U., BENITO-VICENTE, A., JEBARI, S., LARREA-SEBAL, A., SIDDIQI, H., URIBE, K. B., OSTOLAZA, H. & MARTIN, C. 2020. Pathophysiology of Type 2 Diabetes Mellitus. *Int J Mol Sci*, 21.
- GAO, A. W., CHATZISPYROU, I. A., KAMBLE, R., LIU, Y. J., HERZOG, K., SMITH, R. L., VAN LENTHE, H., VERVAART, M. A. T., VAN CRUCHTEN, A., LUYF, A. C., VAN KAMPEN, A., PRAS-RAVES, M. L., VAZ, F. M. & HOUTKOOPER, R. H. 2017. A sensitive mass spectrometry platform identifies metabolic changes of life history traits in *C. elegans*. *Sci Rep*, 7, 2408.
- GARG, E. & ZUBAIR, M. 2023. Mass Spectrometer. [Updated 2023 Jan 21]. In: StatPearls [Internet]. Treasure Island (FL): StatPearls Publishing; 2023 Jan-. Available from: <https://www.ncbi.nlm.nih.gov/books/NBK589702/>.
- GAUTHIER, N. C., MASTERS, T. A. & SHEETZ, M. P. 2012. Mechanical feedback between membrane tension and dynamics. *Trends Cell Biol*, 22, 527-35.
- GELL, D. A. 2018. Structure and function of haemoglobins. *Blood Cells Mol Dis*, 70, 13-42.
- GEORGE, A., PUSHKARAN, S., KONSTANTINIDIS, D. G., KOOCHAKI, S., MALIK, P., MOHANDAS, N., ZHENG, Y., JOINER, C. H. & KALFA, T. A. 2013. Erythrocyte NADPH oxidase activity modulated by Rac GTPases, PKC, and plasma cytokines contributes to oxidative stress in sickle cell disease. *Blood*, 121, 2099-107.
- GERBER, G. K., SCHULTZE, M. & RAPOPORT, S. M. 1970. Occurrence and function of a high-Km hexokinase in immature red blood cells. *Eur J Biochem*, 17, 445-9.
- GHAZVINI, S., ALONSO, R., ALHAKAMY, N. & DHAR, P. 2018. pH-Induced Changes in the Surface Viscosity of Unsaturated Phospholipids Monitored Using Active Interfacial Microrheology. *Langmuir*, 34, 1159-1170.
- GIACCO, F. & BROWNLEE, M. 2010. Oxidative stress and diabetic complications. *Circ Res*, 107, 1058-70.
- GIRI, B., DEY, S., DAS, T., SARKAR, M., BANERJEE, J. & DASH, S. K. 2018. Chronic hyperglycemia mediated physiological alteration and metabolic distortion leads to organ dysfunction, infection, cancer progression and other pathophysiological consequences: An update on glucose toxicity. *Biomed Pharmacother*, 107, 306-328.
- GOI, G., CAZZOLA, R., TRINGALI, C., MASSACCESI, L., VOLPE, S. R., RONDANELLI, M., FERRARI, E., HERRERA, C. J., CESTARO, B., LOMBARDO, A. & VENERANDO, B. 2005. Erythrocyte membrane alterations during ageing affect beta-D-glucuronidase and neutral sialidase in elderly healthy subjects. *Exp Gerontol*, 40, 219-25.

- GOLDIN, A., BECKMAN, J. A., SCHMIDT, A. M. & CREAGER, M. A. 2006. Advanced glycation end products: sparking the development of diabetic vascular injury. *Circulation*, 114, 597-605.
- GONZALEZ-LLEO, A. M., SANCHEZ-HERNANDEZ, R. M., BORONAT, M. & WAGNER, A. M. 2022. Diabetes and Familial Hypercholesterolemia: Interplay between Lipid and Glucose Metabolism. *Nutrients*, 14.
- GOODMAN, S. R. & SHIFFER, K. 1983. The spectrin membrane skeleton of normal and abnormal human erythrocytes: a review. *Am J Physiol*, 244, C121-41.
- GOUJON, A., COLOM, A., STRAKOVA, K., MERCIER, V., MAHECIC, D., MANLEY, S., SAKAI, N., ROUX, A. & MATILE, S. 2019. Mechanosensitive Fluorescent Probes to Image Membrane Tension in Mitochondria, Endoplasmic Reticulum, and Lysosomes. *J Am Chem Soc*, 141, 3380-3384.
- GRAGE, S. L., AFONIN, S., IERONIMO, M., BERDITSCH, M., WADHWANI, P. & ULRICH, A. S. 2022. Probing and Manipulating the Lateral Pressure Profile in Lipid Bilayers Using Membrane-Active Peptides-A Solid-State (19)F NMR Study. *Int J Mol Sci*, 23.
- GWOZDZINSKI, K., PIENIAZEK, A. & GWOZDZINSKI, L. 2021. Reactive Oxygen Species and Their Involvement in Red Blood Cell Damage in Chronic Kidney Disease. *Oxid Med Cell Longev*, 2021, 6639199.
- HA, C. Y., KIM, J. Y., PAIK, J. K., KIM, O. Y., PAIK, Y. H., LEE, E. J. & LEE, J. H. 2012. The association of specific metabolites of lipid metabolism with markers of oxidative stress, inflammation and arterial stiffness in men with newly diagnosed type 2 diabetes. *Clin Endocrinol (Oxf)*, 76, 674-82.
- HAIDEKKER, M. A., L'HEUREUX, N. & FRANGOS, J. A. 2000. Fluid shear stress increases membrane fluidity in endothelial cells: a study with DCVJ fluorescence. *Am J Physiol Heart Circ Physiol*, 278, H1401-6.
- HALE, J. P., WINLOVE, C. P. & PETROV, P. G. 2011. Effect of hydroperoxides on red blood cell membrane mechanical properties. *Biophys J*, 101, 1921-9.
- HAN, X., WANG, C. & LIU, Z. 2018. Red Blood Cells as Smart Delivery Systems. *Bioconjug Chem*, 29, 852-860.
- HAN, Y., RANDELL, E., VASDEV, S., GILL, V., GADAG, V., NEWHOOK, L. A., GRANT, M. & HAGERTY, D. 2007. Plasma methylglyoxal and glyoxal are elevated and related to early membrane alteration in young, complication-free patients with Type 1 diabetes. *Mol Cell Biochem*, 305, 123-31.
- HARRIS, M. I. 1991. Hypercholesterolemia in diabetes and glucose intolerance in the U.S. population. *Diabetes Care*, 14, 366-74.
- HATTORI, Y., HATTORI, S., SATO, N. & KASAI, K. 2000. High-glucose-induced nuclear factor kappaB activation in vascular smooth muscle cells. *Cardiovasc Res*, 46, 188-97.
- HE, W., LIU, Y., WAMER, W. G. & YIN, J. J. 2014. Electron spin resonance spectroscopy for the study of nanomaterial-mediated generation of reactive oxygen species. *J Food Drug Anal*, 22, 49-63.
- HESS, J. R. 2006. An update on solutions for red cell storage. *Vox Sang*, 91, 13-9.
- HIRATA, Y., CAI, R., VOLCHUK, A., STEINBERG, B. E., SAITO, Y., MATSUZAWA, A., GRINSTEIN, S. & FREEMAN, S. A. 2023. Lipid peroxidation increases membrane tension, Piezo1 gating, and cation permeability to execute ferroptosis. *Curr Biol*, 33, 1282-1294 e5.

- HOCHMUTH, R. M. & EVANS, E. A. 1982. Extensional flow of erythrocyte membrane from cell body to elastic tether. I. Analysis. *Biophys J*, 39, 71-81.
- HOCHMUTH, R. M., MOHANDAS, N. & BLACKSHEAR, P. L., JR. 1973. Measurement of the elastic modulus for red cell membrane using a fluid mechanical technique. *Biophys J*, 13, 747-62.
- HOERL, B. J. & SCOTT, R. E. 1978. Plasma membrane vesiculation: a cellular response to injury. *Virchows Arch B Cell Pathol*, 27, 335-45.
- HOLLAN, S. 1996. Membrane fluidity of blood cells. *Haematologia (Budap)*, 27, 109-27.
- HOOGEVEST, P., TIEMESSEN, H. M., J. DRESCHER, S. & FAHR, A. 2021. The Use of Phospholipids to Make Pharmaceutical Form Line Extensions. *European Journal of Lipid Science and Technology*, Volume 123, Issue 4 2000297.
- HORN, A. & JAISWAL, J. K. 2019. Structural and signaling role of lipids in plasma membrane repair. *Curr Top Membr*, 84, 67-98.
- HORNBURG, D., WU, S., MOQRI, M., ZHOU, X., CONTREPOIS, K., BARARPOUR, N., TRABER, G. M., SU, B., METWALLY, A. A., AVINA, M., ZHOU, W., UBELLACKER, J. M., MISHRA, T., SCHUSSLER-FIORENZA ROSE, S. M., KAVATHAS, P. B., WILLIAMS, K. J. & SNYDER, M. P. 2023. Dynamic lipidome alterations associated with human health, disease and ageing. *Nat Metab*, 5, 1578-1594.
- HU, C., VAN DER HEIJDEN, R., WANG, M., VAN DER GREEF, J., HANKEMEIER, T. & XU, G. 2009. Analytical strategies in lipidomics and applications in disease biomarker discovery. *J Chromatogr B Analyt Technol Biomed Life Sci*, 877, 2836-46.
- HUANG, P. L. 2009. A comprehensive definition for metabolic syndrome. *Dis Model Mech*, 2, 231-7.
- HUANG, Y. X., WU, Z. J., MEHRISHI, J., HUANG, B. T., CHEN, X. Y., ZHENG, X. J., LIU, W. J. & LUO, M. 2011. Human red blood cell aging: correlative changes in surface charge and cell properties. *J Cell Mol Med*, 15, 2634-42.
- IGHODARO, O. M. 2018. Molecular pathways associated with oxidative stress in diabetes mellitus. *Biomed Pharmacother*, 108, 656-662.
- INOUYE, M., MIO, T & SUMINO K. 1999. Link between glycation and lipoxidation in red blood cells in diabetes.
- JAIN, S. K. 1989. Hyperglycemia can cause membrane lipid peroxidation and osmotic fragility in human red blood cells. *J Biol Chem*, 264, 21340-5.
- JAY, A. G. & HAMILTON, J. A. 2017. Disorder Amidst Membrane Order: Standardizing Laurdan Generalized Polarization and Membrane Fluidity Terms. *J Fluoresc*, 27, 243-249.
- JUAN, C. A., PEREZ DE LA LASTRA, J. M., PLOU, F. J. & PEREZ-LEBENA, E. 2021. The Chemistry of Reactive Oxygen Species (ROS) Revisited: Outlining Their Role in Biological Macromolecules (DNA, Lipids and Proteins) and Induced Pathologies. *Int J Mol Sci*, 22.
- K, A. A., MUNIANDY, S. & I, S. I. 2007. Role of N-(carboxymethyl)lysine in the development of ischemic heart disease in type 2 diabetes mellitus. *J Clin Biochem Nutr*, 41, 97-105.
- KADRI, L., BACLE, A., KHOURY, S., VANDEBROUCK, C., BESCOND, J., FAIVRE, J. F., FERREIRA, T. & SEBILLE, S. 2021. Polyunsaturated Phospholipids Increase Cell Resilience to Mechanical Constraints. *Cells*, 10.

- KAISER, H. J., LINGWOOD, D., LEVENTAL, I., SAMPAIO, J. L., KALVODOVA, L., RAJENDRAN, L. & SIMONS, K. 2009. Order of lipid phases in model and plasma membranes. *Proc Natl Acad Sci U S A*, 106, 16645-50.
- KALYANARAMAN, B., DARLEY-USMAR, V., DAVIES, K. J., DENNERY, P. A., FORMAN, H. J., GRISHAM, M. B., MANN, G. E., MOORE, K., ROBERTS, L. J., 2ND & ISCHIROPOULOS, H. 2012. Measuring reactive oxygen and nitrogen species with fluorescent probes: challenges and limitations. *Free Radic Biol Med*, 52, 1-6.
- KAMADA, T., YAMASHITA, T., BABA, Y., KAI, M., SETOYAMA, S., CHUMAN, Y. & OTSUJI, S. 1986. Dietary sardine oil increases erythrocyte membrane fluidity in diabetic patients. *Diabetes*, 35, 604-11.
- KARAKUZU, O., CRUZ, M. R., LIU, Y. & GARSIN, D. A. 2019. Amplex Red Assay for Measuring Hydrogen Peroxide Production from *Caenorhabditis elegans*. *Bio Protoc*, 9.
- KARASU, C. 2000. Time course of changes in endothelium-dependent and -independent relaxation of chronically diabetic aorta: role of reactive oxygen species. *Eur J Pharmacol*, 392, 163-73.
- KERWIN, J. L., TUININGA, A. R. & ERICSSON, L. H. 1994. Identification of molecular species of glycerophospholipids and sphingomyelin using electrospray mass spectrometry. *J Lipid Res*, 35, 1102-14.
- KEVAN, L. 2003. *Encyclopedia of Physical Science and Technology. Electron Spin Resonance*.
- KILHOVD, B. K., BERG, T. J., BIRKELAND, K. I., THORSBY, P. & HANSSSEN, K. F. 1999. Serum levels of advanced glycation end products are increased in patients with type 2 diabetes and coronary heart disease. *Diabetes Care*, 22, 1543-8.
- KIM, Y. J., CHO, M. J., YU, W. D., KIM, M. J., KIM, S. Y. & LEE, J. H. 2022. Links of Cytoskeletal Integrity with Disease and Aging. *Cells*, 11.
- KIROV, A., AL-HASHIMI, H., SOLOMON, P., MAZUR, C., THORPE, P. E., SIMS, P. J., TARANTINI, F., KUMAR, T. K. & PRUDOVSKY, I. 2012. Phosphatidylserine externalization and membrane blebbing are involved in the nonclassical export of FGF1. *J Cell Biochem*, 113, 956-66.
- KNIGHT, J., WOOD, K. D., LANGE, J. N., ASSIMOS, D. G. & HOLMES, R. P. 2016. Oxalate Formation From Glyoxal in Erythrocytes. *Urology*, 88, 226 e11-5.
- KOEHRER, P., SAAB, S., BERDEAUX, O., ISAICO, R., GREGOIRE, S., CABARET, S., BRON, A. M., CREUZOT-GARCHER, C. P., BRETILLON, L. & ACAR, N. 2014. Erythrocyte phospholipid and polyunsaturated fatty acid composition in diabetic retinopathy. *PLoS One*, 9, e106912.
- KOLD-CHRISTENSEN, R., JENSEN, K. K., SMEDEGARD-HOLMQUIST, E., SORENSEN, L. K., HANSEN, J., JORGENSEN, K. A., KRISTENSEN, P. & JOHANNSEN, M. 2019. ReactELISA method for quantifying methylglyoxal levels in plasma and cell cultures. *Redox Biol*, 26, 101252.
- KORADE, Z. & KENWORTHY, A. K. 2008. Lipid rafts, cholesterol, and the brain. *Neuropharmacology*, 55, 1265-73.
- KOSTARA, C. E., TSIAFOULIS, C. G., BAIRAKTARI, E. T. & TSIMIHODIMOS, V. 2021. Altered RBC membrane lipidome: A possible etiopathogenic link for the microvascular impairment in Type 2 diabetes. *J Diabetes Complications*, 35, 107998.

- KOZLOV, M. M. & CHERNOMORDIK, L. V. 2015. Membrane tension and membrane fusion. *Curr Opin Struct Biol*, 33, 61-7.
- KOZYRA, K. A. H., J. K.; ENGELKE, M. & DIEHL, H. A. 2003. Concentration and Temperature Dependence of Laurdan Fluorescence in Glycerol. 581 – 588.
- KROGER, J., JACOBS, S., JANSEN, E. H., FRITSCHKE, A., BOEING, H. & SCHULZE, M. B. 2015. Erythrocyte membrane fatty acid fluidity and risk of type 2 diabetes in the EPIC-Potsdam study. *Diabetologia*, 58, 282-9.
- KUCHERENKO, Y. V., BHAVSAR, S. K., GRISCHENKO, V. I., FISCHER, U. R., HUBER, S. M. & LANG, F. 2010. Increased cation conductance in human erythrocytes artificially aged by glycation. *J Membr Biol*, 235, 177-89.
- KUEHNEL, R. M., GANGA, E., BALESTRA, A. C., SUAREZ, C., WYSS, M., KLAGES, N., BRUSINI, L., MACO, B., BRANCUCCI, N., VOSS, T. S., SOLDATI, D. & BROCHET, M. 2023. A Plasmodium membrane receptor platform integrates cues for egress and invasion in blood forms and activation of transmission stages. *Sci Adv*, 9, eadf2161.
- KULIG, W., OLZYNSKA, A., JURKIEWICZ, P., KANTOLA, A. M., KOMULAINEN, S., MANNA, M., POURMOUSA, M., VAZDAR, M., CWIKLIK, L., ROG, T., KHELASHVILI, G., HARRIES, D., TELKKI, V. V., HOF, M., VATTULAINEN, I. & JUNGWIRTH, P. 2015. Cholesterol under oxidative stress-How lipid membranes sense oxidation as cholesterol is being replaced by oxysterols. *Free Radic Biol Med*, 84, 30-41.
- KUMAR, P., SAINI, K., SAINI, V. & MITCHELL, T. 2021. Oxalate Alters Cellular Bioenergetics, Redox Homeostasis, Antibacterial Response, and Immune Response in Macrophages. *Front Immunol*, 12, 694865.
- KUZMIN, P. I., AKIMOV, S. A., CHIZMADZHEV, Y. A., ZIMMERBERG, J. & COHEN, F. S. 2005. Line tension and interaction energies of membrane rafts calculated from lipid splay and tilt. *Biophys J*, 88, 1120-33.
- LABROUCHE, S., FREYBURGER, G., GIN, H., BOISSEAU, M. R. & CASSAGNE, C. 1996. Changes in phospholipid composition of blood cell membranes (erythrocyte, platelet, and polymorphonuclear) in different types of diabetes--clinical and biological correlations. *Metabolism*, 45, 57-71.
- LAI, S. J., OHKAWA, R., HORIUCHI, Y., KUBOTA, T. & TOZUKA, M. 2019. Red blood cells participate in reverse cholesterol transport by mediating cholesterol efflux of high-density lipoprotein and apolipoprotein A-I from THP-1 macrophages. *Biol Chem*, 400, 1593-1602.
- LAI, S. W. T., LOPEZ GONZALEZ, E. J., ZOUKARI, T., KI, P. & SHUCK, S. C. 2022. Methylglyoxal and Its Adducts: Induction, Repair, and Association with Disease. *Chem Res Toxicol*, 35, 1720-1746.
- LAMPARTER, L. & GALIC, M. 2020. Cellular Membranes, a Versatile Adaptive Composite Material. *Front Cell Dev Biol*, 8, 684.
- LANKINEN, M., UUSITUPA, M. & SCHWAB, U. 2018. Genes and Dietary Fatty Acids in Regulation of Fatty Acid Composition of Plasma and Erythrocyte Membranes. *Nutrients*, 10.
- LASCAR, N., BROWN, J., PATTISON, H., BARNETT, A. H., BAILEY, C. J. & BELLARY, S. 2018. Type 2 diabetes in adolescents and young adults. *Lancet Diabetes Endocrinol*, 6, 69-80.

- LEACH, M. D. & COWEN, L. E. 2014. Membrane fluidity and temperature sensing are coupled via circuitry comprised of Ole1, Rsp5, and Hsf1 in *Candida albicans*. *Eukaryot Cell*, 13, 1077-84.
- LEE, H. C. & YOKOMIZO, T. 2018. Applications of mass spectrometry-based targeted and non-targeted lipidomics. *Biochem Biophys Res Commun*, 504, 576-581.
- LEIDL, K., LIEBISCH, G., RICHTER, D. & SCHMITZ, G. 2008. Mass spectrometric analysis of lipid species of human circulating blood cells. *Biochim Biophys Acta*, 1781, 655-64.
- LERNO, L. A., JR., GERMAN, J. B. & LEBRILLA, C. B. 2010. Method for the identification of lipid classes based on referenced Kendrick mass analysis. *Anal Chem*, 82, 4236-45.
- LI, H. & LYKOTRAFITIS, G. 2014. Erythrocyte membrane model with explicit description of the lipid bilayer and the spectrin network. *Biophys J*, 107, 642-653.
- LI, W., YU, X., XIE, F., ZHANG, B., SHAO, S., GENG, C., AZIZ, A. U. R., LIAO, X. & LIU, B. 2018. A Membrane-Bound Biosensor Visualizes Shear Stress-Induced Inhomogeneous Alteration of Cell Membrane Tension. *iScience*, 7, 180-190.
- LI, Z., ZHANG, Z., REN, Y., WANG, Y., FANG, J., YUE, H., MA, S. & GUAN, F. 2021. Aging and age-related diseases: from mechanisms to therapeutic strategies. *Biogerontology*, 22, 165-187.
- LICARI, G., STRAKOVA, K., MATILE, S. & TAJKHORSHID, E. 2020. Twisting and tilting of a mechanosensitive molecular probe detects order in membranes. *Chem Sci*, 11, 5637-5649.
- LIEBER, A. D., YEHUDAI-RESHEFF, S., BARNHART, E. L., THERIOT, J. A. & KEREN, K. 2013. Membrane tension in rapidly moving cells is determined by cytoskeletal forces. *Curr Biol*, 23, 1409-17.
- LIN, L., CAO, B., XU, Z., SUI, Y., CHEN, J., LUAN, Q., YANG, R., LI, S. & LI, K. F. 2016. In vivo HMRS and lipidomic profiling reveals comprehensive changes of hippocampal metabolism during aging in mice. *Biochem Biophys Res Commun*, 470, 9-14.
- LIPPI, G., MERCADANTI, M., ALOE, R. & TARGHER, G. 2012. Erythrocyte mechanical fragility is increased in patients with type 2 diabetes. *Eur J Intern Med*, 23, 150-3.
- LIU, J. H., CHEN, M. M., HUANG, J. W., WANN, H., HO, L. K., PAN, W. H., CHEN, Y. C., LIU, C. M., YE, M. Y., TSAI, S. K., YOUNG, M. S., HO, L. T., KUO, C. D., CHUANG, H. Y., CHAO, F. P. & CHAO, H. M. 2010. Therapeutic effects and mechanisms of action of mannitol during H<sub>2</sub>O<sub>2</sub>-induced oxidative stress in human retinal pigment epithelium cells. *J Ocul Pharmacol Ther*, 26, 249-57.
- LOPEZ, C. A., DE VRIES, A. H. & MARRINK, S. J. 2011. Molecular mechanism of cyclodextrin mediated cholesterol extraction. *PLoS Comput Biol*, 7, e1002020.
- LORENT, J. H., LEVENTAL, K. R., GANESAN, L., RIVERA-LONGSWORTH, G., SEZGIN, E., DOKTOROVA, M., LYMAN, E. & LEVENTAL, I. 2020. Plasma membranes are asymmetric in lipid unsaturation, packing and protein shape. *Nat Chem Biol*, 16, 644-652.
- LOS, D. A. & MURATA, N. 2004. Membrane fluidity and its roles in the perception of environmental signals. *Biochim Biophys Acta*, 1666, 142-57.
- LU, J., LAM, S. M., WAN, Q., SHI, L., HUO, Y., CHEN, L., TANG, X., LI, B., WU, X., PENG, K., LI, M., WANG, S., XU, Y., XU, M., BI, Y., NING, G., SHUI, G. & WANG, W. 2019. Y. Pantoja Estrada, PhD Thesis, Aston University, 2024

- High-Coverage Targeted Lipidomics Reveals Novel Serum Lipid Predictors and Lipid Pathway Dysregulation Antecedent to Type 2 Diabetes Onset in Normoglycemic Chinese Adults. *Diabetes Care*, 42, 2117-2126.
- LU, S., LIAO, Z., LU, X., KATSCHINSKI, D. M., MERCOLA, M., CHEN, J., HELLER BROWN, J., MOLKENTIN, J. D., BOSSUYT, J. & BERS, D. M. 2020. Hyperglycemia Acutely Increases Cytosolic Reactive Oxygen Species via O-linked GlcNAcylation and CaMKII Activation in Mouse Ventricular Myocytes. *Circ Res*, 126, e80-e96.
- LUCHEFELD, I., PIVKIN, I. V., GARDINI, L., ZARE-EELANJEGH, E., GABELEIN, C., IHLE, S. J., REICHMUTH, A. M., CAPITANIO, M., MARTINAC, B., ZAMBELLI, T. & VASSALLI, M. 2024. Dissecting cell membrane tension dynamics and its effect on Piezo1-mediated cellular mechanosensitivity using force-controlled nanopipettes. *Nat Methods*, 21, 1063-1073.
- LUIS A. J. ALVAREZ, B. W., GIULIA OSSATO, BRAM VAN DEN BROEK, KEES JALINK, LIOBA KUSCHEL, M. JULIA ROBERTI AND FRANK HECHT 2019. Application Note: SP8 FALCON: a novel concept in fluorescence lifetime imaging enabling video-rate confocal FLIM.
- LUND, E. K., HARVEY, L. J., LADHA, S., CLARK, D. C. & JOHNSON, I. T. 1999. Effects of dietary fish oil supplementation on the phospholipid composition and fluidity of cell membranes from human volunteers. *Ann Nutr Metab*, 43, 290-300.
- LUO, J., LI, N., PAUL ROBINSON, J. & SHI, R. 2002. Detection of reactive oxygen species by flow cytometry after spinal cord injury. *J Neurosci Methods*, 120, 105-12.
- LUTZ, H. U. & BOGDANOVA, A. 2013. Mechanisms tagging senescent red blood cells for clearance in healthy humans. *Front Physiol*, 4, 387.
- LUX, S. E. T. 2016. Anatomy of the red cell membrane skeleton: unanswered questions. *Blood*, 127, 187-99.
- LYDIC, T. A., RENIS, R., BUSIK, J. V. & REID, G. E. 2009. Analysis of Retina and Erythrocyte Glycerophospholipid Alterations in a Rat Model of Type 1 Diabetes. *JALA Charlottesville Va*, 14, 383-399.
- MAHAMMAD, S. & PARMRYD, I. 2015. Cholesterol depletion using methyl-beta-cyclodextrin. *Methods Mol Biol*, 1232, 91-102.
- MAKKI, B. E. & RAHMAN, S. 2023. Alzheimer's Disease in Diabetic Patients: A Lipidomic Prospect. *Neuroscience*, 530, 79-94.
- MALDONADO, E., MORALES-PISON, S., URBINA, F. & SOLARI, A. 2023. Aging Hallmarks and the Role of Oxidative Stress. *Antioxidants (Basel)*, 12.
- MANAKOVA, K., YAN, H., LOWENGRUB, J. & ALLARD, J. 2016. Cell Surface Mechanochemistry and the Determinants of Bleb Formation, Healing, and Travel Velocity. *Biophys J*, 110, 1636-1647.
- MANGALMURTI, N. S., CHATTERJEE, S., CHENG, G., ANDERSEN, E., MOHAMMED, A., SIEGEL, D. L., SCHMIDT, A. M., ALBELDA, S. M. & LEE, J. S. 2010. Advanced glycation end products on stored red blood cells increase endothelial reactive oxygen species generation through interaction with receptor for advanced glycation end products. *Transfusion*, 50, 2353-61.
- MANNO, S., MOHANDAS, N. & TAKAKUWA, Y. 2010. ATP-dependent mechanism protects spectrin against glycation in human erythrocytes. *J Biol Chem*, 285, 33923-9.

- MAPSTONE, M., CHEEMA, A. K., FIANDACA, M. S., ZHONG, X., MHYRE, T. R., MACARTHUR, L. H., HALL, W. J., FISHER, S. G., PETERSON, D. R., HALEY, J. M., NAZAR, M. D., RICH, S. A., BERLAU, D. J., PELTZ, C. B., TAN, M. T., KAWAS, C. H. & FEDEROFF, H. J. 2014. Plasma phospholipids identify antecedent memory impairment in older adults. *Nat Med*, 20, 415-8.
- MAQSOODA S., B., S. AND KAMAL-ELDIN, A 2012. Haemoglobin-mediated lipid oxidation in the fish muscle: A review. *Elsevier*, 33-43.
- MARCHESI, V. T. 1974. Isolation of spectrin from erythrocyte membranes. *Methods Enzymol*, 32, 275-7.
- MARQUARDT, D., HEBERLE, F. A., GREATHOUSE, D. V., KOEPPE, R. E., STANDAERT, R. F., VAN OOSTEN, B. J., HARROUN, T. A., KINNUN, J. J., WILLIAMS, J. A., WASSALL, S. R. & KATSARAS, J. 2016. Lipid bilayer thickness determines cholesterol's location in model membranes. *Soft Matter*, 12, 9417-9428.
- MASUOKA, N., ZUKERAN, A., TAKEMOTO, K., WANG, D. H. & ISHIHARA, K. 2020. Effect of hydrogen peroxide on normal and acatalasemic mouse erythrocytes. *Toxicol Rep*, 7, 282-287.
- MATHEW, T. K., ZUBAIR, M. & TADI, P. 2023. Blood Glucose Monitoring. *StatPearls*. Treasure Island (FL) ineligible companies. Disclosure: Muhammad Zubair declares no relevant financial relationships with ineligible companies. Disclosure: Prasanna Tadi declares no relevant financial relationships with ineligible companies.
- MATSURA, T. 2014. Oxidized phosphatidylserine: production and bioactivities. *Yonago Acta Med*, 57, 119-27.
- MAULUCCI, G., CORDELLI, E., RIZZI, A., DE LEVA, F., PAPI, M., CIASCA, G., SAMENGO, D., PANI, G., PITOCCHIO, D., SODA, P., GHIRLANDA, G., IANNELLO, G. & DE SPIRITO, M. 2017. Phase separation of the plasma membrane in human red blood cells as a potential tool for diagnosis and progression monitoring of type 1 diabetes mellitus. *PLoS One*, 12, e0184109.
- MAZZANTI, L., FALIOIA, E., RABINI, R. A., STAFFOLANI, R., KANTAR, A., FIORINI, R., SWOBODA, B., DE PIRRO, R. & BERTOLI, E. 1992. Diabetes mellitus induces red blood cell plasma membrane alterations possibly affecting the aging process. *Clin Biochem*, 25, 41-6.
- MCKINNON, K. M. 2018. Flow Cytometry: An Overview. *Curr Protoc Immunol*, 120, 5 1 11-5 1 11.
- MEISTER, A. & ANDERSON, M. E. 1983. Glutathione. *Annu Rev Biochem*, 52, 711-60.
- MELZAK, K. A., MUTH, M., KIRSCHHOFER, F., BRENNER-WEISS, G. & BIEBACK, K. 2020. Lipid ratios as a marker for red blood cell storage quality and as a possible explanation for donor gender differences in storage quality. *Vox Sang*, 115, 655-663.
- MENGSTIE, M. A., CHEKOL ABEBE, E., BEHAILE TEKLEMARIAM, A., TILAHUN MULU, A., AGIDEW, M. M., TESHOME AZEZEW, M., ZEWEDE, E. A. & AGE NEHU TESHOME, A. 2022. Endogenous advanced glycation end products in the pathogenesis of chronic diabetic complications. *Front Mol Biosci*, 9, 1002710.
- MERCIER, V., LARIOS, J., MOLINARD, G., GOUJON, A., MATILE, S., GRUENBERG, J. & ROUX, A. 2020. Endosomal membrane tension regulates ESCRT-III-dependent intra-lumenal vesicle formation. *Nat Cell Biol*, 22, 947-959.

- MILKOVIC, L., CIPAK GASPAROVIC, A., CINDRIC, M., MOUTHUY, P. A. & ZARKOVIC, N. 2019. Short Overview of ROS as Cell Function Regulators and Their Implications in Therapy Concepts. *Cells*, 8.
- MINETTI, G., KAESTNER, L. & DORN, I. 2023. Terminal maturation of human reticulocytes to red blood cells by extensive remodelling and progressive liquid ordering of membrane lipids. *bioRxiv*.
- MINIC, R., ARSIC, A., KOJADINOVIC, M., PALIBRK, A., DORDEVIC, B. & STEVIC, Z. 2023. Erythrocyte fatty acid aberrations in Amyotrophic Lateral Sclerosis: Correlation with disease duration. *J Med Biochem*, 42, 621-629.
- MOHANTY, J. G., NAGABABU, E. & RIFKIND, J. M. 2014. Red blood cell oxidative stress impairs oxygen delivery and induces red blood cell aging. *Front Physiol*, 5, 84.
- MOLDOGAZIEVA, N. T., MOKHOSOEV, I. M., MEL'NIKOVA, T. I., POROZOV, Y. B. & TEREENTIEV, A. A. 2019. Oxidative Stress and Advanced Lipoxidation and Glycation End Products (ALEs and AGEs) in Aging and Age-Related Diseases. *Oxid Med Cell Longev*, 2019, 3085756.
- MONNIER, V. M. 1989. Toward a Maillard reaction theory of aging. *Prog Clin Biol Res*, 304, 1-22.
- MONNIER, V. M., SELL, D. R., ABDUL-KARIM, F. W. & EMANCIPATOR, S. N. 1988. Collagen browning and cross-linking are increased in chronic experimental hyperglycemia. Relevance to diabetes and aging. *Diabetes*, 37, 867-72.
- MONNIER, V. M., SELL, D. R. & GENUTH, S. 2005. Glycation products as markers and predictors of the progression of diabetic complications. *Ann N Y Acad Sci*, 1043, 567-81.
- MORABITO, R., REMIGANTE, A., SPINELLI, S., VITALE, G., TRICHILO, V., LODDO, S. & MARINO, A. 2020. High Glucose Concentrations Affect Band 3 Protein in Human Erythrocytes. *Antioxidants (Basel)*, 9.
- MORLEY, J. E. 2008. Diabetes and aging: epidemiologic overview. *Clin Geriatr Med*, 24, 395-405, v.
- MOURITSEN, O. G. 2010. The liquid-ordered state comes of age. *Biochim Biophys Acta*, 1798, 1286-8.
- MOURITSEN, O. G. & ZUCKERMANN, M. J. 2004. What's so special about cholesterol? *Lipids*, 39, 1101-13.
- MUDDANA, H. S., GULLAPALLI, R. R., MANIAS, E. & BUTLER, P. J. 2011. Atomistic simulation of lipid and Dil dynamics in membrane bilayers under tension. *Phys Chem Chem Phys*, 13, 1368-78.
- MUHLBERGER, T., BALACH, M. M., BISIG, C. G., SANTANDER, V. S., MONESTEROLO, N. E., CASALE, C. H. & CAMPETELLI, A. N. 2021. Inhibition of flippase-like activity by tubulin regulates phosphatidylserine exposure in erythrocytes from hypertensive and diabetic patients. *J Biochem*, 169, 731-745.
- MUNZ, E., JAKOB, P. M. & BORISJUK, L. 2016. The potential of nuclear magnetic resonance to track lipids in planta. *Biochimie*, 130, 97-108.
- MUSTAPHA, S., MOHAMMED, M., AZEMI, A. K., JATAU, A. I., SHEHU, A., MUSTAPHA, L., ALIYU, I. M., DANRAKA, R. N., AMIN, A., BALA, A. A., AHMAD, W., RASOOL, A. H. G., MUSTAFA, M. R. & MOKHTAR, S. S. 2021. Current Status of Endoplasmic Reticulum Stress in Type II Diabetes. *Molecules*, 26.

- NAGABABU, E., CHREST, F. J. & RIFKIND, J. M. 2000. The origin of red cell fluorescence caused by hydrogen peroxide treatment. *Free Radic Biol Med*, 29, 659-63.
- NEELOFAR, K. & AHMAD, J. 2015. Amadori albumin in diabetic nephropathy. *Indian J Endocrinol Metab*, 19, 39-46.
- NOBLE, J. M., THOMAS, T. H. & FORD, G. A. 1999. Effect of age on plasma membrane asymmetry and membrane fluidity in human leukocytes and platelets. *J Gerontol A Biol Sci Med Sci*, 54, M601-6.
- NOMOTO, T., TAKAHASHI, M., FUJII, T., CHIARI, L., TOYOTA, T. & FUJINAMI, M. 2018. Effects of Cholesterol Concentration and Osmolarity on the Fluidity and Membrane Tension of Free-standing Black Lipid Membranes. *Anal Sci*, 34, 1237-1242.
- NONO NANKAM, P. A., MENDHAM, A. E., VAN JAARVELD, P. J., ADAMS, K., FORTUIN-DE SMIDT, M. C., CLAMP, L., BLUHER, M. & GOEDECKE, J. H. 2020. Exercise Training Alters Red Blood Cell Fatty Acid Desaturase Indices and Adipose Tissue Fatty Acid Profile in African Women with Obesity. *Obesity (Silver Spring)*, 28, 1456-1466.
- NOWAK, R. B., ALIMOHAMADI, H., PESTONJAMASP, K., RANGAMANI, P. & FOWLER, V. M. 2022. Nanoscale dynamics of actin filaments in the red blood cell membrane skeleton. *Mol Biol Cell*, 33, ar28.
- NOWOTNY, K., JUNG, T., HOHN, A., WEBER, D. & GRUNE, T. 2015. Advanced glycation end products and oxidative stress in type 2 diabetes mellitus. *Biomolecules*, 5, 194-222.
- OBEAGU, E. I. 2024. Red blood cells as biomarkers and mediators in complications of diabetes mellitus: A review. *Medicine (Baltimore)*, 103, e37265.
- OH, H., MOHLER, E. R., 3RD, TIAN, A., BAUMGART, T. & DIAMOND, S. L. 2009. Membrane cholesterol is a biomechanical regulator of neutrophil adhesion. *Arterioscler Thromb Vasc Biol*, 29, 1290-7.
- OLSHINA, M. A. & SHARON, M. 2016. Mass Spectrometry: A Technique of Many Faces. *Q Rev Biophys*, 49.
- OP DEN KAMP, J. A. 1979. Lipid asymmetry in membranes. *Annu Rev Biochem*, 48, 47-71.
- ORRICO, F., LAURANCE, S., LOPEZ, A. C., LEFEVRE, S. D., THOMSON, L., MOLLER, M. N. & OSTUNI, M. A. 2023. Oxidative Stress in Healthy and Pathological Red Blood Cells. *Biomolecules*, 13.
- PAMPLONA, R. 2011. Advanced lipoxidation end-products. *Chem Biol Interact*, 192, 14-20.
- PARASASSI, T., GRATTON, E., YU, W. M., WILSON, P. & LEVI, M. 1997. Two-photon fluorescence microscopy of laurdan generalized polarization domains in model and natural membranes. *Biophys J*, 72, 2413-29.
- PASCIU, V., NIEDDU, M., SOTGIU, F. D., BARALLA, E. & BERLINGUER, F. 2023. An Overview on Assay Methods to Quantify ROS and Enzymatic Antioxidants in Erythrocytes and Spermatozoa of Small Domestic Ruminants. *Animals (Basel)*, 13.
- PATEL, P. S., SHARP, S. J., JANSEN, E., LUBEN, R. N., KHAW, K. T., WAREHAM, N. J. & FOROUHI, N. G. 2010. Fatty acids measured in plasma and erythrocyte-membrane phospholipids and derived by food-frequency questionnaire and the Y. Pantoja Estrada, PhD Thesis, Aston University, 2024

- risk of new-onset type 2 diabetes: a pilot study in the European Prospective Investigation into Cancer and Nutrition (EPIC)-Norfolk cohort. *Am J Clin Nutr*, 92, 1214-22.
- PATI, S., NIE, B., ARNOLD, R. D. & CUMMINGS, B. S. 2016. Extraction, chromatographic and mass spectrometric methods for lipid analysis. *Biomed Chromatogr*, 30, 695-709.
- PAUL, M., PANDEY, N. K., BANERJEE, A., SHROTI, G. K., TOMER, P., GAZARA, R. K., THATOI, H., BHASKAR, T., HAZRA, S. & GHOSH, D. 2023. An insight into omics analysis and metabolic pathway engineering of lignin-degrading enzymes for enhanced lignin valorization. *Bioresour Technol*, 379, 129045.
- PEARSON, E. R. 2019. Type 2 diabetes: a multifaceted disease. *Diabetologia*, 62, 1107-1112.
- PERTINHEZ, T. A., CASALI, E., LINDNER, L., SPISNI, A., BARICCHI, R. & BERNI, P. 2014. Biochemical assessment of red blood cells during storage by (1)H nuclear magnetic resonance spectroscopy. Identification of a biomarker of their level of protection against oxidative stress. *Blood Transfus*, 12, 548-56.
- PHANIENDRA, A., JESTADI, D. B. & PERIYASAMY, L. 2015. Free radicals: properties, sources, targets, and their implication in various diseases. *Indian J Clin Biochem*, 30, 11-26.
- PIZZINO, G., IRRERA, N., CUCINOTTA, M., PALLIO, G., MANNINO, F., ARCORACI, V., SQUADRITO, F., ALTAVILLA, D. & BITTO, A. 2017. Oxidative Stress: Harms and Benefits for Human Health. *Oxid Med Cell Longev*, 2017, 8416763.
- PONTES, B., MONZO, P. & GAUTHIER, N. C. 2017. Membrane tension: A challenging but universal physical parameter in cell biology. *Semin Cell Dev Biol*, 71, 30-41.
- PRADHAN, S., WILLIAMS, M. A. K. & HALE, T. K. 2022. Changes in the properties of membrane tethers in response to HP1alpha depletion in MCF7 cells. *Biochem Biophys Res Commun*, 587, 126-130.
- QASIM, N., ARIF, A. & MAHMOOD, R. 2023. Hyperglycemia enhances the generation of ROS and RNS that impair antioxidant power and cause oxidative damage in human erythrocytes. *Biochem Cell Biol*, 101, 64-76.
- QUARFORDT, S. H. & HILDERMAN, H. L. 1970. Quantitation of the in vitro free cholesterol exchange of human red cells and lipoproteins. *J Lipid Res*, 11, 528-35.
- QUIJANO, C., TRUJILLO, M., CASTRO, L. & TROSTCHANSKY, A. 2016. Interplay between oxidant species and energy metabolism. *Redox Biol*, 8, 28-42.
- QUINN, P. J., RAINTEAU, D. & WOLF, C. 2009. Lipidomics of the red cell in diagnosis of human disorders. *Methods Mol Biol*, 579, 127-59.
- QUINTERO, M., CABAÑAS, M. & C., A. 2007. A possible cellular explanation for the NMR-visible mobile lipid (ML) changes in cultured C6 glioma cells with growth
- QURESHI, W., SANTAREN, I. D., HANLEY, A. J., WATKINS, S. M., LORENZO, C. & WAGENKNECHT, L. E. 2019. Risk of diabetes associated with fatty acids in the de novo lipogenesis pathway is independent of insulin sensitivity and response: the Insulin Resistance Atherosclerosis Study (IRAS). *BMJ Open Diabetes Res Care*, 7, e000691.

- RABBANI, N. & THORNALLEY, P. J. 2008. Dicarbonyls linked to damage in the powerhouse: glycation of mitochondrial proteins and oxidative stress. *Biochem Soc Trans*, 36, 1045-50.
- RABBANI, N., XUE, M. & THORNALLEY, P. J. 2016. Dicarbonyls and glyoxalase in disease mechanisms and clinical therapeutics. *Glycoconj J*, 33, 513-25.
- RACINE, M. L. & DINENNO, F. A. 2019. Reduced deformability contributes to impaired deoxygenation-induced ATP release from red blood cells of older adult humans. *J Physiol*, 597, 4503-4519.
- RAHBAR, S. 1968. An abnormal hemoglobin in red cells of diabetics. *Clin Chim Acta*, 22, 296-8.
- RAHMAN, I. & ADCOCK, I. M. 2006. Oxidative stress and redox regulation of lung inflammation in COPD. *Eur Respir J*, 28, 219-42.
- RAINS, J. L. & JAIN, S. K. 2011. Oxidative stress, insulin signaling, and diabetes. *Free Radic Biol Med*, 50, 567-75.
- RAMASAMY, R., YAN, S. F. & SCHMIDT, A. M. 2011. Receptor for AGE (RAGE): signaling mechanisms in the pathogenesis of diabetes and its complications. *Ann NY Acad Sci*, 1243, 88-102.
- RANA, S., CHAWLA, R., KUMAR, R., SINGH, S., ZHELEVA, A., DIMITROVA, Y., GADJEVA, V., ARORA, R., SULTANA, S. & SHARMA, R. K. 2010. Electron paramagnetic resonance spectroscopy in radiation research: Current status and perspectives. *J Pharm Bioallied Sci*, 2, 80-7.
- RANDOLPH, C. E., BLANKSBY, S. J. & MCLUCKEY, S. A. 2020. Enhancing detection and characterization of lipids using charge manipulation in electrospray ionization-tandem mass spectrometry. *Chem Phys Lipids*, 232, 104970.
- REDDY, A. S., WARSHAVIAK, D. T. & CHACHISVILIS, M. 2012. Effect of membrane tension on the physical properties of DOPC lipid bilayer membrane. *Biochim Biophys Acta*, 1818, 2271-81.
- REIS, A. & SPICKETT, C. M. 2012. Chemistry of phospholipid oxidation. *Biochim Biophys Acta*, 1818, 2374-87.
- RENNE, M. F. & DE KROON, A. 2018. The role of phospholipid molecular species in determining the physical properties of yeast membranes. *FEBS Lett*, 592, 1330-1345.
- REPSOLD, L. & JOUBERT, A. M. 2018. Eryptosis: An Erythrocyte's Suicidal Type of Cell Death. *Biomed Res Int*, 2018, 9405617.
- RIDONE, P., VASSALLI, M. & MARTINAC, B. 2019. Piezo1 mechanosensitive channels: what are they and why are they important. *Biophys Rev*, 11, 795-805.
- RIPA, I., ANDREU, S., LOPEZ-GUERRERO, J. A. & BELLO-MORALES, R. 2021. Membrane Rafts: Portals for Viral Entry. *Front Microbiol*, 12, 631274.
- ROBERTSON, R. P., HARMON, J., TRAN, P. O. & POITOUT, V. 2004. Beta-cell glucose toxicity, lipotoxicity, and chronic oxidative stress in type 2 diabetes. *Diabetes*, 53 Suppl 1, S119-24.
- ROBINSON, M. & CISTOLA, D. P. 2014. Nanofluidity of fatty acid hydrocarbon chains as monitored by benchtop time-domain nuclear magnetic resonance.
- RODI, P. M., TRUCCO, V. M. & GENNARO, A. M. 2008. Factors determining detergent resistance of erythrocyte membranes. *Biophys Chem*, 135, 14-8.

- RODRIGUEZ-SEGADE, S., RODRIGUEZ, J., GARCIA LOPEZ, J. M., CASANUEVA, F. F. & CAMINA, F. 2012. Estimation of the glycation gap in diabetic patients with stable glycemic control. *Diabetes Care*, 35, 2447-50.
- ROFFAY, C., GARCÍA-ARCOS, J. M., CHAPUIS, P., LÓPEZ-ANDARIAS, J., SCHNEIDER, F., COLOM, A., TOMBA, C., MEGLIO, I., DUNSIG, V., MATILE, S., ROUX, A. & MERCIER, V. 2023. Technical insights into fluorescence lifetime microscopy of mechanosensitive Flipper probes.
- ROFFAY, C., MOLINARD, G., KIM, K., URBANSKA, M., ANDRADE, V., BARBARASA, V., NOWAK, P., MERCIER, V., GARCIA-CALVO, J., MATILE, S., LOEWITH, R., ECHARD, A., GUCK, J., LENZ, M. & ROUX, A. 2021. Passive coupling of membrane tension and cell volume during active response of cells to osmosis. *Proc Natl Acad Sci U S A*, 118.
- ROLFSSON, O., JOHANNSSON, F., MAGNUSDOTTIR, M., PAGLIA, G., SIGURJONSSON, O. E., BORDBAR, A., PALSSON, S., BRYNJOLFSSON, S., GUETHMUNDSSON, S. & PALSSON, B. 2017. Mannose and fructose metabolism in red blood cells during cold storage in SAGM. *Transfusion*, 57, 2665-2676.
- RUDRAPPA, A. B. K. R. T. 2011. Erythrocyte Membrane Lipid Alteration in Type 2 Diabetic Subjects. *Global Journal of Medical Research (USA)*, 11.
- S. ALSALHI, M., DEVANESAN, S., K, E. A., ALSHEBLY, M., AL-QAHTANI, F., FARHAT, K. & MASILAMANI, V. 2018. Impact of Diabetes Mellitus on Human Erythrocytes: Atomic Force Microscopy and Spectral Investigations. *Int J Environ Res Public Health*, 15.
- SAINI, R. K., PRASAD, P., SHANG, X. & KEUM, Y. S. 2021. Advances in Lipid Extraction Methods-A Review. *Int J Mol Sci*, 22.
- SCHEINPFLUG, K., KRYLOVA, O. & STRAHL, H. 2017. Measurement of Cell Membrane Fluidity by Laurdan GP: Fluorescence Spectroscopy and Microscopy. *Methods Mol Biol*, 1520, 159-174.
- SCHUMANN-GILLETT, A. & O'MARA, M. L. 2019. The effects of oxidised phospholipids and cholesterol on the biophysical properties of POPC bilayers. *Biochim Biophys Acta Biomembr*, 1861, 210-219.
- SEELIG, J. & NIEDERBERGER, W. 1973. Deuterium-Labeled Lipids as Structural Probes in Liquid Crystalline Bilayers. A Deuterium Magnetic Resonance Study.
- SENS, P. & PLASTINO, J. 2015. Membrane tension and cytoskeleton organization in cell motility. *J Phys Condens Matter*, 27, 273103.
- SHEHAT, M. G. & TIGNO-ARANJUEZ, J. 2019. Flow Cytometric Measurement Of ROS Production In Macrophages In Response To FcγR Cross-linking. *J Vis Exp*.
- SHENDRIK, P., GOLANI, G., DHARAN, R., SCHWARZ, U. S. & SORKIN, R. 2023. Membrane Tension Inhibits Lipid Mixing by Increasing the Hemifusion Stalk Energy. *ACS Nano*, 17, 18942-18951.
- SHI, Z., GRABER, Z. T., BAUMGART, T., STONE, H. A. & COHEN, A. E. 2018. Cell Membranes Resist Flow. *Cell*, 175, 1769-1779 e13.
- SIMONS, K. & SAMPAIO, J. L. 2011. Membrane organization and lipid rafts. *Cold Spring Harb Perspect Biol*, 3, a004697.
- SITARSKA, E. & DIZ-MUNOZ, A. 2020. Pay attention to membrane tension: Mechanobiology of the cell surface. *Curr Opin Cell Biol*, 66, 11-18.

- SKONIECZNA, M., HEJMO, T., POTERALA-HEJMO, A., CIESLAR-POBUDA, A. & BULDAK, R. J. 2017. NADPH Oxidases: Insights into Selected Functions and Mechanisms of Action in Cancer and Stem Cells. *Oxid Med Cell Longev*, 2017, 9420539.
- SLOTTE, J. P. 2013. Biological functions of sphingomyelins. *Prog Lipid Res*, 52, 424-37.
- SMITH, A. S., NOWAK, R. B., ZHOU, S., GIANNETTO, M., GOKHIN, D. S., PAPOIN, J., GHIRAN, I. C., BLANC, L., WAN, J. & FOWLER, V. M. 2018. Myosin IIA interacts with the spectrin-actin membrane skeleton to control red blood cell membrane curvature and deformability. *Proc Natl Acad Sci U S A*, 115, E4377-E4385.
- SNYDER, L. M., FORTIER, N. L., TRAINOR, J., JACOBS, J., LEB, L., LUBIN, B., CHIU, D., SHOHEET, S. & MOHANDAS, N. 1985. Effect of hydrogen peroxide exposure on normal human erythrocyte deformability, morphology, surface characteristics, and spectrin-hemoglobin cross-linking. *J Clin Invest*, 76, 1971-7.
- SOBCZAK, A. I. S., PITT, S. J., SMITH, T. K., AJJAN, R. A. & STEWART, A. J. 2021. Lipidomic profiling of plasma free fatty acids in type-1 diabetes highlights specific changes in lipid metabolism. *Biochim Biophys Acta Mol Cell Biol Lipids*, 1866, 158823.
- SONG, Y. & JENSEN, M. D. 2021. Red blood cell triglycerides—a unique pool that incorporates plasma-free fatty acids and relates to metabolic health. *J Lipid Res*, 62, 100131.
- SPICKETT, C. M., REIS, A. & PITT, A. R. 2011. Identification of oxidized phospholipids by electrospray ionization mass spectrometry and LC-MS using a QQLIT instrument. *Free Radic Biol Med*, 51, 2133-49.
- STILLWELL, W. & WASSALL, S. R. 2003. Docosahexaenoic acid: membrane properties of a unique fatty acid. *Chem Phys Lipids*, 126, 1-27.
- STIRBAN, A., GAWLOWSKI, T. & RODEN, M. 2014. Vascular effects of advanced glycation endproducts: Clinical effects and molecular mechanisms. *Mol Metab*, 3, 94-108.
- SUBCZYNSKI, W. K., PASENKIEWICZ-GIERULA, M., WIDOMSKA, J., MAINALI, L. & RAGUZ, M. 2017. High Cholesterol/Low Cholesterol: Effects in Biological Membranes: A Review. *Cell Biochem Biophys*, 75, 369-385.
- SUHLING, K. H., L.; LEVITT, J; 2015. Fluorescence lifetime imaging (FLIM): Basic concepts and some recent developments.
- SUN, K., D'ALESSANDRO, A. & XIA, Y. 2017. Purinergic control of red blood cell metabolism: novel strategies to improve red cell storage quality. *Blood Transfus*, 15, 535-542.
- SURYAWANSHI, N. P., BHUTEY, A. K., NAGDEOTE, A. N., JADHAV, A. A. & MANOORKAR, G. S. 2006. Study of lipid peroxide and lipid profile in diabetes mellitus. *Indian J Clin Biochem*, 21, 126-30.
- SUVITAIVAL, T., BONDIA-PONS, I., YETUKURI, L., POHO, P., NOLAN, J. J., HYOTYLAINEN, T., KUUSISTO, J. & ORESIC, M. 2018. Lipidome as a predictive tool in progression to type 2 diabetes in Finnish men. *Metabolism*, 78, 1-12.
- SUZEN, S., GURER-ORHAN, H. & SASO, L. 2017. Detection of Reactive Oxygen and Nitrogen Species by Electron Paramagnetic Resonance (EPR) Technique. *Molecules*, 22.
- TAKAKUWA, Y. 2000. Protein 4.1, a multifunctional protein of the erythrocyte membrane skeleton: structure and functions in erythrocytes and nonerythroid cells. *Int J Hematol*, 72, 298-309.

- TAM, M. F., RICE, N. W., MAILLETT, D. H., SIMPLACEANU, V., HO, N. T., TAM, T. C. S., SHEN, T. J. & HO, C. 2013. Autoxidation and oxygen binding properties of recombinant hemoglobins with substitutions at the alphaVal-62 or betaVal-67 position of the distal heme pocket. *J Biol Chem*, 288, 25512-25521.
- TANG, W. H., MARTIN, K. A. & HWA, J. 2012. Aldose reductase, oxidative stress, and diabetic mellitus. *Front Pharmacol*, 3, 87.
- TAPIA, J., VERA, N., AGUILAR, J., GONZALEZ, M., SANCHEZ, S. A., COELHO, P., SAAVEDRA, C. & STAFORELLI, J. 2021. Correlated flickering of erythrocytes membrane observed with dual time resolved membrane fluctuation spectroscopy under different D-glucose concentrations. *Sci Rep*, 11, 2429.
- TETZ, L. M., KAMAU, P. W., CHENG, A. A., MEEKER, J. D. & LOCH-CARUSO, R. 2013. Troubleshooting the dichlorofluorescein assay to avoid artifacts in measurement of toxicant-stimulated cellular production of reactive oxidant species. *J Pharmacol Toxicol Methods*, 67, 56-60.
- THOMAS, S. N., FRENCH, D., JANNETTO, P. J., RAPPOLD, B. A. & CLARKE, W. A. 2022. Liquid chromatography-tandem mass spectrometry for clinical diagnostics. *Nat Rev Methods Primers*, 2, 96.
- THOMAS, T., CENDALI, F., FU, X., GAMBONI, F., MORRISON, E. J., BEIRNE, J., NEMKOV, T., ANTONELLOU, M. H., KRIEBARDIS, A., WELSBY, I., HAY, A., DZIEWULSKA, K. H., BUSCH, M. P., KLEINMAN, S., BUEHLER, P. W., SPITALNIK, S. L., ZIMRING, J. C. & D'ALESSANDRO, A. 2021. Fatty acid desaturase activity in mature red blood cells and implications for blood storage quality. *Transfusion*, 61, 1867-1883.
- TOMAIUOLO, G. 2014. Biomechanical properties of red blood cells in health and disease towards microfluidics. *Biomicrofluidics*, 8, 051501.
- TSUGAWA, H., CAJKA, T., KIND, T., MA, Y., HIGGINS, B., IKEDA, K., KANAZAWA, M., VANDERGHEYNST, J., FIEHN, O. & ARITA, M. 2015. MS-DIAL: data-independent MS/MS deconvolution for comprehensive metabolome analysis. *Nat Methods*, 12, 523-6.
- TURPIN, C., CATAN, A., GUERIN-DUBOURG, A., DEBUSSCHE, X., BRAVO, S. B., ALVAREZ, E., VAN DEN ELSEN, J., MEILHAC, O., RONDEAU, P. & BOURDON, E. 2020. Enhanced oxidative stress and damage in glycated erythrocytes. *PLoS One*, 15, e0235335.
- URBAN, P. L. 2016. Quantitative mass spectrometry: an overview. *Philos Trans A Math Phys Eng Sci*, 374.
- VAHEDI, A., BIGDELOU, P. & FARNOUD, A. M. 2020. Quantitative analysis of red blood cell membrane phospholipids and modulation of cell-macrophage interactions using cyclodextrins. *Sci Rep*, 10, 15111.
- VAISERMAN, A. & LUSHCHAK, O. 2019. Developmental origins of type 2 diabetes: Focus on epigenetics. *Ageing Res Rev*, 55, 100957.
- VAN DER PAAL, J., NEYTS, E. C., VERLACKT, C. C. W. & BOGAERTS, A. 2016. Effect of lipid peroxidation on membrane permeability of cancer and normal cells subjected to oxidative stress. *Chem Sci*, 7, 489-498.
- VENN-WATSON, S., LUMPKIN, R. & DENNIS, E. A. 2020. Efficacy of dietary odd-chain saturated fatty acid pentadecanoic acid parallels broad associated health benefits in humans: could it be essential? *Sci Rep*, 10, 8161.

- VERDE, C., GIORDANO, D., BELLAS, C. M., DI PRISCO, G. & ANESIO, A. M. 2016. Polar Marine Microorganisms and Climate Change. *Adv Microb Physiol*, 69, 187-215.
- VESTERGAARD, M., HAMADA, T., MORITA, M. & TAKAGI, M. 2010. Cholesterol, lipids, amyloid Beta, and Alzheimer's. *Curr Alzheimer Res*, 7, 262-70.
- VILLASANTA-GONZALEZ, A., MORA-ORTIZ, M., ALCALA-DIAZ, J. F., RIVAS-GARCIA, L., TORRES-PENA, J. D., LOPEZ-BASCON, A., CALDERON-SANTIAGO, M., ARENAS-LARRIVA, A. P., PRIEGO-CAPOTE, F., MALAGON, M. M., EICHELMANN, F., PEREZ-MARTINEZ, P., DELGADO-LISTA, J., SCHULZE, M. B., CAMARGO, A. & LOPEZ-MIRANDA, J. 2023. Plasma lipidic fingerprint associated with type 2 diabetes in patients with coronary heart disease: CORDIOPREV study. *Cardiovasc Diabetol*, 22, 199.
- VINCENT, A. M., RUSSELL, J. W., LOW, P. & FELDMAN, E. L. 2004. Oxidative stress in the pathogenesis of diabetic neuropathy. *Endocr Rev*, 25, 612-28.
- VISKUPICOVA, J., BLASKOVIC, D., GALINIAK, S., SOSZYNSKI, M., BARTOSZ, G., HORAKOVA, L. & SADOWSKA-BARTOSZ, I. 2015. Effect of high glucose concentrations on human erythrocytes in vitro. *Redox Biol*, 5, 381-387.
- VISTOLI, G., DE MADDIS, D., CIPAK, A., ZARKOVIC, N., CARINI, M. & ALDINI, G. 2013. Advanced glycooxidation and lipoxidation end products (AGEs and ALEs): an overview of their mechanisms of formation. *Free Radic Res*, 47 Suppl 1, 3-27.
- WACZULIKOVA, I., SIKUROVA, L. & CARSKY, J. 2002. Fluidity gradient of erythrocyte membranes in diabetics: the effect of resorcylicidene aminoguanidine. *Bioelectrochemistry*, 55, 53-5.
- WANG, Q. & ZENNADI, R. 2020. Oxidative Stress and Thrombosis during Aging: The Roles of Oxidative Stress in RBCs in Venous Thrombosis. *Int J Mol Sci*, 21.
- WANG, Q. & ZENNADI, R. 2021. The Role of RBC Oxidative Stress in Sickle Cell Disease: From the Molecular Basis to Pathologic Implications. *Antioxidants (Basel)*, 10.
- WANG, Q. & ZOU, M. H. 2018. Measurement of Reactive Oxygen Species (ROS) and Mitochondrial ROS in AMPK Knockout Mice Blood Vessels. *Methods Mol Biol*, 1732, 507-517.
- WANG, W., YANG, H., JOHNSON, D., GENSLER, C., DECKER, E. & ZHANG, G. 2017. Chemistry and biology of omega-3 PUFA peroxidation-derived compounds. *Prostaglandins Other Lipid Mediat*, 132, 84-91.
- WANG, Y., YANG, P., YAN, Z., LIU, Z., MA, Q., ZHANG, Z., WANG, Y. & SU, Y. 2021. The Relationship between Erythrocytes and Diabetes Mellitus. *J Diabetes Res*, 2021, 6656062.
- WANG-SATTLER, R., YU, Z., HERDER, C., MESSIAS, A. C., FLOEGEL, A., HE, Y., HEIM, K., CAMPILLOS, M., HOLZAPFEL, C., THORAND, B., GRALLERT, H., XU, T., BADER, E., HUTH, C., MITTELSTRASS, K., DORING, A., MEISINGER, C., GIEGER, C., PREHN, C., ROEMISCH-MARGL, W., CARSTENSEN, M., XIE, L., YAMANAKA-OKUMURA, H., XING, G., CEGLAREK, U., THIERY, J., GIANI, G., LICKERT, H., LIN, X., LI, Y., BOEING, H., JOOST, H. G., DE ANGELIS, M. H., RATHMANN, W., SUHRE, K., PROKISCH, H., PETERS, A., MEITINGER, T., RODEN, M., WICHMANN, H. E., PISCHON, T., ADAMSKI, J. & ILLIG, T. 2012. Novel biomarkers for pre-diabetes identified by metabolomics. *Mol Syst Biol*, 8, 615.

- WATALA, C. & JOZWIAK, Z. 1990. The phospholipid composition of erythrocyte ghosts and plasma lipoproteins in diabetes type 1 in children. *Clin Chim Acta*, 188, 211-9.
- WAUGH, R. & EVANS, E. A. 1979. Thermoelasticity of red blood cell membrane. *Biophys J*, 26, 115-31.
- WAUTIER, J. L. & SCHMIDT, A. M. 2004. Protein glycation: a firm link to endothelial cell dysfunction. *Circ Res*, 95, 233-8.
- WILKERSON, J. L., SUMMERS, S. A. & HOLLAND, W. L. 2019. Listen to your heart when ceramide's calling for higher glucose. *EBioMedicine*, 41, 3-4.
- WINTERBOURN, C. C. 2014. The challenges of using fluorescent probes to detect and quantify specific reactive oxygen species in living cells. *Biochim Biophys Acta*, 1840, 730-8.
- WRONA, M. & WARDMAN, P. 2006. Properties of the radical intermediate obtained on oxidation of 2',7'-dichlorodihydrofluorescein, a probe for oxidative stress. *Free Radic Biol Med*, 41, 657-67.
- WU, D. & YOTNDA, P. 2011. Production and detection of reactive oxygen species (ROS) in cancers. *J Vis Exp*.
- WU, J., LEWIS, A. H. & GRANDL, J. 2017. Touch, Tension, and Transduction - The Function and Regulation of Piezo Ion Channels. *Trends Biochem Sci*, 42, 57-71.
- WU, Z., BAGAROLO, G. I., THOROE-BOVELETH, S. & JANKOWSKI, J. 2020. "Lipidomics": Mass spectrometric and chemometric analyses of lipids. *Adv Drug Deliv Rev*, 159, 294-307.
- XIAO, D. & CHANG, W. 2023. Phosphatidylserine in Diabetes Research. *Mol Pharm*, 20, 82-89.
- XU, H., LI, W., HUANG, L., HE, X., XU, B., HE, X., CHEN, W., WANG, Y., XU, W., WANG, S., KONG, Q., XU, Y. & LU, W. 2023. Phosphoethanolamine cytidyltransferase ameliorates mitochondrial function and apoptosis in hepatocytes in T2DM in vitro. *J Lipid Res*, 64, 100337.
- XU, Z., DOU, W., WANG, C. & SUN, Y. 2019. Stiffness and ATP recovery of stored red blood cells in serum. *Microsyst Nanoeng*, 5, 51.
- YAN, Q., GOMIS PEREZ, C. & KARATEKIN, E. 2024. Cell Membrane Tension Gradients, Membrane Flows, and Cellular Processes. *Physiology (Bethesda)*, 39, 0.
- YANG, D. R., WANG, M. Y., ZHANG, C. L. & WANG, Y. 2024. Endothelial dysfunction in vascular complications of diabetes: a comprehensive review of mechanisms and implications. *Front Endocrinol (Lausanne)*, 15, 1359255.
- YANG, J., ZHENG, X., MAHDI, A., ZHOU, Z., TRATSIKOVICH, Y., JIAO, T., KISS, A., KOVAMEES, O., ALVARSSON, M., CATRINA, S. B., LUNDBERG, J. O., BRISMAR, K. & PERNOW, J. 2018. Red Blood Cells in Type 2 Diabetes Impair Cardiac Post-Ischemic Recovery Through an Arginase-Dependent Modulation of Nitric Oxide Synthase and Reactive Oxygen Species. *JACC Basic Transl Sci*, 3, 450-463.
- YANG, K. & HAN, X. 2011. Accurate quantification of lipid species by electrospray ionization mass spectrometry - Meet a key challenge in lipidomics. *Metabolites*, 1, 21-40.
- YANG, S. T., KREUTZBERGER, A. J. B., LEE, J., KIESSLING, V. & TAMM, L. K. 2016. The role of cholesterol in membrane fusion. *Chem Phys Lipids*, 199, 136-143.

- YONAR, D., KILIC SULOGLU, A., SELMANOGLU, G. & SUNNETCIOGLU, M. M. 2019. An Electron paramagnetic resonance (EPR) spin labeling study in HT-29 Colon adenocarcinoma cells after Hypericin-mediated photodynamic therapy. *BMC Mol Cell Biol*, 20, 16.
- YOON, Y. Z., HONG, H., BROWN, A., KIM, D. C., KANG, D. J., LEW, V. L. & CICUTA, P. 2009. Flickering analysis of erythrocyte mechanical properties: dependence on oxygenation level, cell shape, and hydration level. *Biophys J*, 97, 1606-15.
- YOUNESSI, P. & YOONESSI, A. 2011. Advanced glycation end-products and their receptor-mediated roles: inflammation and oxidative stress. *Iran J Med Sci*, 36, 154-66.
- ZALBA, S. & TEN HAGEN, T. L. 2017. Cell membrane modulation as adjuvant in cancer therapy. *Cancer Treat Rev*, 52, 48-57.
- ZAVODNIK, I. B., PIASECKA, A., SZOSLAND, K. & BRYSEWSKA, M. 1997. Human red blood cell membrane potential and fluidity in glucose solutions. *Scand J Clin Lab Invest*, 57, 59-63.
- ZHANG, Q., MONROE, M. E., SCHEPMOES, A. A., CLAUSS, T. R., GRITSENKO, M. A., MENG, D., PETYUK, V. A., SMITH, R. D. & METZ, T. O. 2011. Comprehensive identification of glycated peptides and their glycation motifs in plasma and erythrocytes of control and diabetic subjects. *J Proteome Res*, 10, 3076-88.
- ZHANG, Y. L., FRANGOS, J. A. & CHACHISVILIS, M. 2006. Laurdan fluorescence senses mechanical strain in the lipid bilayer membrane. *Biochem Biophys Res Commun*, 347, 838-41.
- ZHONG, Y., XU, Y., TAN, Y., ZHANG, X., WANG, R., CHEN, D., WANG, Z. & ZHONG, X. 2023. Lipidomics of the erythrocyte membrane and network pharmacology to explore the mechanism of mangiferin from *Anemarrhenae rhizoma* in treating type 2 diabetes mellitus rats. *J Pharm Biomed Anal*, 230, 115386.
- ZHOU, Z., MAHDI, A., TRATSIKOVICH, Y., ZAHORAN, S., KOVAMEES, O., NORDIN, F., URIBE GONZALEZ, A. E., ALVARSSON, M., OSTENSON, C. G., ANDERSSON, D. C., HEDIN, U., HERMESZ, E., LUNDBERG, J. O., YANG, J. & PERNOW, J. 2018. Erythrocytes From Patients With Type 2 Diabetes Induce Endothelial Dysfunction Via Arginase I. *J Am Coll Cardiol*, 72, 769-780.
- ZHU, R., AVSIEVICH, T., POPOV, A. & MEGLINSKI, I. 2020. Optical Tweezers in Studies of Red Blood Cells. *Cells*, 9.
- ZIDOVETZKI, R. & LEVITAN, I. 2007. Use of cyclodextrins to manipulate plasma membrane cholesterol content: evidence, misconceptions and control strategies. *Biochim Biophys Acta*, 1768, 1311-24.

# Supplementary Data

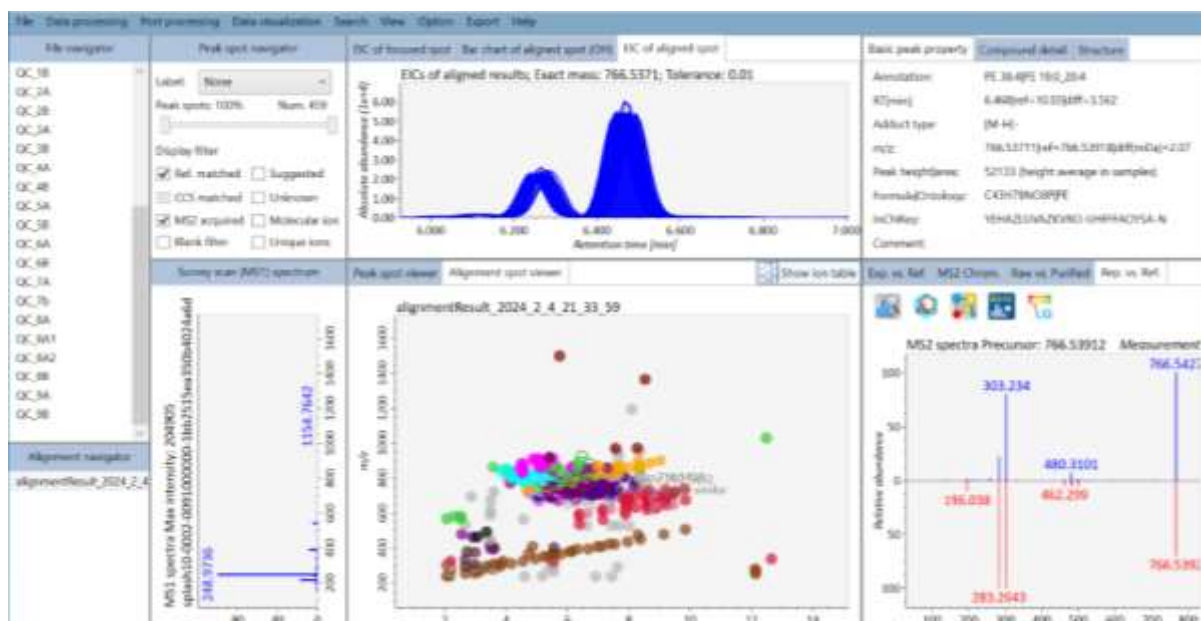


Figure S 1. Quality controls (QCs) obtained using negative ion mode. The top left panel lists different QCs sample files analysed. The middle panel shows the extracted ion chromatograms (EICs) for  $m/z$  766.5371, corresponding to PE 38:4|PE 18:0\_20:4, from different QC samples aligned by similar retention times. This helps assess the reproducibility and retention time alignment of the lipids across different QC samples. Top right panel shows detailed information about the specific ion detected including phospholipid type, retention time (in minutes), adduct type (in this case  $[M-H]^-$ ),  $m/z$  (766.5371), and the formula ( $C_{43}H_{78}NO_8P$ ). Bottom right panel shows the replicate (Rep) fragments in blue and the reference (Ref) fragments in red. Comparing replicate data to reference data allows for the assessment of consistency between replicate samples and the reference, ensuring that replicate analyses produce results consistent with expected fragments. This comparison helps verify the accuracy and reliability of mass spectrometry data. Additionally, MS Dial matches spectra against mass spectral libraries such as MassBank or LipidBlast (Tsugawa *et al.*, 2015). Bottom middle panel shows the detected precursor ions which are displayed as spots in the alignment spot viewer, with each type of phospholipid denoted by a different colour. Compound identification is performed based on a weighted similarity score that considers retention time, accurate mass, and MS/MS spectra.

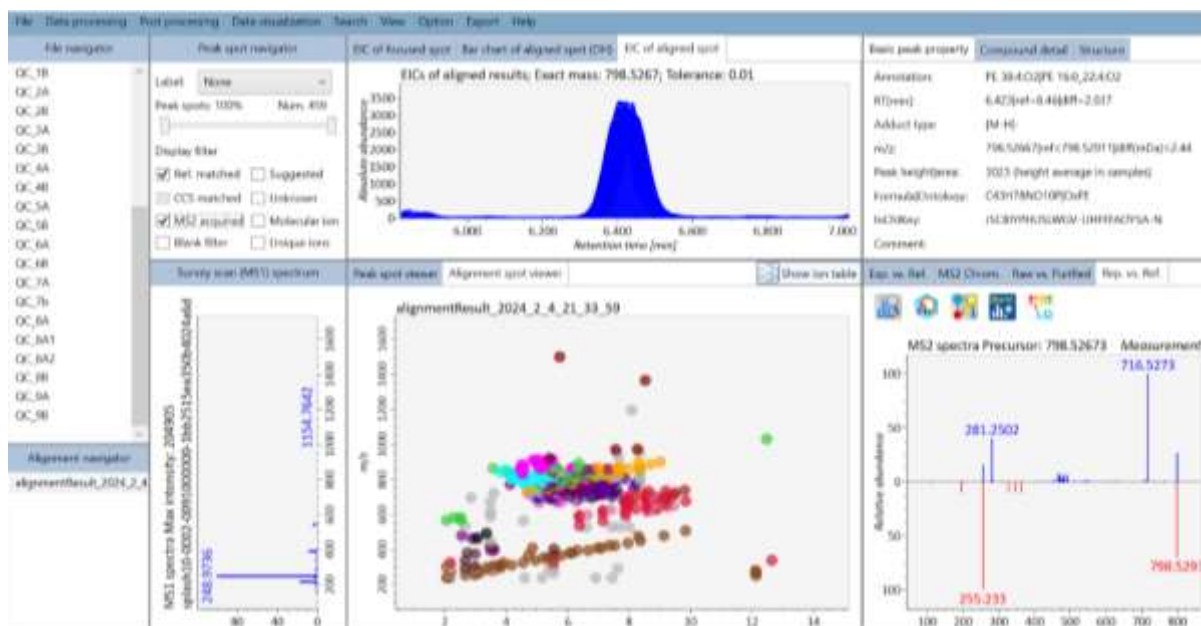


Figure S 2. Quality controls (QCs) obtained using negative ion mode.

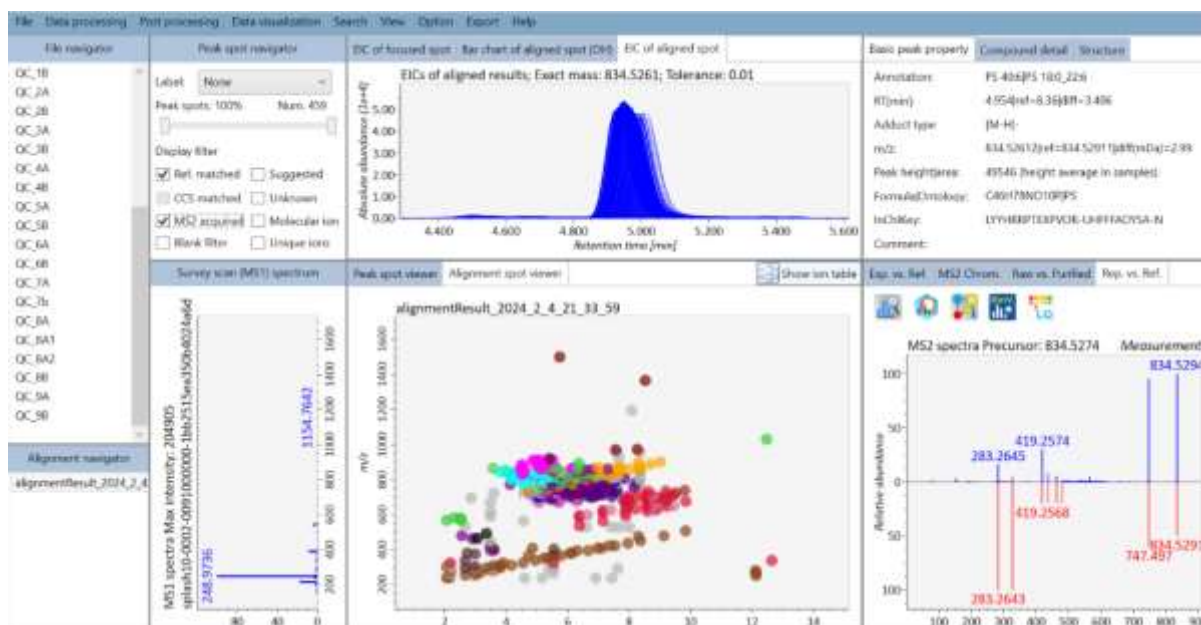


Figure S 9. Quality controls (QCs) obtained using negative ion mode.

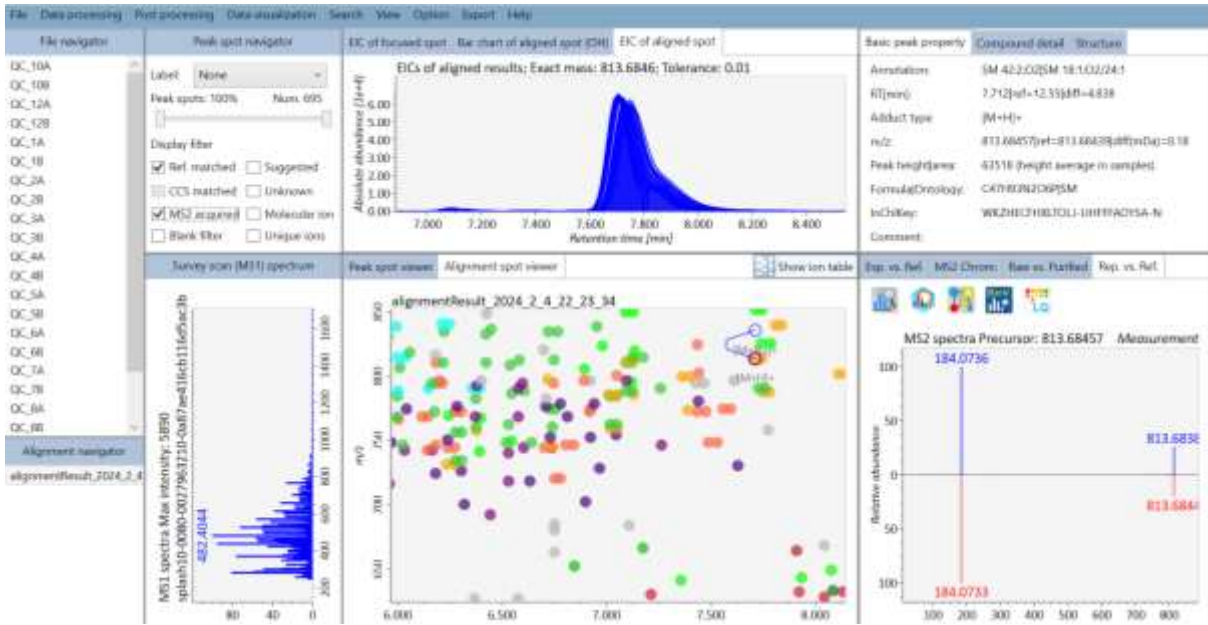


Figure S 10. Quality controls (QCs) obtained using positive ion mode.

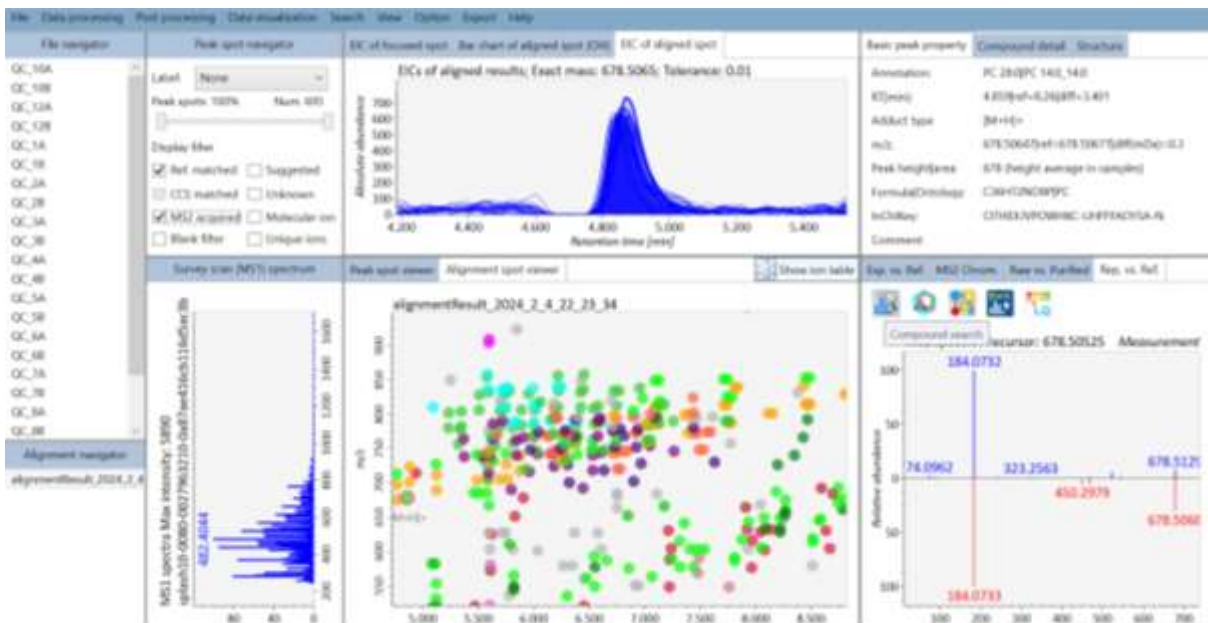


Figure S 11. Quality controls (QCs) obtained using positive ion mode.

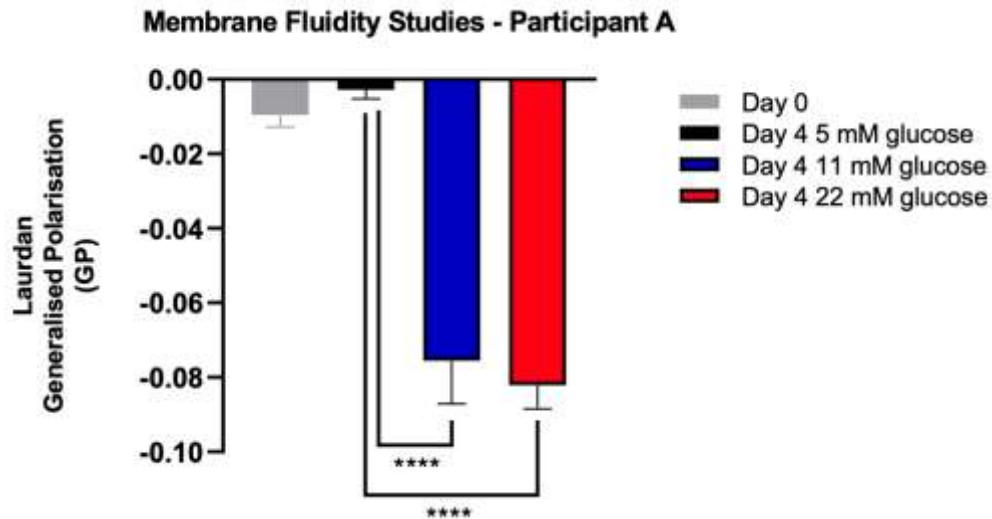


Figure S 12. Membrane fluidity studies. Results obtained for participant A, long term glucose treatment. Results shown as means  $\pm$  SD of three technical replicates. One-way ANOVA followed by Tukey post hoc test were carried out. No significance was found between day 0 and day 4 at 5 mM glucose. P values of  $<0.0001$  were obtained between 5 mM-11 mM, and 5 mM-22 mM glucose.

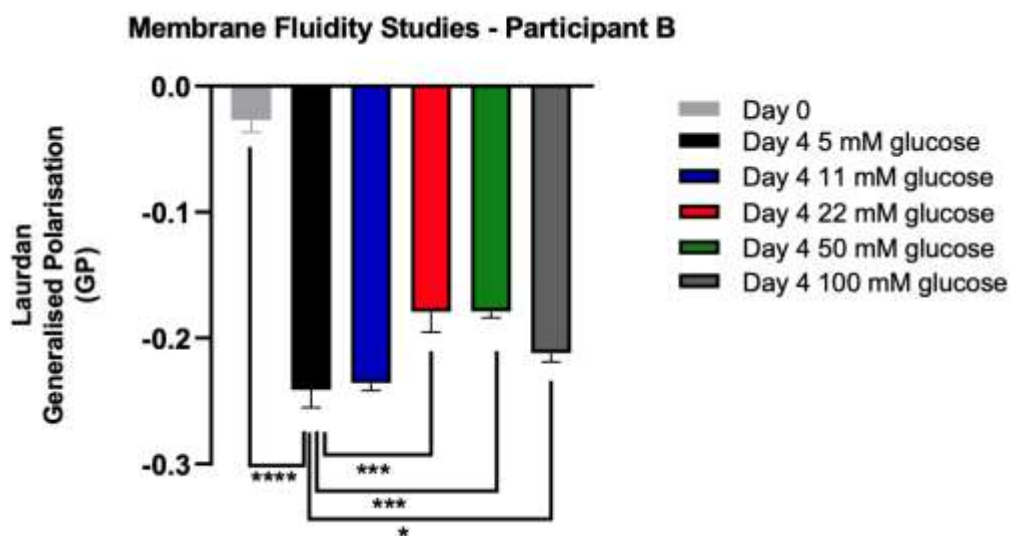


Figure S 13. Membrane fluidity studies. Results obtained for participant B, long term glucose treatment. Results shown as means  $\pm$  SD of three technical replicates. One-way ANOVA followed by Tukey post hoc test were carried.  $P < 0.0001$  was obtained between day 0 and day 4 at 5 mM glucose. No significance was observed between 5 mM-11 mM glucose. P values of 0.0001 were obtained between 5 mM-22 mM and 5 mM-50 mM glucose.  $P < 0.05$  was obtained between 5 mM-100 mM glucose.

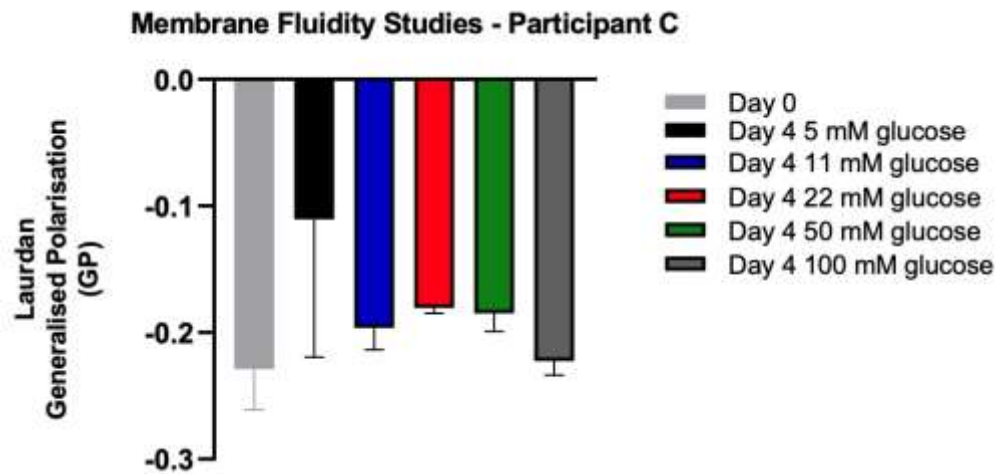


Figure S 14. Membrane fluidity studies. Results obtained for participant C, long term glucose treatment. Results shown as means  $\pm$  SD of three technical replicates. One-way ANOVA followed by Tukey post hoc test showed no significance between the treatments.

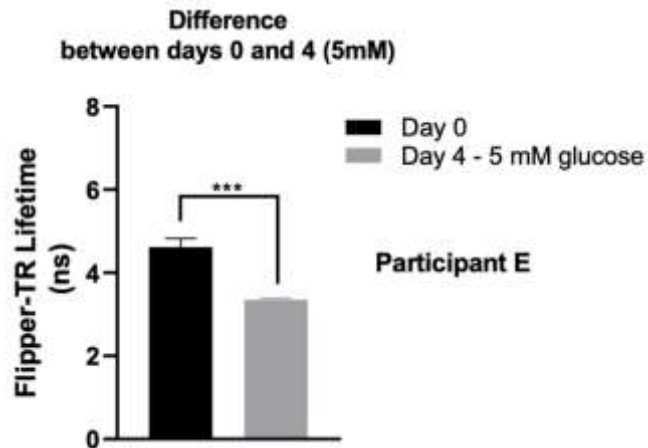


Figure S 15. Erythrocyte membrane tension assayed by Flipper-TR on untreated erythrocytes and those aged in media containing 5 mM for participant E. Results shown as means  $\pm$  SD of three technical replicates. A *t*-test showed significant difference between untreated and aged cells ( $P < 0.0005$ ).

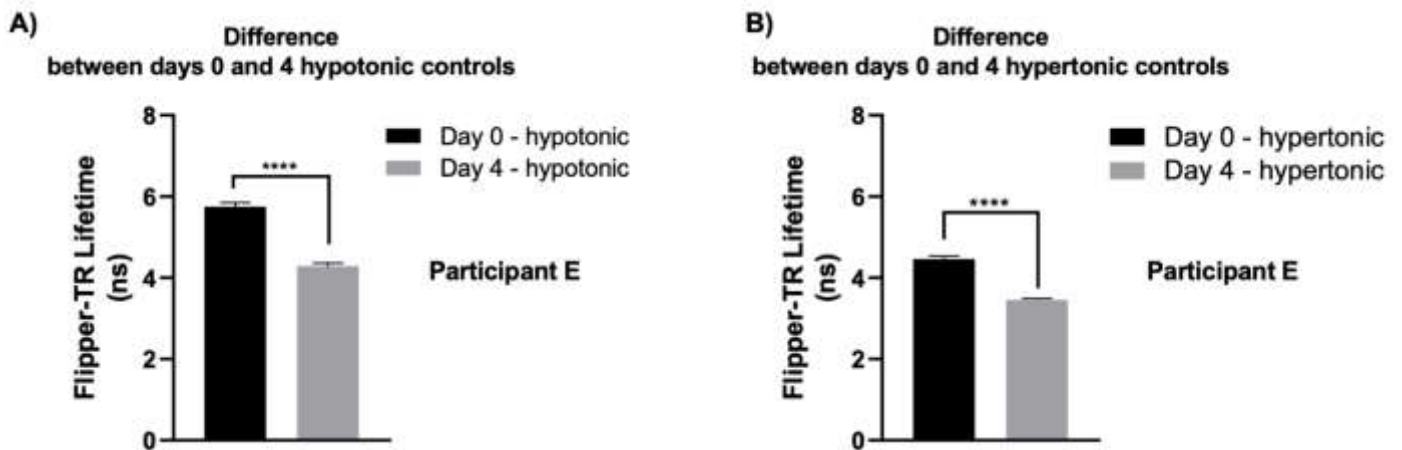


Figure S 16. Membrane tension of fresh (day 0) and aged (day 4, 5 mM glucose) erythrocytes when exposed to hypotonic (A) and hypertonic solutions (B), which was assayed by Flipper-TR. Erythrocytes belonged to participant E. Results shown as means  $\pm$  SD of three technical replicates. A *t*-test showed significant difference between the hypotonic ( $P < 0.0001$ ) and hypertonic ( $P < 0.0001$ ) controls.

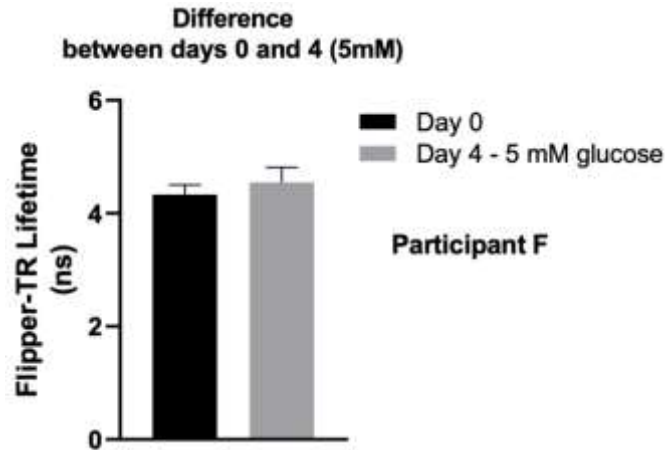


Figure S 17. Erythrocyte membrane tension assayed by Flipper-TR on untreated erythrocytes and those aged in media containing 5 mM for participant F. Results shown as means  $\pm$  SD of three technical replicates. A *t*-test showed no significant difference between untreated and aged cells.

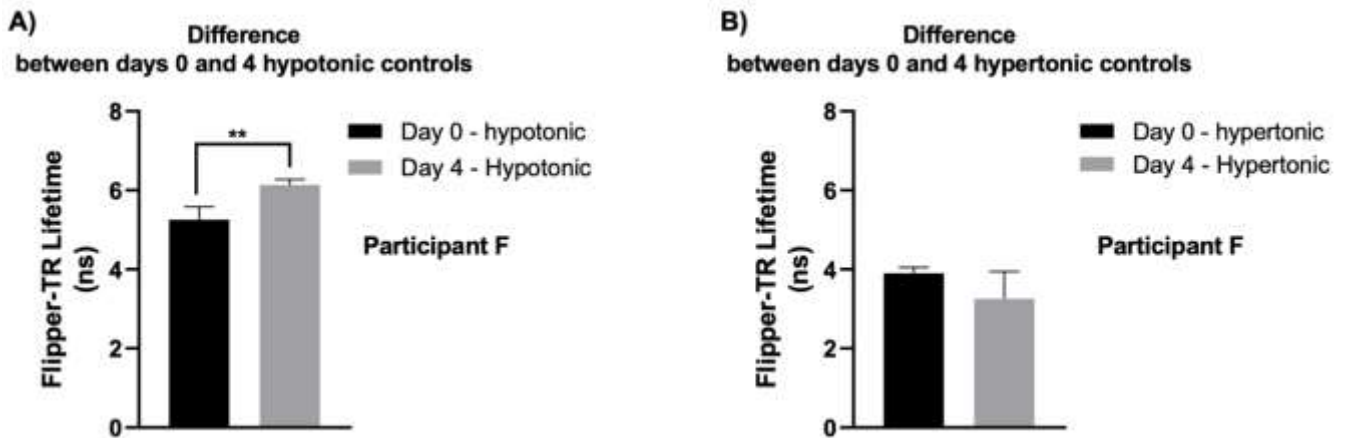


Figure S 18. Membrane tension of fresh (day 0) and aged (day 4, 5 mM glucose) erythrocytes when exposed to hypotonic (A) and hypertonic solutions (B), which was assayed by Flipper-TR. Erythrocytes belonged to participant F. Results shown as means  $\pm$  SD of three technical replicates. A *t*-test showed significant difference between the hypotonic controls ( $P < 0.005$ ), but not for hypertonic.

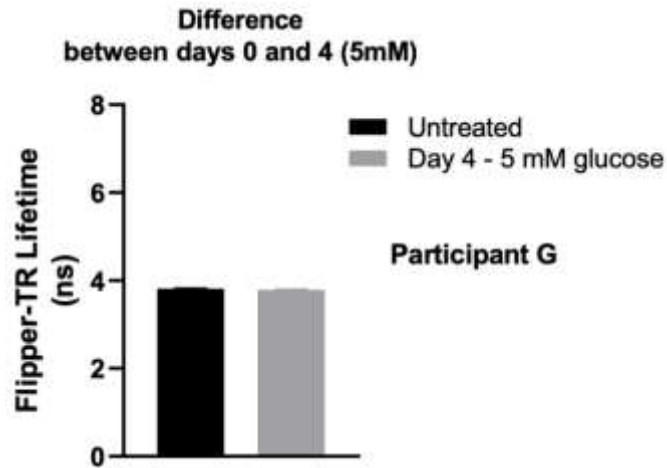


Figure S 19. RBC membrane tension assayed by Flipper-TR on untreated erythrocytes and those aged in media containing 5 mM for participant G. Results shown as means  $\pm$  SD of three technical replicates. A *t*-test showed no significant difference between untreated and aged cells.

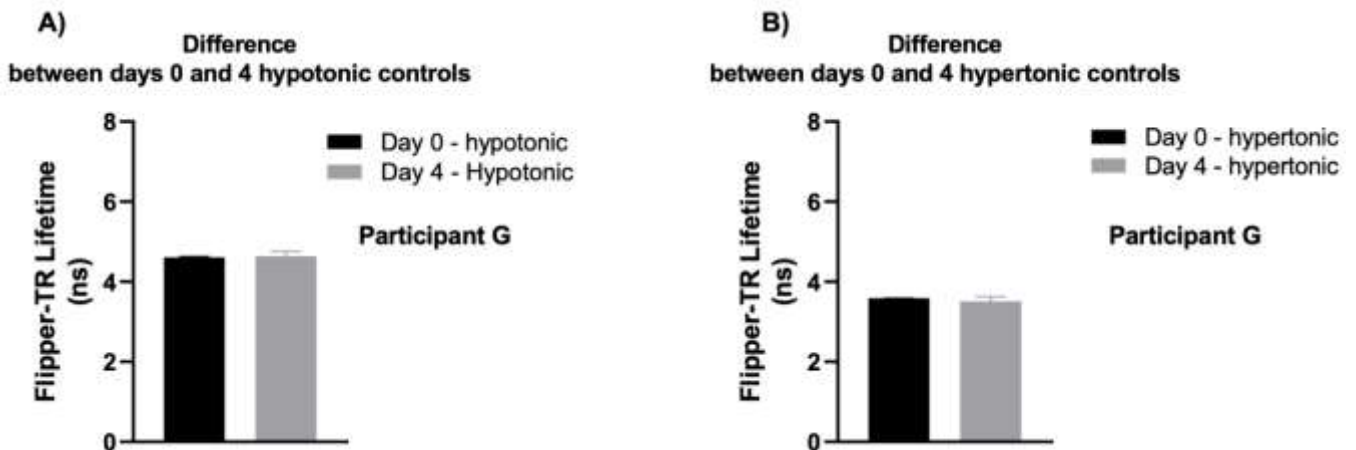


Figure S 20. Membrane tension of fresh (day 0) and aged (day 4, 5 mM glucose) erythrocytes when exposed to hypotonic (A) and hypertonic solutions (B), which was assayed by Flipper-TR. Erythrocytes belonged to participant G. Results shown as means  $\pm$  SD of three technical replicates. A *t*-test showed significant difference between the hypotonic controls ( $P < 0.005$ ), but not for hypertonic.

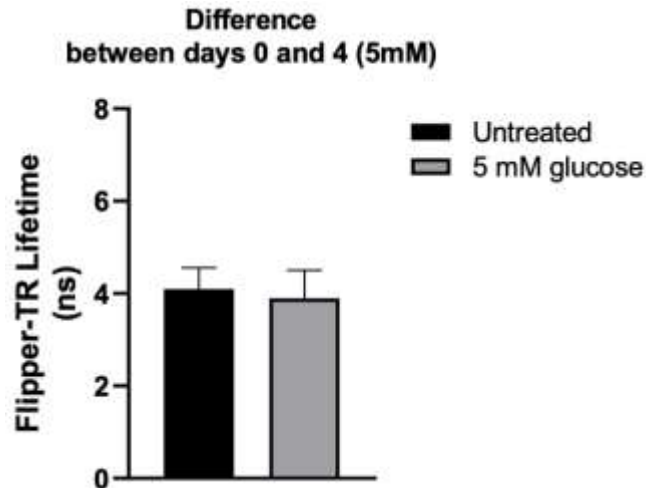


Figure S 21. Erythrocyte membrane tension assayed by Flipper-TR on untreated erythrocytes and those aged in media containing 5 mM. The combined results are shown as means  $\pm$  SD of three biological replicates ( $n=3$ ). A  $t$ -test showed no significant difference between untreated and aged cells.

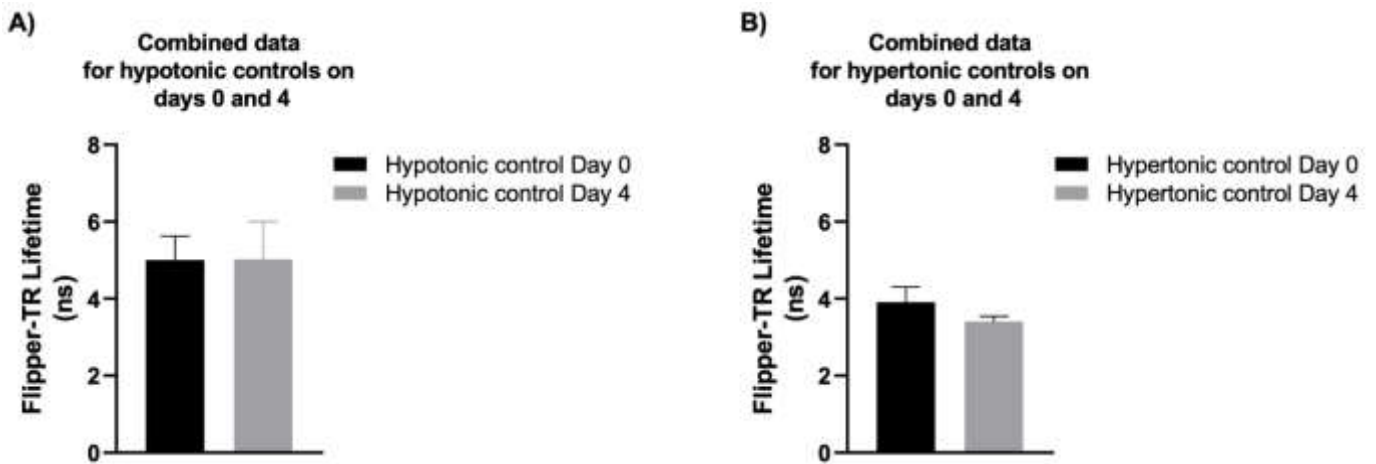


Figure S 22. RBC membrane tension assayed by Flipper-TR on cells treated with hypotonic (A) and hypertonic (B) solutions on days 0 and 4. The combined results are shown as means  $\pm$  SD of three biological replicates ( $n=3$ ). A  $t$ -test showed no significant difference between untreated and aged cells.